The role of the Smc5/6 complex and the Mms21 SUMO Ligase in the maintenance of genomic integrity

Marcelino Bermúdez López

Dipòsit Legal: L.1224-2014
http://hdl.handle.net/10803/284851

The role of the Smc5/6 complex and the Mms21 SUMO Ligase in the maintenance of genomic integrity està subjecte a una llicència de Reconeixement-NoComercial-SenseObraDerivada 3.0 No adaptada de Creative Commons

(c) 2014, Marcelino Bermúdez López

The role of the Smc5/6 complex and the Mms21 SUMO ligase in the Maintenance of Genomic Integrity

MARCELINO BERMÚDEZ LÓPEZ

Universitat de Lleida, *September 2014*

Universitat de Lleida
Departament de Ciències Mèdiques Bàsiques

The role of the Smc5/6 complex and the Mms21 SUMO ligase in the Maintenance of Genomic integrity

MARCELINO BERMÚDEZ LÓPEZ
September 2014

Thesis submitted for the degree of Doctor (PhD)

Thesis Director: **Dr. Jordi Torres-Rosell**
Universitat de Lleida, IRBLleida

IRBLleida
Institut de Recerca Biomèdica

Acknowledgments

A mis padres. Lo sois todo, de verdad! Sin vosotros nada de esto hubiera sido posible… Y no lo digo por la simple obviedad de que sin vosotros no estaría en este mundo y demás. Me refiero al apoyo incondicional que siempre me habéis ofrecido y por estar siempre a mi lado aconsejándome y guiándome en cada momento importante de mi vida. Por las charlas de los domingos, en las que no importa el tiempo, solo buscar nuevos horizontes. GRACIAS! No me cansaré de decirlo jamás.

A Alex, mi querido hermano. Por mogollón de cosas. Por todo lo que nos ayudas. Por tu santa paciencia para enseñarme lo que sé de diseño gráfico y ayudarme a maquetar la tesis con un mínimo de criterio estético, je,je,je,je. Gracias por aguantar mis nervios e inseguridades y estar siempre disponible para lo que sea. Gracias peque!

A mis tíos. Por estar siempre a mi lado cuando os he necesitado y por todo el apoyo que me habéis ofrecido desde siempre.

Al GRAN AMIGO de la familia. Por todo. Por tus consejos, por tu apoyo, por enseñarnos que no existe distancia y por ofrecernos soluciones ante cualquier situación. Sin tu inmensa ayuda jamás hubiera podido llevar esta pequeña barquita a puerto. Sinceramente GRACIAS!

A Jordi Torres, mi director de tesis. Hay momentos que marcan toda una vida. Recuerdo aquel primer contacto-entrevista en la terracita de la tercera planta del CMB. Estabas recién llegado de Londres lleno de aspiraciones, energía y vitalidad. Me cautivaste. Aquella tarde decidimos emprender un viaje juntos. Gracias por darme la oportunidad de empezar mi formación como 'científico'.

A Martí Aldea y Carme Gallego, los 'Master and Commander del CYC'. Gracias por acogerme en vuestro grupo como uno más, y enseñarme a estirar la neurona.

A Eloi Garí por estar siempre dispuesto a resolver cualquier duda. Por enseñarme a hacer clonajes y por buscar la solución a cualquier problema técnico que surgiera.

A Neus Colomina, por su vitalidad, por "aquest Western és de llibre, de llibre!!" Ha sido muy gratificante trabajar a tu lado. Siempre dando ánimos. No me olvido de tus nenas: Emma y Núria. Qué buenos momentos hemos pasado juntos! Cuando llegaban al Lab lo revolucionaban totalmente; y a mí, la verdad, es que me gustaba engrescarlas con actividades como ir a robar material de vidrio a la primera planta y demás actividades truculentas, je,je,je,je ...

A Serafí y Rose, mis grandes amigos. Hemos forjado una gran amistad. Estoy y estaré eternamente agradecido por acogerme en vuestra casa durante ocho meses cuando me exilié a Londres. Me acogisteis como un hermano! Para mi aquello fue muy importante, ya lo sabéis. Recuerdo aquellas caminatas enormes por London en las que me sacabais a pasear y las compras compulsivas en el Morrison en las el 70% eran cosas tan imprescindibles como galletas, chocolate, pizzas y cakes… Hicisteis que mi estancia de trabajo fuera como unas vacaciones en familia. Thanks guys!!

A Sònia Rius, mi fiel amiga. Por no cambiar nunca y por ser como eres, íntegra y leal. A parte de tu amistad, valoro tu gran profesionalidad y tu manera metódica y ordenada de trabajar en el Lab. Te admiro por ello! Siempre estás dispuesta a ayudarme, no importa lo ocupada que estés. Tu amistad ha hecho que los días arduos fueran más llevaderos. Gracias Susi!

A Sera y Sònia, nuevamente, por todo lo que hemos compartido juntos como grupo y lo que está por venir. Por las interminables "asambleas", comidas y cenas. Por las escapadas de desconexión. Por estar siempre ahí cuando nos hemos necesitado. Por las charlas de friki series y friki pelis en general. Habéis sido un gran apoyo. GRACIAS!

A Fangoria, Depeche mode, The Lord of the Rings BSO soundtrack, al enigmático CD popurrí de los viernes y a la colección de flamenco jondo. Habéis sido mis fieles compañeros durante estos años de interminables horas de laboratorio. Suerte de estas playlists llenas de energía y ritmo que sonaban una y otra vez en el Lab a todo volumen.

A Marta Rafel, la Marteta. Mi hermana mayor del laboratorio. Por todo lo que hemos compartido en el Lab y fuera de él. Por las interminables horas de gabinete de crisis que teníamos. Por los "pita-pita-puta-mura!", los "just to imagine!" y los "lost to the river!" Qué no se nos olviden muestras escapadas a la máquina de gorrinadas a media tarde! je,je,je, Dios, hemos ingerido una cantidad de bollería espantosa; pero lo volvería a hacer con sumo gusto. Lo que nos hemos reído y lo bien que nos lo hemos pasado.

To Galal, my friend. We spent a great time in the lab and living together. We built up such a nice friendship. I wish you all the best!

A Inma Montoliu. Por tu amistad y la ayuda que me ofreciste estando en el CYC. Por tu vitalidad arrolladora y tu forma de ser. Siempre tendrás un rinconcito en mi corazón.

A los mindundis del CYC, los presentes y pasados, que han sido unos cuantos. Por los buenos y malos momentos. Por las escapadas semanales al chinaco de turno (verdad Sera, Sonia y Marta?) Dios, lo bien que nos lo pasábamos! Sería el exceso de glutamato? … Por las comilonas de navidad en la que forma compulsiva montábamos una mega mesa en la que no faltaba de nada y comíamos hasta reventar múltiples platos seguidos de postres, turrones, polvorones y demás delicias culinarias. Y los carnavales! Si, habéis leído bien! Por crear la tradición de disfrazarse de las temáticas más inverosímiles y liarla parda por todo el CMB. Y pensar que a mí no me gustaba disfrazarme…

A Enric Herrero por darme la posibilidad de empezar como 'mindundi de prácticas' mientras estudiaba medicina y permitirme integrarme en tu laboratorio como un miembro más. He tenido el gran privilegio de trabajar contigo y tenerte como profesor. Sin olvidarme de todas las veces que me has ayudado con nuestro amigo común, *S. cerevisiae.*

A Felip Vilella, mi querido amigo. Por aceptarme los veranos como 'tu niño de prácticas'. Tú estimulaste mi agrado por la ciencia y el laboratorio. Eres mi modelo a seguir: currante como el que más, meticuloso y perfeccionista. Recuerdo cuando me pasabas los protocolos con la teoría y me los explicabas con gran entusiasmo y dedicación. Aquel verano fue el inicio de mi carrera científica, aunque sólo era un mindundín.

A Lidia Piedrafita, mi Mami del CMB. Qué decirte que no sepas.? Admiro muchísimo tu amistad y tu profesionalidad. De hecho, no sé si te acordarás, pero hicimos juntos mi primer Western. Dios, que proeza! Llegar al Lumi y ver bandas fue lo más! En todos estos años he tenido el privilegio de aprender muchísimo de ti tanto en el terreno personal como profesional.

A Anna Casanovas por tu desbordante entusiasmo. Aún recuerdo la primera clase de Neuroanatomía de segundo de Medicina, la facilidad con la que trasmitías los conceptos y tu pasión por la docencia. No la pierdas nunca! Si un día me dedicara a la docencia, me gustaría tener tu vitalidad y dedicación.

A Luís Aragón. Por darme la oportunidad de hacer una estancia breve versión extendida en tu laboratorio. Por mostrar una gran motivación en los proyectos que estamos llevando a cabo y por proponerme nuevos retos a diario.

To Jon Baxter. For being so patient with me and teaching me all I know about topology. We had such a great time talking about DNA topology and Smc5/6. I really enjoyed that. I learned so much from you. Thanks!

I would like to say thanks to all members of the cell cycle group in London, especially to Joanne Leonard, Nick Sen, Raúl Torres, Ale Canteli, Glòria Palou, Charlotte Mikura, Jonay and Adam Jarmuz for being so nice with me and making me feel like being at home. We are building such a good friendship! Joanne, thanks for the critical reading of my manuscript. I really appreciate your effort,dedication and friendship.

A mis padres
A mi hermano

Abstract

Mitotically growing cells devote most efforts to accurately duplicate and transmit their chromosomes to daughter cells. Precise delivery requires the assembly of protein connections to pair replicated sister chromatids; but also the removal of DNA joint molecules that link them, including recombination intermediates and ongoing DNA replication forks. The individual action of several enzymes, including resolvases and dissolvases, is capable of removing such structures.

The Structural Maintenance of Chromosomes (SMC) Smc5/6 complex has a poorly understood function in chromosome repair and segregation. In this study, we show that the dissolution of DNA-mediated connections requires the Smc5/6 complex. *smc5/6* mutants fail to remove chromosome linkages, leading to gross chromosome segregation defects. Besides, we show that these connections are mainly due to the accumulation of recombination intermediates and replication forks, and are not mediated by catenanes. The accumulation could be either due to upregulation of junction formation, or to defects in their removal. To discern between these two possibilities, we have designed an assay to restore Smc5/6 function after induction of chromosome linkages. Our assay demonstrates that the Smc5/6 complex is capable of promoting chromosome disjunction in metaphase-arrested cells, thus restoring chromosome segregation. The Smc5/6 complex is also the docking site for a SUMO E3 ligase, a feature that highlights its potential signalling skills. However, it is unknown how this E3 ligase is regulated. Our initial characterization of the lysines targeted by SUMO suggests that Smc5 SUMOylation is required for its recruitment to sites of DNA damage and proper DNA repair. The activity of the SUMO ligase is induced in response to DNA damage, a phenomenon that requires the presence of an active homologous recombination pathway. Our results also show that the SUMO ligase domain is required for chromosome disjunction, and indicate that the Smc5/6-Mms21 complex operates as a giant SUMO ligase, requiring all of its sub-complexes for its E3 activity *in vivo*. Moreover, we show that Mms21-dependent SUMOylation requires the ATPase function of the complex, a step that is part of the ligase mechanism that assists Ubc9 function.

Consequently, we propose that the structural maintenance of chromosomes function and the SUMO ligase activity of the Smc5/6 complex cooperate in the removal of chromosome junctions, to prevent chromosome missegregation and aneuploidy, and to ensure the maintenance of the genome integrity.

Resumen

Las células dedican la mayor parte de su esfuerzo a duplicar y transmitir con precisión sus cromosomas a las células hijas. La precisa distribución requiere el ensamblaje de conexiones proteicas para emparejar las cromátidas hermanas replicadas; pero también la eliminación de estructuras de ADN que las unen, incluyendo los intermediarios de recombinación y horquillas de replicación. La acción individual de varias enzimas, incluyendo "resolvasas" y "disolvasas", es capaz de eliminar tales estructuras.

El complejo de mantenimiento estructural de los cromosomas (SMC) Smc5/6 tiene una función pobremente entendida en la reparación y segregación de cromosomas. En este estudio, mostramos que la disolución de conexiones mediadas por ADN requiere el complejo Smc5/6. Los mutantes del complejo Smc5/6 presentan fallos en la resolución de uniones cromosómicas, lo que provoca una mala segregación. Además, mostramos que estas conexiones se deben principalmente a la acumulación de intermediarios de recombinación y a horquillas de replicación, y no por encadenados. Esta acumulación puede ser debida a un incremento en la formación de uniones entre cromátidas hermanas o a un defecto en su eliminación. Para discernir entre ambas posibilidades, diseñamos un ensayo para restaurar la función Smc5/6 después de la inducción de uniones en los cromosomas. Éste demuestra que el complejo Smc5/6 es capaz de promover la disolución de estas uniones en células paradas en metafase, restaurando así la segregación cromosómica. El complejo Smc5/6 es también el sitio de acoplamiento para una SUMO E3 ligasa, hecho que le confiere una posible función señalizadora. Sin embargo, se desconoce cómo se regula dicha actividad. Nuestra caracterización inicial de las lisinas diana por SUMOilación sugiere que la SUMOilación de Smc5 es necesaria para su reclutamiento a los sitios de daño en el ADN y para su adecuada reparación. La actividad de la SUMO ligasa se induce en respuesta a daño en el ADN, un fenómeno que requiere la presencia de una vía de recombinación homóloga activa. Nuestros resultados también muestran que el dominio SUMO ligasa es necesario para la segregación cromosómica, e indican que el complejo Smc5/6-Mms21 funciona como una SUMO ligasa gigante, que requiere todos sus subcomplejos para su actividad E3 *in vivo.* Por otra parte, mostramos que la SUMOilación dependiente de Mms21 requiere la función ATPasa del complejo, un paso que es parte del mecanismo que ayuda a la función de Ubc9.

En consecuencia, proponemos que la función del complejo Smc5/6 y la actividad SUMO ligasa de Mms21 cooperan en la eliminación de las uniones cromosómicas, para evitar la segregación incorrecta de cromosomas y posibles aneuploidías, asegurando el mantenimiento de la integridad del genoma.

Resum

Les cèl·lules dediquen la major part dels esforços a duplicar i transmetre amb precisió els seus cromosomes a les cèl·lules filles. La precisa distribució requereix l'assemblatge de connexions proteiques per aparellar les cromàtides germanes replicades; però també l'eliminació d'estructures d'ADN que les uneixen, incloent els intermediaris de recombinació i forquilles de replicació. L'acció individual de diversos enzims, incloent "resolvases" i "disolvases", és capaç d'eliminar aquestes estructures.

El complex de manteniment estructural dels cromosomes (SMC) Smc5/6 té una funció pobrament entesa en la reparació i segregació dels cromosomes. En aquest estudi, mostrem que la dissolució de connexions mitjançades per ADN requereix el complex Smc5/6. Els mutants del complex Smc5/6 presenten errors en la resolució d'unions cromosòmiques, fet que provoca una mala segregació. A més, mostrem que aquestes connexions es deuen principalment a l'acumulació d'intermediaris de recombinació i a forquilles de replicació, i no per encadenats. Aquesta acumulació pot ser deguda a un increment en la formació d'unions entre cromàtides germanes o a un defecte en la seva eliminació. Per diferenciar entre ambdues possibilitats, vam dissenyar un assaig per restaurar la funció Smc5/6 després de la inducció d'unions en els cromosomes. Aquest demostra que el complex Smc5/6 és capaç de promoure la dissolució d'aquestes unions en cèl·lules aturades en metafase, restaurant així la segregació cromosòmica. El complex Smc5/6 és també el lloc d'acoblament per a una SUMO E3 lligasa, fet que li confereix una possible funció senyalitzadora. No obstant això, es desconeix com es regula aquesta activitat. La nostra caracterització inicial de les lisines diana per SUMOilació suggereix que la SUMOilació de Smc5 és necessària per al seu reclutament als llocs de dany en l'ADN i per a la seva adequada reparació. L'activitat de la SUMO lligasa s'indueix en resposta a dany en l'ADN, un fenomen que requereix la presència d'una via de recombinació homòloga activa. Els nostres resultats també mostren que el domini SUMO ligasa és necessari per a la segregació cromosòmica, i indiquen que el complex Smc5/6-Mms21 funciona com una SUMO lligasa gegant, que requereix tots els seus sub-complexes per a la seva activitat E3 *in vivo*. D'altra banda, mostrem que la SUMOilació dependent de Mms21 requereix la funció ATPasa del complex, un pas que és part de la mecanisme que ajuda a la funció de Ubc9.

En conseqüència, proposem que la funció del complex Smc5/6 i l'activitat SUMO ligasa de Mms21 cooperen en l'eliminació de les unions cromosòmiques, per evitar la segregació incorrecta dels cromosomes i possibles aneuploïdies, assegurant el manteniment de la integritat del genoma.

Table of contents

Acknowledgments 7
Abstract 13
Resumen 15
Resum 17
Table of contents 19
List of Figures 23
List of Tables 25
List of abbreviations 27

1. Introduction 29

1.1. The *S. cerevisiae* cell cycle 31
1.1.1. Overview 31
1.1.2. Chromosome replication 33
1.1.3. Chromosome condensation 35
1.1.4. Chromosome segregation 36

1.2. DNA damage response and repair 37
1.2.1. DNA replication checkpoint 37
1.2.2. DNA damage repair mechanisms 40
1.2.3. Double-strand break repair 42
1.2.4. Processing of recombination intermediates 44
1.2.5. DNA damage tolerance 45

1.3. SMC complexes 47
1.3.1. The cohesin complex 48
1.3.2. The condensin complex 50
1.3.3. The Smc5/6 complex 50
1.3.3.1. Localisation of the Smc5/6 complex 51
1.3.3.2. The Smc5/6 complex and DNA damage repair 52
1.3.3.3. The role of the Smc5/6 complex in DSB repair 53
1.3.3.4. The Smc5/6 complex and the segregation of the rDNA locus 56
1.3.3.5. The Smc5/6 complex and telomere function 57
1.3.3.6. The Smc5/6 complex and chromosome cohesion 59
1.3.3.7. The role of the Smc5/6 complex in chromosome topology 59
1.3.3.8. The Smc5/6-mediated SUMOylation and genome stability 60

1.4. SUMOylation 61
1.4.1. The SUMOylation cycle 61
1.4.1.1. SUMO conjugation 61
1.4.1.2. SUMO deconjugation 62
1.4.2. The consensus motifs for SUMO conjugation 63
1.4.3. Molecular consequences of SUMOylation 65

2. Objectives 67

3. Materials and methods 71

3.1. *S. cerevisiae* strains and general yeast methods 73
3.1.1. *S. cerevisiae* strains 73
3.1.2. Media 78
3.1.3. Yeast growth conditions 79
3.1.4. Competent yeast cell preparation 79
3.1.5. Yeast cell transformation 79
3.1.6. Genomic integration for protein tagging or gene deletion 80
3.1.7. Phenotype analysis by growth test on plates 80
3.1.8. Cell cycle synchronizations 80

3.2. General bacterial methods 81
3.2.1. Plasmids 81
3.2.2. Bacteria growth conditions 81
3.2.3. *DH5α* competent cell transformation 82
3.2.4. *MCD1061* competent cell transformation 82
3.2.5. Positive clone selection by ‘plasmid jet-prep’ 82

3.3. Cytological methods 83
3.3.1. Yeast fixation for microscopy 83
3.3.2. Optical and fluorescence microscopy 83
3.3.3. Flow cytometry analysis 83

3.4. DNA methods 84
3.4.1. Primers 84
3.4.2. Isolation of plasmid DNA from *E. coli* 87
3.4.3. Isolation of genomic DNA from *S. cerevisiae* 71
3.4.4. Polymerase chain reaction (PCR) 88
3.4.5. Yeast colony PCR 88
3.4.6. Site-directed mutagenesis 88
3.4.7. DNA restriction analysis 89
3.4.8. Separation of DNA fragments by gel electrophoresis 89
3.4.9. Purification of DNA fragments from agarose gels 89
3.4.10. Ligation of DNA fragments 89
3.4.11. DNA sequencing 90
3.4.12. Chromatin Immunoprecipitation 90
3.4.13. Real time PCR analysis 91
3.4.14. Pulsed field gel electrophoresis 91
3.4.15. DNA combing 92
3.4.16. 2D gels for X-shaped DNA molecule detection 92
3.4.17. 2D gels for catenated plasmid detection 93
3.4.18. Southern blot 94

3.5. Protein methods 95
3.5.1. Protein extraction under denaturing conditions 95
3.5.2. Post alkaline protein extraction 95
3.5.3. SUMO and SUMO-conjugates purification 95
3.5.4. Co-immunoprecipitation 96
3.5.5. Protein chromatin-binding assay 97
3.5.6. SDS-PAGE 97
3.5.7. Coomassie staining 98
3.5.8. Western blot 98

4. Results 101
4.1. The role of the Smc5/6 complex in sister chromatid disjunction 103
4.1.1. *smc5/6* mutants are hypersensitive to MMS 103
4.1.2. Bulk replication fork progression is not impaired in *smc5/6* mutants 104
4.1.3. An MMS pulse does not affect S phase progression in wild type cells 107
4.1.4. *smc5/6* mutant cells undergo aberrant mitosis after an MMS pulse 108
4.1.5. *smc5/6* mutant cells accumulate replication and recombination intermediates after an MMS pulse 113
4.1.6. Suppression of SCJ formation is beneficial in *smc5/6* mutants 117
4.1.7. Smc6 promotes resolution of SCJs 120

4.2. Characterization of the Nse2 SUMO ligase activity regulation 123
4.2.1. Detection of SUMOylated proteins *in vivo* 123
4.2.2. Several subunits of the Smc5/6 complex are SUMOylated in an Nse2-dependent manner 124
4.2.3. Nse2 binding to Smc5 is essential for viability and required for the Smc5/6 complex SUMOylation 127
4.2.4. The Ubc9 fusion-directed SUMOylation suppresses the phenotype of the *nse2ΔC* mutant 130
4.2.5. Nse2-mediated SUMOylation requires an active and intact Smc5/6 complex 132
4.2.6. Esc2 promotes the SUMO ligase activity of Nse2 141
4.2.7. The ATPase function of Smc5 is required for the Nse2-dependent SUMOylation 142

4.3. Characterization of the Smc5/6 complex SUMOylation in response to DNA damage 146
4.3.1. The DNA damage checkpoint in not required for the MMS-induced SUMOylation of Smc5 146
4.3.2. SCJ formation activates the Nse2-dependent SUMOylation 147

4.4. Identification of the SUMOylation sites of Smc5 149
4.4.1. Smc5 is not SUMOylated at the Ubc9 consensus sites 149
4.4.2. Smc5 is SUMOylated in both coiled-coils 150

4.5. The role of the Smc5/6 complex in replisome swivelling 155
4.5.1. *top2-td* mutant cells accumulate catenated plasmids 155
4.5.2. Catenane distribution is not altered in *smc6-9* mutant cells 158
4.5.3. Catenane distribution is not impaired in *smc6-56* mutant cells 161
4.5.4. *smc5-4* mutant cells accumulate more catenanes 162

5. Discussion 165
5.1. The role of the Smc5/6 complex in sister chromatid disjunction 167
5.1.1. *smc5/6* mutants are able to complete bulk DNA replication when replicating in the presence of MMS 167
5.1.2. An MMS pulse allowed characterizing the genome-wide segregation problems in *smc5/6* mutant cells 168
5.1.3. *smc5/6* mutants accumulate replication and recombination intermediates after an MMS pulse 169
5.1.4. The Smc5/6 complex has a role in resolution of SCJs 170
5.1.5. How does the Smc5/6 complex resolve SCJs? 171

5.2. Characterization of the Nse2 SUMO ligase activity regulation 172
5.2.1. Nse2 docking to Smc5 is required for the Smc5/6 complex SUMOylation and DNA damage repair 172
5.2.2. The phenotype of *nse2ΔC* mutant cells is suppressed by its fusion to Ubc9 174
5.2.3. Nse2-mediated SUMOylation requires an active and intact Smc5/6 complex 174
5.2.4. Esc2 promotes the SUMO ligase activity of Nse2 176
5.2.5. The ATPase function in Smc5 is required for Nse2-dependent SUMOylation 177
5.2.6. How could Nse2 sense ATP binding by Smc5? 178

5.3. Characterization of the Smc5/6 complex SUMOylation in response to DNA damage 179

5.4. Identification of the Smc5 SUMOylation sites 180

5.5. The role of the Smc5/6 complex in chromosome topology 181

6. Conclusions 187

7. Reference List 189

List of figures

Introduction

Figure 1. *S. cerevisiae* cell cycle 31
Figure 2. Topological transitions at the fork 34
Figure 3. Chromosome condensation 35
Figure 4. The S-phase checkpoint response 39
Figure 5. DNA damage and the associated DNA repair pathways 41
Figure 6. DSB repair pathways 43
Figure 7. Processing of Holliday junctions 45
Figure 8. The postreplicational repair pathway 46
Figure 9. The architecture of SMC proteins 47
Figure 10. The role of the Smc5/6 complex in DSB repair 55
Figure 11. DNA repair in the rDNA locus in *S. cerevisiae* 57
Figure 12. The role of the Smc5/6 complex in telomeres 58
Figure 13. The SUMO cycle 63
Figure 14. SUMO consensus motifs 64

Results

Figure 16. *smc5/6* mutants are hypersensitive to MMS 104
Figure 17. Bulk replication fork progression is not affected in *smc5/6* mutants 105
Figure 18. *smc6-9* and *smc6-1* mutants accumulate sister chromatid junctions when replicating in the presence of MMS 106
Figure 19. Cell cycle progression is not impaired by an MMS pulse in wild type cells 107
Figure 20. *smc5/6* mutant cells undergo aberrant mitosis after an MMS pulse 110
Figure 21. *smc6-9* mutant cells fail to segregate centromeric sequences after an MMS pulse 111
Figure 22. *smc6-9* mutant cells show an activation of the DNA damage checkpoint in the second cell cycle after an MMS pulse 112
Figure 23. *smc5/6* mutants accumulate DNA-mediated structures after an MMS pulse 114
Figure 24. *smc5/6* mutants accumulate protein/topological-independent linkages after an MMS pulse 115
Figure 25. *smc6* mutant cells accumulate SCJs and unfinished replication intermediates after an MMS pulse 116
Figure 26. Homologous recombination has a negative effect in *smc5/6* mutants 118
Figure 27. Blocking the template switch pathway is beneficial in *smc6-9* mutants 119
Figure 28. Smc6 promotes SCJs resolution *in vivo* 120
Figure 29. *SMC6* reactivation increases chromosome resolution in a PFG 121
Figure 30. *SMC6* reactivation prevents nuclear missegregation after an MMS pulse 122
Figure 31. Strategy for purification of SUMO-conjugated proteins 123
Figure 32. Several subunits of the Smc5/6 complex are SUMOylated and the SUMOylation increases in response to MMS 124
Figure 33. The SUMOylation of Smc5, Smc6 and Nse4 are Nse2-dependent 125
Figure 34. Nse2 degradation decreases the SUMOylation levels of Smc5/6 127

Figure 35. The Nse2 docking to Smc5 is essential for viability and required for Smc6 SUMOylation 128
Figure 36. *nse2ΔC* mutant cells are sensitive to MMS 130
Figure 37. The Ubc9 fusion-directed SUMOylation suppresses the phenotype of the *nse2ΔC* mutant 131
Figure 38. The SUMO ligase activity of Nse2 is reduced when the Nse3 docking to Smc5 is impaired 133
Figure 39. The SUMO ligase activity of Nse2 is affected when the Nse5 docking to Smc5 is impaired 135
Figure 40. A functional *SMC6* is required for the activation of Nse2 137
Figure 41. The degradation of Nse4, Nse5 and Nse6 decreases the SUMOylation levels of the Smc5 139
Figure 42. The SUMOylation of the cohesin complex is affected when the integrity of the Smc5/6 complex is compromised 140
Figure 43. The Smc5 SUMOylation is affected in *esc2* null cells 142
Figure 44. The ATPase function of the Smc5/6 complex is required for activation of the Nse2 SUMO ligase 143
Figure 45. *smc5-K75I* is not SUMOylated in Nse2-Ubc9 cells 145
Figure 46. The MMS-induced SUMOylation of Smc5 is not controlled by Mre11, Mec1 or Rad53 146
Figure 47. Homologous recombination is required for the MMS-induced SUMOylation of Smc5 147
Figure 48. Replication fork collapse in HU activates the SUMO ligase activity of Nse2 148
Figure 49. Smc5 is not SUMOylated at the Ubc9 consensus sites 150
Figure 50. The *smc5-K-all-*R mutant is lethal 151
Figure 51. Strategy used to generate *smc5-single-domain-K-*R mutants 152
Figure 52. Smc5 is SUMOylated in both coiled-coils 153
Figure 53. The recruitment of *smc5(cc1,2 K-R)* to DSB is impaired 154
Figure 54. Top2 depletion provokes accumulation of catenated dimers 156
Figure 55. Visualization of catenated dimers by 2D gel electrophoresis 157
Figure 56. Catenane distribution is not impaired in *smc6-9* mutant cells in a *top2-td* background 159
Figure 57. Catenane distribution is not impaired in *smc6-9* mutant cells in a *top2-4* background 160
Figure 58. Catenane distribution is not impaired in *smc6-56* mutant cells 162
Figure 59. *smc5-4* mutant cells show a higher accumulation of catenanes 163

List of tables

Table 1. Strains used in this study 73

Table 2. Plasmids used in this study 81

Table 3. Primers used in this study 84

Table 4. Antibodies used in this study 99

Table 5. Nuclear segregation phenotype after an MMS pulse 108

List of abbreviations

aa	aminoacids
ADN	ácido desoxirribunucleico
ALT	alternative lengthening of telomeres
APC	anaphase promoting complex
ARS	autonomously replicating sequence
BER	base excision repair
BIR	break induced replication
bp	base pair
Cdk	cyclin-dependent kinase
CEN	centromere
CFP	cyan fluorescent protein
cm	centimetre
CPD	cyclobutane pyrimidine dimers
dHJ	double Holliday junction
DNA	deoxyribonucleic acid
dNTP	deoxynucleotide tri-phosphate
DSB	double-strand break
dsDNA	double-stranded DNA
FACS	fluorescence-activated cell sorting
GCR	gross chromosomal rearrangement
GFP	green fluorescent protein
h	hour
HJ	Holliday junction
IR	ionizing radiation
JM	joint molecule
kb	kilobases
LOH	loss of heterozygosis
M	molar
mA	milliampere
min	minute
ml	millilitre
mM	millimolar
MMEJ	microhomology-mediated end joining
MMR	mismatch repair
MMS	methyl methansulphonate
NDSM	negatively charged amino acid-dependent SUMO motif
NER	nucleotide excision repair
ng	nanogram
NHEJ	non-homologous end joining
nm	nanometre
Nse	non-SMC element
º	degree
ºC	degree Celsius
OD_{600}	optical density measured at 600 nanometres-wavelength
PCNA	proliferating cell nuclear antigen
PCR	polymerase chain reaction

PDSM	phosphorylation-dependent SUMO motifs
PFGE	pulsed-field gel electrophoresis
PIAS	protein inhibitor of activated STAT
PML	promyelocytic leukaemia
Pol	DNA polymerase
Pre-RC	pre-replicative complex
PRR	postreplication repair
rDNA	ribosomal DNA
RER	ribonucleotide excision repair
RFC	replication factor C
RPA	replication protein A
rpm	revolution per minute
s	second
SAC	spindle assembly checkpoint
SC	synthetic complete
SCC	sister chromatid cohesion
SDSA	synthesis-dependent strand annealing
SENP	sentrin-specific protease
SIM	SUMO-interacting motif
SMC	structural maintenance of chromosomes
SPB	spindle pole body
SSA	single strand annealing
ssDNA	single-stranded DNA
STUBL	SUMO-targeted ubiquitin ligase
SUMO	small ubiquitin-like modifier
TLS	translesion synthesis
tRNA	transfer RNA
TS	template switch
U	units
UV	ultraviolet
V	volts
v/v	volume/volume
w/v	weight/volume
αF	α-factor
μg	microgram
μl	microliter
μM	micromolar

INTRODUCTION

1.1. The *S. cerevisiae* cell cycle

1.1.1. Overview

The eukaryotic cell cycle is a sequence of biological events that allow one cell to grow and divide into two daughter cells. It is controlled by the specific coordination of many proteins and deregulation of this complicated cycle has been implicated in a wide variety of human diseases, such as cancer. The complex molecular machinery that coordinates all cell cycle events is highly conserved among eukaryotes. Since its discovery, much of the work has been conducted in fission and budding yeast. The availability of the complete genome sequence (Goffeau et al., 1996), together with ease in genetic manipulation and fast growth rate under laboratory conditions make the budding yeast, *Saccharomyces cerevisiae,* an ideal model organism for cell cycle studies.

The cell cycle involves the cyclical progression through four phases: G1 (Gap 1), S (Synthesis), G2 (Gap 2) and M (Mitosis) (see Figure 1). Progression through the eukaryotic cell cycle is controlled by the cyclins and the cyclin-dependent kinases (Cdks). Importantly, the three major classes of cyclins, called G1/S, S, and M cyclins, whose activity is highly regulated (Bloom and Cross, 2007), oscillate during the cell cycle to generate a series of cyclin-Cdk complexes that are abruptly switched on at specific cell-cycle transitions; phosphorylating numerous substrates required for progression through the cell cycle.

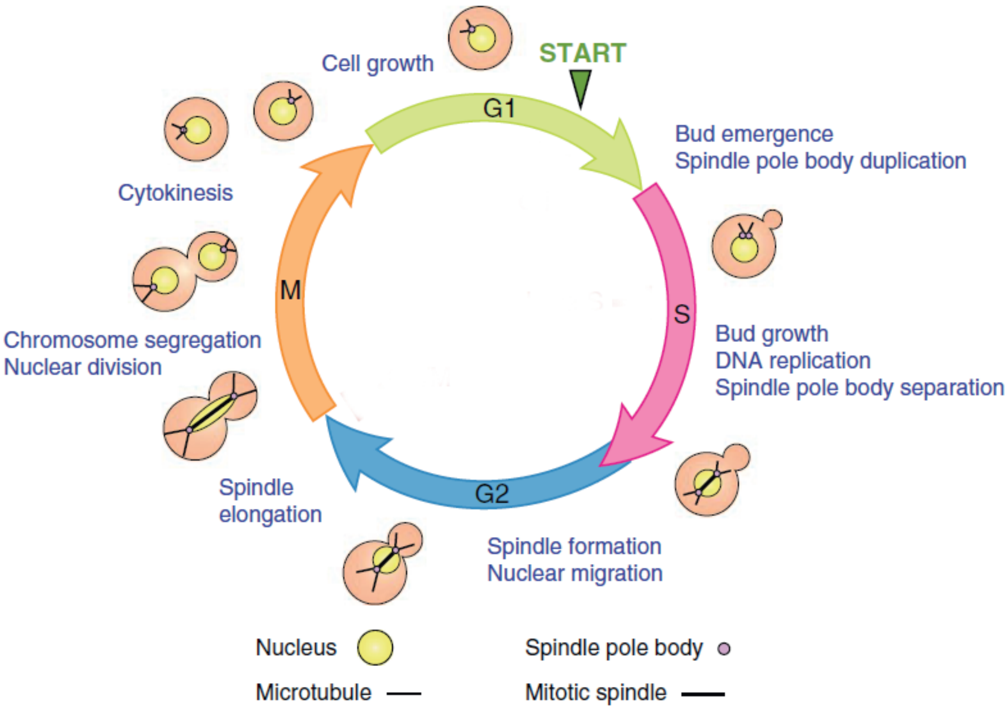
Cell growth
START
G1
Bud emergence
Spindle pole body duplication
S
Bud growth
DNA replication
Spindle pole body separation
G2
Spindle formation
Nuclear migration
Spindle elongation
Chromosome segregation
Nuclear division
M
Cytokinesis
Nucleus
Spindle pole body
Microtubule
Mitotic spindle

Figure 1. *S. cerevisiae* **cell cycle**

The budding yeast cell cycle, illustrating the specific cellular morphologies at each cell cycle stage. Figure taken from Finn et al., 2012.

In G1, a high rate of protein synthesis increases cell size and mass until budding yeast cells reach the restriction point, or START. In order to decide whether to enter the cell cycle and to divide or not, cells integrate external signals such as the availability of nutrients and the presence of mating pheromones. Under nutrient-restrictive or starvation conditions, cells typically arrest growth and enter a quiescent state called G0. Otherwise, cells may undergo cell division. Several internal signals, such as cell size, growth rate, different forms of cell stress, and the presence of DNA damage can also block the passage through START in budding yeast (Dirick et al., 1995). When budding yeast cells enter the cell cycle, the spindle pole body (SPB) duplicates in late G1 (Jaspersen and Winey, 2004) and the actin filaments start to assembly to form the bud (Pruyne and Bretscher, 2000). During this period, post-Golgi secretory vesicles, and cargo containing membrane-bound organelles also travel along the actin cables to deliver organelles such as vacuoles, mitochondria, late Golgi complexes, and peroxisomes to the daughter cell (Fagarasanu et al., 2010; Pruyne et al., 2004). The next stage, S phase, is devoted to DNA synthesis. During this phase, cohesion is established between newly born sister chromatids, and kinetochores are assembled at the centromeres in preparation for the chromosome segregation (Hirano, 2000; Tanaka et al., 2005). In *S. cerevisiae*, the start of M phase overlaps with the end of S phase because mitotic spindle assembly begins in late S phase (Forsburg and Nurse, 1991). When cells sense the correct signals, they progress to the final phase of the cycle where chromosomes are pulled apart by the action of the mitotic spindle (mitosis). Finally, the cytoplasm is split into two (cytokinesis) and septation occurs to seal the bud neck, releasing the daughter cell (Westhorpe and Straight, 2013).

The order and timing of critical cell cycle transitions requires the presence of surveillance mechanisms, collectively known as checkpoints, that implement any necessary delay in cell cycle progression until the problem is solved. These delays provide time to resolve the problems, thereby preventing any unwanted consequences (Cooper, 2006). In that sense, elimination of checkpoints may increase the susceptibility of the cell to environmental perturbations and genome instability. Whereas wild type cells are able to induce a cell cycle delay under stress conditions, checkpoint mutants progress to the next stage (Hartwell and Weinert, 1989). There are several cell cycle checkpoints in eukaryotic cells. The first of these encountered is the START checkpoint, located at the G1/S transition, and passage through this commits cells to division. As previously described, it is regulated by cell growth and protein synthesis levels: in the absence of nutrients, or in the presence of mating pheromones, cells are not allowed to enter the cell cycle (Hartwell et al., 1974). The next major checkpoint is the DNA damage checkpoint, which ensures that DNA replication is successfully completed and the genome is ready for mitosis, and its activation provides a delay to allow the DNA repair machinery to resolve the damage. The details of this checkpoint will be discussed in more detail below. The final major checkpoint is located at the metaphase to anaphase transition and is referred to as the spindle assembly checkpoint (SAC). The role of this checkpoint is to delay anaphase entry until all kinetochores are properly attached to microtubules. Treating cells with a microtubule-depolymerizing drug, such as nocodazole, can artificially trigger this checkpoint (Foley and Kapoor, 2013).

1.1.2. Chromosome replication

DNA replication, which is a tightly regulated process, initiates from multiple different sites throughout the genome called origins of replication. These sites in *S. cerevisiae* have a specific sequence known as autonomously replicating sequences (ARS). However, other organisms have more relaxed DNA sequence requirements for initiation (Kearsey and Cotterill, 2003). In metazoans, they are placed into initiation zones or clusters, which are activated at different moments during DNA replication (Gilbert, 2007; Jackson and Pombo, 1998).

The first step is the assembly of the pre-replicative complex (pre-RC) at the origin of replication which includes the binding of numerous proteins including the origin recognition complex 1-6 (ORC1-6) (Bell and Stillman, 1992; Gavin et al., 1995), cell division cycle 6 (Cdc6) and chromatin licensing and DNA replication factor 1 (Cdt1) to DNA; followed by the recruitment of the mini-chromosome maintenance (MCM2-7) complex, which is the active replicative helicase (Mendez and Stillman, 2003). Replication is then initiated in early S phase when Sld2 and Sld3 are phosphorylated by the S phase Cdk and the Cdc7-Dbf4 kinase complex (also known as Dbf4-dependent kinase (DDK)) (Krude et al., 1997; Lei et al., 1997). Their phosphorylation allows them to interact with Dpb11, which in turn facilitates the loading of Cdc45 and the go-ichi-ni-san (GINS) complex. They have an essential role in origin firing and fork progression (Ilves et al., 2010; Mimura and Takisawa, 1998; Takayama et al., 2003). When the origin of replication fires, the MCM complex unwinds the parental strands leading to the eviction of nucleosomes ahead of the fork (Groth et al., 2007) and the GINS complex maintains protein-protein interactions within the replication complex (replisome) (Gambus et al., 2006; Labib et al., 2000; Pacek and Walter, 2004).

There are three DNA polymerases associated with the replisome, the polymerase α-primase and the replicative polymerases δ and ε, which replicate the lagging and leading strands, respectively. The replisome also contains accessory factors, such as the clamp proliferating cell nuclear antigen (PCNA; also known as Pol30 in *S. cerevisiae*), and the clamp loader replication factor C (RFC) (Stukenberg et al., 1991). DNA replication is semi-discontinuous due to the structure of DNA: there is a leading strand, on which DNA nucleotides are added to the initial primer, and a lagging strand, on which primers are synthesized and elongated throughout DNA synthesis forming the Okazaki fragments. RFC and PCNA regulate the polymerase switch (Stukenberg et al., 1994), and are also required for the interaction of flap endonuclease-1 (FEN-1) and DNA ligase I, which process and seal the Okazaki fragments.

The unwinding of the double helix by the action of the replicative helicase complex induces a torsional stress that leads to the formation of positive supercoiling ahead of the fork (Alexandrov et al., 1999; Peter et al., 1998). This torsional stress is reduced by the action of topoisomerase 1 (Top1), a Type I topoisomerase that can alter supercoiling by making single-strand breaks, allowing the uncut strand to pass through the break before resealing the nick (Wang, 2002); see Figure 2). Since each topoisomerase molecule needs around 150 base pair (bp) to bind to DNA (Bates and Maxwell, 1989), the accessibility of topoisomerases to DNA could be impaired when two forks approach one another in replication termination. This could lead to the accumulation of positive supercoiling ahead of the forks, jeopardizing the replication process. However, if the replication fork were free to rotate along the axis of the DNA helix, the torsional stress in front of the fork could diffuse through the replication fork and redistribute both ahead and behind the fork. This replisome swivelling would generate intertwinings in the sister chromatids in its wake (Postow et al., 2001; Wang, 2002). These intertwinings, which are called precatenanes (Peter et al., 1998), need to be removed before chromosome segregation by the action of topoisomerase 2 (Top2), an enzyme that introduces transient double-strand breaks in a DNA double helix, through which it passes a segment of uncut DNA before resealing the break resolving catenations (Lucas et al., 2001; Zechiedrich et al., 1997) (see Figure 2).

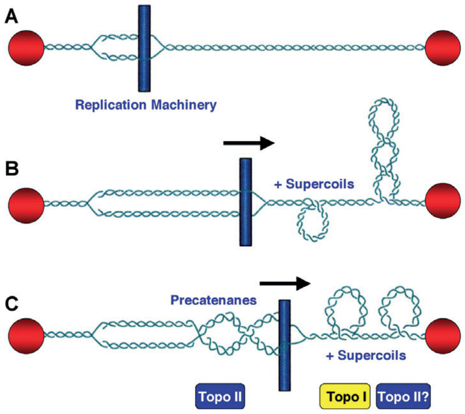

Figure 2. Topological transitions at the fork

Model for topoisomerase function and topological stress associated with DNA replication. The replication machinery is represented by a rod moving through the double helix. DNA ends are anchored to hypothetical immobile structures existing in the nucleus. a) upon initiation of DNA replication, the two strands of duplex DNA are separated, and the replication fork is formed. b) movement of the replication machinery through the immobilized DNA template strands induces acute overwinding (i.e. positive supercoiling) ahead of the fork.) if the replisome rotates around the helical axis of the DNA, compensatory underwinding (i.e. negative supercoiling) behind the replication machinery allows some of the torsional stress in the prereplicated DNA to be translated to the newly replicated daughter molecules in the form of precatenanes. If these precatenanes are not resolved, they ultimately lead to the formation of catenated duplex daughter chromosomes. Topoisomerase I is proposed to work ahead of the replication fork to remove positive DNA supercoils, whereas topoisomerase II is proposed to work primarily behind the fork to remove precatenanes. Figure taken form McClendon et al., 2005.

1.1.3. Chromosome condensation

A diploid human cell contains about 2 m of DNA (Lander et al., 2001; Venter et al., 2001), which must be highly packaged into chromosomes before segregation. The question of how cells pack such big heavily charged polymers into a nucleus has puzzled scientists ever since the discovery of the structure of DNA in 1953 (Watson and Crick, 1953).

In eukaryotic cells, the basic level of DNA compaction is the nucleosome, which consists of a histone octamer containing two copies of each histone H2A, H2B, H3 and H4, around which 147 bp of DNA are wound in 1.7 left-handed super-helical turns (Luger et al., 1997). This conformation is referred to as 'beads on a string' due to its appearance under the electron microscope. Since the diameter of the nucleosome is 10 nm, this structure is also called the 10 nm fibre (see Figure 3). The DNA wrapping around histones neutralizes the negative charge of DNA (Fussner et al., 2011). The N-terminal tails of histone proteins, which extrude from the nucleosome (Luger et al., 1997), are subjected to a large variety of posttranslational modifications, including phosphorylation, acetylation, methylation, ubiquitination and SUMOylation. These modifications regulate the DNA-nucleosome interactions and the interaction between the nucleosome and other proteins and can thus influence chromatin composition and structure (Xu et al., 2009).

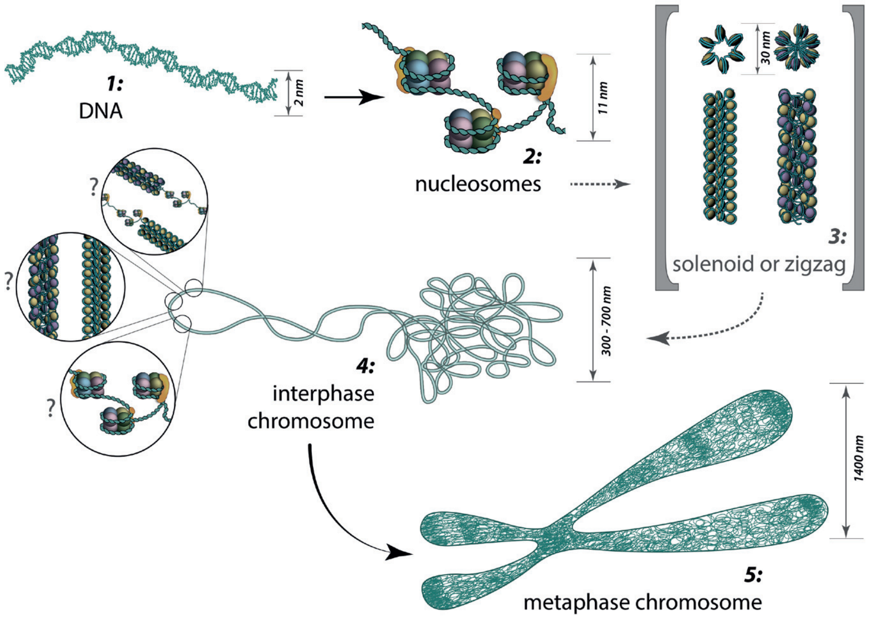

Figure 3. Chromosome condensation

DNA is wrapped around a histone octamer to form nucleosomes. Then, DNA forms into the 30 nm fibre through the presence of histone H1. Finally this fibre is further compacted into higher-order structures. Figure taken from MBInfo Wiki, Retrieved 5/8/2014 from http://www.mechanobio.info/figure/figure/1389944285515.jpg.html.

It has been proposed that the ‘beads on a string’ nucleosome array is then further coiled around itself to form a higher structure referred to as the 30 nm fibre. This structure requires the presence of histone H1 (Heermann, 2012). This conformation is the source of some controversy as a number of studies have failed to find evidence supporting its existence (Fussner et al., 2011; Fussner et al., 2012). When cells enter mitosis, chromosomes must be further condensed, resulting in the formation of mitotic chromosomes. Condensation ensures that chromosomes are small enough to be completely segregated in anaphase, thus preventing their cleavage during cytokinesis. The formation of mitotic chromosomes is a dynamic process, that requires the contribution of different proteins and complexes in constant exchange (Earnshaw and Laemmli, 1983), including cohesin, condensin (Hirano and Mitchison, 1994), Top2 (Earnshaw et al., 1985; Lewis and Laemmli, 1982), and a number of signalling molecules. Detailed examination of condensed chromosomes has revealed that the process of condensation involves the formation of looped and folded structures (see Figure 3), which themselves are further folded to form a higher-order structure. Condensation of chromosomes is an irregular process with no preference over locations of particular sequences within specific folded loop structures (Strukov and Belmont, 2009).

1.1.4. Chromosome segregation

With each round of cell division, cells face the challenge of transmitting an exact copy of the genome to the two newly formed daughter cells both in terms of replication and segregation. Importantly, chromosome segregation errors are frequently seen in cancer cells (Gordon et al., 2012; Janssen et al., 2011; Ricke et al., 2008; Sheltzer et al., 2011).

The purpose of mitosis is to divide the replicated chromosomes before cytokinesis. Budding yeast mitosis has distinctive features that are not observed in higher eukaryotes: *S. cerevisiae* undergoes a ‘closed’ mitosis, characterized by a lack of nuclear envelope breakdown. Therefore, the mitotic spindle has to form inside the nucleus and the spindle poles are embedded in the nuclear envelope (Bouck et al., 2008). In contrast to vertebrate cells, microtubules have access to chromosomes throughout the cell cycle (Goshima and Yanagida, 2000). To ensure that each daughter cell inherits an identical copy of the genome, cohesion between the newly replicated sister chromatids is established during S phase, and maintained until the onset of anaphase. Sister chromatid cohesion (SCC) is essential to allow the proper bi-orientation of chromosomes on the metaphase plate, and is provided by a ring-shaped protein complex known as cohesin. Once all chromosomes are attached to microtubules, the spindle assembly checkpoint (SAC) is inactivated, cohesion is destroyed, and sister chromatids are irreversibly separated.

From a cell cycle point of view, the transition from metaphase to anaphase requires the proteolytic destruction of proteins (Enserink and Kolodner, 2010; Morgan, 1999). Entry into anaphase is triggered by the activation of the anaphase promoting complex (APC) associated with the activator protein Cdc20, which promotes the degradation of a large number of proteins, including mitotic cyclins (Shirayama et al., 1999; Wasch and Cross, 2002), and the separase inhibitor securin (Pds1 in budding yeast). The degradation of Pds1 allows the separase protease (Esp1 in budding yeast) to cleave Scc1, thereby triggering the opening of cohesin rings and chromosome segregation (Uhlmann et al., 1999). Additionally, mitotic exit requires reversing Cdk-dependent phosphorylation, which is largely carried out by the Cdc14 phosphatase in budding yeast (Azzam et al., 2004; Stegmeier and Amon, 2004). Finally, cytokinesis produces two daughter cells through the coordinated contraction of the actomyosin ring (Sanchez-Diaz et al., 2008).

1.2. DNA damage response and repair

Every day cells have to cope with a wide range of DNA lesions that compromise the integrity of our genome. These lesions arise from three different sources. First, exogenous sources, such as the exposure to the ultraviolet (UV) component of the sunlight and numerous genotoxic substances can affect the integrity of the DNA. Moreover, chromosomes can also be broken by ionizing radiation or cosmic rays. Second, some reactive products arising from normal cell metabolism can compromise the DNA structure. In order to counteract the toxicity of these molecules, cells have a complex antioxidant defence system and low molecular-mass scavengers, such as glutathione. DNA can suffer some spontaneous reactions, such as nucleotide hydrolysis and spontaneous deamination which will lead to abasic sites and miscoding nucleotides, respectively (Lindahl, 1993). Finally, errors during DNA replication can also jeopardise the integrity of our genome.

Independently of the nature of the DNA damaging agent, the most common consequence is the activation of the DNA damage checkpoint, which leads to cell cycle arrest. This provides time for the repair machinery to restore DNA integrity. Although the DNA repair process is highly efficient, sometimes there are some errors that can lead to mutations and chromosome aberrations, such as deletions (loss of heterozygosity), translocations, inversions and duplication events which are related to premature ageing and cancer predisposition (Hoeijmakers, 2001). If the cell is unable to repair the lesion and cannot bypass its effects on replication, transcription or chromosome segregation, cells may initiate the apoptosis program.

1.2.1. DNA replication checkpoint

The DNA damage checkpoint is a surveillance pathway, present in eukaryotic cells, that monitors replication and is able to trigger a cellular response to preserve genome integrity in case of sensing replicative stress (Osborn et al., 2002). Although it was originally described as a signal transduction pathway delaying cell cycle progression to provide time to allow replication to finish (Enoch and Nurse, 1990), nowadays it is accepted to be a highly regulated and interconnected pathway that coordinates a wide variety of cellular processes in order to maintain cell viability providing genome stability (Labib and de, 2011).

When a replication fork encounters a DNA lesion, the fork can either stall or collapse. Briefly, a stalled fork is one whose movement has been compromised. Even under normal conditions, replication forks do sometimes stop for minutes (Calzada et al., 2005; Deshpande and Newlon, 1996). On the other hand, a collapsed fork is one in which some elements of the replisome are no longer associated with the site of synthesis (Yao and O'Donnell, 2010). Forks are prevented from collapse by the checkpoint pathway, and possibly other mechanisms (Labib and de, 2011). It has been described that in some specific places, such as tRNA genes and centromeres, replication fork stabilization by the checkpoint is a key factor in maintaining genome stability (Zegerman and Diffley, 2009).

The central elements in the DNA damage checkpoint cascade are the phosphoinositide 3-kinases (PI3)-related Mec1 (ATR in humans) and Tel1 (ATM in humans) (Mallory and Petes, 2000). The highly conserved effector kinases Rad53 (CHK2 in humans) and Chk1 (CHK1 in humans) are directly targeted by PI3-related kinases and are responsible for the amplification of the checkpoint signal, as well as for the phosphorylation of key proteins that modulate different aspects of cellular physiology (Longhese et al., 2003).

The main signal able to trigger the activation of the checkpoint is the generation of extended ssDNA tracks (Zou and Elledge, 2003), which are due to the uncoupling between the DNA unwinding and DNA synthesis (Byun et al., 2005), or the uncoupling between the leading and lagging strand synthesis due to the presence of damaged templates (Branzei and Foiani, 2009). ssDNA tracks are rapidly coated by the single strand DNA-binding protein RPA complex (composed of Rfa1, Rfa2, and Rfa3) which recruits the apical kinase Mec1 to stalled forks through the action of its associated factor Ddc2 (ATRIP in humans) (Zou and Elledge, 2003). Then, Mec1 phosphorylates several factors, such as Rad53 and Mrc1 (CLASPIN in humans) (Tanaka and Russell, 2001). The latter is required for full Rad53 kinase activation (Alcasabas et al., 2001) and prevents uncoupling between helicase unwinding and DNA synthesis at stalled forks by somehow tethering helicases to DNA polymerases (Nedelcheva-Veleva et al., 2006). Other factors, such as the Topb1, the Mre11-Rad50, Xrs2 (MRX) complex, the Rad24-Rfc2-5 complex, the Ddc1-Rad17-Mec3 (also known as 9-1-1) complex have also been implicated in the replication checkpoint response (Finn et al., 2012) (see Figure 4). The DNA checkpoint pathway modulates the cellular physiology in response to replication stress through phosphorylation by the Mec1, Rad53, and Dun1 kinases. Among other processes, they are responsible for inhibition of late origin firing through down-regulation of Sld3 and Dbf4; transcription of other replication factors, such as MBF targets; and increasing the dNTP pool through stimulation of the ribonucleotide reductase activity, which should also help to successfully complete replication (Labib and de, 2011).

One of the most important roles of DNA damage response is to maintain fork stability (Lopes et al., 2001). Checkpoint mutants fail to resume DNA synthesis after removal of replication stress and accumulate DNA breaks (Feng et al., 2011a). Collapsed replication forks, in checkpoint deficient cells, are characterized by the accumulation of abnormal replication intermediates (Lopes et al., 2001), which reflects the nucleolytic activity of exonuclease 1 (Exo1)(Cotta-Ramusino et al., 2005). Exo1 induces fork instability and therefore lethality in checkpoint deficient cells as they proceed to replicate damaged templates (Segurado and Diffley, 2008). Rad53-mediated Exo1 phosphorylation (Morin et al., 2008) suppresses its exonuclease activity preventing fork breakdown and the accumulation of aberrant structures at stalled forks (Segurado and Diffley, 2008) (see Figure 4).

Finally, normal cellular physiology needs to be restored when the replication stress is overcome. This requires shutting-down the checkpoint cascade, as well as the reversal of post-translational modifications. When DNA replication resumes, ssDNA tracks shorten, limiting further Ddc2-mediated recruitment and activation of Mec1 (Jossen and Bermejo, 2013). Moreover, in *S. cerevisiae*, several phosphatases, such as Ptc2, Ptc3, and Pph3/Psy2 are involved in Rad53 dephosphorylation, which tightly correlates with the down-regulation of its activity (O'Neill et al., 2007).

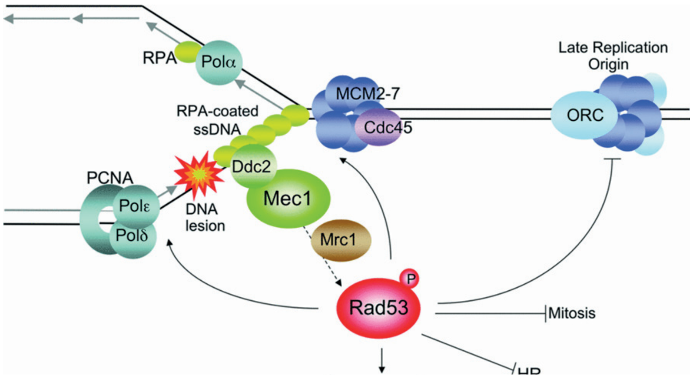

Figure 4. The S-phase checkpoint response

The accumulation of ssDNA tracks causes the activation of the checkpoint. Then, the RPA bound to ssDNA recruits Ddc2 and Mec1 to the stalled forks. Mec1 phosphorylates the mediator Mrc1 and the effector kinase Rad53 activating them. Rad53 maintains stable and functional DNA replication forks, inhibits firing of late origins, activates gene expression and prevents entry into mitosis and unscheduled recombination. Abbreviations: HR, homologous recombination; PCNA, proliferating cell nuclear antigen. Figure taken from Segurado and Tercero, 2009.

1.2.2. DNA damage repair mechanisms

To repair the wide variety of lesions that could compromise the integrity of DNA, cells have evolved sophisticated DNA repair systems to cope with most, if not all, the possible insults (see Figure 5). Studies in *S. cerevisiae* have a central role in elucidating the highly conserved mechanisms that promote eukaryotic genome stability.

Direct reversal of DNA damage

This pathway repairs DNA damage in a single-step reaction. However, it is only effective in a very limited number of DNA lesions, such as specific UV lesions and base methylation (Yi and He, 2013). The cyclobutane pyrimidine dimers (CPDs), which are produced by ultraviolet B (UVB) and UVC radiations, are repaired using a photo-reactivation reaction by the DNA photolyase Phr1 (Sancar, 2008). Direct repair is also involved in removing methyl groups from modified bases, such as O6-methylguanine (O6-MeG) in a reaction carried out by the methyltransferase Mgt1 in budding yeast (Sassanfar and Samson, 1990).

Base excision repair

Base excision repair (BER) is involved in repairing abasic sites, single-strand breaks (SSB), and chemically modified bases generated by normal cellular metabolism, exposure to some alkylating agents, or some spontaneous reactions (Dianov and Hubscher, 2013). BER deficiency affects genome stability and it is implicated in many human diseases, including premature aging (Lombard et al., 2005), neurodegeneration (Caldecott, 2008) and cancer (Bartkova et al., 2005). First, a wide range of glycosylases recognizes DNA lesions. Then, they flip the suspected base out of the helix. After base excision, a DNA polymerase will fill the abasic site and the strand will be resealed (Mol et al., 1999).

Nucleotide excision repair

Nucleotide excision repair (NER) removes multiple different lesions that cause DNA helix distortions, which could jeopardize replication and transcription. This pathway is very important in repairing lesions caused by environmental mutagens and chemical carcinogen-induced bulky adducts (Cadet et al., 2005). Loss of NER in humans is associated with the disease xeroderma pigmentosum, which is characterized by an extreme sensitivity to sunlight and >1000-fold incidence of sun-induced skin cancer. After recognizing the lesion, DNA incisions are made flanking the damage to remove it (Prakash and Prakash, 2000). These will generate a 20-25 nucleotide gap that will be filled by a DNA polymerase, and sealed by a DNA ligase (Boiteux and Jinks-Robertson, 2013).

Mismatch repair

The mismatch repair (MMR) pathway detects helical distortions due to mispairing of bases during DNA replication (Hsieh and Yamane, 2008). Since MMR reduces the number of replication-associated errors, defects in MMR increase the spontaneous mutation rate. In that sense, failures in this pathway provoke microsatellite instability, which is observed in the hereditary non-polyposis colorectal cancer (HNPCC) and in a variety of sporadic cancers (Arends, 2013).

Ribonucleotide excision repair

The ribonucleotide excision repair pathway is a pathway that senses the misincorporation of ribonucleotides into genomic DNA during the replication process. The RNA:DNA hybrids affect DNA conformation (Wahl and Sundaralingam, 2000), which will lead to genome instability (Nick McElhinny et al., 2010; Watt et al., 2011). The RNAase H is a family of proteins that cleave the RNA moiety in RNA:DNA hybrids (Cerritelli and Crouch, 2009).

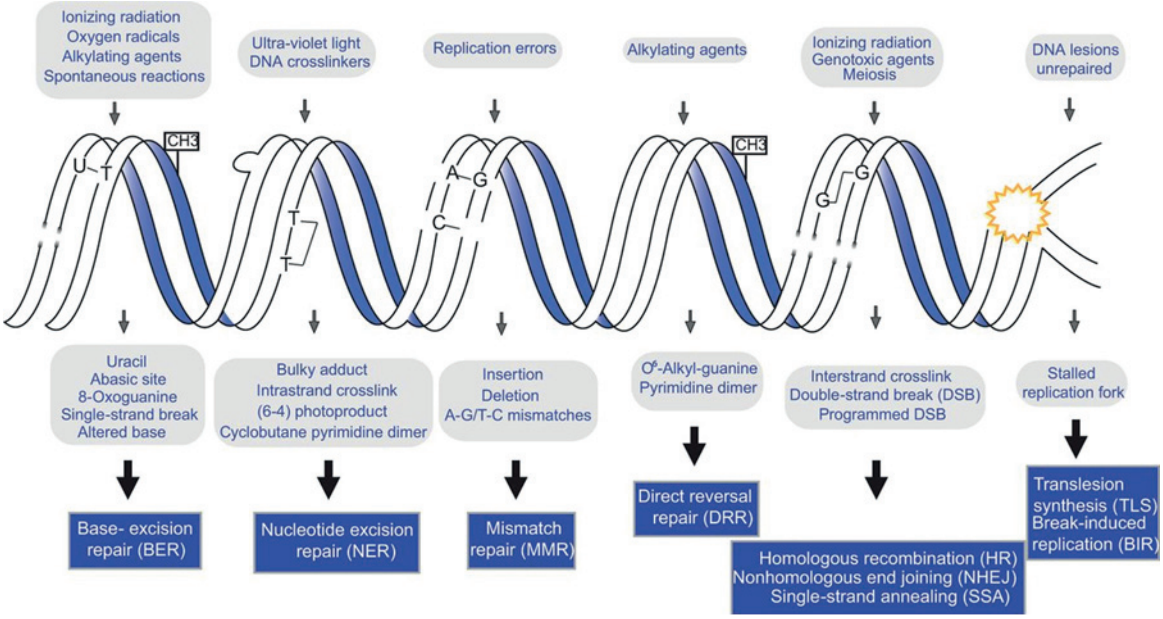
Ionizing radiation
Oxygen radicals
Alkylating agents
Spontaneous reactions
Ultra-violet light
DNA crosslinkers
Replication errors
Alkylating agents
Ionizing radiation
Genotoxic agents
Meiosis
DNA lesions
unrepaired
U
T
CH3
T
T
A
G
C
CH3
G
G
Uracil
Abasic site
8-Oxoguanine
Single-strand break
Altered base
Bulky adduct
Intrastrand crosslink
(6-4) photoproduct
Cyclobutane pyrimidine dimer
Insertion
Deletion
A-G/T-C mismatches
O6-Alkyl-guanine
Pyrimidine dimer
Interstrand crosslink
Double-strand break (DSB)
Programmed DSB
Stalled
replication fork
Base- excision
repair (BER)
Nucleotide excision
repair (NER)
Mismatch
repair (MMR)
Direct reversal
repair (DRR)
Homologous recombination (HR)
Nonhomologous end joining (NHEJ)
Single-strand annealing (SSA)
Translesion
synthesis (TLS)
Break-induced
replication (BIR)

Figure 5 DNA damage and the associated DNA repair pathways

The DNA backbone can be attacked by several endogenous or exogenous agents (for instance, ionizing radiation, alkylating agents, or oxygen radicals), leading to the activation of DNA repair enzymes. Figure taken from Genois et al., 2014.

1.2.3. Double-strand break repair

DNA double-strand breaks (DSBs) are one of the most cytotoxic forms of DNA damage. They can occur accidentally during normal cell metabolism or by exposure of cells to exogenous agents, such as ionizing radiation (IR) or some classes of chemotherapeutic drugs. In addition, DSBs appear during programmed recombination events, such as meiosis, budding yeast mating-type interconversion, and lymphocyte development (Paques and Haber, 1999; Soulas-Sprauel et al., 2007).

Classically, two pathways of DSB repair have been defined: non-homologous end joining (NHEJ) and homologous recombination (HR). As their names imply, NHEJ involves direct ligation of the broken ends, whereas HR requires an undamaged homologous sequence to serve as a template for repair of both broken strands. There is another repair modality called microhomology-mediated end joining (MMEJ) that utilizes annealing of short homologous sequences (microhomologies) revealed during the resection step to align ends prior to ligation (Hartlerode and Scully, 2009).

Non-homologous end joining (NHEJ) is particularly important during G0, G1 and early S phase in mitotic cells (Delacote and Lopez, 2008; Takata et al., 1998). Briefly, the two DNA ends are aligned by the action of the Ku complex which will protect them from degradation (Walker et al., 2001). Then, the two ends will be joined together and ligated (Grawunder et al., 1997). The mechanism of this pathway leads to loss of information, which could lead to genome instability.

Homologous recombination (HR) is a conserved DNA repair mechanism involved in meiosis, DNA double-strand breaks (DSBs) repair, DNA gap filling, and interstrand crosslinks repair. Moreover it is required for telomere stability in absence of telomerase and for the recovery of stalled or broken replication forks (Li and Heyer, 2008). However, recombination is also potentially dangerous as it can lead to gross chromosomal rearrangements and potentially lethal intermediates (Kolodner et al., 2002). Not surprisingly, defects in HR define a number of human cancer predisposition syndromes associated with genome instability.

When a DSB occurs within a repetitive sequence, the repeats may provide homology regions that can anneal to form a continuous chromosome in a process called single-strand annealing (SSA). Alternatively, 5´ end resection will generate 3´ protruding tails (Mimitou and Symington, 2008) followed by formation of Rad51 filaments that invade into homologous template to form a displacement loop (D-loop) to prime DNA synthesis from the 3´-OH of the broken chromosome on an intact template. After D-loop formation, DSB repair pathway has three branches that generate different products: first, extended DNA synthesis and subsequent D-loop disruption and reannealing to the second end repairs the break via synthesis-dependent strand annealing (SDSA) (Resnick, 1976). Second, if an intact replication fork is formed, the D-loop can be extended to the end of the chromosome. This pathway is defined as break-induced replication (BIR) resulting in loss of heterozygosity (LOH) (Malkova et al., 1996). Finally, the 3´ overhang could be extended by DNA synthesis and the second end could be captured forming a double Holliday junction (dHJ) intermediate (Symington and Gautier, 2011). The dHJ intermediate can then be dissolved or resolved by different mechanisms generating different products (see below for more detail).

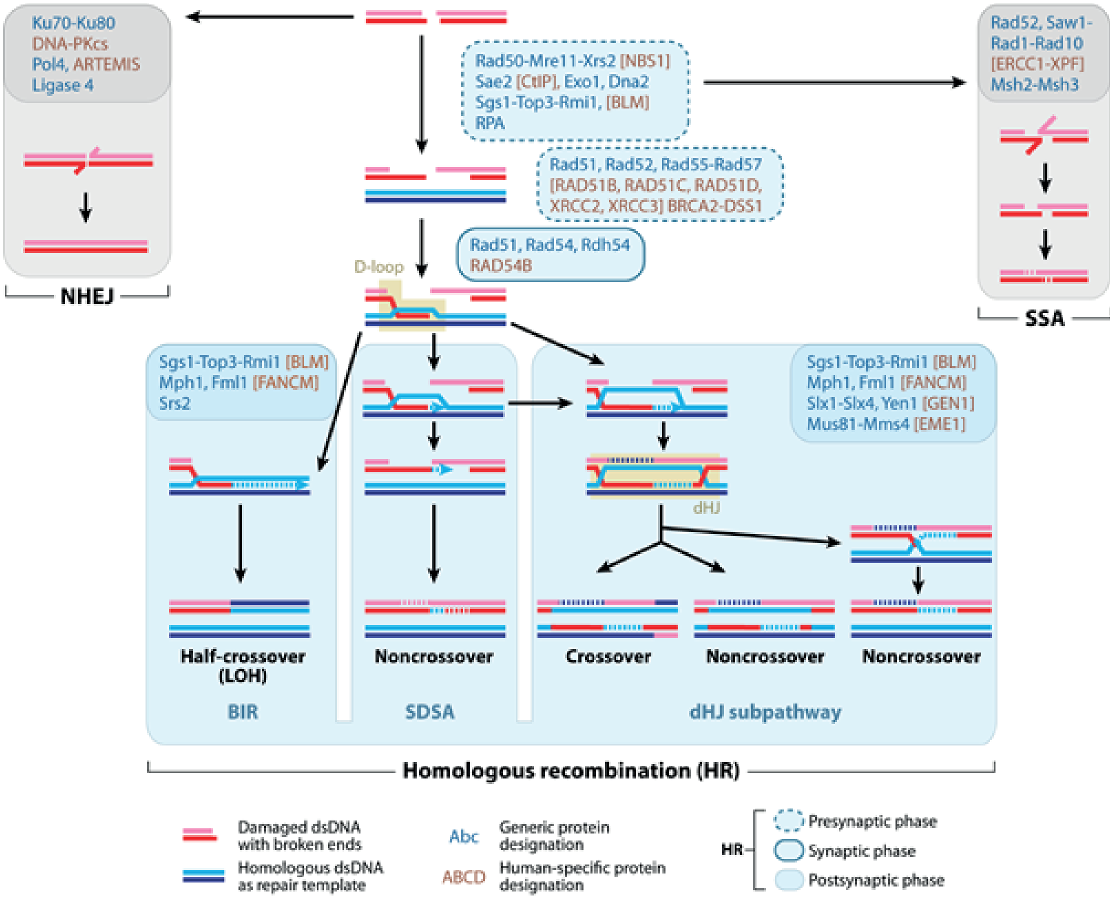
Ku70-Ku80
DNA-PKcs
Pol4, ARTEMIS
Ligase 4
NHEJ
Rad50-Mre11-Xrs2 [NBS1]
Sae2 [CtIP], Exo1, Dna2
Sgs1-Top3-Rmi1, [BLM]
RPA
Rad52, Saw1-
Rad1-Rad10
[ERCC1-XPF]
Msh2-Msh3
SSA
Rad51, Rad52, Rad55-Rad57
[RAD51B, RAD51C, RAD51D,
XRCC2, XRCC3] BRCA2-DSS1
Rad51, Rad54, Rdh54
RAD54B
D-loop
Sgs1-Top3-Rmi1 [BLM]
Mph1, Fml1 [FANCM]
Srs2
Sgs1-Top3-Rmi1 [BLM]
Mph1, Fml1 [FANCM]
Slx1-Slx4, Yen1 [GEN1]
Mus81-Mms4 [EME1]
dHJ
Half-crossover
(LOH)
BIR
Noncrossover
SDSA
Crossover
Noncrossover
Noncrossover
dHJ subpathway
Homologous recombination (HR)
Damaged dsDNA
with broken ends
Homologous dsDNA
as repair template
Abc
Generic protein
designation
ABCD
Human-specific protein
designation
HR
Presynaptic phase
Synaptic phase
Postsynaptic phase

Figure 6. DSB repair pathways

Protein names refer to the budding yeast *Saccharomyces cerevisiae* (blue). Where different in human, names (brown) are given in brackets. Broken lines indicate new DNA synthesis and stretches of heteroduplex DNA that upon mismatch repair (MMR) can lead to gene conversion. Abbreviations: BIR, break-induced replication; dHJ, double Holliday junction; NHEJ, non-homologous end joining; LOH, loss of heterozygosity; SDSA, synthesis-dependent strand annealing; SSA, single-strand annealing. Figure taken from Heyer, W.D et al, 2010.

1.2.4. Processing of recombination intermediates

The activation of some DNA repair mechanisms, such as homologous recombination; or the activation of some DNA damage bypass, such as template switching, lead to the formation of DNA junctions that need to be resolved before cells enter anaphase. Therefore, failures in resolving these linkages will provoke chromosome missegregation leading to genome instability.

In order to overcome this problem, cells have acquired a collection of endonucleases that recognize and cleave DNA joint molecules with different substrate specificity (Schwartz and Heyer, 2011). In *S. cerevisiae*, four resolvases have been determined to cleave Holliday junction intermediates: Mus81-Mms4, Slx1-4, Yen1 and Rad1-Rad10 (Svendsen and Harper, 2010). Recent investigations indicate that some structure-specific nucleases are activated during mitosis by the cell cycle machinery to remove DNA joint molecules (JMs): the Mus81-Mms4 complex is upregulated by Cdk and Polo kinase-dependent phosphorylation as cells enter mitosis (Matos et al., 2013) and the Yen1 resolvase becomes nuclear and active later on, as Cdk activity declines and the Cdc14 phosphatase removes the inhibitory phosphates (Blanco et al., 2014).

Importantly, depending how these enzymes process DNA joint molecules, a crossover or non-crossover product is generated. Although crossovers play an important role promoting genetic diversity during meiosis, they present a threat in mitosis, causing loss of heterozygosity when recombination occurs between homologous chromosomes; or translocations, inversions, deletions and gene duplications when crossovers occur between repeated regions on the same chromosome or other non-homologous chromosomes. To minimize crossover products, mitotically growing cells tend to dissolve (as opposed to ‘resolve’) HJs using the RecQ family of proteins. The RecQ proteins form an evolutionarily conserved family of DNA helicases that are important for the maintenance of genomic stability. Five RecQ helicases have been identified in humans: BLM, RECQ1, REQL4, RECQ5 and WRN. These proteins have received considerable interest due to their putative roles in the suppression of cancer and premature ageing in humans. For instance, mutations in BLM cause Bloom´s syndrome, which is characterized by an increased cancer predisposition and premature ageing (Monnat, Jr., 2010). In budding yeast there is one RecQ helicase, called Sgs1, which shares a number of features with BLM. BLM and Sgs1 associate with and stimulate the activity of a type IA topoisomerase (Top3 in yeast; hTOPOIIIα in humans) (Ui et al., 2005). Additionally, both Sgs1-Top3 and BLM-hTOPOIIIα associate with a conserved OB fold-containing protein (Rmi1 in yeast; BLAP75/hRMI1 and BLAP18/RMI2 in humans), which appears to stimulate the enzymatic function of Sgs1-Top3 (Yang et al., 2010). The Sgs1-Top3-Rmi1 complex acts cooperatively as a ‘dissolvasome’ processing DNA structures that arise during DNA replication and HR repair generating non-crossover products (Chu and Hickson, 2009; Mankouri and Hickson, 2007) (see Figure 7).

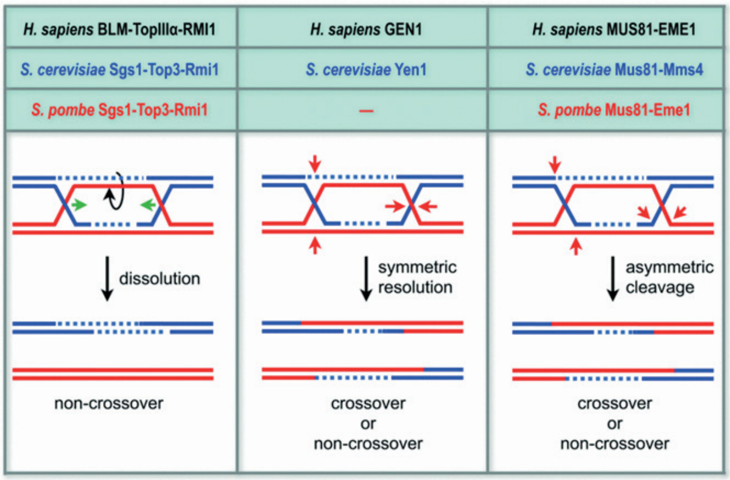
H. sapiens BLM-TopIIIα-RMI1
H. sapiens GEN1
H. sapiens MUS81-EME1
S. cerevisiae Sgs1-Top3-Rmi1
S. cerevisiae Yen1
S. cerevisiae Mus81-Mms4
S. pombe Sgs1-Top3-Rmi1
—
S. pombe Mus81-Eme1
dissolution
symmetric resolution
asymmetric cleavage
non-crossover
crossover or non-crossover
crossover or non-crossover

Figure 7. Mechanisms for the resolution of Holliday junctions

> Three possible pathways for the resolution of Holliday junctions in eukaryotic cells. Double-Holliday junctions produced by strand exchanges between homologous molecules (blue and red) can be resolved by 'dissolution' mediated by the BLM complex, symmetrical cleavage by GEN1/Yen1 or by asymmetric cleavage mediated by MUS81–EME1 complex. Green arrows indicate junction migration. Red arrows indicate cleavage sites. Broken lines indicate newly synthesized DNA. Yen1 resolvase is absent from *S. pombe*. Figure taken from West S.C., 2009.

1.2.5. DNA damage tolerance

Since cells are particularly vulnerable to DNA damage during DNA replication (Branzei and Foiani, 2009), they have acquired DNA damage tolerance mechanisms to allow replication fork progression in the presence of damage without the need to repair it. This pathway is called postreplication repair (PRR). Studies in *S. cerevisiae* suggest two pathways for PRR: translesion synthesis (TLS) and the damage avoidance by template switching (TS) which are error-prone and error-free, respectively (see Figure 8). Mutations in the error-free branch of PPR lead to a strong mutagenic phenotype in *S. cerevisiae* (Chang and Cimprich, 2009). In mammalian cells, the predominant pathway is the TLS, which uses specialized DNA damage-tolerant polymerases that, unlike replicative polymerases, contain flexible active sites and so they can replicate through damaged bases (Sale et al., 2012).

The central step of PRR is the posttranslational modification of PCNA (Pol30 in budding yeast). PCNA is monoubiquitylated on lysine 164 (K164) by the Rad18-Rad6 ubiquitin ligase complex in response to replication blocks (Hoege et al., 2002). When a replication fork stalls, the replication protein A (RPA) complex coats the ssDNA generated (Chang et al., 2006). This leads to Rad18 recruitment and stimulation of its E3 ligase activity, promoting K164 monoubiquitilation (Davies et al., 2008). Although K164 is the principal ubiquitylation site in PCNA, in *S. cerevisiae* K107 has also been implicated in DNA damage response triggered by DNA ligase I deficiency (Das-Bradoo et al., 2010). Work from the past decade has shown that K164 monoubiquitilation promotes the interaction with the Y-family TLS polymerases that are able to replicate through damaged bases (Sale et al., 2012) (see Figure 8).

In some circumstances, the monoubiquitylated K164 can be extended to a K63-linked ubiquitin chain (Hoege et al., 2002). This modification has been suggested to trigger an alternative error-free DNA damage tolerance pathway that involves regression of stalled forks followed by template switching in order to use the newly synthesized strand as a template to bypass DNA lesions (Ulrich and Walden, 2010). In *S. cerevisiae*, PCNA polyubiquitylation is mediated by the E3 ligase Rad5 in conjunction with the methansulphonate sensitive 2 (Mms2)-Ubc13 E2 complex (Hoege et al., 2002). The exact mechanism that triggers the switch from mono- to polyubiquitilation remains elusive (see Figure 8). Moreover, PCNA is also SUMOylated during S phase in budding yeast (Hoege et al., 2002; Parker et al., 2008; Stelter and Ulrich, 2003). SUMOylation of PCNA, mediated by the SUMO E3 ligase Siz1, preferentially occurs on K164 and to a lesser extent K127. This may suppress monoubiquitylation of PCNA and recruitment of TLS polymerases during unperturbed replication (Hoege et al., 2002). In *S. cerevisiae*, PCNA SUMOylation recruits the anti-recombinase Srs2, a 3´-5´ helicase that suppresses unwanted recombination events during S phase by disrupting Rad51 nucleoprotein filaments (Krejci et al., 2003; Papouli et al., 2005; Pfander et al., 2005) (see Figure 8).

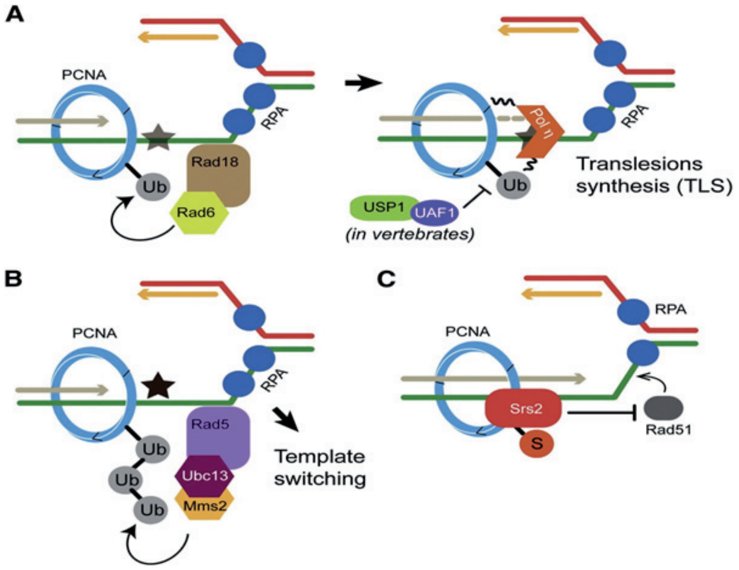

Figure 8. The postreplicational repair pathway

a) When the replication forks encounter a lesion (star) the Rad18-Rad6 complex is recruited to the fork leading to K164 PCNA monoubiquitilation. Then, the Y-family polymerases such as Polη are recruited to the fork to bypass the lesion in the process termed translesion synthesis (TLS). In vertebrates, the deubiquitinating complex USP1-UAF1 removes ubiquitin from PCNA. b) PCNA can be polyubiquitilated by the E3 Rad5 and the Ubc13/Mms2 dimeric E2, which promotes template switching. c) PCNA SUMOylation on K164 recruits Srs2, which blocks unscheduled recombination events within S phase. Figure from Jackson and Durocher, 2013.

1.3. SMC complexes

The structural maintenance of chromosomes (SMC) proteins are involved in the structural and functional organization of chromosomes from bacteria to humans (Losada and Hirano, 2005; Nasmyth and Haering, 2005). They participate in many chromosome functions, such as sister chromatid cohesion (SCC), chromosome condensation, transcription, DNA repair and recombination.

SMC proteins are large polypeptides that contain two nucleotide-binding motifs (known as Walker A and Walker B) located at the N- and C-terminal parts of the protein, respectively. These walker domains are separated by two long coiled-coils and a hinge domain. One SMC monomer folds back on itself through antiparallel coiled-coil interactions, creating an ATP-binding head domain at one end and placing the hinge domain at the other (Haering et al., 2002; Melby et al., 1998). Then, two monomers interact with each other through the hinge domain forming a V-shaped molecule (Hirano and Hirano, 2002). It has been determined that the length of each arm is ~50 nm, which is equivalent to ~150 bp of double-stranded DNA (dsDNA). Binding to ATP has been proposed to induce engagement of ATPase heads in SMC complexes, while its hydrolysis is supposed to bring them apart. The nucleotide binding, engagement and hydrolysis functions are essential for the activity of SMC complexes (Hirano and Hirano, 2004).

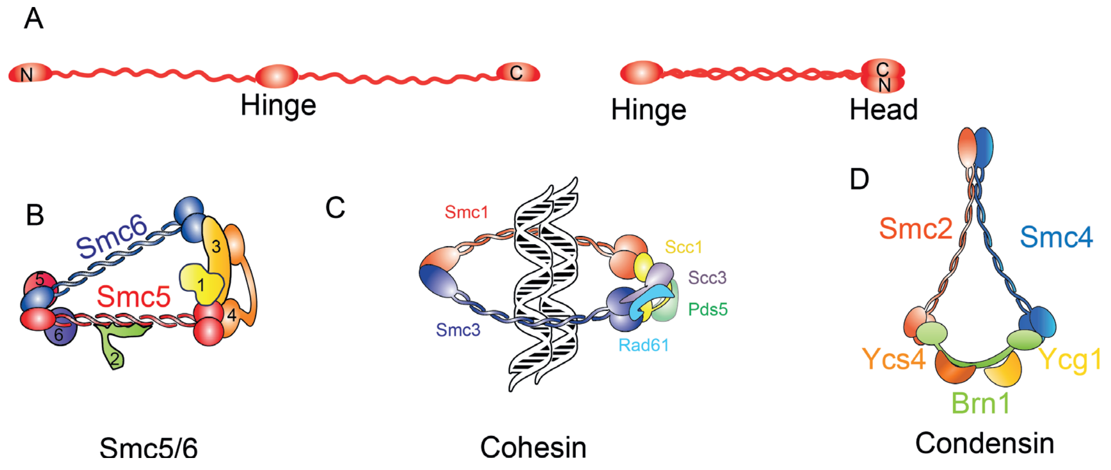

Figure 9. The architecture of SMC proteins.

a) Each SMC complex is formed of self-folded anti-parallel coiled coils that contain at one end the ATP-binding cassette (head domain) and a dimerization domain at the other end (hinge domain). b) Smc5/6 complex in budding yeast; in fission yeast, the Nse5-Nse6 heterodimer interacts with the ATPase heads; in both yeast, Nse2 interacts with the coiled coil region of Smc5. c) The core subunits of cohesin are Smc1 and Smc3, which associate with Scc1, Scc3, and to other less stably associated proteins, including Pds5 and Rad61. The complex has been proposed to embrace replicated sister chromatids. d) The condensin complex is formed by Smc2 and Smc4, which associate with Brn1, Ycs4 and Ycg1. The illustration depicts the open ring structure of cohesin as opposed to the more closed 'lollipop' structure of condensin. Figure from Seba Almedawar, Cell cycle lab.

Unlike bacteria, which only contain a single SMC protein, eukaryotes have six different SMC proteins that form heterodimers in specific combinations (see Figure 9). First, the Smc1-Smc3 pair constitutes the core of the cohesin complex that mediates sister-chromatid cohesion (Haering et al., 2002). Second, the Smc2-Smc4 heterodimer form the core of the condensin complex, which is required for chromosome condensation (Hirano, 2005). Finally, the Smc5-Smc6 heterodimer form a third complex implicated in DNA damage repair (Lehmann, 2005). Cohesin and condensin conformations are remarkably different. Whereas the hinge domain of condensin adopts a 'closed' conformation, which places the coiled-coils in close proximity forming a 'lollipop-like' structure, the coiled-coils in the cohesin complex display a more open structure (Anderson et al., 2002). Apart from the SMC subunits, all SMC complexes interact with non-SMC proteins that collectively regulate their function (see Figure 9).

1.3.1. The cohesin complex

The main role of cohesin is sister chromatid cohesion (Guacci et al., 1997; Michaelis et al., 1997). However, cohesin has been implicated in a wide range of other functions, including pairing of homologous chromosomes during meiosis (Thomas et al., 2005); double-strand break repair in mitotic (Sjogren and Nasmyth, 2001) and meiotic cells (Kim et al., 2010); assembly of replication factories during S phase (Guillou et al., 2010) and the axes of synaptonemal complexes during meiotic prophase (Kim et al., 2010); co-orientation of sister kinetochores during the first meiotic division (Sakuno et al., 2009); transcriptional control in yeast (Lin et al., 2011), flies (Pauli et al., 2008), fish (Horsfield et al., 2007) and mammals (Wendt et al., 2008); regulation of the recombination process that generates a full repertoire of T-cell receptors (Seitan et al., 2011); and lastly chromatin morphology during interphase (Schmidt et al., 2010).

The core components of the cohesin complex are two SMC proteins, Smc1 and Smc3. In addition two non-SMC proteins, Mcd1/Scc1/Rad21 and Scc3, also interact with the heterodimer. Mcd1/Scc1/Rad21 is a kleisin protein (Schleiffer et al., 2003) that binds to the head domain of Smc3 and Smc1 through its N- and C-terminal part, respectively (Haering et al., 2002). This interaction creates a ring-like structure which allows the physical entrapment of sister chromatids (Haering et al., 2002). Scc1 also interacts with Scc3, which is predicted to be a HEAT (Huntington, Elongation Factor 3, PR65/A, TOR) repeat-containing protein. In addition, there are several meiosis-specific subunits and some variants in vertebrate cells. For more information about the importance of cohesin variants in vertebrate cells read (Remeseiro and Losada, 2013).

The cohesin complex is loaded onto chromosomes during G1. This process requires the loading complex Scc2-Scc4 (Ciosk et al., 2000), ATP hydrolysis by the SMC heads and transient separation of the hinge regions (Gruber et al., 2006; Hu et al., 2011). Interestingly, cohesin is constantly being exchanged from chromatin throughout interphase (Gerlich et al., 2006). This feature may be important to facilitate replication and transcription (Fay et al., 2011; Terret et al., 2009) and depends on Wapl and Pds5. This destabilizing action on cohesin has been called ‘antiestablishment’ (Shintomi and Hirano, 2009). The action of Pds5-Wapl is particularly important for the prophase pathway that drives dissociation of most of the cohesin from chromatin at the onset of mitosis in metazoans (Gandhi et al., 2006).

In order to establish cohesion during DNA replication, the cohesin complex needs to become cohesive. Eco1, which is a cohesin acetyltransferase (CoATs), acetylates two lysine residues (K112 and K113) located in the head domain of Smc3 during S phase (Zhang et al., 2008). This neutralizes the antiestablishment action of Pds5-Wapl, most probably by affecting the conformation of the ring. In vertebrates, Smc3 acetylation enables the recruitment of sororin to Pds5, which displaces Wapl promoting cohesion (Nishiyama et al., 2010). Moreover, in *S. cerevisiae*, apart from Smc3 acetylation, cohesin SUMOylation is also required for sister chromatid cohesion and non-SUMOylated cohesin complexes are not cohesive despite being acetylated (Almedawar et al., 2012).

Cohesin is released from chromatin in two steps in metazoan mitosis, at prophase and anaphase. At the beginning of mitosis, in prophase, vertebrate Scc3 and sororin are phosphorylated by Polo and Cdk1, respectively; which allow Wapl and Pds5 to evict the majority of cohesin from chromosome arms (Dreier et al., 2011). At this stage, a small proportion of cohesin remains at the centromeres protected by Shugoshin (Sgo) and the protein phosphatase 2A (PP2A) (Kitajima et al., 2006). When cells enter anaphase, the ubiquitin-ligase anaphase promoting complex (APC) gets activated and induces the degradation of securin, which is normally bound to separase, inhibiting it. Once securin is degraded, separase is released and is able to cut Scc1 (Uhlmann et al., 1999). When Scc1 is cleaved and sister chromatids are decatenated by the action of Top2 (Wang et al., 2008), they are now free to be pulled apart by the mitotic spindle.

In addition to its function in sister-chromatid cohesion, cohesin plays critical roles in the DNA damage response. Several studies have confirmed a role in DNA repair in different organisms, such as *S. cerevisiae*, chicken, and humans (Sjogren and Nasmyth, 2001; Sonoda et al., 2001). Cohesin participates in DSB repair promoting homologous recombination. In *S. cerevisiae*, cohesin and its positive regulators, including Scc2, Pds5 and Eco1, are all required for DSB repair during G2 (Sjogren and Nasmyth, 2001). Moreover, cohesin is involved in DNA damage checkpoint activation. Several studies have established the role of cohesin in intra-S phase checkpoint activation in human cells. In response to DNA damage (IR, UV, HU), ATM or ATR phosphorylates two residues (S957 and S966) on SMC1, and phosphorylation of these two sites is required for S phase checkpoint activation. (Kitagawa et al., 2004; Yazdi et al., 2002). In addition to SMC1, SMC3 is also phosphorylated by ATM at S1083 in response to IR (Luo et al., 2008).

1.3.2. The condensin complex

Condensin is a large complex evolutionarily conserved from bacteria to humans (Hirano, 2012). It is involved in chromosome organization and condensation during mitosis and meiosis. They fold chromatin fibres into highly compact chromosomes to ensure correct segregation (Freeman et al., 2000; Hirano et al., 1997). It also prevents unwanted intrachromosomal recombination events at the rDNA locus, which helps ensure its stability (Tsang et al., 2007b) and regulates rDNA condensation during interphase upon nutrient starvation in budding yeast (Tsang et al., 2007a).

Condensin is formed by the Smc2-Smc4 heterodimer. In addition, three accessory subunits (Brn1, Ycs4, Ycg1) bind to the SMC heterodimer and regulate its activity. Kleisin I/Brn1, a member of the kleisin family (Schleiffer et al., 2003), interacts with Smc2 and Smc4 through its N- and C-terminal parts, respectively. Its interaction with the Smc2-Smc4 heterodimer forms a ring-shaped structure (Bhat et al., 1996; Hirano et al., 1997). All three accessory subunits of condensin are required for its association with chromatin and function in chromosome condensation (Lavoie et al., 2002). Most eukaryotes have two isoforms of condensin, called condensin I and II. They differ in the composition of the accessory subunits, which may explain the differential localization patterns, dynamics and functions of the two condensin complexes (Ono et al., 2004). Whereas condensin I-depleted cells show a swollen chromosome shape, condensin II depletion produces a curly shape. Depletion of both complexes produces a fuzzy appearance with cloud-like chromosomes (Ono et al., 2003).

Chromosome condensation is a dynamic process, and condensin is required not only to assemble chromosomes, but also to maintain them in a condensed state throughout mitosis (D'Ambrosio et al., 2008). A wide range of evidence suggests that mitotic Cdk-dependent phosphorylation stimulates the ATPase and supercoiling activities of *Xenopus* condensin I (Kimura et al., 1998). In budding yeast, Cdk-mediated phosphorylation of Smc4 primes condensin to be hyperphosphorylated by the Polo-like kinase Cdc5 enhancing its DNA supercoiling activity (St-Pierre et al., 2009). Condensin binds to specific sites along chromosomes, which likely involves the topological entrapment of DNA (Thadani et al., 2012).

1.3.3. The Smc5/6 complex

The Smc5/6 complex is formed by the Smc5-Smc6 heterodimer and 6 non-SMC elements, Nse1-6 (see Figure 9 and Table 3). Since its discovery in *S. pombe* in 1995 (Lehmann et al., 1995), it has been described in other eukaryotes, such as *S. cerevisiae* (Fujioka et al., 2002), *X. laevis* (Tsuyama et al., 2006), *A. thaliana* (Watanabe et al., 2009), *C. glabrata* (Miyazaki et al., 2006) and humans (Taylor et al., 2001).

Biochemical and two-hydrid experiments in yeast indicate that there are different subentities in the Smc5/6 complex: the first of them is formed by Smc5, Smc6 and Nse2; Nse1, Nse3 and Nse4 form the second subcomplex; and finally, Nse5 and Nse6 form the third subcomplex (Duan et al., 2009b; Hudson et al., 2011; Pebernard et al., 2006; Sergeant et al., 2005). In *S. pombe*, the Nse1-Nse3-Nse4 heterotrimer and the Nse5-Nse6 heterodimer both interact with the heads of Smc5 and Smc6 (Palecek et al., 2006; Pebernard et al., 2006). In *S. cerevisiae* the Nse5-Nse6 subcomplex binds to the Smc5-Smc6 hinge domains (Duan et al., 2009b).

Similarly to cohesin and condensin, the heads of Smc5 and Smc6 are brought together by the kleisin protein Nse4 (Palecek et al., 2006), also known as Rad62 (Morikawa et al., 2004), although Nse4 seems to be unable to interact with Smc6 on its own. Nse4 is related to the EID (E1A-like inhibitor of differentiation) family of proteins (Hudson et al., 2011). In budding and fission yeast, the N-terminal part of Nse4 binds to Nse3 (Hudson et al., 2011). In humans, there are two Nse4 proteins (NSE4a and NSE4b/EID3) containing both N- and C-terminal kleisin domains (Palecek et al., 2006; Taylor et al., 2008), which also interact with Nse3 (Guerineau et al., 2012). However, unlike Scc1, Nse4 is not cleaved at any specific cell cycle stage (Palecek et al., 2006).

Nse1 contains a RING (really interesting new gene) finger domain, common to ubiquitin E3 ligases (McDonald et al., 2003). *In vitro* experiments failed to demonstrate the ubiquitin E3 ligase activity from purified human and fission yeast Nse1 (Pebernard et al., 2008a). However, when Nse3 was added to the ubiquitination reaction, a strong *in vitro* ubiquitin ligase activity was detected (Doyle et al., 2010). Nse3 is a melanoma-associated antigen gene (MAGE)-like protein. These proteins are specifically expressed in some cancers. They are involved in gene transcription and apoptosis (Feng et al., 2011b). Recently, it has been described that they also bind to and enhance the ubiquitin ligase activity of other E3 RING ligases (Doyle et al., 2010). Nse6 contains ARM/HEAT repeats, also present in the cohesin loading factor Scc2 (Pebernard et al., 2006), while no conserved domains have been described in Nse5.

Nse2, also known as Mms21 is a SUMO E3 ligase. It contains a characteristic catalytic Siz/PIAS (SP)-RING domain at its C-terminus. Several experiments in yeast and human cells have demonstrated that Nse2 is able to transfer SUMO to several different substrates (Andrews et al., 2005; Potts and Yu, 2005; Zhao and Blobel, 2005). Nse2 binds to the coiled-coil region of Smc5 (Duan et al., 2009a). The importance of this subunit will be discussed in more detail below.

1.3.3.1. Localisation of the Smc5/6 complex

The Smc5/6 complex is primarily enriched at repetitive regions in the genome, including the rDNA array and telomeric sequences, but also at other discrete loci, as shown by immunofluorescence on chromosome spreads (Torres-Rosell et al., 2005). ChIP-on-chip analyses has provided a more detailed insight into the global chromosomal localization of the Smc5/6 complex in budding (Lindroos et al., 2006) and fission yeast (Pebernard et al., 2008b).

In G1, the Smc5/6 complex shows a strong association with telomeric regions in budding yeast. The complex seems to associate with DNA during S phase (Lindroos et al., 2006), an observation that has also been reported in *X. laevis* (Tsuyama et al., 2006). In G2/M, the complex localizes to all centromeric regions and shows a scattered distribution in intergenic regions. This pattern is very similar to the chromosomal localization of cohesin (Lengronne et al., 2004). The recruitment of Smc5/6 in budding yeast is controlled by Scc2, a loading factor required for cohesin recruitment onto chromatin (Ciosk et al., 2000). In *scc2-4* cells, the binding of Smc5/6 to chromatin is impaired, showing a 40% reduction compared to their wild type counterparts. However, whereas the centromeric association is almost abolished in *scc2-4* mutant cells, the rDNA-dependent association is not affected (Lindroos et al., 2006). In fission yeast, Smc5/6 is transiently loaded at centromeres when they are replicated in early S phase (Pebernard et al., 2008b).

Double-strand breaks (DSBs), as well as replication fork collapse, triggers Smc5/6 relocalization to the damaged sites (Lindroos et al., 2006; Pebernard et al., 2008b). This might reflect the requirement of the complex in DSB repair and in restarting collapsed replication forks (Ampatzidou et al., 2006). Similar results were obtained in MMS-treated cells in *S. pombe*, indicating that Smc5/6 is also important for replication on damaged templates (Pebernard et al., 2008b).

Immunostaining experiments in human cells showed that Smc5/6 associates with chromatin during interphase and dissociates from the nucleus in mitosis (Gallego-Paez et al., 2014; Taylor et al., 2001). However, fractionation and immunoblotting analysis revealed a small amount of Smc5/6 in the chromatin-enriched fraction in mitosis (Gallego-Paez et al., 2014). In humans, Smc5/6 associates with chromatin in early G1; whereas in yeast and *X. laevis* it associates during DNA replication (Gallego-Paez et al., 2014; Lindroos et al., 2006; Tsuyama et al., 2006).

1.3.3.2. The Smc5/6 complex and DNA damage repair

Since the initial isolation of *SMC6*, previously called *RAD18* in *S. pombe* (Nasim and Smith, 1975), and *NSE2* in *S. cerevisiae* (Prakash and Prakash, 1977b) in screens for yeast genes involved in response to DNA damage, the Smc5/6 complex has been related to DNA damage repair. Years later, it was reported that *smc6* mutants were sensitive to ultraviolet (UV) and γ-rays in *S. pombe* (Lehmann et al., 1995). In fact, subsequent studies have uncovered mutations in every member of the Smc5/6 complex that render cells sensitive to DNA damaging agents, such as UV, ionizing radiation (IR), methyl methanesulfonate (MMS), Mitomycin C, and hydroxyurea (HU) in yeast, *Arabidopsis*, chicken, *Drosophila,* mouse, *Xenopus* and humans (Ampatzidou et al., 2006; Andrews et al., 2005; Cost and Cozzarelli, 2006; de et al., 2006; Fousteri and Lehmann, 2000; Fujioka et al., 2002; Hu et al., 2005; McDonald et al., 2003; Miyabe et al., 2006; Morikawa et al., 2004; Onoda et al., 2004; Pebernard et al., 2004; Pebernard et al., 2006; Potts et al., 2006; Potts and Yu, 2005; Sheedy et al., 2005; Torres-Rosell et al., 2005; Zhao and Blobel, 2005). The function of Smc5/6 at damaged sites seems to be related to the processing of recombinogenic structures arising at blocked forks. In fact, genetic analyses have related the Smc5/6 complex with the homologous recombination pathway. In *S. pombe*, the *smc6-X* and *rhp51 Rad51⊿* mutations are epistatic in IR (Lehmann et al., 1995), an observation that has also been reported in budding yeast and chicken cells (Cost and Cozzarelli, 2006; Stephan et al., 2011a).

The Smc5/6 complex plays important roles at damaged replication forks too. When replication forks encounter a DNA lesion, the replisome can stall; and if it cannot proceed beyond the damage, it might eventually collapse (Branzei and Foiani, 2005). The Smc5/6 complex re-localizes to collapsed forks in yeast (Bustard et al., 2012; Irmisch et al., 2009; Lindroos et al., 2006). Replication forks can restart through homologous recombination (Arnaudeau et al., 2001). Several *smc5/6* hypomorphic alleles, such as *smc6-74*, *smc6-X* in *S. pombe*, are hypersensitive to replication arrest by hydroxyurea (HU) (Ampatzidou et al., 2006; Miyabe et al., 2006; Pebernard et al., 2004; Pebernard et al., 2006; Verkade et al., 1999). Interestingly, deletion of *RAD51* (blocking HR) can partially rescue these defects (Ampatzidou et al., 2006; Miyabe et al., 2006). The HU hypersensitivity and accumulation of X-shaped DNA molecules in *smc6-74* mutant cells can be rescued by overexpression of Brc1, a BRCA1 C-terminal domain protein (Rtt107 in budding yeast) (Ampatzidou et al., 2006; Sheedy et al., 2005). Brc1 is required for efficient DNA repair during S phase. It has been proposed that when the activity of the Smc5/6 complex is compromised, the accumulated HR intermediates can be repaired through an alternative Brc1-dependent mechanism, which requires the activity of several nucleases, such as Slx1/4 and Mus81/Eme1 (Sheedy et al., 2005). It has been described that the Smc5/6 complex has an early function in replication fork rescue in *S. pombe*: Smc5/6 is required for the loading of RPA and Rad52 onto stalled replication forks to maintain them in a recombination-competent configuration. *smc6-X* mutant cells show a reduced level of Rad52 and RPA association at stalled forks compared to wild-type cells (Irmisch et al., 2009).

1.3.3.3. The role of the Smc5/6 complex in DSB repair

Smc5/6 is recruited to DSBs in budding yeast (de et al., 2006; Lindroos et al., 2006). The recruitment is only significant when the DSB is induced in G2/M-arrested cells (de et al., 2006) and it requires Mre11 and Rtt107; but, neither the checkpoint nor the cohesin loader Scc2 (Leung et al., 2011; Lindroos et al., 2006; Ullal et al., 2011) (see Figure 10). Recruitment of Smc5/6 to DSBs promotes sister chromatid recombination: hypomorphic *smc6* alleles in budding yeast (de et al., 2006) show reduced sister chromatid exchanges (SCE) in response to DSB. Analogously, the Smc5/6 complex enhances sister chromatid alignment after DNA damage in plants and flies, thereby facilitating correct DSB repair by recombination between sister chromatids (Chiolo et al., 2011; Watanabe et al., 2009; Xu et al., 2013).

The meiotic program also induces DSBs to trigger recombination between homologues. In 2004 Pebernard and colleagues showed that *nse1*, *nse2* and *nse3* mutants show reduced spore viability after meiotic divisions in *S. pombe* (Pebernard et al., 2004). More recently, Wehrkamp-Richter and colleagues described that the low spore viability in *nse6* mutant cells is due to the accumulation of joint molecules resembling HJs (Wehrkamp-Richter et al., 2012). *smc6-9* budding yeast mutant cells also undergo aberrant meiotic divisions due to unresolved linkages between chromosomes during prophase I. These defects are not meiotic recombination-dependent, as *smc6-9 spo11Δ* mutants are also affected, a situation that might be explained by the essential function of the Smc5/6 complex during pre-meiotic S phase, where the complex acts to correct excessive linkages between chromosomes (Farmer et al., 2011). Lilienthal and colleagues demonstrated that the Smc5/6 complex prevents excessive joint molecule formation and aids in joint molecule resolution during meiotic divisions. In the absence of a functional Smc5/6 complex, overall joint molecules levels are 2-3 fold higher than in wild-type cells (Lilienthal et al., 2013). The dual function of the Smc5/6 complex in prevention and resolution of joint molecules was supported by two other independent works in meiosis (Copsey et al., 2013; Xaver et al., 2013).

SMC5 and SMC6 are highly expressed in human testis and they localize to meiotic chromosomes, supporting a meiotic function of the complex in human cells (Taylor et al., 2001). In mouse cells, the Smc5/6 complex has a role in spermatogonial differentiation and meiosis. Smc6 is present in differentiating spermatogonia and colocalizes with heterochromatic regions, such as pericentromeric regions, which are rich in repetitive sequences (Verver et al., 2013). Another study identified Smc6 along the chromatid axes in metaphase I and anaphase I chromosomes, as well as in mitotic chromosomes (Gomez et al., 2013). The recruitment of the Smc5/6 complex to heterochromatin is conserved in fission yeast, rodents and flies. In yeast cells, Smc6 is strongly enriched in the pericentromeric regions (Lindroos et al., 2006; Pebernard et al., 2008b; Yong-Gonzales et al., 2012). In *Drosophila*, Smc6 has a key role in the suppression of homologous recombination events in heterochromatic domains in somatic cells by inhibiting the recombinase Rad51 within these domains (Chiolo et al., 2011).

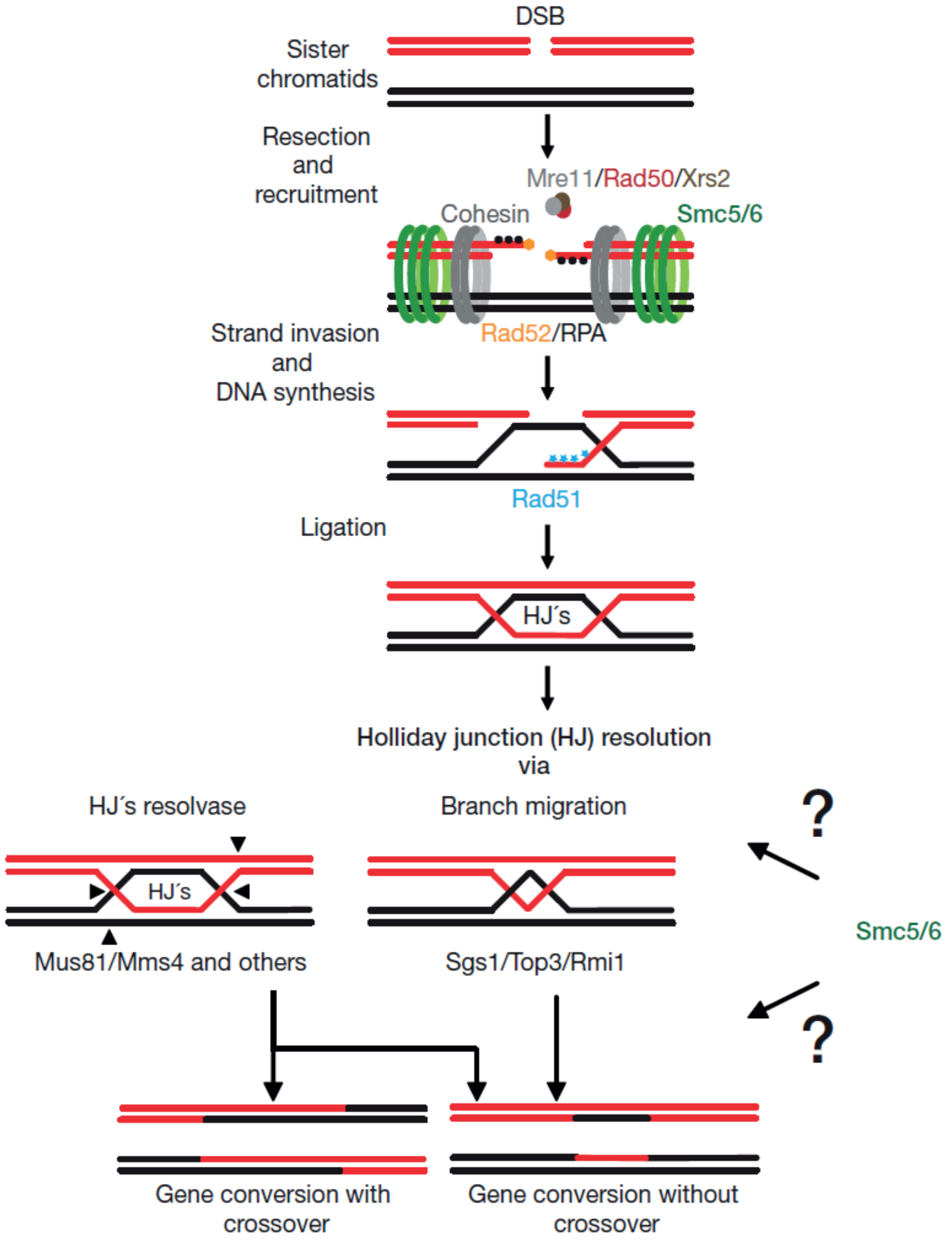
DSB
Sister chromatids
Resection and recruitment
Mre11/Rad50/Xrs2
Cohesin
Smc5/6
Rad52/RPA
Strand invasion and DNA synthesis
Rad51
Ligation
HJ´s
Holliday junction (HJ) resolution via
HJ´s resolvase
Branch migration
HJ´s
Mus81/Mms4 and others
Sgs1/Top3/Rmi1
?
Smc5/6
?
Gene conversion with crossover
Gene conversion without crossover

Figure 10. The role of the Smc5/6 complex in DSB repair

The Smc5/6 complex promotes sister chromatid recombination by recruiting the cohesin complex to the region of the DSB site. When the function of the Smc5/6 complex or cohesin is impaired, chromatids will be misaligned, and this can affect the repair process. Based on its known function in damaged replication forks, the Smc5/6 complex might also act in parallel with Mus81-Mms4, Sgs1-Top3-Rmi1 and other factors in the resolution of DSB-induced double HJs. Figure taken from Kegel and Sjogren, 2010.

1.3.3.4. The Smc5/6 complex and the segregation of the rDNA locus

The ribosomal DNA (rDNA) array has around 150 tandem repeats on the right arm of chromosome XII (Petes, 1979). Each 9.1 Kb repeat contains the *35S* and *5S* rRNA genes which are highly transcribed in opposite directions by RNA polymerase I and RNA polymerase III, respectively (Warner, 1999). Once transcribed, the *35S* rRNA precursor is processed into the *18S*, *5.8S* and *25S* rRNAs before all four rRNA molecules are assembled into a functional ribosome. This process is coordinated within a specialized region of the nucleus called the nucleolus. Due to the highly repetitive sequence of the rDNA, this site shows a high rate of recombination. Unscheduled recombination events between rDNA repeats can affect the number of copies and therefore compromise the rDNA stability (Kobayashi et al., 1998).

The Smc5/6 complex is enriched in the rDNA in *S. cerevisiae* (Torres-Rosell et al., 2005) and in *S. pombe* (Ampatzidou et al., 2006). Interestingly, *smc5/6* mutants show a fragmented and irregular rDNA shape (Torres-Rosell et al., 2005; Zhao and Blobel, 2005) and show massive defects in segregation of the rDNA locus and the right telomere of chromosome XII (Torres-Rosell et al., 2005). This defect per se seems sufficient to induce lethality in *smc5/6* mutant cells. However, the fact that Smc5/6 is required for viability in cells where chromosomal rDNA has been deleted (and are kept alive by expression of a unit of the rDNA from a multicopy plasmid) indicates that the complex has other essential functions beyond rDNA and full chromosome XII segregation (Torres-Rosell et al., 2005). The rDNA segregation failures are due to the presence of unresolved recombination intermediates and the failure to complete replication of this highly transcribed locus. In fact, elimination of *35S* transcription, unidirectional replication and recombination suppress the *smc6-9* missegregation phenotype (Torres-Rosell et al., 2007a). Interestingly, no known checkpoint is defective in *smc6-9* mutant cells. This indicates that either cellular checkpoints do not recognize the DNA structures accumulated in *smc6-9* cells or that the Smc5/6 complex is part of a thus far unidentified checkpoint (Torres-Rosell et al., 2007a).

The Smc5/6 complex and Rad52 SUMOylation prevent unscheduled recombination events within the nucleolus: HR events cannot be prevented when the function of the Smc5/6 complex and Rad52 SUMOylation are impaired, a situation that compromises the stability of the rDNA locus (Torres-Rosell et al., 2007b) (see Figure 11). This function might be extended to other heterochromatin-like loci. In *Drosophila* cells Smc5/6 is enriched in heterochromatic repetitive DNAs and it is also required to exclude Rad51 from this domain to prevent aberrant recombination events (Chiolo et al., 2011).

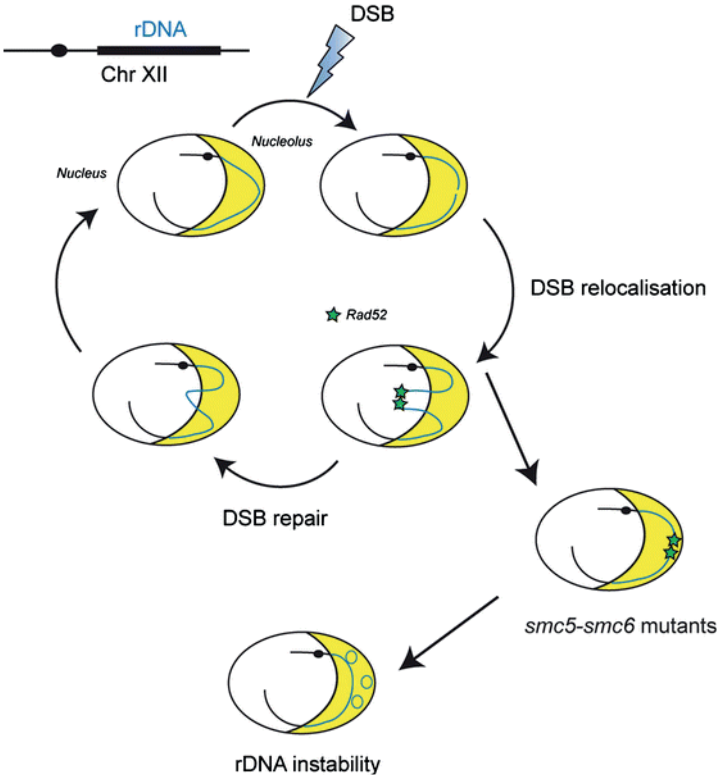

Figure 11. DNA repair in the rDNA locus in *S. cerevisiae*

DSBs generated in the rDNA array are relocated to the nucleus in order to be repaired by Rad52-mediated recombination. When the function of the Smc5/6 complex is impaired, DSBs are not relocated to the nuclear compartment and undergo Rad52-mediated repair in the nucleolus. This could lead to rDNA instability due to the repetitive nature of the rDNA. Figure taken from de et al., 2009.

1.3.3.5. The Smc5/6 complex and telomere function

Telomeres are repetitive DNA sequences placed at the ends of each chromosome (Blackburn, 2001). They are shortened in each cell division due to the end-replication problem of the lagging strand (Harley et al., 1990). In order to circumvent this problem, cells maintain the number of telomeric repeats using an enzyme called telomerase (Smogorzewska and de, 2004). In the absence of telomerase, the progressive loss of telomere fragments affects cell proliferation and leads to senescence (Bodnar et al., 1998).

There is another pathway, present in some cancer cells, called alternative lengthening of telomeres (ALT) based on homologous recombination (Henson et al., 2002). One characteristic feature of ALT cells is the localization of telomeres in promyelocytic leukaemia (PML) bodies, called ALT-associated PML bodies (APBs) (Yeager et al., 1999). Interestingly, the Smc5/6 complex localizes to APBs in ALT human cells and is required for targeting telomeres to APBs. In fact, several subunits of the shelterin telomere-binding complex are SUMOylated in an NSE2-dependent manner. NSE2 stimulates the SUMOylation of four of the six known components of the shelterin complex, including TRF1, TRF2, TIN2 and RAP1. Furthermore, depletion of NSE2 in ALT human cells inhibits shelterin SUMOylation and its recruitment to PML bodies (Potts and Yu, 2007). The proposed model for APB assembly is that APB formation can be initiated by the recruitment of NSE2, which will SUMOylate shelterin components. The initial nucleation event triggers the recruitment of other proteins such as DNA recombination and repair factors to allow telomere extension (Brouwer et al., 2009) (see Figure 12).

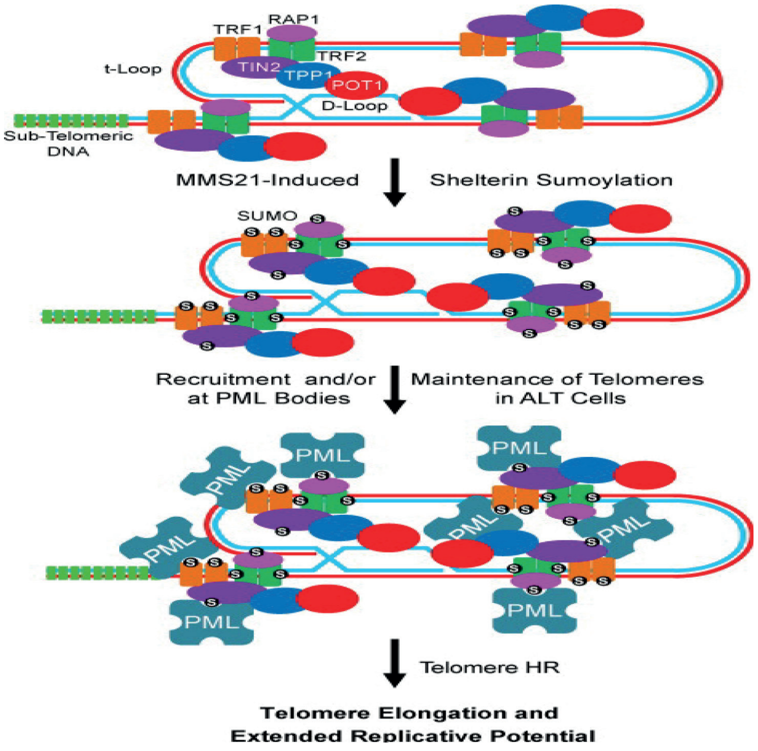
TRF1
RAP1
TRF2
t-Loop
TIN2
TPP1
POT1
D-Loop
Sub-Telomeric DNA
MMS21-Induced
Shelterin Sumoylation
SUMO
S
Recruitment and/or at PML Bodies
Maintenance of Telomeres in ALT Cells
PML
Telomere HR
Telomere Elongation and Extended Replicative Potential

Figure 12. Model for the role of the Smc5/6 complex in the recruitment of telomeres to PML bodies in ALT cells

Nse2 stimulates the SUMOylation of TRF1, TRF2, TIN2, and RAP1, which promotes the recruitment of telomeres to PML bodies in ALT cells. The relocalization of telomeres to PML bodies promotes telomere elongation by HR. Abbreviations: PML, promyelocytic leukaemia bodies; ALT, alternative lengthening of telomeres. Figure taken from Potts, 2009.

As previously described, Smc5/6 is highly associated with telomeres in budding yeast (Lindroos et al., 2006; Torres-Rosell et al., 2005). In *S. pombe*, MMS-induced DNA damage increases its association in an Nse2-dependent manner (Pebernard et al., 2008b). Although *nse2* mutants show a normal telomere length compared to wild type cells (Hang et al., 2011), they show a significant perturbation in subtelomeric silencing, suggesting an alteration in chromatin modifications (Wan et al., 2013). In *S. cerevisiae*, the limited cell division potential of about 70 generations in telomerase-lacking cells is significantly reduced to about 50-55 generations when the function of the Smc5/6 complex is compromised, indicating an increased rate of senescence. This is due to the accumulation of recombination intermediates at telomeres in senescing yeast cells in the absence of a functional Smc5/6 complex (Chavez et al., 2010).

Another study also showed that *smc5/6* mutants have a significant reduction in the generation of 3´ single-stranded overhangs on unprotected telomeres by Yku80 or Cdc13 inactivation. The authors suggest that the Smc5/6 complex facilitates 5´ resection or any other mechanism that generates 3´-overhangs, providing the ssDNA substrate required for telomere recombination and telomere maintenance without telomerase (Noel and Wellinger, 2011).

1.3.3.6. The Smc5/6 complex and chromosome cohesion

Some functions of the cohesin complex seem to be regulated by Smc5/6, especially under conditions of DNA damage. All subunits of the cohesin complex are SUMOylated and this modification seems to partially depend on the Nse2 SUMO ligase in the Smc5/6 complex. Interestingly, Eco1-mediated Smc3 acetylation and cohesin SUMOylation are both required for the entrapment of sister chromatids during S phase (Almedawar et al., 2012). Under conditions of DNA damage, specific SUMOylation-deficient *scc1* alleles are recruited to DSBs but are defective in establishing damage-induced cohesion both at DSBs and undamaged chromosomes (McAleenan et al., 2012). In chicken DT40 cells, *SMC5* knockdown reduces sister chromatid cohesion (Stephan et al., 2011a). Similarly, *SMC5* or *NSE2* knockdown by RNAi provokes a highly extended metaphase arrest with prematurely separated sister chromatids in HeLa cells (Behlke-Steinert et al., 2009). Very recently, it has been reported that NSE2-dependent SCC1 SUMOylation promotes sister chromatid recombination through counteracting WAPL in DSB repair (Wu et al., 2012). Somewhat strikingly, Scc1 SUMOylation has been linked to a negative role in sister chromatid cohesion: Scc1 becomes polySUMOylated in a Siz2-dependent manner in *pds5* mutants (D'Ambrosio and Lavoie, 2014), a situation that mark it for destruction by the SUMO-targeted ubiquitin ligase (STUBL) Slx5-Slx8 (Mullen and Brill, 2008).

1.3.3.7. The role of the Smc5/6 complex in chromosome topology

ChIP-on-chip experiments have shown that the frequency of Smc5/6 interaction sites along chromosome increases in linear correlation with chromosome length (Lindroos et al., 2006), a situation that could be explained if the Smc5/6 complex directly or indirectly sensed topological stress that accumulates during DNA replication. In fact, cells lacking functional type I topoisomerases show a length-dependent inhibition of late replication. The same replication delay is observed in s*mc6* and *nse2* mutant cells, suggesting that Smc5/6 senses topological stress and helps to reduce it. One possibility to account for these observations would be that Smc5/6 may allow replisome swivelling as a mechanism to reduce the torsional stress generated ahead of the fork (Kegel et al., 2011).

Other evidence points to a link between the Smc5/6 complex and chromosome topology. For example, *nse2-11* and *smc6-56* show synthetic growth defects when combined with mutations in *TOP2* (Takahashi et al., 2008), and the fission yeast *smc6-74* mutant is synthetically lethal with temperature sensitive *top2-191* at semipermissive temperature (Verkade et al., 1999). Interestingly, the overexpression of the protease separase increases survival in *smc6-74 top2-191* mutant cells, indicating that this mutant suffers from a misregulation of cohesin association (Outwin et al., 2009). It is possible that Smc5/6 and Top2 may physically cooperate on chromosomes, since both SMC6 and TOP IIα colocalize at centromeres, mitotic and meiotic chromatid axes, and in etoposide-induced chromatin fibres connecting lagging chromosomes in human cells (Gomez et al., 2013). Moreover, the redistribution of TOP IIα from interphase binding sites to the centromeric region in mitosis is blocked in SMC6-depleted cells (Gallego-Paez et al., 2014).

1.3.3.8. The Smc5/6-mediated SUMOylation and genome stability

NSE2, also known as *MMS21*, was described for the first time in a genetic screen for methyl methanesulfonate (MMS)-sensitive mutants in budding yeast (Prakash and Prakash, 1977a; Prakash and Prakash, 1977b). Like all other subunits in the Smc5/6 complex, *NSE2* is an essential gene in budding yeast (Andrews et al., 2005; Zhao and Blobel, 2005). Although the gene is essential for viability, its SUMO ligase domain is not. However, cells bearing mutations in the Siz/PIAS-like (SPL) RING domain of Nse2 are sensitive to a broad range of DNA damaging agents, such as hydroxyurea (HU), ionizing radiation (IR), MMS and ultraviolet (UV) light (Andrews et al., 2005; McDonald et al., 2003; Pebernard et al., 2004; Sergeant et al., 2005; Zhao and Blobel, 2005). *nse2* mutants show constitutive activation of Rad53 (Rai et al., 2011), reduced viability after exposure to DNA damage and high levels of chromosome missegregation, indicating a role for SUMOylation in efficient DNA repair. *nse2* mutant plants show a short-root phenotype, with shorter and fewer cells, caused by an apical root meristem cell proliferation defect and reduced sensitivity to exogenous cytokinins (Huang et al., 2009; Zhang et al., 2013). NSE2 maintains root stem cells survival by ameliorating DSB damage and thus ensures the normal structure and function of the root stem cell niche (Xu et al., 2013). Moreover, NSE2 has a role in the drought tolerance response by regulating stomatal opening and closing (Zhang et al., 2013).

As most other E3 ligases, Nse2 is autoSUMOylated *in vitro* and *in vivo* (Andrews et al., 2005; Potts and Yu, 2005; Zhao and Blobel, 2005). Only a limited number of Smc5/6-mediated SUMOylation substrates have been identified so far, most of which are involved in DNA repair, kinetochore function and chromosome integrity: human SMC6, RAP1, SA2, SCC1, TIN2, TRAX, TRF1, and TRF2 are SUMOylated in a NSE2-dependent manner (Potts and Yu, 2005; Potts and Yu, 2007); Nse3, Nse4 and Smc6 are SUMO-targets of Nse2 in fission yeast (Andrews et al., 2005; Pebernard et al., 2008b); and Smc2, Smc4, Brn1, Ku70, Smc5, Ndc10, Bir1, RNA pol I, Fob1, Tof2, and Snf1 are SUMOylated in a Nse2-dependent manner in budding yeast (Albuquerque et al., 2013; Simpson-Lavy and Johnston, 2013; Yong-Gonzales et al., 2012; Zhao and Blobel, 2005).

1.4. SUMOylation

Posttranslational modifications expand the complexity of a cell's proteome and regulate its properties. Small molecules, such as phosphate, methyl, and acetyl groups, or entire polypeptides, can be attached to proteins. The best-characterized example of a protein that modifies other proteins is ubiquitin, a highly conserved 76-residue polypeptide present in eukaryotes. Initially, ubiquitin was identified for its ability to target proteins for degradation by the *26S* proteasome (Elsasser et al., 2002; Young et al., 1998). Ubiquitin chains formed on Lys48 of ubiquitin result in proteasomal targeting, whereas Lys63-linked chains have non-proteasomal roles, including functions in DNA repair (McDowell et al., 2010).

Since the discovery of ubiquitin in the mid-70s, an entire family of small proteins related to ubiquitin, called ubiquitin-like proteins (Ubls) has been identified. This family includes several proteins, such as ISG15, SUMO, Nedd8, FAT10, and ATG8 (van der Veen and Ploegh, 2012). Small ubiquitin-like modifier (SUMO) proteins are small polypeptides (~10 kDa) (Kerscher et al., 2006). They are expressed by all eukaryotes, but are absent in bacteria and archaea. Some organisms, such as yeast, worms and flies, have a single SUMO gene, whereas plants and vertebrates express several SUMO proteins. The human genome encodes four distinct SUMO isoforms, SUMO1-4, with different expression patterns (Guo et al., 2004; Melchior, 2000). SUMO2 and SUMO3 are often referred to as SUMO2/3 because they share 97% identity. By contrast, SUMO2/3 shares only ~50% sequence identity with SUMO-1 (Rosas-Acosta et al., 2005; Saitoh and Hinchey, 2000; Vertegaal et al., 2006). Whereas SUMO2/3 is able to form chains, SUMO1 seems to act as a chain terminator on SUMO2/3 polymers (Matic et al., 2008). A proline residue at position 90 prevents the processing of SUMO4, which makes it unlikely that the protein is conjugated *in vivo* (Owerbach et al., 2005).

1.4.1. The SUMOylation cycle

1.4.1.1. SUMO conjugation

Similar to ubiquitin, conjugation of SUMO to a target protein is mediated by a cascade of enzymes responsible for SUMO activation, transfer and substrate-selective conjugation of the modifier. Like ubiquitin, SUMO proteins are synthesized as inactive precursors that must first undergo a C-terminal cleavage by the Sentrin/SUMO-specific protease (SENP). This cleavage exposes a di-glycine motif that allows SUMO to be conjugated to a lysine residue in target proteins (see Figure 13).

SUMO proteins are then activated in an ATP-dependent manner by the E1 activating heterodimer Sae1-Sae2 in mammals or Aos1/Uba2 in budding yeast (Gong et al., 1999).

This step involves the formation of a thioester bond between the active site cysteine residue of Sae2 and the C-terminal glycine residue of SUMO. SUMO is then passed to the active site cysteine of the conjugating enzyme Ubc9 (ubiquitin-conjugating 9), again via a thioester linkage (Desterro et al., 1997; Gong et al., 1997; Johnson and Blobel, 1997; Lee et al., 1998; Schwarz et al., 1998). Importantly, Ubc9 is the only known SUMO-conjugating enzyme and Ubc9 itself binds directly to the consensus SUMOylation motif on substrate proteins (Rodriguez et al., 2001; Sampson et al., 2001). The target protein consensus motif comprises ΨKX(D/E) (where Ψ is a large hydrophobic consensus residue). See below for more details.

Although Ubc9 can directly transfer SUMO to some target lysines, it frequently requires the assistance of a SUMO E3 ligase *in vivo*. Most of the E3 SUMO ligases harbour a RING finger-like domain, called Siz/PIAS (SP) RING motif. This domain is required for ligase activity, and acts as a binding platform that coordinates the contact between the SUMO-Ubc9 complex and its substrate (Hochstrasser, 2001). In mammals, the most important family of SUMO E3 ligases is the PIAS (protein inhibitor of activated STAT) family (Kahyo et al., 2001; Kotaja et al., 2002; Nishida and Yasuda, 2002; Schmidt and Muller, 2002). Several other proteins lacking an SP-RING domain have been reported to function as SUMO E3 ligases, including TOPORS, MUL1, PC2, HDAC4, HDAC7, the G-protein Rhes, TRAF7, and the nucleoporin RanBP2 (Braschi et al., 2009; Gao et al., 2008; Gregoire and Yang, 2005; Kagey et al., 2003; Morita et al., 2005; Pichler et al., 2002; Subramaniam et al., 2009; Weger et al., 2005).

S. cerevisiae has four SP-RING SUMO ligase genes: *SIZ1* and *SIZ2* (Johnson and Gupta, 2001), the meiosis-specific *ZIP3* (Cheng et al., 2006); and *NSE2*, a component of the Smc5/6 complex (Zhao and Blobel, 2005).

1.4.1.2. SUMO deconjugation

Protein SUMOylation is a highly dynamic process that can be readily reversed by Sentrin-specific proteases (SENPs). These enzymes cleave precisely between the terminal glycine of SUMO and the substrate lysine. Certain SUMO proteases are also responsible for SUMO precursor maturation and thus indirectly affect SUMO conjugation (Hickey et al., 2012). In humans, there are six SENPs: SENP1-3 and SENP5-7 (Mukhopadhyay and Dasso, 2007). Moreover, recent studies have identified three new SUMO proteases in humans: DESI1 (deSUMOylating isopeptidase 1), DESI2 (Shin et al., 2012) and USPL1 (ubiquitin-specific protease-like 1) which share little sequence similarity with the SENP protease class (Schulz et al., 2012). SUMO proteases show different subcellular distribution and paralogue specificity (Hickey et al., 2012). In *S. cerevisiae*, the two SENPs, Ulp1 and Ulp2, also show distinct localization and functions. *ulp1Δ* mutants undergo cell cycle arrest that cannot be rescued by either pro-Smt3 or mature Smt3, suggesting that Ulp1 is required for both pro-

Smt3 maturation and Smt3 cleavage from substrate proteins (Li and Hochstrasser, 1999). Another Smt3-specific protease, Ulp2 acts to remove Smt3 from substrate proteins but does not appear to be involved in the maturation of pro-Smt3 (Li and Hochstrasser, 2000). In addition, yeast strains lacking *ULP2* show an accumulation of Smt3 polymers, suggesting that Ulp2 functions in the processing and editing of Smt3 chains (Bylebyl et al., 2003).

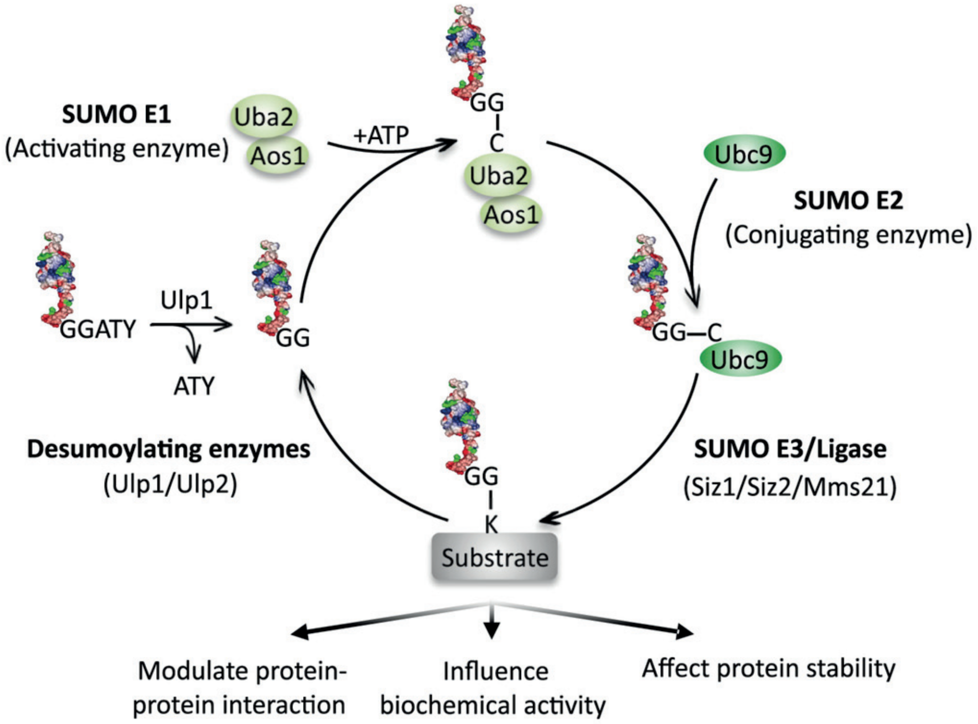
SUMO E1
(Activating enzyme)
Uba2
Aos1
+ATP
GG
C
Uba2
Aos1
Ubc9
SUMO E2
(Conjugating enzyme)
GGATY
Ulp1
ATY
GG
GG—C
Ubc9
Desumoylating enzymes
(Ulp1/Ulp2)
GG
K
Substrate
SUMO E3/Ligase
(Siz1/Siz2/Mms21)
Modulate protein-protein interaction
Influence biochemical activity
Affect protein stability

Figure 13. The SUMO cycle

Before the attachment, SUMO must be cleaved to expose two glycine residues (GG) by the SENP/Ulp proteases. The processed SUMO proteins are then activated by conjugation to the E1 heterodimer Uba2-Aos1, after which it is transferred to the E2 enzyme Ubc9. Finally, SUMO is ligated to substrate proteins by an isopeptide bond between the terminal glycine of SUMO and the ε-amino group in the substrate. The efficiency of the ligation reaction is aided by SUMO ligase E3 proteins, which interact with both target proteins and the E2 enzyme, thereby acting as bridging factors. SUMO polypeptides are removed from target proteins by the action of SENPs, which recycle SUMO. Three commonly seen effects of substrate SUMOylation are also shown. Abbreviations: SUMO, Small Ubiquitin-like Modifier; SENP, Sentrin/SUMO-specific protease; SAE, SUMO-activating enzyme; Ubc9, ubiquitin-conjugating 9. Figure taken from Cremona et al., 2012.

1.4.2. The consensus motifs for SUMO conjugation

Many SUMO-modified proteins identified contain an acceptor lysine within a ΨKX(D/E) consensus motif, where Ψ is a large hydrophobic residue (Rodriguez et al., 2001). These residues directly interact with the SUMO-Ubc9 complex and thus have a critical role in regulating the stability of interactions between the E2 and the substrate (Sampson et al., 2001). The consensus motif adopts an extended conformation, wherein the acceptor lysine fits into a hydrophobic groove on Ubc9 (Bernier-Villamor et al., 2002; Lin et al., 2002).

In addition to the canonical four amino acid SUMO consensus motifs, longer sequences that include both SUMO consensus motifs and additional elements have been identified in some substrates (see Figure 14). These include phosphorylation-dependent SUMO motifs (PDSMs) and negatively charged amino acid-dependent SUMO motifs (NDSMs). PDSM are present in proteins that are substrates for modification by pro-directed kinases (Yang and Gregoire, 2006) and comprise a SUMO consensus motif located adjacent to a phosphorylation site, ΨKX(D/E)XXSP. NDSMs have negatively charged residues located at the C-terminal part of the consensus site to increase the interaction with Ubc9 (Mohideen et al., 2009; Yang et al., 2006). In most studies, SUMO consensus motifs adopt similar polarity in their interactions with the E2 enzyme. However, recent studies have uncovered new motifs for SUMO conjugation, such as inverted consensus motifs and N-terminal hydrophobic cluster motifs (Matic et al., 2010) (see Figure 14).

Whereas SUMO consensus motifs mediate interactions between E2 and substrates, SUMO-interacting motifs (SIMs) mediate non-covalent interactions between SUMO and SIM-containing proteins (Kerscher, 2007). They contain a short stretch of hydrophobic amino acids, (V/I)X(V/I)(V/I), which are flanked by acidic residues (Song et al., 2005). SIMs have been uncovered in a wide range of proteins, including SUMO enzymes, SUMO substrates, SUMO-binding proteins and SUMO-targeted ubiquitin ligases (Kerscher, 2007; Perry et al., 2008).

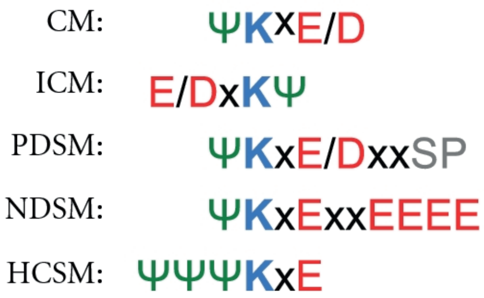

Figure 14. SUMO consensus motifs

Amino acid sequence alignment of the canonical SUMO consensus motifs. Ψ represents a hydrophobic amino acid. K is the lysine modified by SUMO and X represents any amino acid. Amino acids shown as blue: basic; red: acid; green: hydrophobic; and gray: phospho-serine. Abbreviations: CM, canonical consensus motif; ICM, inverted consensus motif; PDSM, phosphorylation-dependent SUMO motif; NDSM, negatively charged amino-acid-dependent SUMO motif; HCSM, hydrophobic cluster SUMO motif. Figure taken from Da Silva-Ferrada et al., 2012.

1.4.3. Molecular consequences of SUMOylation

The effects of SUMOylation cannot be predicted easily, as they depend on the function of the target protein. However, SUMO may lead to one of these non-mutually exclusive effects: SUMOylation of proteins can affect protein stability or enzymatic activity, alter localization, or mediate novel protein-protein interactions with other proteins containing SUMO-interacting motifs (SIMs) (Geiss-Friedlander and Melchior, 2007; Kerscher, 2007). In many cases, SUMOylation enhances the assembly of large multiprotein complexes. As previously described, SUMOylation is required to assemble the shelterin complex in the promyelocytic leukaemia (PML) nuclear bodies to allow telomere elongation in telomerase-negative cells (Chung et al., 2011). Moreover, SUMOylation may mask the binding site of a protein that interacts with the substrate protein, essentially acting to occlude the interaction in a SUMO-dependent manner. For instance, SUMOylation of the ubiquitin-conjugating enzyme E2-25K inhibits its interaction with the ubiquitin E1 enzyme leading to a decrease in its capability to conjugate ubiquitin to substrate proteins (Pichler et al., 2005). Finally, the diverse effects of SUMOylation can also be explained through interactions with other posttranslational modifications, such as ubiquitilation and acetylation (Wilkinson and Henley, 2010).

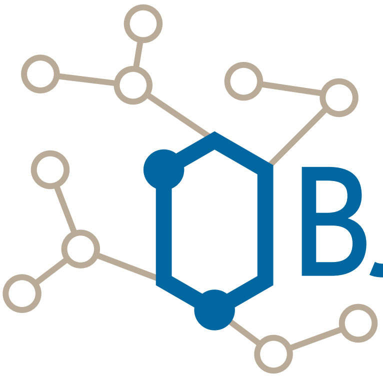

OBJECTIVES

smc5/6 mutants show a fragmented and irregular rDNA shape (Torres-Rosell et al., 2005; Zhao and Blobel, 2005) and show massive defects in segregation of the rDNA locus and the right telomere of chromosome XII (Torres-Rosell et al., 2005). Although this defect per se must be sufficient to induce lethality in *smc5/6* mutant cells, the fact that Smc5/6 is required for viability in cells where the chromosomal rDNA has been deleted (and are kept alive by expressing a unit of the rDNA from a multicopy plasmid) indicates that the complex has other essential functions beyond rDNA and full chromosome XII segregation. The presence of an E3 SUMO ligase as a member of the complex, suggests that some of its functions might be regulated by SUMOylation. However, despite multiple experiments in yeast and human cells have demonstrated that the Nse2 SUMO ligase is required for efficient DNA repair (Andrews et al., 2005; Potts and Yu, 2005; Zhao and Blobel, 2005), little is known about how the activity of this enzyme is regulated and which factors control its ability to transfer SUMO. Using *Saccharomyces cerevisiae* as a model organism, this work aims to:

- **Determine if the Smc5/6 complex has a genome-wide function in chromosome segregation.**
- **Uncover the regulation of the SUMO ligase activity of Nse2.**
- **Test the relevance of Smc5 SUMOylation.**
- **Investigate the role of the Smc5/6 complex in chromosome topology.**

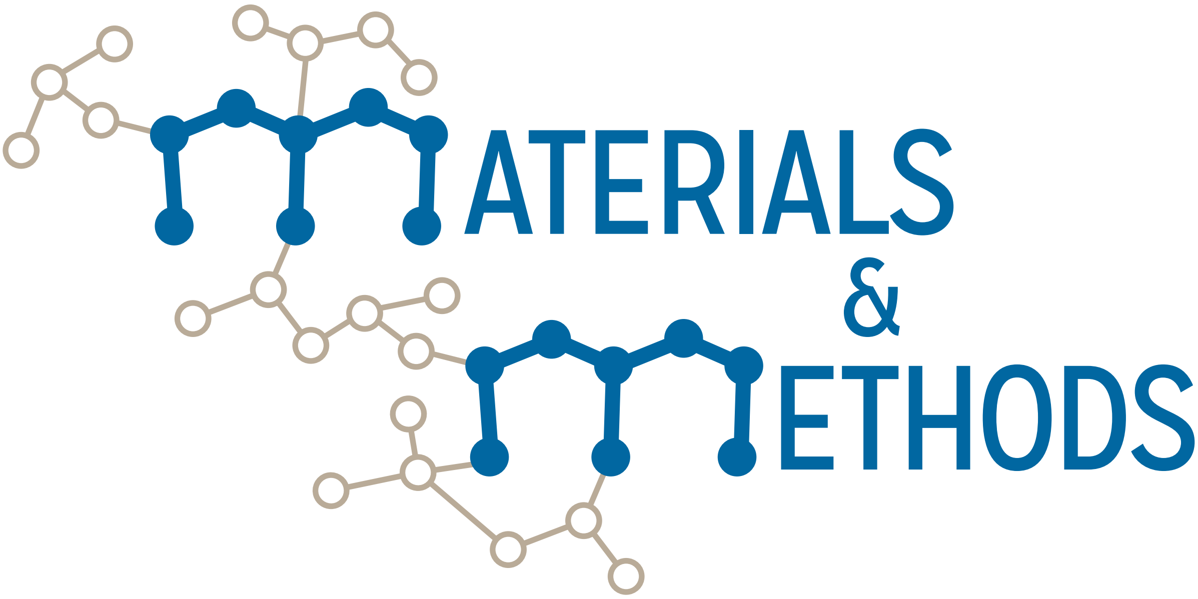

MATERIALS & METHODS

3.1. *S. cerevisiae* strains, growth conditions and general yeast methods

3.1.1. *S. cerevisiae* strains

A list of strains used in this study is provided in Table 1 below.

Strain		Genotype	Reference
AS499		*MATa ura3 lys2 ade2 trp1 his3 leu2 bar1-Δ, pep4::HIS3*	L. Aragon's lab
BY4741		*MATa his3Δ1 leu2Δ0 met15Δ0 ura3Δ0*	EUROSCARF
W303		*MATa ade2-1 trp1Δ2 can1-100 leu2-3,112 his3-11,15 ura3-52*	
YTR27	BY4741	*SMC5-9myc:TRP*	This study
YTR28	BY4741	*SMC6-9myc:TRP*	This study
YTR53	BY4741	*smc6-9:HIS3MX6*	This study
YTR82	AS499	*NSE3-9myc:TRP*	This study
YTR83	AS499	*NSE4-9myc:TRP*	This study
YTR109	BY4741	*rad24::kanMX4*	EUROSCARF
YTR110	BY4741	*mrc1::kanMX4*	EUROSCARF
YTR111	BY4741	*ddc1::kanMX4*	EUROSCARF
YTR114	BY4741	*mec3::kanMX4*	EUROSCARF
YTR119	BY4741	*smc5-6:natMX*	This study
YTR128	AS499	*rad52::kanMX4*	This study
YTR149	AS499	*rad9::KanMX4*	This study
YTR176	BY4741	*mms4::kanMX4*	EUROSCARF
YTR178	BY4741	*top3::kanMX4*	EUROSCARF
YTR179	BY4741	*rrm3::kanMX4*	EUROSCARF
YTR186	BY4741	*mus81::kanMX4*	EUROSCARF
YTR188	BY4741	*slx1::kanMX4*	EUROSCARF
YTR189	BY4741	*slx4::kanMX4*	EUROSCARF
YTR193	BY4741	*rad57::kanMX4*	EUROSCARF
YTR196	BY4741	*rad55::kanMX4*	EUROSCARF
YTR250	BY4741	*apn2::kanMX4*	EUROSCARF
YTR252	BY4741	*exo1::kanMX4*	EUROSCARF
YTR337	AS499	*MATa ura3 lys2 ade2 trp1 his3 leu2 bar1-Δ, pep4::HIS3*	L. Aragon's lab
YTR358	BY4741	*srs2::kanMX4*	EUROSCARF
YTR359	BY4741	*sgs1::kanMX4*	EUROSCARF
YTR400	BY4741	*rad1::kanMX4*	EUROSCARF
YTR401	BY4741	*rad10::kanMX4*	EUROSCARF
YTR402	BY4741	*rad18::kanMX4*	EUROSCARF
YTR405	BY4741	*rad27::kanMX4*	EUROSCARF
YTR454	AS499	*mms2::kanMX4*	EUROSCARF

YTR456	AS499	*smc6-9:natMX mms2::kanMX4*	This study
YTR474	BY4741	*mag1::kanMX4*	EUROSCARF
YTR484	AS499	*rad6::kanMX4*	This study
YTR486	AS499	*rad18::kanMX4*	This study
YTR488	AS499	*smc6-9:natMX4 rad6::kanMX4*	This study
YTR489	AS499	*smc6-9:natMX4 rad18::kanMX4*	This study
YTR493	AS499	*smc6-9:natMX4 TUB1-GFP:URA*	This study
YMB499	AS499	*smc6-9:natMX4 his3::pHIS3-lacI-NLS-GFP HIS3 CEN3:256xlacO:URA3*	This study
YTR506	AS499	*his3::pHIS3-lacI-NLS-GFP HIS3 CEN3::256xlacO:URA3*	This study
YTR516	AS499	*his3::pHIS3-lacI-NLS-GFP HIS3 CEN3::256xlacO:URA3 smc6-9:natMX4*	This study
YTR539	AS499	*nse2ΔC::hphMX4*	This study
YTR557	BY4741	*6his-Flag-SMT3:kanMX6*	This study
YTR569	BY4741	*6his-Flag-SMT3:kanMX6 siz1::hphMX4*	This study
YTR570	BY4741	*6his-Flag-SMT3:kanMX6 nse2ΔC::hphMX4*	This study
YTR571	BY4741	*6his-Flag-SMT3:kanMX6 siz2::natMX4*	This study
YTR572	BY4741	*6his-Flag-SMT3:kanMX6 siz1::natMX4 siz2::hphMX4*	This study
YTR608	BY4741	*smc6::kanMX4 pRS415-smc6-1*	This study
YTR613	BY4741	*smc5::kanMX4 pRS415-smc5-11*	This study
YTR633	BY4741	*GAL-3HA-SMC6:HIS bar1::URA pRS415-smc6-1*	This study
YTR718	AS499	*smc6-9:natMX4 Pol30-Myc-7his:KanMX4*	This study
YTR735	AS499	*POl30-Myc-7his:KanMX4*	This study
YTR737	AS499	*pol30-K127R-Myc-7his:KanMX4*	This study
YTR739	AS499	*pol30-K164R-Myc-7his:KanMX4*	This study
YTR755	AS499	*POL30-Myc-7his:KanMX4 rad5::hphMX4*	This study
YTR756	AS499	*POL30-Myc-7his:KanMX4 siz1::hphMX4*	This study
YTR774	BY4741	*rtt101::kanMX4*	EUROSCARF
YTR775	BY4741	*rtt107::kanMX4*	EUROSCARF
YTR778	BY4741	*top1::kanMX4*	EUROSCARF
YTR786	AS499	*nse5-2-9myc:TRP*	This study
YTR788	AS499	*nse3-2-9myc:TRP*	This study
YTR793	BY4741	*6his-Flag-SMT3:kanMX6 nse2ΔC::hphMX4 SMC5-9myc:HIS*	This study
YTR794	BY4741	*6his-Flag-SMT3:kanMX6 SMC5-9myc:HIS*	This study
YTR811	BY4741	*6his-Flag-SMT3:kanMX6 siz1::hphMX4 SMC5-9myc:HIS*	This study
YTR813	BY4741	*6his-Flag-SMT3:kanMX6 siz2::natMX4 SMC5-9myc:HIS*	This study
YTR823	BY4741	*6his-Flag-SMT3.kanMX6 siz1::natMX4 siz2::hphMX4 SMC5-9myc:HIS*	This study
YTR844	BY4741	*6his-Flag-SMT3:kan SMC6-9myc:TRP*	This study
YTR846	AS499	*6his-Flag-SMT3:kan NSE1-9myc:TRP*	This study
YTR848	AS499	*6his-Flag-SMT3:kan NSE6-9myc:TRP*	This study
YTR850	AS499	*6his-Flag-SMT3:kan NSE5-9myc:TRP*	This study
YTR852	AS499	*6his-Flag-SMT3:kan NSE2-9myc:TRP*	This study
YTR854	AS499	*6his-Flag-SMT3:kan NSE3-9myc:TRP*	This study

YTR856	BY4741	*6his-Flag-SMT3:kan NSE4-9myc:TRP*	This study
YTR896	AS499	*rad5::kanMX4*	This study
YTR907	W303	*6his-Flag-SMT3:kanMX4*	This study
YTR912	W303	*SMC5-9myc:TRP*	This study
YTR953	W303	*6his-Flag-SMT3:kanMX4 pSMC5p-SMC5:9myc*	This study
YTR954	W303	*6his-Flag-SMT3:kanMX4 pSMC5p-smc5(K-16-R):9myc*	This study
YTR1064	BY4741	*sae2::kanMX4*	EUROSCARF
YTR1065	BY4741	*apn1::kanMX4*	EUROSCARF
YTR1066	BY4741	*yen1::kanMX4*	EUROSCARF
YTR1067	BY4741	*rad2::kanMX4*	EUROSCARF
YTR1068	BY4741	*mph1::kanMX4*	EUROSCARF
YMB1072	W303	*6his-Flag-SMT3:kanMX4 pSMC5p-smc5(K-all-R):9myc*	This study
YMB1074	BY4741	*GAL-3HA-SMC5:kanMX4 pSMC5p-SMC5:9myc*	This study
YMB1075	BY4741	*GAL-3HA-SMC5:kanMX4 pSMC5p-smc5(wa K-R):9myc*	This study
YMB1076	BY4741	*GAL-3HA-SMC5:kanMX4 pSMC5p-smc5(h K-R):9myc*	This study
YMB1077	BY4741	*GAL-3HA-SMC5:kanMX4 pSMC5p-smc5(wb K-R):9myc*	This study
YMB1080	BY4741	*GAL-3HA-SMC5:kanMX4 pSMC5p-smc5(K-all-R):9myc*	This study
YMB1081	BY4741	*GAL-3HA-SMC5:kanMX4 YCplac22*	This study
YTR1089	BY4741	*dna2-1*	
YMB1110	BY4741	*6his-Flag-SMT3:kanMX6 nse2⊿C::hphMX4 NSE4-9myc:HIS*	This study
YMB1117	AS499	*6his-Flag-SMT3:kan SMC5-6HA:HIS*	This study
YMB1120	AS499	*6his-Flag-SMT3:kan nse5-2-9myc:TRP SMC5-6HA:HIS*	This study
YTR1154	AS499	*SCC1-GFP:kanMX4*	This study
YMB1156	AS499	*SCC1-GFP:kanMX4 smc6-9:natMX4*	This study
YTR1162		*MATalpha ade1-100 leu2,3-112 lys5 ura3-52 trp::hisG ho⊿ hml::ADE1 hmr::ADE1 ade3::GAL-HO DDC2-GFP:kanMX4*	L. Aragon's lab
YTR1172		*MATalpha ade1-100 leu2,3-112 lys5 ura3-52 trp::hisG ho⊿ hml::ADE1 hmr::ADE1 ade3::GAL-HO DDC2-GFP:kanMX4 smc5::smc5(cc1,cc2 K-R)-9myc:hphNT*	This study
YTR1178		*MATalpha ade1-100 leu2,3-112 lys5 ura3-52 trp::hisG ho⊿ hml::ADE1 hmr::ADE1 ade3::GAL-HO DDC2-GFP:kanMX4 SMC5-9myc:hphNT*	This study
YTR1268	W303	*top2-4:ADE2*	This study
CCG1297	AS499	*TetR-YFP:ADE2 TetO(5.6Kb):194Kb ChrXII:HIS3*	This study
CCG1298	AS499	*TetR-YFP:ADE2 TetO(5.6Kb):450Kb ChrXII:URA3*	This study
YMB1328	AS499	*nse5-2-9myc:TRP SMC5-6Flag:kanMX*	This study
YMB1330	AS499	*nse3-2-9myc:TRP SMC5-6Flag:kanMX*	This study
YMB1345	AS499	*nse3-2-9myc:TRP 6his-Flag-SMT3:kan SMC5-6HA:hphNT*	This study
YTR1355		*MATa ade2-1 ura3-1 his3-11,15 trp1-1 leu2-3,112 can1-100 ura3-1::ADH1-OsTIR1-9Myc:URA3*	YGRC
YTR1356		*MATa ade2-1 ura3-1 his3-11,15 trp1-1 leu2-3,112 can1-100 ura3-1::ADH1-OsTIR1-9Myc:URA3 MCM4-AID:kanMX*	This study
YMB1410	AS499	*NSE5-9myc:TRP SMC5-6Flag:kanMX*	This study

YMB1424	AS499	*NSE3-9myc:TRP SMC5-6Flag:kanMX*	This study
YMB1430	AS499	*nse3-2-9myc:TRP SMC5-6Flag:kanMX MMS21-6HA:HIS*	This study
YMB1432	AS499	*nse5-2-9myc:TRP SMC5-6Flag:kanMX MMS21-6HA:HIS*	This study
YTR1435	AS499	*SMC5-6HA:HIS 6his-Flag-SMT3:hphNT ura3-1::ADH1-Os-TIR1-9myc:URA3*	This study
YTR1444	BY4741	*GAL-3HA-SMC6:HIS bar1::URA 6his-Flag-SMT3:kanMX4 SMC5-9myc:TRP*	This study
YMB1446	AS499	*NSE5-9myc:TRP SMC5-6Flag:kanMX MMS21-6HA:HIS*	This study
YMB1448	AS499	*NSE3-9myc:TRP SMC5-6Flag:kanMX MMS21-6HA:HIS*	This study
YMB1452	AS499	*SMC5-6HA:HIS 6his-Flag-SMT3:hphNT ura3-1::ADH1-Os-TIR1-9myc:URA3 NSE4-AID:kanMX*	This study
YMB1454	AS499	*SMC5-6HA:HIS 6his-Flag-SMT3:hphNT ura3-1::ADH1-Os-TIR1-9myc:URA3 NSE5-AID:kanMX*	This study
YMB1456	AS499	*SMC5-6HA:HIS 6his-Flag-SMT3:hphNT ura3-1::ADH1-Os-TIR1-9myc:URA3 NSE6-AID:kanMX*	This study
YMB1458		*MATa ade1-100 leu2,3-112 lys5 ura3-52 trp1::hisG ho*Δ *hml::ADE1 hmr::ADE1 ade3::GAL-HO 6his-Flag-SMT3:hphNT SMC5-9myc:natNT*	This study
YMB1530	W303	*mre11::TRP 6HisFlag-SMT3:kanMX SMC5-9myc:HIS3*	This study
YMB1536		*MATa ade1-100 leu2,3-112 lys5 ura3-52 trp1::hisG ho*Δ *hml::ADE1 hmr::ADE1 ade3::GAL-HO 6his-Flag-SMT3:hphNT SMC5-9myc:natNT Rad52::LEU*	This study
YMB1556	BY4741	*GAL-3HA-SMC6:HIS bar1::URAca 6his-Flag-SMT3:kanMX4 SMC5-9myc:TRP pRS415-smc6-1*	This study
YMB1557	AS499	*ura3-1::ADH1-OsTIR1-9Myc:URA3 6his-Flag-SMT3:hphNT NSE2-AID:kanMX*	This study
YMB1606	W303	*rad53::HIS3 sml1-1 6HisFlag-SMT3:kanMX SMC5-9myc:HIS3*	This study
YMB1608	W303	*mec1::TRP 6HisFlag-SMT3:KanMX SMC5-9myc:HIS3*	This study
YMB1773	BY4741	*6his-Flag-SMT3:kan SMC6-9myc:TRP nse2*Δ*C::hphMX4*	This study
YMB1738	W303	*6his-Flag-SMT3:kanMX4 SMC5-9myc:TRP*	This study
CCG1761	AS499	*smc6-9:natMX4*	This study
YTR1766	BY4741	*6his-Flag-SMT3:kanMX6 SMC5-9myc:HIS mms21::mms21-3HA-UBC9:hphNT*	This study
YTR1768	BY4741	*6his-Flag-SMT3:kanMX6 SMC5-9myc:HIS mms21::mms21*Δ*C-3HA-UBC9:hphNT*	This study
CCG1800	AS499	*rad52::kanMX4*	This study
CCG1804	AS499	*smc6-9:His3MX6 rad52::kanMX4*	This study
YMB1815	BY4741	*6HisFLAG-SMT3::kanMX6 SMC5-9myc:HIS ESC2-6HA:natMX*	This study
YMB1817	BY4741	*ESC2-6HA:natMX*	This study
YM1830	BY4741	*GAL-3HA-SMC6:HIS bar1::URAca 6his-Flag-SMT3:kanMX4 SMC3-9myc:hphNT*	This study
YMB1839		*MATa ade1-100 leu2,3-112 lys5 ura3-52 trp1::hisG ho*Δ *hml::ADE1 hmr::ADE1 ade3::GAL-HO 6his-Flag-SMT3:hphNT SMC5-9myc:natNT esc2::kanMx*	This study

YMB1852		*MATa ade2-1 ura3-1 his3-11,15 trp1-1 leu2-3,112 can1-100 ura3-1::ADH1-OsTIR1-9Myc:URA3 6HisFLAG-SMT3:kanMX6*	This study
YMB1899	AS499	*ura3-1::ADH1-OsTIR1-9myc:URA3 6his-Flag-SMT3:KanMX NSE2-AID:hphNT SMC6-6HA:natNT*	This study
YMB1916	BY4741	*GAL-3HA-SMC5:kanMX bar1::URAca pADH1p-SMC5:9myc*	This study
YMB1917	BY4741	*GAL-3HA-SMC5:kanMX bar1::URAca pADH1p-smc5(cc1,cc2 K-R):9myc*	This study
YMB1918	BY4741	*GAL-3HA-SMC5:kanMX bar1::URAca pADH1p-smc5(cc1 K-R):9myc*	This study
YMB1919	BY4741	*GAL-3HA-SMC5:kanMX bar1::URAca pADH1p-smc5(cc2 K-R):9myc*	This study
YMB1920	BY4741	*GAL-3HA-SMC5:kanMX bar1::URAca pSMC5p-smc5(16-K-R):9myc*	This study
CCG1920	AS499	*TetR-YFP:ADE2 TetO(5.6Kb):194Kb ChrXII HIS3 smc6-9:natMX4*	This study
YMB1921	W303	*6his-Flag-SMT3:kanMX4 pSMC5p-SMC5:9myc*	This study
CCG1922	AS499	*TetR-YFP:ADE2 TetO(5.6Kb):450Kb ChrXII:URA3 smc6-9:natMX4*	This study
YMB1922	W303	*6his-Flag-SMT3:kanMX4 pSMC5p-smc5(wa K-R):9myc*	This study
YMB1923	W303	*6his-Flag-SMT3:kanMX4 pSMC5p-smc5(h K-R):9myc*	This study
YMB1924	W303	*6his-Flag-SMT3:kanMX4 pSMC5p-smc5(wb K-R):9myc*	This study
YMB1925	W303	*6his-Flag-SMT3:kanMX4 pADH1p-SMC5:9myc*	This study
YMB1926	W303	*6his-Flag-SMT3:kanMX4 pADH1p-smc5(cc1K-R):9myc*	This study
YMB1927	W303	*6his-Flag-SMT3:kanMX4 pADH1p-smc5(cc2K-R):9myc*	This study
YMB1928	W303	*6his-Flag-SMT3:kanMX4 pADH1p-smc5(cc1,cc2 K-R):9myc*	This study
YMB1937	BY4741	*GAL-3HA-SMC5:kanMX bar1::URAca 6His-Flag-SMT3:hphNT NSE4-6HA:NatMX pADH1p-SMC5:9myc*	This study
YMB1938	BY4741	*GAL-3HA-SMC5:kanMX bar1::URAca 6His-Flag-SMT3:hphNT NSE4-6HA:NatMX pADH1p-smc5(K75I):9myc*	This study
YMB1949	W303	*6his-Flag-SMT3:kanMX4 pADH1p-Smc5(K75I):9myc*	This study
YMB1950	AS499	*MMS21-3HA:HIS pADH1p-SMC5:9myc*	This study
YMB1951	AS499	*MMS21-3HA:HIS pADH1p-SMC5(K75I):9myc*	This study
YMB2045	BY4741	*GAL-3HA-SMC6:HIS bar1::URAca 6his-Flag-SMT3:kanMX4 SMC5-9myc:TRP MMS21-6HA:natNT*	This study
YMB2137	AS499	*ura3-1::ADH1-OsTIR1-9Myc:URA3 6HisFlag-SMT3:kanMX NSE2-AID:hphNT SMC6-6HA:NatNT pGALp-NSE2-3HA*	This study
YMB2138	AS499	*ura3-1::ADH1-OsTIR1-9Myc:URA3 6HisFlag-SMT3:kanMX NSE2-AID:hphNT SMC6-6HA:natNT pGALp-nse2(5BD):3HA*	This study
YMB2141	W303	*SMC5-9myc:TRP pGALpNSE2:3HA*	This study
YMB2142	W303	*SMC5-9myc:TRP pGALp-nse2(5BD):3HA*	This study

YMB2145	BY4741	*GAL-3HA-SMC5:kanMX bar1::URAca pADH1p-smc5(K75I):9myc*	This study
YMB2162	BY4741	*6his-Flag-SMT3:kanMX6 nse2ΔC::hphMX4 SMC1-6HA:NatNT*	This study
YMB2164	BY4741	*6his-Flag-SMT3:kanMX6 SMC3-6HA:NatNT*	This study
YMB2166	BY4741	*6his-Flag-SMT3:kanMX6 nse2ΔC::hphMX4 SMC3-6HA:NatNT*	This study
YMB2210	AS499	*MMS21-6HA:natNT*	This study
YMB2214	BY4741	*6his-Flag-SMT3:kanMX6 SMC1-6HA:NatNT*	This study
YMB2230	W303	*6his-Flag-SMT3:kanMX6 mms21::mms21-3HA-UBC9:hphNT pADH1p-SMC5:9myc*	This study
YMB2231	W303	*6his-Flag-SMT3:kanMX6 mms21::mms21-3HA-UBC9:hphNT pADH1p-smc5(K75I):9myc*	This study
YMB2266	AS499	*nse5-2-9myc:TRP 6His-Flag-SMT3:kanMx SMC3-6HA:NatNT*	This study
YMB2309	BY4741	*GAL-3HA-SMC6:HIS bar1::URAca 6his-Flag-SMT3:kanMX4 SMC5-9myc:TRP pRS415-smc6-1 NSE2-6HA:NatNT*	This study
YMB2315	BY4741	*6his-Flag-SMT3:kanMX6 SMC5-9myc:HIS NSE2-6HA:NatNT*	This study
CCG3227		*MATa ade2-1 trp1-1 can1-100 leu2-3, 112 his3-11,15 GAL psi+ura3::URA3/GPD-TK(7x) RAD5 p415-ADH hENT1::LEU2 bar1::natMX4*	L. Aragon's lab
CCG3229		*MATa ade2-1 trp1-1 can1-100 leu2-3, 112 his3-11,15 GAL psi+ura3::URA3/GPD-TK(7x) RAD5 p415-ADH hENT1::LEU2 bar1::natMX4 smc6-9:natMX4*	L. Aragon's lab
CCG8603	W303	*top2-4:ADE2 pRS316*	L. Aragon's lab
CCG9119	W303	*UBR1::pGAL-myc-UBR1 (HIS3), leu2::pCM244 x3 pRS316*	L. Aragon's lab
CCG9120	W303	*UBR1::pGAL-myc-UBR1 (HIS3), leu2::pCM244 x3 pRS316 kanMX-tTA-tetO2-UB-DHFRts-myc-top2*	L. Aragon's lab
CCG10435	W303	*smc6-9:natMX4*	L. Aragon's lab
CCG10542	W303	*UBR1::pGAL-myc-UBR1 (HIS3), leu2::pCM244 x3 pRS316 kanMX-tTA-tetO2-UB-DHFRts-myc-top2 smc6-9:natMX4*	L. Aragon's lab
CCG10649	W303	*top2-4:ADE2 pRS316 smc6-9:natMX4*	L. Aragon's lab

Table 1. Strains used in this study

3.1.2. Media

Yeast media were prepared according to standard recipes. Yeast extract peptone medium (YP; 1% yeast extract, 2% peptone) and synthetic complete minimal dropout medium (SC; 0.17% yeast nitrogen base without amino-acids and $(NH_4)_2SO_4$ (YNB-AA/AS), 0.5% $(NH_4)_2SO_4$, 0.13% dropout) were used. Solid plates were prepared adding agar powder at a final concentration of 2%. Media were autoclaved at 121ºC for 15 minutes before use.

Yeast strains were grown on different carbon sources, depending on the requirements: glucose (gluc), galactose (gal), or raffinose (raff), all at a final concentration of 2%, sterilized by filtration. Yeast cells were also grown on media containing 100 µg/ml nourseothricin, 300 µg/ml hygromycin B or 200 µg/ml geneticin to select for strains carrying *NAT*, *HPH* or *KAN* markers respectively. For liquid media and plates containing genotoxins, methyl methanesulfonate (MMS) or hydroxyurea (HU) was added at different final concentrations depending on the experiment.

3.1.3. Yeast growth conditions

Liquid cultures were generally inoculated at 25ºC from freshly streaked plates in flasks (with the volume of the flask approximately 5 times the volume of the culture), shaken at high speed (150 rotations per minute, rpm), generally overnight, until the culture reached mid-log phase. The culture density was photometrically determined (an OD_{600} of 1 is approximately equal to $3x10^7$ cells/ml). On agar plates, yeast cells were generally grown at 25ºC for 72 hours and stored at 4ºC for up to 3 weeks. For long-term storage, cells were frozen at -80ºC in media containing 15% glycerol.

3.1.4. Competent yeast cell preparation

Yeast competent cells were prepared using a modified version of the quick lithium acetate and freezing method described by Janke et al. (Janke et al., 2004): Briefly, cells from an exponentially growing culture (OD_{600} ≈0.4-0.8) were harvested at 3,000 rpm for 2 minutes, washed once in sterile distilled water and once in SORB buffer (100 mM lithium acetate, 10 mM Tris-HCl, 1 mM EDTA, 1 M sorbitol, adjusted to pH 8.0 with acetic acid). Then, cells were resuspended in SORB buffer (360 µl per 50 ml of original culture) and denatured salmon sperm DNA was added to a final concentration of 1 mg/ml. Finally, yeast competent cells were divided into 50 µl aliquots and they were frozen at -80ºC for long-term storage.

3.1.5. Yeast cell transformation

The yeast transformation method used was based on Janke et al. (Janke et al., 2004): either 0.2 µg of circular DNA or 1 µg of linear DNA were added to a 50 µl aliquot of yeast competent cells. Then, 300 µl of PEG buffer (100 mM LiOAc, 10 mM Tris-HCl, 1 mM EDTA, 40% PEG-3350, pH8.0) were added and the cell suspension was incubated for 30 minutes at room temperature. Then, DMSO was added to a final concentration of 10% and they were heat shocked at 42ºC for 15 minutes. Afterwards, cells were either resuspended in sterile distilled water and plated on selective media; or resuspended in YPD and incubated rocking at room temperature for approximately 3 hours before being plated on antibiotic resistance selective media.

3.1.6. Genomic integration for protein tagging or gene deletion

Insertions of epitope tags were performed as described by Janke et al. (Janke et al., 2004; Knop et al., 1999): Briefly, cassettes containing a selectable marker, and an appropriate epitope tag, were amplified using primers that will direct integration by homologous recombination at a specific locus (see below for list of primers). For gene deletions, a strain with the deleted gene was used from EUROSCARF (European *Saccharomyces cerevisiae* archive for functional analysis). After genomic DNA preparation (see below), the deletion was amplified with primers that anneal 400 bp away from the start and the selective marker, respectively. Finally, the PCR product was transformed into yeast to delete the endogenous locus.

Hypomorphic *smc5/6* alleles were generated by random mutagenesis PCR using the GeneMorph PCR mutagenesis Kit (from Stratagene) (Torres-Rosell et al., 2005). The *nse2ΔC* allele was obtained by introducing a stop codon after the position 552 (cys183) in the *NSE2* gene.

YIplac vectors (Gietz and Sugino, 1988) were used to integrate some constructs into the yeast genome. In order to allow homologous recombination, plasmids were linearized by site-specific cleavage in the auxotrophy marker before transformation.

Positive transformants in which the recombination event had occurred were checked by colony PCR, Western blot, growth tests or microscopy (described below).

3.1.7. Phenotype analysis by growth test on plates

Cells were generally inoculated in liquid media at 25ºC from freshly streaked plates until the culture reached mid-log phase. Then, 10-fold serial dilutions from $OD_{600}\approx1.0$ on fresh media were spotted (as 2 µl drops) onto solid media, incubated at the appropriate temperature for 3-4 days and then photographed.

3.1.8. Cell cycle synchronizations

In order to synchronize cells in G1, exponentially growing cultures were treated with alpha factor (from Genescript). For *BAR1+* strains, the final concentration used was 10^{-6} M and 10^{-8} M for *bar1Δ* cells. They were maintained in the presence of alpha factor until >95% had been arrested in G1. The release from alpha factor was conducted by washing cells twice with pre-warmed media and resuspending them in media containing 0.1 mg/ml protease from *S. griceus* (pronase; from Sigma), to digest the remaining alpha factor.

To arrest cells in metaphase, nocodazole (from Sigma) was used at a final concentration of 15 µg/ml in the presence of 1% DMSO. For prolonged metaphase arrests, the concentration of nocodazole was raised to 22.5 µg/ml. In order to release cells from the nocodazole arrest, cultures were washed twice with pre-warmed media and resuspended in media containing 1% DMSO.

3.2. General bacterial methods

3.2.1. Plasmids

A list of plasmids used in this study is provided in Table 2 below.

Name	Description	Reference
pTR927	*YCplac22-SMC5p-SMC5:9myc*	This study
pTR943	*YCplac22-SMC5p-smc5(K-16-R):9myc*	This study
pTR999	*YCplac22-SMC5p-smc5(wa K-R):9myc*	This study
pTR1000	*YCplac22-SMC5p-smc5(h K-R):9myc*	This study
pTR1002	*YCplac22-SMC5p-smc5(wb K-R):9myc*	This study
pTR1094	*YCplac22-ADH1p-SMC5:9myc*	This study
pMB1132	*YCplac22-SMC5p-smc5(K-all-R):9myc*	This study
pTR1150	*YCplac22-ADH1p-smc5(cc1 K-R):9myc*	This study
pTR1151	*YCplac22-ADH1p-smc5(cc2 K-R):9myc*	This study
pTR1152	*YCplac22-ADH1p-smc5(cc1,cc2 K-R):9myc*	This study
p1238	*YCplac22*	
pTR1621	*YCplac22-ADH1p-SMC5(K75I):9myc*	This study
p1787	*pRS315*	
p1788	*pRS316*	
pNC2275	*pRS315-GALp-MMS21:3HA*	This study
pNC2277	*pRS315-GALp-MMS21(5BD):3HA*	This study

Table 2. Plasmids used in this study

3.2.2. Bacteria growth conditions

E. coli cultures were grown either in Luria-Bertani broth (LB; 1% peptone, 0.5% yeast extract, 0.5% NaCl) at 37°C with high shaking (200 rpm) or on LB agar plates at 37°C. Bacteria on plates were stored at 4°C for up to 7 days. For long-term storage, cells were frozen at -80°C in media containing 20% glycerol.

3.2.3. *DH5*α competent cells transformation

Subcloning Efficiency™ *DH5*α competent cells (from Invitrogen) were generally used for bacterial transformation. 50 μl of cells were mixed with 1 to 5 μl (1-10 ng) of plasmid DNA and incubated on ice for 30 minutes. Then, cells were heat shocked for 20 seconds at 42°C, followed by 2 minutes incubation on ice. After this, 1 ml of pre-warmed LB media was added, and cells were incubated at 37°C for 1 hour at 225 rpm. Transformed cells were selected by plating the cell suspension on LB agar plates containing antibiotic (either 50 μg/ml ampicillin or 30 μg/ml kanamycin). Finally, cells were allowed to grow overnight at 37°C.

3.2.4. *MCD1061* competent cells transformation

The *E. coli MCD1061* strain was used to achieve DNA recombination between a plasmid and an insert within the cell. To prepare competent cells, 100 ml LB culture at $OD_{600} \approx 0.5$ were spun down at 6,000 rpm for 5 minutes at 4ºC and incubated in 10 ml of $CaCl_2$ buffer (60 mM $CaCl_2$, 10 mM HEPES, pH 7.0) on ice for 2 hours. After this, cells were spun down at 4,000 rpm for 4 minutes at 4ºC and resuspended in 2 ml of $CaCl_2$ buffer with glycerol (60 mM $CaCl_2$, 10 mM HEPES, 15% glycerol, pH 7.0). Finally, 300 μl aliquots were made and frozen at -80ºC.

5 to 10 μl (10-50 ng) of plasmid DNA and insert were added to an aliquot of competent cells and incubated on ice for 30 minutes. Then, cells were heat shocked for 2 minutes at 42°C, followed by 2 minutes incubation on ice. After this, 1 ml of pre-warmed LB media was added, and cells were incubated at 37°C for 1 hour. Transformed cells were selected by plating the cell suspension on LB agar plates containing antibiotic (either 50 μg/ml ampicillin or 30 μg/ml kanamycin). Finally, they were allowed to grow overnight at 37°C.

3.2.5. Positive clone selection by 'plasmid jet-prep'

Putative positive transformants were inoculated in 500 μl of LB media containing antibiotic overnight. Then, cells were harvested at 12,000 rpm for 2 minutes and all supernatant was removed. After this, 50 μl of lysis buffer (2% Triton™ X-100, pH 12.4) and 50 μl of phenol:chloroform (5:1) were added. Cells were shaken for 30 seconds and spun down at 12,000 rpm for 5 minutes. Afterwards, DNA was precipitated by adding 4 μl of 2% acetic acid, 4 μl of 3 M sodium acetate, 100 μl of 100% ethanol and spun down at 12,000 rpm for 5 minutes at RT. Finally, DNA was resuspended in 10 μl of sterile distilled water and checked by DNA restriction analysis (see below).

3.3. Cytological methods

3.3.1. Yeast fixation for microscopy

Cells were centrifuged at 12,000 rpm for 30 seconds and washed in ice-chilled distilled water. Then, cells were resuspended in 4% paraformaldehyde solution and incubated for 5 minutes at RT. After cell fixation, cells were washed once in potassium phosphate/sorbitol buffer (0.1 M K_2PO_4, 1.2 M sorbitol, pH 7.5) and resuspended in a small volume of potassium phosphate/sorbitol buffer. Fixed yeast cells were stored for up to 2 weeks at 4°C.

3.3.2. Optical and fluorescence microscopy

Yeast cells carrying green fluorescent protein (GFP)-tagged proteins were analyzed by fluorescence microscopy after DNA staining. DNA was stained using 4,6,-diamidino-2-phenylindole (DAPI) at a final concentration of 1 µg/ml in the presence of a mounting solution (Slow fade® Antifade, form Invitrogen) and 0.4% Triton™ X-100. For fluorescence microscopy, series of z-focal plane images were collected with a DP30 monochrome camera mounted on an upright BX51 Olympus fluorescence microscope. Image stacks were z-projected using the ImageJ software.

3.3.3. Flow cytometry analysis

To perform flow cytometry analysis, cells were fixed in 70% ethanol for at least 1 hour at room temperature. After cell fixation, cells were pelleted at 4,000 rpm for 2 minutes and resuspended in saline-sodium citrate buffer (SSC; 0.15 M NaCl, 15 mM sodium citrate, pH 7.0) plus 0.1 mg/ml RNAse A (from Qiagen) and incubated overnight at 50°C. Following RNA digestion, proteinase K (from Qiagen) was added at a final concentration of 0.1 mg/ml and cells were incubated for a further hour at 50°C. Then, cells were spun down at 3,000 rpm for 2 minutes and all the supernatant was removed. Finally, cell pellets were resuspended in SSC buffer containing 5 µg/ml propidium iodide and subsequently incubated in darkness at room temperature for at least 1 hour and stored for up to two weeks at 4°C. Before analysis, samples were sonicated for 8 seconds at power 10 in a Soniprep 150 sonicator (from MSE). Flow cytometric analyses were performed using a FACSCanto™ II flow cytometer (from BD). Finally, the WinMDI 2.9 software was used to represent the FACS profiles.

3.4. DNA methods

3.4.1. Primers

A list of primers used in this study is provided in Table3 below.

Number	Description	Sequence
CYO1201	5'-NotI-SMC5	GTAAGGCGGCCGCCATGACCAGTCTAATAGATTTGGGCA
CYO1202	3'-SacI-SMC5	AGGAATGAGCTCTTAATCGAATGAGTAGTTAGAAGTT
CYO1290	5'-KpnI-Smc5	GTAAGGGTACCATGACCAGTCTAATAGATTTGG
CYO1291	3'-XhoI-Smc5	AGAAGCTCGAGCATCGAATGAGTAGTTAGAAGTTT
CYO1353	SMC5-500	TTTAATTGGTATTGCTCGAACATCTAG
CYO1354	SMC5+500	AATAGGTAATTGTAAAGGGCTGTTCTC
CYO1355	SMC5(22)5'	ACCAGTCTAATAGATTTGGGCA
CYO1356	SMC5(622)5'	ATAAGGTCAATCGATGCAAGCT
CYO1357	SMC5(1411)5'	GAGGTCCGTGATGCTGTGTTGA
CYO1358	SMC5(1946)5'	CAAACTAATTTTTATCAGGGATC
CYO1359	SMC5(2706)5'	CGAACTGAGAGAGTTGGAGCAC
CYO1360	SMC5(3263)5'	ATGATACATTTCGGTGAAACTTC
CYO1361	SMC5(50)3'	CGATCTTGGCTCTGTATCTTCTC
CYO1362	SMC5(657)3'	TTGCAAGCTTTGCTCATTTCCT
CYO1363	SMC5(1413)3'	CATTTCTGGATGCTCTCTAACC
CYO1364	SMC5(1944)3'	CTGCTCATTTGACATGATTGAT
CYO1365	SMC5(2704)3'	CGACTGCTGAGGAACCGTGTG
CYO1366	SMC5(3256)3'	ATCGAATGAGTAGTTAGAAGTTTC
CYO1453	5'-ADH1p-SMC5	GAGAATTCATCGATGATAAAAGCTATATCCCTAGC
CYO1454	3'-ADH1p-SMC5	GATCCCGGCGAGCTCAAGCTTGGCGTAATCATGGT
CYO1734	SMC5(935)5'	CCATTTGCAAATACTAAGAAGAC
CYO1735	SMC5(913)3'	CTCTTCCACCTGATTTTCCAAAGTCTTCTTAGTATTTGCAAAT
CYO1736	SMC5(2380)5'	AATTTGAAGCCCAAAATATGGATG
CYO1737	SMC5(2409)3'	AAATCAGCTTCCCTCTCATTG
CYO1738	SMC5(1099)5'	TCATCAAAAAGAAAAACCAGAACGAATATTATAGAGGAAGAACCA
CYO1739	SMC5(1077)3'	TGGTTCTTCCTCTATAATATTCG
CYO1740	SMC5(2257)5'	AGATATTGATGATCAGATCCAAC
CYO1741	SMC5(2236)3'	ATGTCTTTGCTTGAGTAATAGTTGTTGGATCTGATCATCAATATC
CYO1753	SMC5(1090)5'	AAACCAGAACGAATATTATAGAG

CYO1754 SMC5(1110)3’	CTGTAGTTTTTTGGTTCTTCCTCTATAATATTC
CYO1755 SMC5kr(2285)3’	AGCAAATGTCTTTGtctGAGTAATAGTTGTTGGATC
CYO1756 SMC5kr(2710)5’	ACCATTTGCAAATACTAGAAG
CYO1757 SMC5kr(2734)3’	TCTTCCACCTGATTTTCCAAAGTTCTTCTAGTATTTGCAAATGGT
CYO1788 5’ SMC5 K75I	TTGGGCCAAACGGATCTGGGATATCTACTTTCGTATGCGCAGT
CYO1789 3’ SMC5 K75I	ACTGCGCATACGAAAGTAGATATCCCAGATCCGTTTGGCCCAA
CYO1795 S2-SMC5	CATCTATATGTGTATAATTAATTATGCAATAGTGAAAGAATCGATGAATTCGAGCTCG
CYO1804 5’ SMC5 D1014A	GAAATCAATCAAGGTATGGACTCTAG
CYO1805 3’ SMC5 D1014A	AGCAACCACTCTAAATGGTGCAGAG
CYO1836 S3-Smc5	AAGATGATACATTTCGGTGAAACTTCTAACTACTCATTCGATCGTACGCTGCAGGTCGAC
CYO1839 3’ SMC5 P305E	TTCTTTTTTATCCTTCAGTATAGCC
CYO1840 5’ SMC5 P305E	TTCGCAAATACTAAGAAGACTTTG
CYO1841 3’ SMC5 HLP393E-DLEL	TAGATCTGTTTGTGCTAATATTTCCTG
CYO1842 5’ SMC5 HLP393E	GAATTGAAAAGCGTATTTGAAGATATAGA
CYO1843 3’ SMC5 P271E	GAGTAGTTGGGAGTGTAACTC
CYO1844 5’ SMC5 P271E	GAGTATGTGAAAGTAAAGGACCA
CYO1875 3’ SMC5 P393E	TAGATGTGTTTGTGCTAATATTTCCTG
CYO1876 5’ SMC5 P393E	GAAGAGAAAAGCGTATTTGAAGATATAGA
CYO1047 Nse2(138)	TCAATTAGTGGATTCTACATCTCCT
CYO1048 Nse2+527	CCGCCTTTATGTATATCACTTTGAG
CYO1389 5’-XhoI-NSE2	GTAAGCTCGAGATGGCCTTGAACGATAATCCTAT
CYO1390 3’-XhoI-NSE2	AGAAGCTCGAGcTAAAACATCGATGGCTTGACTAC
CYO1430 S3-nse2Δc	ACGAAGACGATCTACAAATAGAAGGTGGTAAAATTGAATTGACTCGTACGCTGCAGGTCGAC
CYO1431 3’-XhoI-NSE2(480)	AGAAGCTCGAGcTACACAAGTTGGATCATTCCATA
CYO1432 5’-XhoI-NSE2(471)	GTAAGCTCGAGATGACTTGTGTAATACCGGATCTGCA
CYO1473 5’-KpnI-NSE2	GTAAGGGTACCATGGCCTTGAACGATAATCCTAT
CYO1490 3’-SacI-NSE2	AGAAGGAGCTCTAAAACATCGATGGCTTGACTACT
CYO1491 3’-SacI-NSE2(480)	AGAAGGAGCTCTACACAAGTTGGATCATTCCATAT
CYO1512 3’-KpnI-NSE2(480)	AGAAGGGTACCTACACAAGTTGGATCATTCCATA
CYO1513 3’-KpnI-NSE2	AGAAGGGTACCTAAAACATCGATGGCTTGACTAC
CYO1554 Nse2 (134)	AAACAAATTGATGAGACCAT
CYO1555 Nse2 3’ (ATG)	GGATTATCGTTCAAGGCCAT
CYO1621 NSE2(323)	CCTGTCCGCAAATCGACCTTTCTAC
CYO1622 NSE2(-471)	TGGATCATTCCATATGTACGGCAAC
CYO1692 NSE2 5’	AGGGAATATTAAGCTTGGTAC
CYO1693 NSE2 3’	GAGATGTAGAATCCACTAATTG
CYO1699 NSE2 M1 5’	CACCTGCAGCTCCAAAATCAGGTAAGTACTTCC
CYO1700 NSE2 M1 3’	CACTCTTAGCGATCGGATTATCGTTCAAGGCCATGG

CYO1701 NSE2 M2	GAGACGCTAGCAATATATATCAACAATGCTAC
CYO1702 NSE2 M2 3’	GAGCATGAGCATTATGGAAGTACTTACCTG
CYO1820 S2-ESC2	ACGTAAAGAGCCGGAGTTCGGCCTTTTTTAGCAAATTGCGCATCGATGAATTCGAGCTCG
CYO1821 S3-ESC2	CAGGATATGGAAGATGAAGACATGGTTGATGTCATTATTGATCGTACGCTGCAGGTCGAC
CYO1822 5’-ESC2 -334	CTCGAACAAAAAATGGAATGTTG
CYO1823 3’-ESC2 +314	AACCTAGCACGAAAAAGCTGAAG
CYO1831 5’ ESC2 -403	TTAGTTTTTAGGACATGAAACTGC
CYO1720 MRE11-254	CTAACAAAAACAAAGTCAGAGTTCAC
CYO1721 MRE11+314	TTGAATACTTTCCTATGCTCTTAATG
CYO1834 S2-SMC1	TTAGTTATTTGACGGGTTATAGCAGAGGTTGGTTTCATAGAATCGATGAATTCGAGCTCG
CYO1835 S3-SMC1	TCGTCGAAGATCATAACTTTGGACTTGAGCAATTACGCAGAACGTACGCTGCAGGTCGAC
CYO1818 S2-SMC3	CAAAACTGATATTTTTATATACAAATCGTTTCAAATATCTCATCGATGAATTCGAGCTCG
CYO1819 S3-SMC3	GCAATCGGATTCATTAGAGGTAGCAATAAATTCGCTGAAGTCCGTACGCTGCAGGTCGAC
CYO907 RAD5-289	CTGGACCTTTCTGCACGGATAA
CYO908 RAD5+282	TTCCACCTACACTTTCTGTCATAATG
CYO1125 RAD51-212	TACCCTATGCTACGCGTCATT
CYO1126 RAD51+211	TCATGGGTGACAGACAATACG
CYO1724 RAD52-274	TTGGCGTCTGTATCATCTGCT
CYO1725 RAD52+300	ATACAAATATGGCAACTCGGA
CYO 1073 SMT3+154	GGAAAGAGGCGTGGACAAAACTAT
CYO 1074 SMT3-222	TATGAATATGTTGGGTTACCCAGC
CYO913 RAD18-300	TTGCAGAAGAGGCAGGAAAAA
CYO914 RAD18+299	ACTTCTTTGCCTAATCCAGTGG
CYO915 RAD18-441	TAATCTGATGGATTCATCGCAAACG
CYO910 RAD6-294	GTGTGAGCTAACCATGCTTACACTA
CYO911 RAD6+301	AAAGATACGGGTATCGGCAGTTA
CYO912 RAD6-462	AAGCGGTCTTTTAGATACAAGCTTG
CYO901 MMS2-263	GTCCACTCAATGCACTGAAGAA
CYO902 MMS2+269	GCAACAGTCTTTCTGTCGTCTGTTT
CYO903 MMS2-417	TGTAACGCCTGAATCTGACGATTAC
CYO1724 RAD52-274	TTGGCGTCTGTATCATCTGCT
CYO1725 RAD52+300	ATACAAATATGGCAACTCGGA
CYO1821 S3-NSE6	GTTGAAATTTCTATCCTGAAGGGAATATTAAATTTGTTTTCTAAAATCAGGCGTACGCTGCAGGTCGAC
CYO1822 S2-NSE6	CAGTCAACTGGTCAAATCAACAGATCAATGTTCAGTCATCATGACTGTTAATCGATGAATTCGAGCTCG
CYO1823 S3-NSE2	AAAGAATCTCAGGAACAGGATAAAAGAAGTAGTCAAGCCATCGATGTTTTACGTACGCTGCAGGTCGAC

CYO1824 S2-NSE2	GAACTTCGGGCCGAAGGGCTCGGATAAGAGAAACAATAATTTTGTTTTCAATCGATGAATTCGAGCTCG
CYO1825 S3-NSE4	ACTTGGCGAAAACTAATAAAGAAATACAACATCACTTCACCATTCTTAGACCGTACGCTGCAGGTCGAC
CYO1826 S2-NSE4	AAAAAAAAAAAAAAACTGTACATATTATATGCAGCGCTCTATCGCTGTTAATCGATGAATTCGAGCTCG

Table 3. List of primers used

3.4.2. Isolation of plasmid DNA from *E. coli*

Single colonies were either streaked on LB plates or inoculated in LB liquid media containing antibiotic overnight. To extract plasmid DNA, the GenElute™ Plasmid Miniprep Kit (from Sigma) was used following the manufacturer's instructions.

3.4.3. Isolation of genomic DNA from *S. cerevisiae*

Isolation of genomic DNA from *S. cerevisiae* was performed as described by Hoffman, Cs (Hoffman, 2001) with minor modifications: approximately 5 OD_{600} of cells were washed in ice-chilled distilled water and resuspended in 200 µl of breaking buffer (2% Triton™ X-100, 10 mM Tris-HCl, 1% SDS, 1 mM EDTA, 100 mM NaCl, pH 8.0,), 200 µl of phenol:chloroform (5:1) and 200 µl of glass beads. Cells were vortexed for 4 minutes at RT. Then, 200 µl of Tris-EDTA buffer (TE; 10 mM Tris-HCl, 1 mM EDTA, pH 8.0) were added and cells were spun down at 13,000 rpm for 5 minutes at RT to clear the cell suspension. The clean upper phase was transferred to a clean eppendorf tube and 1 ml of ice-chilled 100% ethanol was added to precipitate DNA. The mixture was placed on ice for 20 minutes to increase DNA precipitation. Then, DNA was spun down at 13,000 rpm for 5 minutes at 4ºC and the supernatant was removed. The DNA pellet was resuspended in 400 µl of TE buffer and 3 µl of 10 mg/ml RNAse A were added and incubated at 37ºC for 5 minutes to digest RNA. DNA was precipitated by adding 6.5 µl of ammonium acetate 6.2 M and 1 ml of ice-chilled 100% ethanol. The DNA extract was placed on ice for 20 minutes and spun down at 13,000 rpm for 5 minutes at 4ºC. The DNA pellet was washed with ice-chilled 70% ethanol and spun down at 13,000 rpm for 5 minutes. Finally, the DNA pellet was air dried, resuspended in 100 µl of TE buffer and stored at 4ºC.

3.4.4. Polymerase chain reaction (PCR)

The Expand High Fidelity PCR System (from Roche) was generally used. 2.6 U (0.75 µl) enzyme per 50 µl reaction were used with 1.5 mM $MgCl_2$, 200 µM dNTPs and 300 µM primers. For products with high GC content, DMSO was added to a final concentration of 5%. The thermal cycles used were: initial denaturation step of 94ºC for 3 minutes; followed by amplification cycles at 94ºC for 30 seconds (denaturation), 52-65ºC (depending on the melting temperature of the primers) for 30 seconds (annealing), 1 minute/kb either at 72ºC (for PCR products up to 3 kb) or at 68ºC (for PCR products larger than 3 kb) (elongation); repeated 10 times. For the next 25 cycles, 5 seconds were added in each successive elongation cycle. A final elongation step was performed at 72ºC for 10 minutes.

3.4.5. Yeast colony PCR

The SupraTherm™ Taq DNA Polymerase (from Genecraft) was used to perform yeast colony PCR. 1 U (0.2 µl) enzyme per 20 µl reaction was used with 2 mM $MgCl_2$, 200 µM dNTPs and 500 µM primers. Colonies were picked into a PCR tube and microwaved at 1,200 watts for 30 seconds and placed on ice for 30 seconds. Then, 20 µl of SupraTherm™ mix were added to the PCR tube and vortexed. The thermal cycles used were: initial denaturation step of 94ºC for 5 minutes; followed by amplification cycles at 94ºC for 30 seconds (denaturation), 52-60ºC (depending on the melting temperature of the primers) for 30 seconds (annealing), 1 minute/Kb at 72ºC (elongation); repeated 35 times. A final elongation step was performed at 72ºC for 10 minutes.

3.4.6. Site-directed mutagenesis

The QuikChange XL Site-Directed Mutagenesis Kit (from Stratagene) was used to perform site-directed mutagenesis. Briefly, the desired mutation was incorporated into primers (designed using the QuikChange Primer Design programme available at http://www.stratagene.com/qcprimerdesign. Incorporation of the primers during PCR generates a mutated plasmid containing staggered nicks. PCR was performed using the standard reaction mix containing 50 ng of template DNA and 125 ng of each primer. The thermal cycles used were: initial denaturation step of 95ºC for 30 seconds; followed by amplification cycles at 95ºC for 30 seconds (denaturation), 55ºC for 1 minute (annealing), 1 minute/kb at 68ºC (elongation) repeated 12-18 times.

Following PCR amplification, parental DNA (not containing the mutation) was digested by the addition of 1 µl *DpnI* (10 U/µl), an enzyme that specifically digests methylated and hemimethylated DNA, and incubated for 1 hour at 37ºC. The nicked vector containing the desired mutation was then transformed into XL10-Gold Ultracompetent® cells (provided with the kit). 2 µl of the digested PCR mix were added to 50 µl of competent cells that had been previously treated with β-mercaptoethanol. The mixture was incubated on ice for 30 minutes, and then heat shocked at 42ºC for 30 seconds. Afterwards, cells were immediately chilled on ice for 2 minutes before being resuspended in 1 ml of LB media and allowed to grow for 1 hour at 37ºC. Finally, cells were plated onto LB plates containing antibiotic (either 50 μg/ml ampicillin or 30 μg/ml kanamycin) and they were allowed to grow overnight at 37ºC.

3.4.7. DNA restriction analysis

Restriction enzymes were used for sequence-specific cleavage of DNA. To digest 1 μg of DNA, 1 μl of restriction enzyme (10 units) was usually used. The reaction conditions were chosen according to the manufacturer's instructions. Samples were incubated at the recommended temperature for either 2 hours or overnight in a total reaction volume of 50 μl.

3.4.8. Separation of DNA fragments by gel electrophoresis

Ficoll loading buffer (FLB; 0.25% Bromophenol Blue, 0.25% xylene cyanol, 25% ficoll-400) was added to DNA samples and they were run on 0.8-2% agarose gels (depending on the size of the DNA fragments) in Tris-acetate EDTA buffer (TAE; 40 mM Tris-HCl, 20 mM acetic acid, 1 mM EDTA, pH 8.0) at 5 V/cm (distance between the electrodes of the unit). After gel electrophoresis, DNA was stained in 1 μg/ml ethidium bromide solution for 20-30 minutes and visualized using an UV transilluminator.

3.4.9. Purification of DNA fragments from agarose gels

To visualize the DNA, 1 μl of 1/100 dilution of SYBR® Green I Nucleic Acid Gel Stain (from Invitrogen) was added per 1 μg DNA. After separating the DNA fragments by gel electrophoresis (see previous section), the DNA fragment was excised from the gel using a clean scalpel and purified using the QIAquick Gel Extraction Kit (from Qiagen) following the manufacturer´s instructions.

3.4.10. Ligation of DNA fragments

Digested inserts were ligated into digested and dephosphorylated vectors using the Rapid DNA Dephos and Ligation kit (from Roche), which enables fast and efficient dephosphorylation and ligation of sticky and blunt-end DNA. For standard ligation reactions, the molar ratio of vector to insert was 1:3. The protocol was performed following the manufacturer´s instructions.

3.4.11. DNA sequencing

DNA sequencing reactions were carried out by Servei cientificotècnic de Proteòmica i genòmica (SCT-P&G) of the University of Lleida, Spain.

3.4.12. Chromatin Immunoprecipitation

Chromatin immunoprecipitation experiments were performed according to Nelson et al. (Nelson et al., 2006) with minor modifications: 50 ml of culture at $OD_{600} \approx 0.5$ were fixed with formaldehyde at a final concentration of 1.42% for 15 minutes at room temperature. Then, formaldehyde was quenched with glycine at a final concentration of 125 mM for 5 minutes at room temperature and cells were harvested by centrifugation at 4,000 rpm for 2 minutes. The pellet was washed with phosphate buffered saline buffer (PBS; 137 mM NaCl, 2.7 mM KCl, 10 mM Na_2HPO_4, 2 mM KH_2PO_4, pH 7.4), transferred to a screw cap tube, frozen in liquid nitrogen and stored at -80°C.

Pellets were resuspended in 100 µl of immunoprecipitation buffer (IP buffer; 150 mM NaCl, 50 mM Tris-HCl pH 7.5, 5 mM EDTA pH 8.0, 0.5% NP-40, 1% Triton™ X-100) supplemented with PMSF at a final concentration of 1 mM and complete protease inhibitor cocktail (from Roche). Then, 500 µl of glass beads were added and cells were lysed by two 20 seconds cycles at power 6.5 in a FastPrep® FP120 machine, with 5 minutes on ice in between cycles. Afterwards, 300 µl of IP buffer containing PMSF and protease inhibitors were added. Tubes were pierced with a hot needle and placed on top of new eppendorfs and spun down at 1,000 rpm for 2 minutes at 4°C to collect lysate minus glass beads. Samples were pelleted at 13,000 rpm for 1 minute at 4°C. The nuclear pellet was resuspended thoroughly in 1 ml of IP buffer containing PMSF and protease inhibitors. Then, chromatin was sonicated for 1 hour (15 seconds ON, 15 seconds OFF at high power in a Diagenode Biorupter. At this point, sonicated chromatin can be stored at -80°C.

20 µl (30% of sample) were taken for input and 400 µl for IP. After clarification at 13,000 rpm for 1 minute at 4°C, input DNA was precipitated from the supernatant by the addition of KOAc to a final concentration of 0.3 M and 2.75 volumes of 100% ethanol. The mixture was incubated at -20°C overnight, spun down at 13,000 rpm for 5 minutes and the supernatant discarded. 100 µl of 10% Chelex® 100 suspension (from BioRad) were added to the dried pellet and the sample boiled for 20 minutes. The supernatant was cleaned using the PCR purification kit (from Qiagen) according to the manufacturer´s instructions, eluted in 250 µl of sterile distilled water and stored at -20°C.

2 µg of antibody (from Roche) were added to 400 µl of chromatin for the IP, and

samples were incubated in an ultrasonic water bath for 30 minutes at 4°C. After clarification at 13,000 rpm for 2 minutes at 4°C, the supernatant was added to 100 µl of 50:50 slurry of Protein G beads (from Roche), which had been previously equilibrated in IP buffer. Beads were incubated overnight on a rotating platform at 4°C. Then, they were washed 3 times in IP buffer, and 250 µl of 10% Chelex® 100 suspension (from Bio-Rad) were added and boiled for 20 minutes. After spinning down at 13,000 rpm for 1 minute, the supernatant was transferred into a fresh tube and stored at -20°C. Finally, the relative occupancy of the immunoprecipitated factor was analysed by real time PCR (see below).

3.4.13. Real time PCR analysis

PCR reactions were performed using the SensiMix™ NoRef Kit (from Quantace). Reactions were carried out according to the manufacturer´s instructions in a total volume of 20 µl, containing either 3 µl of Input or IP DNA and oligonucleotide primer pairs at a final concentration of 1.5 µM. DNA amplification was performed with the CFX96™ Real-time-system (from Bio-Rad) and analyzed using the CFX manager™ software (from Bio-Rad).

The primers used for the analysis of an induced HO-break at the MAT locus were previously described by Shroff et al. (Shroff et al., 2004). The melting curve of each primer pair was analysed to confirm the absence of contaminant PCR products. The relative occupancy of the immunoprecipitated factor at the locus was estimated using the following equation: $2^{(CtIP\text{-}CtInput)}$, where CtIP and CtInput are mean threshold cycles of PCR done in triplicate on Input and IP DNA samples, respectively.

3.4.14. Pulsed field gel electrophoresis

Pulsed field gel electrophoresis (PFGE) was performed as described by Lengronne, A et al. (Lengronne et al., 2001) with minor modifications: A volume of cell culture containing 7 OD_{600} of yeast was taken for each time point. Cells were pelleted and washed twice with 50 mM EDTA pH 8.0 and resuspended in 50 µl of 50 mM EDTA pH 8.0, 100 µl of solution 1 (1 M sorbitol, 0.06 M EDTA pH 8.0, 0.1 M sodium citrate, 0.5% β-mercaptoethanol, 1 mg/ml zymolyase 100T) and 300 µl of 1% low melting point agarose (from Sigma), tempered at 50ºC. Then, the mixture was immediately poured into 4 PFGE moulds. Following polymerization at room temperature, plugs were displaced from their moulds into 1,6 ml of Buffer 2 (0.45 M EDTA pH 8.0, 7.5% β-mercaptoethanol, 0.01 M Tris-HCl pH 7.0, 10 µg/ml RNAse A) and incubated overnight at 37°C in order to degrade the cell wall. Then, all buffer was removed and plugs were incubated in 1,6 ml of PK buffer (10 mM Tris-HCl pH 7.5, 250 mM EDTA pH 8.0, 1% sarcosyl, 1 mg/ml Proteinase K) at 37°C overnight. After proteinase K treatment, plugs were washed and 1,6 ml of storage solution (0.05 M

EDTA pH 8.0, 50% glycerol) were added. Plugs were stored at 4°C for up to 3 months.

PFGE was run in 0.5x Tris-borat-EDTA buffer (TBE; 89 mM Tris-base, 89 mM boric acid, 2 mM EDTA, pH 8.0) for 24 hours at 6 V/cm (initial switching time: 60 seconds; final: 120 seconds). After DNA electrophoresis, gels were stained in 1 μg/ml ethidium bromide solution for 20 minutes and DNA was visualized using an UV transilluminator.

3.4.15. DNA combing

Chromosome combing was performed by Dr. Audrey Ceschia in Dr Pasero's lab (Montpellier) as described in Tourriere et al. (Tourriere et al., 2005) with minor modifications: Cells were embedded in agarose moulds and genomic DNA was purified as for pulse field gel electrophoresis (see above). Then, chromosomal DNA was resuspended in 50 mM 2-(N-morpholino) ethanesulfonic acid (MES) pH 5.5 at a final concentration of 200 ng/ml in a Teflon reservoir. Silanized coverslips were dipped into the DNA solution for 5 minutes and pulled out at a constant speed (0.3 mm/sec). Then, coverslips were baked at 60°C overnight, mounted on microscope slides and stored at −20°C until use. Coverslips were incubated for 30 minutes in 1 M NaOH to denature the DNA and they were neutralized in phosphate-buffered saline buffer (PBS; 137 mM NaCl, 2.7 mM KCl, 10 mM Na_2HPO_4, 2 mM KH_2PO_4, pH 7.4. Then, coverslips were washed with 2x saline-sodium citrate buffer (SSC; 0.3% sodium chloride, 30 mM trisodium citrate, pH 7.0) supplemented with 50% formamide and they were subsequently processed for immunofluorescence. BrdU was detected with a rat monoclonal antibody (clone BU1/75; from AbCys) and a secondary antibody coupled to Alexa Fluor 488 (from Molecular Probes). DNA molecules were counterstained with an anti-guanosine antibody (from Argene) and an anti-mouse IgG coupled to Alexa Flour 546 (from Molecular Probes). Replication gaps were scored as regions positive for the anti-guanosine signal but negative for the anti-BrdU one. The length of DNA fibres was measured using lambda phage DNA molecules as standard.

3.4.16. 2D gels for X-shaped DNA molecules detection

Total genomic DNA was isolated mainly according to Allers, T. and Lichten, M. (Allers and Lichten, 2000) with some modifications: 200 ml culture OD_{600}≈0.4 were arrested by addition of sodium azide at a final concentration of 0.1% and cooled down in ice. Cells were harvested by centrifugation, washed in ice-chilled water, and incubated in spheroplasting buffer (1 M sorbitol, 100 mM EDTA pH 8.0, 0.1% β-mercaptoethanol, 100 U zymoliase/ml) for 20 minutes at 37°C. Once yeast cells were spheroplasted, cells were spun down at 4.000 rpm for 10 minutes at 4°C. Then, 2 ml of water, 200 μl of 100 mg/ml RNAse A, and 2.5 ml of Solution I (2% cetyl-trimethyl-ammonium-bromide (CTAB), 1.4 M NaCl, 100 mM Tris-HCl pH 7.5, and 25 mM EDTA pH 8.0) were sequentially added to the spheroplasted pellet and samples were incubated for 30 minutes at 50°C. Afterwards, 200 µl of 20 mg/ml Proteinase K were added and the incubation was prolonged at 50°C for 1 hour 30 minutes. Then, samples were centrifuged at 4,000 rpm for 10 minutes and the cellular debris pellet was kept for further extraction, while the DNA present in the supernatant was extracted with 2.5 ml of chloroform/isoamylalcohol (24:1). DNA was precipitated by addition of 2 volumes of Solution II (1% CTAB, 50 mM Tris-HCl pH 7.5, and 10 mM EDTA pH 8.0) and centrifuged at 12,000 rpm for 10 minutes. Pellet was resuspended in 2 ml of Solution III (1.4 M NaCl, 10 mM Tris-HCl pH 7.6, and 1 mM EDTA pH 8.0). Residual DNA in the cellular debris pellet was also extracted by resuspending in 2 ml of Solution III and incubating at 50°C for 30 minutes, followed by extraction in 1 ml of chloroform/isoamylalcohol (24:1). The upper phase was pooled together with the main DNA preparation. Then, total DNA was precipitated with 1 volume of isopropanol, washed with 70% ethanol, air dried, and finally resuspended in Tris-EDTA buffer (TE; 10 mM Tris-HCl, 1 mM EDTA, pH 8.0).

After purification, DNA concentration was determined, digested with *HindIII* and *EcoRV* and separated by electrophoresis. 2D gel electrophoresis was carried out as originally described by Brewer B.J. and Fangman W.L. (Brewer and Fangman, 1987) using the following conditions: first dimension: 0.4% agarose gel in 1x Tris-borat-EDTA buffer (TBE; 89 mM Tris-base, 89 mM boric acid, 2 mM EDTA) run at 0.6 V/cm for 24 hours at room temperature. For the second dimension, the dissolved agarose was poured around the excised agarose lane from the first dimension and run in 1% agarose gel in TBE buffer supplemented with 0.3 µg/ml ethidium bromide at 3 V/cm for 11 hours at 4°C. Finally, DNA molecules present in the *ARS305* were detected by Southern blot (See below).

3.4.17. 2D gels for catenated plasmid detection

DNA extraction for catenated plasmid analysis was performed as described by Baxter et al. (Baxter et al., 2011): a volume of cell culture containing 30 OD_{600} of yeast was taken for each time point. Frozen pellets were resuspended in lysis buffer (50 mM Tris-HCl, 100 mM NaCl, 10 mM EDTA, 1% SDS, pH 8.0) and the cell wall was digested by incubation with 80 units of lyticase (from Sigma) and 1% β-mercaptoethanol at 37°C for 5 minutes. Then, DNA was extracted with phenol/chloroform/isoamylalcohol (25:24:1) and the aqueous layer collected using phase lock tubes (from 5 prime) by spinning down at 12,000 rpm for 10 minutes at RT. DNA was precipitated with 2 volumes of 100% ice-chilled ethanol and washed with 70% ethanol before being re-solubilized in 10 mM Tris-HCl, pH 8.0.

Neutral-neutral two-dimensional (2D) gel electrophoresis was carried out as described by Martinez-Robles M.L. et al. (Martinez-Robles et al., 2009): the first dimension was performed in a 0.4% agarose gel in 1x Tris-borat-EDTA buffer (TBE; 89 mM Tris-base, 89 mM boric acid, 2 mM EDTA) run at 0.9 V/cm at room temperature for 24 hours. The second dimension was performed in a 1% agarose gel in TBE buffer, run perpendicular with respect to the first dimension. The dissolved agarose was poured around the excised agarose lane from the first dimension and run at 4.5 V/cm in a cold chamber for 15 hours. The different forms of the *pRS316* plasmid were detected by Southern blot (see below).

3.4.18. Southern blot

Agarose gels were prepared for Southern blot by incubating the gels in depurinating solution (0.125 M HCl) for 15 minutes, in denaturing solution (0.4 M NaOH, 1 M NaCl) for 30 minutes and finally in neutralizing solution (1.5 M NaCl, 0.5 M Tris-HCl, pH 7.5) for 30 minutes. After these incubations, DNA was transferred onto a positively-charged nylon membrane (Hybond-N+; from GE Healthcare) via upward capillary transfer in 20x sodium citrate buffer (SSC; 3 M NaCl, 300 mM Sodium citrate, pH 7.0). Then, DNA was immobilized by UV irradiation using the autocrosslinking function of the UV Stratalinker 2400 (from Stratagene) and washed in 5x SSC.

DNA probes were amplified by PCR either from wild type genomic DNA or plasmids, and purified using the QIAquick PCR Purification Kit (from Qiagen). 500 ng of DNA were labelled with fluorescein-12-dUTP with the Fluorescein-High Prime labelling system (from Roche). Then, labelled probe was boiled for 5 minutes and chilled on ice. Membranes were blocked in blocking solution (0.1% SDS, 5% dextran sulphate, 5% Rapid-Hyb (from GE Healthcare) in 5X SSC buffer) for 1 hour, and then they were hybridized with the probe overnight at 60°C.

Blots were washed twice in 1x SSC with 0.1% SDS at 60ºC for 10 minutes and twice in 0.5X SSC with 0.1% SDS at 60°C for 10 minutes. After a brief wash in antibody buffer (AB; 150 mM NaCl, 100 mM Tris-HCl, pH 7.5), blots were blocked in AB buffer plus 1% dried skimmed milk for 1 hour at room temperature with gentle agitation and then incubated for 1 hour with alkaline phosphatase conjugated anti-fluorescein F(ab)2 antibody (dilution 1:250,000; from Roche) in AB buffer plus 0.5% dried skimmed milk. Afterwards, blots were washed three times in AB buffer plus 0.2% Tween® 20 for 10 minutes each. After washes, membranes were incubated with the CDP-Star™ reagent (from GE Healthcare) followed by exposure to high performance chemiluminescence films (Amersham hyperfilm™ ECL from GE Healthcare), to detect the signal.

3.5. Protein methods

3.5.1. Protein extraction under denaturing conditions

Yeast protein extracts were prepared under denaturing conditions as described by Gallego, C et al. (Gallego et al., 1997): briefly, 5 OD_{600} were used for Western blot analysis. 15 µl of 5 M urea were added and immediately boiled for 2 minutes. After addition of an equal volume of glass beads, cell suspension was broken by one 45 seconds cycle at power 5.5 in FastPrep® FP120 machine. Then, 50 µl of SR buffer (2% SDS, 0.125 M Tris–HCl, pH 6.8) were added, vortexed, boiled for 2 minutes and centrifuged at 12,000 rpm for 2 minutes at RT. The protein concentration in the supernatants was determined by a Micro DC protein assay (from Bio-Rad). After protein quantification, loading buffer at a final concentration of 125 mM Tris-HCl pH 6.8, 5% sacarose, 0.0125% bromophenol blue, 0.025% sodium azide, 2% SDS supplemented with 4% β-mercaptoethanol was added. Finally, samples were boiled at 95ºC for 2 minutes and loaded onto a SDS-PAGE gel and analysed by Western blot (see below).

3.5.2. Post alkaline protein extraction

Post alkaline protein extraction was performed based on Kushnirov, V.V et al. (Kushnirov, 2000) for rapid protein extraction, such as checking transformants by Western blot: 2.5 OD_{600} of cells were harvested by centrifugation from liquid culture or scraped off from an agar plate and resuspended in 100 µl of sterile distilled water. Then, 100 µl of 0.2 M NaOH were added, and they were incubated for 5 minutes at room temperature. Afterwards, cells were pelleted at 13,000 rpm for 30 seconds and resuspended in 50 µl of 2x SSR buffer (10% sacarose, 0.025% bromophenol blue, 0.05% sodium azide, 4% SDS, 250 mM Tris-HCl, pH 6.8) supplemented with 4% β-mercaptoethanol. Then, samples were boiled at 95ºC for 3 minutes and pelleted at 12.000 rpm for 2 minutes. Finally, the supernatant was loaded onto a SDS-PAGE gel and analysed by Western blot (see below).

3.5.3. SUMO and SUMO-conjugates purification

Pull-down experiments were performed as previously described by Sacher, M et al. (Sacher et al., 2005) with minor modifications: Briefly, 200 OD_{600} of cells were harvested at 4,000 rpm for 2 minutes, washed once with ice-chilled water, and the cell pellet frozen at -80ºC. Cells were resuspended in 500 µl of Buffer A (8 M Urea, 100 mM KH_2PO_4, 10 mM Tris-HCl, 0.05% Tween® 20, pH 8.0), an equal volume of glass beads was added, and cells were lysed by one 45 seconds cycle at power 5.5 in a FastPrep® FP120 machine. Then, tubes were pierced with a hot needle and placed onto new eppendorfs and spun down at 1,000 rpm for 2 minutes to collect cell lysate minus glass beads. Cell lysate was clarified by centrifugation at 14,000 rpm for 10 minutes at 4ºC. Protein concentration was determined using a Micro DC protein assay (from Bio-Rad). Afterwards, cell extract was scaled up to 5 ml in buffer A and 50 µl of Ni-NTA beads (from Qiagen) were added. To reduce non-specific binding, imidazole was added to a final concentration of 15 mM. Proteins were bound overnight at 4ºC on a rotating platform. After binding, beads were washed 3 times in Buffer A containing 2 mM imidazole, followed by 5 washes in Buffer B (8 M Urea, 100 mM KH_2PO_4, 10 mM Tris-HCl, 0.05% Tween, pH 6.3). Bound proteins were eluted from the beads using 25 µl of 2x SSR buffer (10% sacarose, 0.025% bromophenol blue, 0.05% sodium azide, 4% SDS, 250 mM Tris-HCl, pH 6.8) supplemented with 4% β-mercaptoethanol; boiled at 95ºC for 2 minutes. Eluates were loaded onto SDS-PAGE gels and analysed by Western blot (see below). In all cases, SUMO pull-downs were loaded next to protein extracts to confirm the slower mobility of SUMO conjugates with respect to the unmodified protein.

3.5.4. Co-immunoprecipitation

Myc-tagged proteins were immunoprecipitated using anti-Myc antibodies (9E10; from Roche) coupled to protein G Dynabeads (from Invitrogen). HA-tagged and Flag-tagged proteins were immunoprecipitated using anti-HA Affinity matrix (from Roche) and Anti-FLAG® M2 Affinity Gel (from Sigma), respectively.

Co-immunoprecipitation experiments were performed based on Arumugam et al. (Arumugam et al., 2003) with minor modifications: 100 OD_{600} of cells were harvested at 4,000 rpm for 2 minutes, washed once with ice-chilled water, and cell pellet frozen at -80ºC. Cells were resuspended in 500 µl of pre-chilled lysis buffer (50 mM HEPES, 150 mM KCl, 1.5 mM $MgCl_2$, 0.5 mM DTT, 0.5% Triton™ X-100, pH 7.5) supplemented with Complete protease inhibitor cocktail tablets (from Roche), and an equal volume of glass beads was added. Then, cells were lysed by one 45 seconds-cycle at power 5.5 in a FastPrep® FP120 machine. Tubes were pierced with a hot needle and placed onto new eppendorfs and spun down at 1,000 rpm for 2 minutes to collect cell lysate minus glass beads. Afterwards, cell lysate was clarified by centrifugation at 14,000 rpm for 10 minutes at 4ºC and protein concentration was determined using a Micro DC protein assay (from Bio-Rad). Then, 30 µl of beads were added to the lysate and the suspension was incubated for 2 hours at 4ºC. After protein binding, beads were washed with IPP150 buffer (10 mM Tris-HCl, 150 mM NaCl, 0.1% Triton™ X-100, pH 7.5) three times and eluted in 40 µl of 2x SSR buffer (10% sacarose, 0.025% bromophenol blue, 0.05% sodium azide, 4% SDS, 250 mM Tris-HCl pH 6.8) supplemented with 4% β-mercaptoethanol; boiled at 95ºC for 2 minutes. Finally, eluted proteins were loaded onto SDS-PAGE gels and analysed by Western blot (see below).

3.5.5. Protein chromatin-binding assay

Protein chromatin-binding assays were performed as described by Liang, C & Stillman, B (Liang and Stillman, 1997) with minor modifications: 15 OD_{600} of cells were harvested and sodium azide was added to a final concentration of 0.1%. Cells were spheroplasted according to Conradt, B et al. (Conradt et al., 1992). They were incubated at room temperature for 10 minutes in 1 ml of pre-spheroplasting buffer (100 mM KH_2PO_4/K_2HPO_4 pH 9.4, 10 mM DTT, 0.1% sodium azide), followed by incubation in 1 ml of spheroplasting buffer (100 mM KH_2PO_4/K_2HPO_4 pH 7.5, 0.6 M sorbitol, 10 mM DTT) containing 3 µl of 10 mg/ml of zymoliase 100T at 37°C for 10 minutes with occasional mixing, until the OD_{600} of a 1:100 dilution of the cell suspension (in water) dropped to <10% of the value before digestion. Then, spheroplasts were washed with 1 ml of ice-chilled spheroplasts washing buffer (SWB; 100 mM KCl, 50 mM HEPES-KOH pH 7.5, 2.5 mM $MgCl_2$, and 0.4 M Sorbitol), pelleted at 1,200 rpm for 1 minute at 4°C, and resuspended in an equal pellet volume (50 µl) of extraction buffer (EB; 100 mM KCl, 50 mM HEPES-KOH pH 7.5, 2.5 mM $MgCl_2$) supplemented with Complete protease inhibitor cocktail tablets (from Roche). Spheroplasts were lysed by adding Triton™ X-100 to a final concentration of 0.25% and incubated on ice for 5 minutes with gentle mixing. The suspension was split into two tubes (one for whole cell extract (WCE) and the other for chromatin pellet (CP)). Afterwards, lysate was underlayered with 50% volume of 30% sucrose (volume refers to the volume of the spheroplasts suspension in EB buffer; the same below), and spun down at 12,000 rpm for 10 minutes at 4°C. Then, the pellet was washed with 25% volume of EBX buffer (EB buffer supplemented with 0.25% Triton™ X-100), and spun down again at 10,000 rpm for 5 minutes at 4°C. An equal volume of 2×SSR buffer (10% sacarose, 0.025% bromophenol blue, 0.05% sodium azide, 4% SDS, 250 mM Tris-HCl, pH 6.8) supplemented with 4% β-mercaptoethanol was added to each fraction (chromatin pellet (CP) and whole cell extract (WCE)), boiled for 3 minutes at 95°C and spun down at 10,000 rpm for 1 minute. Finally, samples were loaded onto SDS-PAGE gel and analysed by Western blot (see below).

3.5.6. SDS-PAGE

The Mini-PROTEAN® 3 system (from Bio-Rad) and the NuPAGE® Novex® gel system (from Invitrogen) were used for SDS-PAGE.

Acrylamide gels were prepared according to the Laemmli SDS-PAGE gel formulation. The stacking casting solution was made with 5% acrylamide, 0.13% bis-acrylamide, 125 mM Tris-HCl pH 6.8, 0.1% SDS, 0.067% ammonium persulfate, 0.1% *N,N,N´,N´* tetramethylethylenediamine (TEMED). The resolving casting solution was made in a 6-12% acrylamide solution depending on the size of the protein, in all cases with an acrylamide:bis-acrylamide ratio of 37.5:1, in 375 mM Tris-HCl pH 8.8, 0.1% SDS, 0.067% ammonium persulfate, 0.1%

N,N,N´,N´ tetramethylethylenediamine (TEMED). These gels were run using the Mini-PROTEAN® 3 system (from Bio-Rad) at 20 mA/gel constant for 60-120 minutes (depending on the protein) in running buffer (25 mM Tris-HCl, 192 mM glycine, 0.1% SDS, pH 8.9).

Pre-cast 4-12% Bis-Tris gels (from Invitrogen) were run using the NuPAGE® Novex® gel system in NuPAGE® MOPS SDS buffer (50 mM MOPS, 50 mM Tris-base, 0.1% SDS, 1 mM EDTA, pH 7.7) at 200 V constant for 60-120 minutes (depending on the protein).

3.5.7. Coomassie staining

SDS-PAGE gels and polyvinylidene fluoride (PVDF) membranes were stained with Coomassie staining solution (0.1% Coomassie brilliant blue, 25% isopropanol, 10% acetic acid) for 20 minutes and distained with distaining solution (10% acetic acid, 10% isopropanol) for 20 minutes and then air dried.

3.5.8. Western blot

SDS-PAGE gels were transferred to polyvinylidene fluoride (PVDF) membrane using either the TE70X semi-dry blotter system (from Hoefer) or the XCell II™ blot module (from Invitrogen). The Bio-Rad system was used in conjunction with transfer buffer (48 mM Tris-base, 39 mM Glycine, 0.0375% SDS) containing 10-20% methanol for 1 hour at 1 mA/cm^2 constant. The NuPAGE® system was used with NuPAGE® transfer buffer (12 mM Tris-base, 96 mM glycine, pH 8.3) containing 10-20% methanol for 2 hours at 25 V constant.

PVDF membranes were blocked in 5% dried skimmed milk in Tris-buffered saline buffer (TBS; 20 mM Tris-HCl, 125 mM NaCl, pH8.0) supplemented with 0.1% Tween® 20 (TBST) for either 1 hour at RT or overnight at 4ºC. Then, the blocked membranes were incubated with the primary antibody (see Table 4) for either 1 hour at room temperature or overnight at 4°C. After several washes in TBST buffer, membranes were incubated with the secondary peroxidase-linked antibody (see Table 4) for one hour. Then, membranes were washed in TBST buffer several times and they were incubated with the Immobilon Western Chemiluminescent HRP Substrate (from Millipore) for 5 minutes. Finally, the chemiluminescent signal detection was performed with a CCD camera-based system (Lumi-Imager) from Boehringer Mannheim.

Antibody	Specie		Clone	Company	Dilution
Anti-c-myc	Mouse	monoclonal	Clone 9E10	Roche	1:5,000
Anti-HA	Rat	monoclonal	Clone 3F10	Roche	1:5,000
Anti-FLAG	Mouse	monoclonal	Clone M2	Sigma	1:5,000
Anti-Smt3	Rabbit	polyclonal		Abcam	1:5,000
Anti-Rpd3 (yC-19)	Goat	polyclonal		Santa Cruz	1:5,000
Anti-Histone H3	Rabbit	monoclonal	Clone A3S	Millipore	1:5,000
Anti-Hexokinase	Rabbit	polyclonal		GenWay	1:5,000
Anti-Rad53 (yC-19)	Goat	polyclonal		Santacruz	1:5,000
Anti -BrdU	Rat	monoclonal	BU1/75 (ICR1)	Abcam	1:50
Anti-Guanosine	Mouse			Argene	1:10
Anti-Fluorescein-AP, Fab fragments	Sheep			Roche	1:250,000
Anti-Mouse IgG-HRP	Sheep			GE	1:12,500
Anti-Rat IgG-HRP	Goat			Santa Cruz	1:12,500
Anti-Rabbit IgG-HRP	Goat			GE	1:12,500
Anti-Goat IgG-HRP	Rabbit			Santa Cruz	1:12,500
Anti-Rat IgG Alexa Fluor® 488	Goat			Life tech.	1:200
Anti-Mouse IgG Alexa Fluor® 546	Goat			Life tech.	1:200

Table 4. List of antibodies

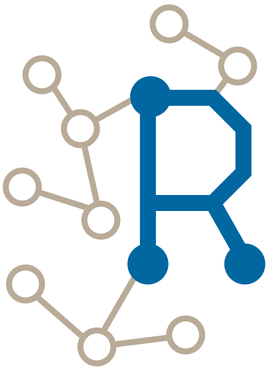

RESULTS

4.1. The role of the Smc5/6 complex in sister chromatid disjunction

smc6-9 mutant cells fail to segregate the distal part of chromosome XII at the restrictive temperature. They show sister chromatid junctions (SCJs) and replication intermediates in the rDNA at anaphase onset which lead to rDNA missegregation. However, the fact that the entire deletion of the rDNA array does not suppress the thermosensitivity of *smc6-9* mutant cells indicates that the Smc5/6 complex has further essential non-nucleolar functions (Torres-Rosell et al., 2007a). Based on this, we decided to investigate whether the Smc5/6 complex had a genome-wide function in chromosome segregation.

To address this question, DNA replication, chromosome segregation and DNA damage checkpoint activation were studied in *smc5/6* mutants in response to the alkylating agent methyl methanesulfonate (MMS).

4.1.1. *smc5/6* mutants are hypersensitive to MMS

MMS is an alkylating agent that produces DNA methyl adducts (Roberts et al., 1971). The predominant lesions induced are N^7-methylguanine (N7meG) followed by N^3-methyladenine (N3meA) (Wyatt and Pittman, 2006). Only 0.3% of total alkylations induced by MMS are O^6-methylguanine (O6meG), the major toxic and mutagenic lesion produced by methylating agents (Roberts et al., 1971). Alkylation damage has been previously demonstrated to disturb cell cycle progression and origin firing in yeast (Tercero and Diffley, 2001) and human cells (Painter, 1977). It inhibits replication elongation in a manner that is dose-dependent and related to the overall alkylation grade (Groth et al., 2010). If the MMS-induced DNA damage is not repaired, mainly by BER (Boiteux and Guillet, 2004), during DNA replication the alkylated bases will either (i) force the replisome to replicate through the damaged site using translesion synthesis polymerases, or (ii) activate some bypass mechanisms based on homologous recombination and template switch in order to proceed with DNA replication (Jackson and Durocher, 2013).

First, we tested the MMS sensitivity of two *smc6* mutants (*smc6-9* and *smc6-1*). Although these two alleles are both sensitive to MMS, the *smc6-9* allele, which contains E903G and S908P mutations, displays a higher sensitivity. The *smc6-1* allele, which contains E97G, E378G, H379R, M432V and K770R mutations, displays higher temperature sensitivity but is slightly less sensitive to MMS than the *smc6-9* allele (see Figure 16). Furthermore, *nse2ΔC* mutant cells, which contain a deletion of the SUMO ligase domain of Nse2, also display a high sensitivity to MMS. This indicates that Nse2-dependent SUMOylation is required in the presence of DNA damage (see Figure 16).

These results are supported by several studies that have uncovered mutations in every subunit of the Smc5/6 complex that render cells sensitive to many DNA damaging agents, such as UV, ionizing radiation, and MMS (Ampatzidou et al., 2006; Andrews et al., 2005; Cost and Cozzarelli, 2006; de et al., 2006; Fousteri and Lehmann, 2000; Fujioka et al., 2002; Hu et al., 2005; Lehmann et al., 1995; McDonald et al., 2003; Miyabe et al., 2006; Miyazaki et al., 2006; Morikawa et al., 2004; Onoda et al., 2004; Pebernard et al., 2004; Pebernard et al., 2006; Potts et al., 2006; Potts and Yu, 2005; Sheedy et al., 2005; Torres-Rosell et al., 2005; Zhao and Blobel, 2005).

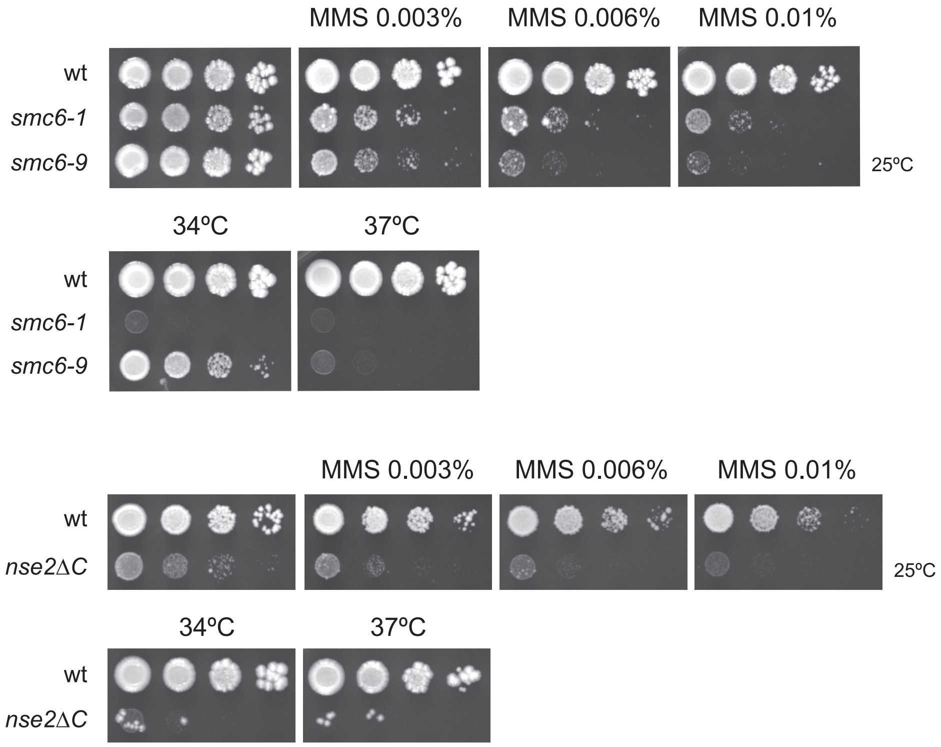

Figure 16. ***smc5/6* mutants are hypersensitive to MMS**

Serial dilutions of wild type (BY4741), *smc6-1* (YTR608), *smc6-9* (YTR53), nse2ΔC (YTR570) cells. They were spotted on YPD plates or YPD plates containing the indicated amounts of MMS. Note that *smc5/6* mutants are sensitive to MMS.

4.1.2. Bulk replication fork progression is not impaired in *smc5/6* mutants

In order to determine whether the Smc5/6 complex has a role in replication fork progression in the presence of MMS, wild type, *smc6-9* and *nse2ΔC* cells were arrested in G1 with alpha factor at the permissive temperature. After G1 synchronization, cells were shifted to 37ºC for 30 minutes to inactivate *smc5/6*. Then, they were released into fresh media containing 0.02% MMS at 37ºC. Wild type cells go through a very long and slow S phase when replicating in the presence of MMS (Tercero and Diffley, 2001). As shown in Figure 17, FACS analysis indicates that *smc6-9* and *nse2ΔC* mutant cells enter S phase and complete bulk DNA replication with wild type kinetics. Under these conditions, the DNA damage checkpoint is activated, which causes cell cycle arrest. Interestingly, *smc5/6* mutants do not show defects in S phase progression when replicating in the presence of MMS. These results strongly suggest that the Smc5/6 complex is not required for general replication fork progression in the presence of MMS-induced DNA damage

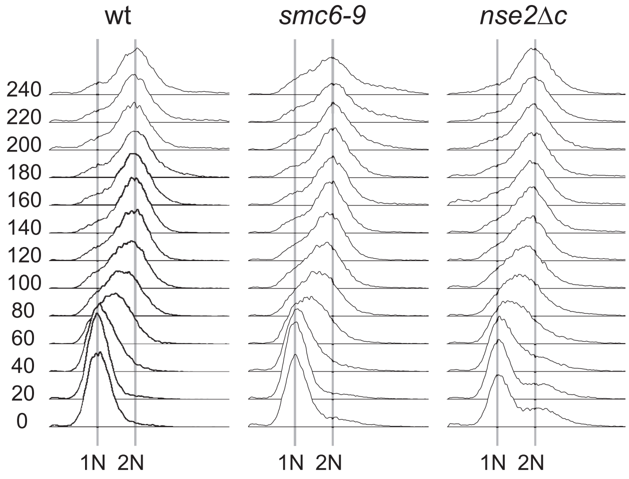

Figure 17. Bulk replication fork progression is not affected in *smc5/6* mutant cells

FACS analysis of wild type (AS499), *smc6-9* (CCG1761) and *nse2ΔC* (YMB539) cells replicating in the presence of 0.02% MMS. Cells were arrested with alpha factor at the permissive temperature. Once arrested, they were shifted to 37ºC for 30 minutes and released into 0.02% MMS at 37ºC. FACS analysis shows that they replicate with the same kinetics, reaching 2N DNA content at the same time (≈180 minutes). All three remain arrested for up to 4 hours in G2/M, showing wild type checkpoint activation.

However, two-dimensional (2D) gel electrophoresis revealed that *smc6-9* and *smc6-1* mutant cells accumulate sister chromatid junctions (SCJs) when replicating in the presence of MMS in the *ARS305* (see Figure 18). Similar results have been obtained using different *smc5/6* mutants: *mms21-CH* (Branzei et al., 2006), *mms21-11* and *smc6-P4* (Chen et al., 2009; Chen et al., 2013; Choi et al., 2010), *smc6-56* (Yong-Gonzales et al., 2012), and *mms21-SP* (Chavez et al., 2011). Therefore the aforementioned data provide compelling support for the idea that *smc5/6* mutants accumulate SCJs during replication of a damaged DNA template.

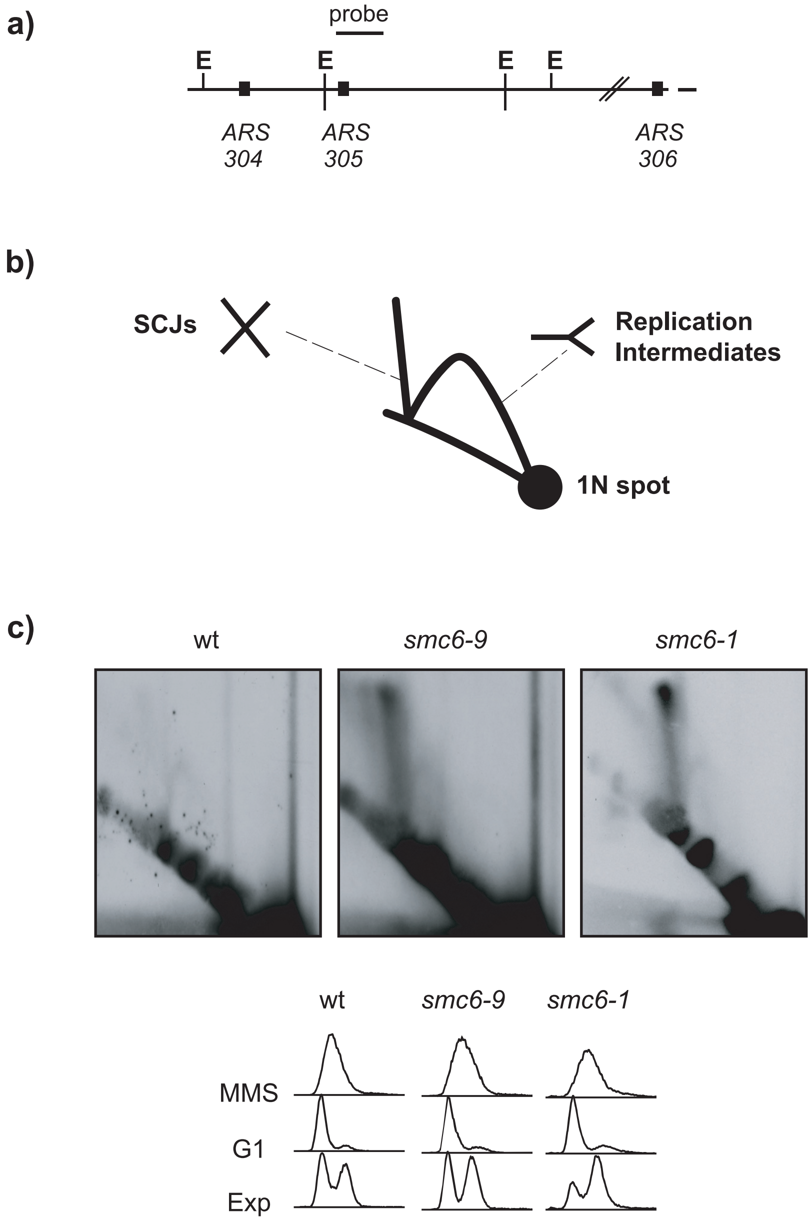
a)
probe
E
E
E
E
ARS 304
ARS 305
ARS 306
b)
SCJs
Replication Intermediates
1N spot
c)
wt
smc6-9
smc6-1
wt
smc6-9
smc6-1
MMS
G1
Exp

Figure 18. ***smc6-9*** **and** ***smc6-1*** **mutants accumulate sister chromatid junctions when replicating in the presence of MMS**

a) Diagram of the region analysed by replication 2D gel electrophoresis. The diagram shows *EcoRV* restriction sites (E) and the localization of the probe used to analyse the *ARS305*. b) Schematic representation of the visualized structures by replication 2D gel electrophoresis. c) s*mc5/6* mutants accumulate sister chromatid junctions. Exponentially growing cultures of wild-type (BY4741), *smc6-1* (YTR608) and *smc6-9* (YTR53) mutant cells were arrested in G1 and released into S phase at the restrictive temperature in the presence of 0.033% MMS for 3 hours. Samples were taken and processed for 2D gel electrophoresis and FACS analysis. Note the accumulation of X-shaped DNA molecules forming sister chromatid junctions (SCJs) in both *smc6* mutants. FACS analysis revealed that cells are still in S phase after 3 hours from the G1 release into MMS.

4.1.3. An MMS pulse does not affect S phase progression in wild type cells

Although MMS-induced DNA damage has been extensively used, its effects on chromosome segregation have not been previously addressed because activation of the DNA damage checkpoint precludes anaphase entry (Tercero and Diffley, 2001). In order to circumvent this problem, we set up a more physiological approach based on a pulse of 0.01% MMS for 30 minutes while cells are arrested in G1. Then, cells are washed thoroughly and allowed to enter S phase in the absence of the DNA alkylating agent. Under such conditions, FACS analysis revealed that wild type cells do not experience a significant delay in cell cycle entry or progression through S phase (see Figure 19), and start chromosome segregation with similar kinetics to unchallenged cells. In our hands, yeast cells treated this way frequently took a long time to complete cytokinesis, leading to the appearance of re-budded cells with >2N DNA content.

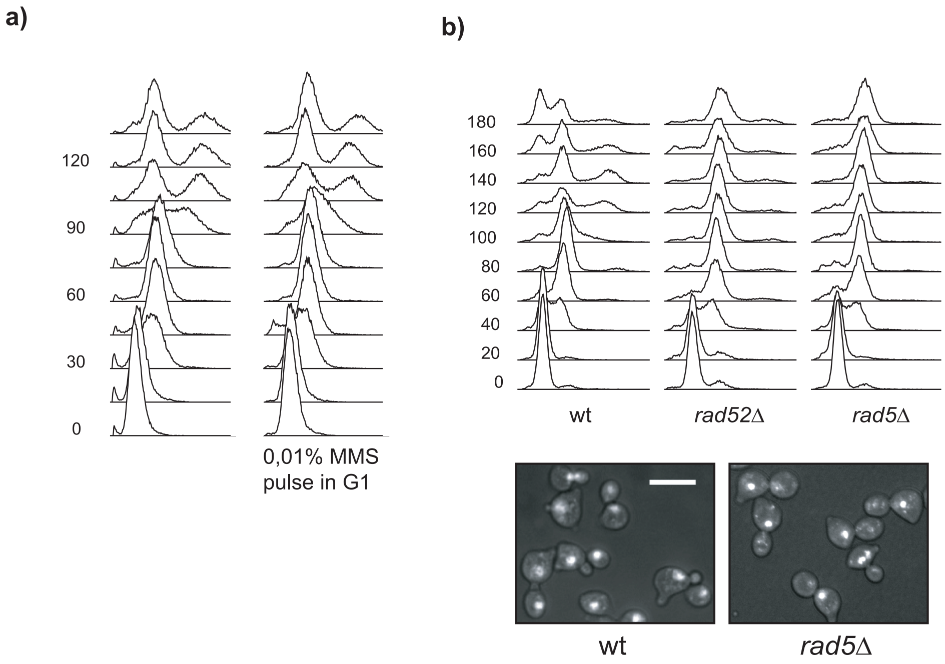

Figure 19. Cell cycle progression is not impaired by an MMS pulse in wild type cells

a) An MMS pulse does not impair cell cycle progression in wild type cells. Wild type cells (AS499) were arrested in G1 with alpha factor at 25ºC. Then, the culture was split into two and one half was treated with 0.01% MMS for 30 minutes. Both cultures were subsequently washed, resuspended in fresh media and allowed to enter the cell cycle in the absence of MMS. Note that both cultures proceed through S phase with similar kinetics. b) An MMS pulse prevents nuclear segregation in *rad52⊿* and *rad5⊿* mutant cells. Wild type (AS499), *rad52⊿* (CCG1800) and *rad5⊿* (YTR896) cells were treated as previously described. Samples were taken at the indicated time points for FACS analysis. Note that contrary to wild type cells, *rad5⊿* and *rad52⊿* cells arrest in G2/M. Representative micrographs of DAPI-stained nuclei of wild type and *rad5⊿* cells at 120 minutes after G1 release. Note that whereas in wild type cells the nuclei are segregated, in *rad5⊿* mutant cells only one nuclear mass can be detected, indicative of G2/M arrest.

DNA damage bypass mechanisms, which lead to sister chromatid junction formation, are required in the presence of MMS. Inactivation of the homologous recombination pathway (*rad52* null cells) or the error-free branch of the postreplicational repair pathway (*rad5* null cells) prevent the formation of sister chromatid junctions (SCJs) after an MMS treatment (Branzei et al., 2006; Liberi et al., 2005). *rad52Δ* and *rad5Δ* mutant cells arrest for a prolonged time in G2/M after an MMS pulse (see Figure 19). These findings indicate that the MMS pulse conditions are acute enough to require SCJ formation through HR and the error-free branch of the PRR pathway to bypass the MMS-induced DNA damage.

4.1.4. *smc5/6* mutant cells undergo aberrant mitosis after an MMS pulse

Using this experimental condition we tested several genes involved in DNA repair and/or SCJ metabolism. Interestingly, cells bearing single deletions in base excision repair, nucleotide excision repair or in the DNA damage and S phase checkpoints progress and segregate the nuclei with the same kinetics and efficiency as wild type cells (see Table 5). Similarly, although the combined action of a helicase and a topoisomerase has been proposed to dissolve some types of SCJs (Liberi et al., 2005; Wu and Hickson, 2003), nuclear segregation was unaffected in single helicase or topoisomerase mutants. This finding suggests that, despite the accumulation of SCJs in *sgs1Δ* and *top3Δ* mutant during continuous MMS damage (Liberi et al., 2005), the Sgs1-Top3 pair is not essential for removal of SCJs, at least under our experimental conditions. In addition, deletion of other yeast DNA nucleases, such as *EXO1*, *SLX1*, *SLX4*, *MMS4*, *MUS81*, *RAD2*, *MRE11*, *SAE2* and *YEN1*) leads to no obvious nuclear missegregation after an MMS pulse (see Table 5). Overall these results indicate that no single nuclease is essential for the removal of SCJs when cells are subjected to a low dose of alkylating damage.

		Phenotype
Homologous recombination	*rad52Δ* (YT128)	G2/M arrest
	rad57Δ (YT193)	G2/M arrest
Post-replicational repair	*rad5Δ* (YT896)	G2/M arrest
Base excision repair	*mag1Δ* (YT474)	wild type
	apn1Δ (YT1065)	wild type
	apn2Δ (YT250)	wild type
Nucleotide excision repair	*rad1Δ* (YT400)	wild type
	rad10Δ (YT401)	wild type
	rad2Δ (YT1067)	wild type
DNA damage checkpoint	*ddc1Δ* (YT111)	wild type
	rad9Δ (YT149)	wild type
	rad24Δ (YT109)	wild type
S phase checkpoint	*mrc1Δ* (YT110)	wild type
	mph1Δ (YT1068)	wild type

Helicases	*sgs1⊿* (YT359)	wild type
	srs2⊿ (YT358)	wild type
	rrm3⊿ (YT179)	wild type
Topoisomerases	*top1⊿* (YT778)	wild type
	top3⊿ (YT178)	wild type
Other DNA nucleases	*exo1⊿* (YT252)	wild type
	slx1⊿ (YT188)	wild type
	slx4⊿ (YT189)	wild type
	mms4⊿ (YT176)	wild type
	mus81⊿ (YT186)	wild type
	rad27⊿ (YT405)	wild type
	mre11⊿ (YT114)	wild type
	sae2⊿ (YT1064)	wild type
	dna2-1 (YT1089)	wild type
	yen1⊿ (YT1066)	wild type
Smc5/6 complex	*smc6-9* (YT1761)	Missegregation
	smc6-1 (YT608)	Missegregation
	nse2⊿C (YT539)	Missegregation
	smc5-6 (YT118)	Missegregation
	smc5-11 (YT613)	Missegregation

Table 5. Nuclear segregation phenotype after 0.01% MMS pulse in G1 arrested cells

In order to determine whether the Smc5/6 complex is required under these experimental conditions, *smc5/6* mutants (*smc5-6*, *sm5-11*, *smc6-1*, *smc6-9* and *nse2⊿C*) were arrested in G1 with alpha factor at 25ºC. Once arrested, cells were treated with 0.01% MMS and the temperature was shifted to 37ºC (restrictive temperature) to inactivate the function of the complex. After 30 minutes, cells were washed to remove the MMS and they were allowed to enter S phase in the absence of the alkylating agent. FACS analysis indicates that *smc5/6* mutant cells enter S phase and complete bulk DNA replication with wild type kinetics, indicating no gross defects in completion of DNA replication after an MMS pulse (see Figure 20). Microscopic analysis indicates that nuclear segregation starts on time in *smc5/6* mutant cells after an MMS pulse (see Figure 20). However, *smc6* mutant cells display an abnormally high proportion of anaphase cells and are defective in generation of binucleated cells (see Figure 20), suggesting chromosome disjunction problems. Moreover, at the time of entry into the second cell cycle (80 minutes onwards), *smc6* mutant cells display massive nuclear segregation defects: ~30% of the *smc6-9* and *smc6-1* population display missegregated nuclei at time 120 minutes, and ~70% of those that grow a second bud from 80-120 minutes have distributed unequal masses of DNA between mother and daughter cells, or have simply failed to divide the nucleus (see Figure 20). As expected, only *smc6* mutant cells that had inherited the larger DNA mass were able to start a new cell cycle and re-bud. FACS analysis also revealed the presence of cells with less than 1N (<1N) DNA content at later time points in the cell cycle, indicative of gross chromosome segregation defects in *smc6* mutant cells.

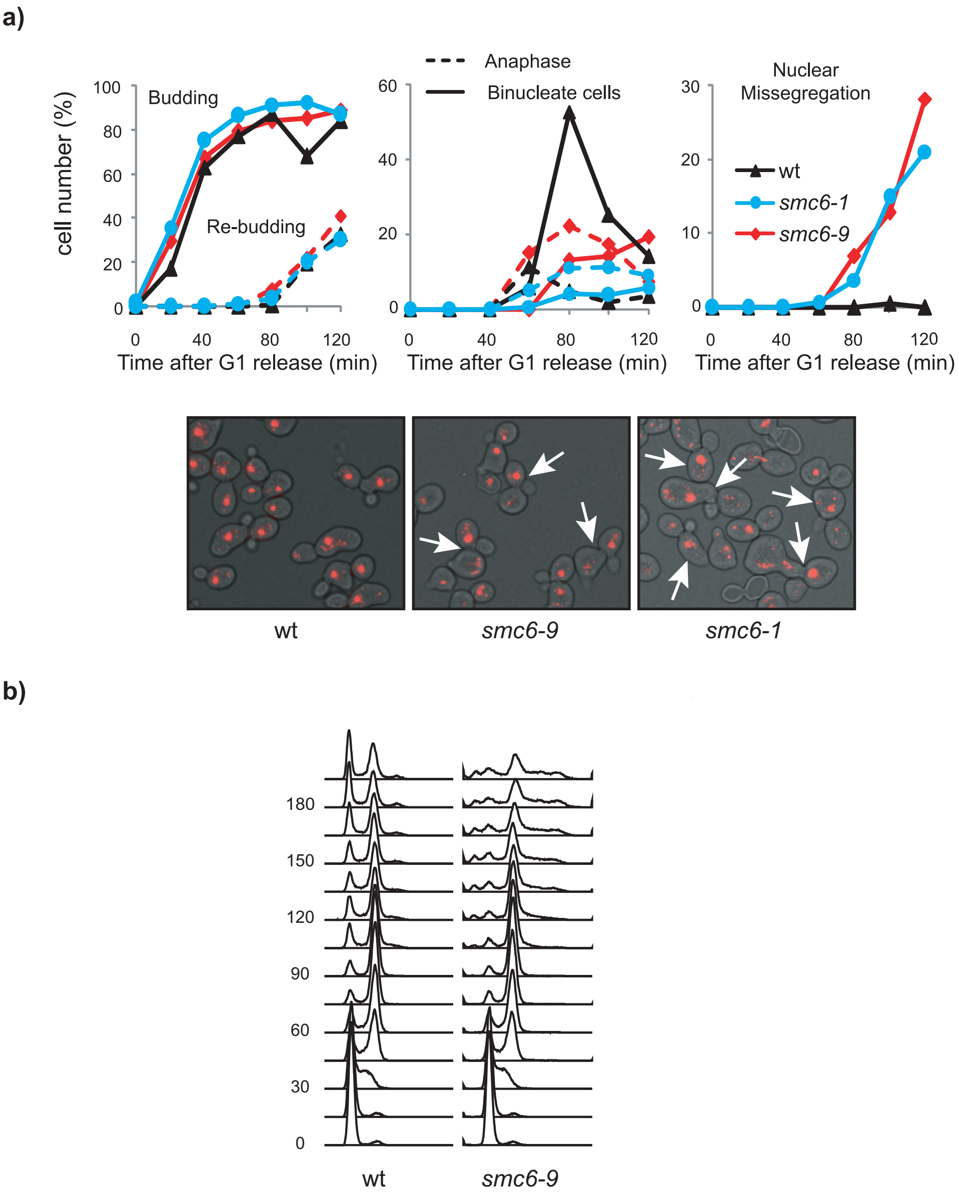

Figure 20. ***smc5/6*** **mutant cells undergo aberrant mitosis after an MMS pulse**

a) *smc6* mutants show nuclear missegregation after an MMS pulse. Wild type (BY4741), *smc6-1* (YTR608) and *smc6-9* (YTR53) cells were treated as previously described. After DAPI staining, cells were scored for budding, re-budding, anaphase nucleus and binucleated cells. Note the high percentage of nuclear missegregation. Representative micrographs of DAPI stained cells at 120 minutes after G1 release are shown. *smc6* mutant cells display unequal segregation of DNA masses (white arrows). b) *smc6-9* mutant cells show cells with <1N DNA content after an MMS pulse. FACS analysis from the previous panel shows that wild type and *smc6-9* cells progress with similar kinetics during the first cell cycle. Note the appearance of cells with less than 1N (<1N) DNA content in the *smc6-9* culture from 105 minutes onwards.

In order to evaluate the chromosome segregation defects in more detail, we analysed the fate of chromosomal tags inserted at different positions in the genome after an MMS pulse. Yeast cells fail to segregate the rDNA and rDNA-distal sequences on chromosome XII after inactivation of the Smc5/6 complex in unchallenged conditions. However, centromeres and the rDNA-centromeric flank on chromosome XII are faithfully segregated after *smc5/6* inactivation in the absence of DNA damage (Torres-Rosell et al., 2005). In contrast, *smc6-9* mutant cells fail to segregate centromere III, centromere XII and the rDNA-centromeric flank after an MMS pulse (see Figure 21, red area). Centromeres are the first loci to be separated and segregated by the spindle apparatus, and normally lead chromosome arms. To our surprise, many *smc6-9* mutant cells with an anaphase nucleus displayed a single dot, instead of two dots leading the segregating nuclei. A more detailed analysis indicates that 18%, 35% and 58% of *smc6-9* cells undergoing anaphase have failed to resolve centromere III, centromere XII and the rDNA centromeric flank, respectively (N=94; 262; 263). In contrast, only 2%, 0% and 6.7% of wild type anaphase cells show remaining cohesion at these loci (N=94; 72; 45). Therefore, *smc6-9* mutant cells accumulate chromosome linkages after MMS damage, which prevent chromosome segregation.

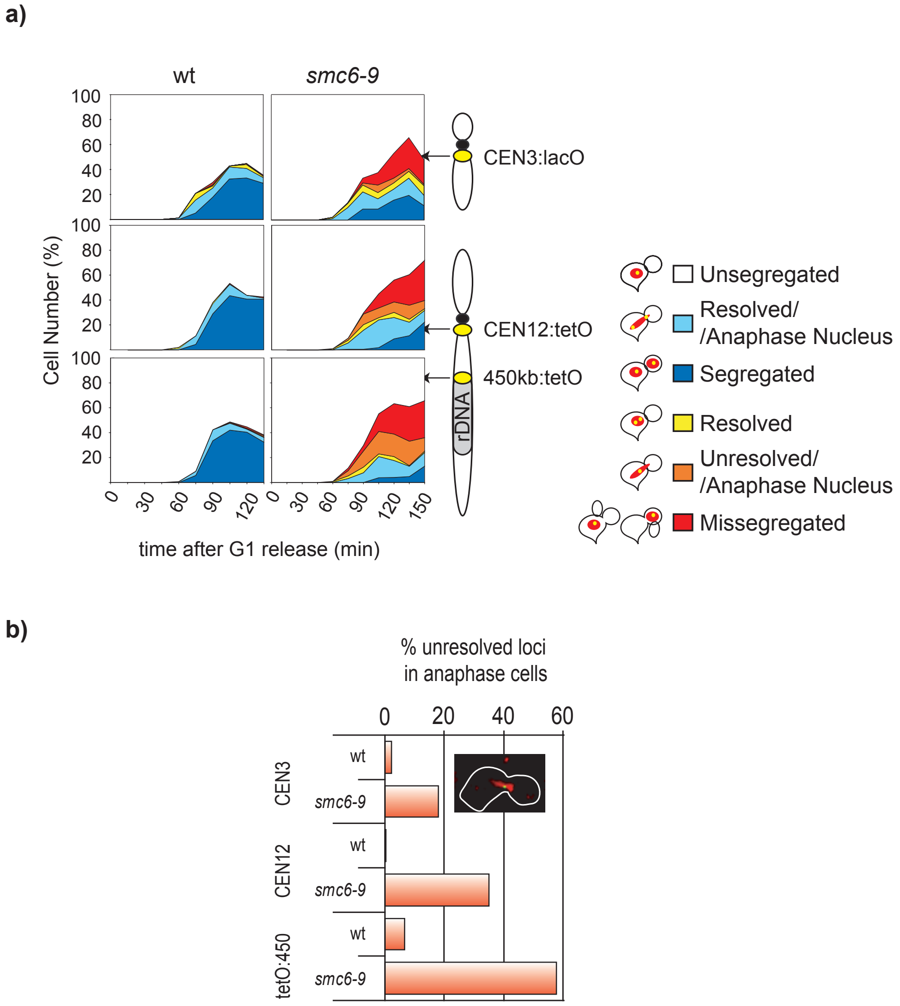

Figure 21. ***smc6-9* mutant cells fail to segregate centromeric sequences after an MMS pulse**

a) s*mc6-9* shows a high proportion of unresolved and missegregated chromosomal tags after an MMS pulse. Wild type (YTR506, CCG1297, CCG1298) and *smc6-9* (YTR516, CCG1920, CCG1922) cells carrying the indicated chromosome tags were treated as previously described. Samples were taken at different time points after G1 release, stained with DAPI and microscopically examined for localization of chromosome tags. Data are presented as stacked percentages of cells in each category. Both wild type and *smc6-9* mutant cells start anaphase around 75 minutes after G1 release. Wild type cells first go through an anaphase stage with segregating tags (light blue), and then complete nuclei and tag segregation (dark blue). In contrast, very few *smc6-9* mutant cells complete a successful anaphase and many mutant cells display aberrant morphologies. Note the presence of *smc6-9* anaphase cells that fail to resolve CEN3 or CEN12 tags (orange), and cells that fail to complete tag segregation (red). b) *smc6-9* cells show a high percentage of unresolved loci with an anaphase nuclei. Anaphase nuclei from (a) were scored according to the resolution of the tags. Note that *smc6-9* mutant cells show a high proportion of unresolved loci.

However, the centromere resolution problems indicate that the chromosome linkages present in *smc6-9* cells are not concentrated at or displaced towards the ends of the chromosome, but scattered throughout the genome. The higher frequency of anaphase misresolution for the rDNA-centromeric flank compared to the centromere indicates that the linkage accumulation probability increases with distance from the centromere, as expected for random DNA damage.

smc6-9 mutant cells activate Rad53 as they enter a second cell cycle at the restrictive temperature (Torres-Rosell et al., 2005). Analysis of Rad53 phosphorylation in *smc6* mutant cells shows that the DNA damage checkpoint is not activated during the first S phase after an MMS pulse (see Figure 22), which is in accordance with the absence of G2/M arrest. However, the appearance of the slower mobility forms of Rad53 coincides with the entry into the second cell cycle. These results suggest that the brief treatment with MMS does not produce, in most of the cells, a sufficient number of stalled forks to activate a checkpoint response during the first cell cycle (Sanchez et al., 1996; Tercero et al., 2003).

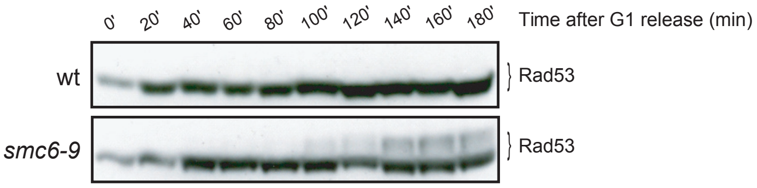

Figure 22. ***smc6-9*** **mutant cells show an activation of the DNA damage checkpoint in the second cell cycle after an MMS pulse**

Wild type (AS499) and *smc6-9* (CCG1761) mutant cells were treated as previously described. Samples were taken for FACS and Western blot analysis of Rad53. Note the presence of phosphorylated forms of Rad53 after 100 minutes in *smc6-9* mutant cells.

4.1.5. *smc5/6* mutant cells accumulate replication and recombination intermediates after an MMS pulse

The nuclear segregation problems in *smc6* mutant cells could stem from defects in dissolution of DNA linkages, but also from defects in removal of catenanes or protein-based cohesion. In order to discern between them, we prepared intact chromosomes in agarose plugs. Importantly, sister chromatids that are glued together by protein or RNA are resolved during intact chromosome preparation. Catenated sister chromatids are also resolved during migration and reorientation of chromosomes in a pulsed field gel electrophoresis (PFGE)(Baxter and Diffley, 2008). Therefore, only sister chromatids that are linked by DNA-mediated structures, such as replication or recombination intermediates, will fail to migrate into the gel when subjected to a pulsed electric field.

Wild type and *smc5/6* mutant cells (*smc6-1*, *smc6-9*, and *nse2ΔC*) were treated with an MMS pulse, as previously described and processed for PFGE. Figure 23 shows that chromosomes do not enter the PFG while they are replicating in S phase (40 to 80 minutes). This is due to the presence of branched replication intermediates. It is widely accepted that PFGE prevents chromosomes containing replication forks or branched recombination intermediates from entering the gel (Azvolinsky et al., 2006; Hennessy et al., 1991). Following S phase completion, when these structures disappear, chromosomes from wild type cells enter into the gel (80 minutes onwards). In contrast, chromosomes from *smc5/6* mutant cells fail to enter into the gel even at later time points (see Figure 23). Gel quantifications show that up to 160% of wild type chromosomes enter into the gel after S phase (relative to G1), while only 14% of those from *smc6-9* mutant cells are able to do so. Interestingly, larger chromosomes from *smc5/6* mutant cells tend to enter less into the gel, suggesting that they are more likely to carry DNA linkages, as expected for random DNA damage (see Figure 23). These observations indicate that SUMOylation by Nse2 together with a functional Smc5/6 complex are required to prevent the accumulation of DNA-mediated linkages.

Although protein-mediated linkages (mainly based on the cohesin complex) are degraded during preparation of intact chromosomes; and catenated sister chromatids can be resolved by PFGE (Holm et al., 1989), we decided to rule out any further contribution from these two possibilities. It has been proposed that the Smc5/6 complex has a role in cohesin removal in *S. pombe* (Outwin et al., 2009). To confirm that the missegregation phenotype seen in *smc6-9* mutant cells is not due to problems in cohesion removal, a GFP-tagged version of Scc1 was used. As seen in Figure 24, nuclear Scc1-GFP signal appears during S phase and disappears when cells enter into anaphase with the same kinetics in wild type and *smc6-9* mutant cells. This suggests that the chromosome linkages seen in *smc5/6* mutant cells are cohesin-independent. Moreover, chromosomes of *top2-4* mutant cells arrested in G2/M, although being catenated can be resolved in a PFG, while those in *smc6-9* mutant cells cannot (see Figure 24). Overall, these observations indicate that *smc5/6* mutants accumulate DNA-mediated linkages that prevent chromosome segregation and that protein or catenation-based linkages are not significant in this process.

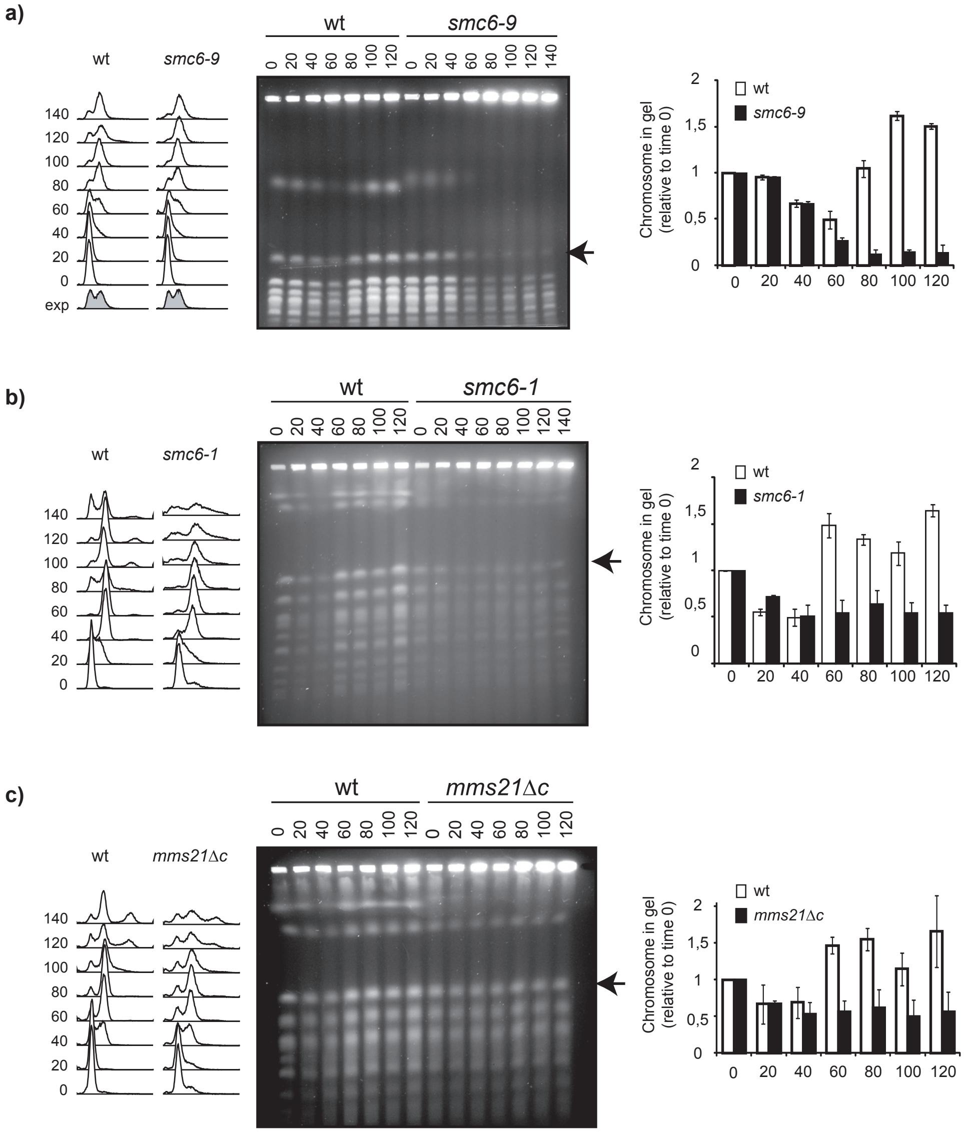

Figure 23. ***smc5/6*** **mutants accumulate DNA-mediated structures after an MMS pulse**

(a) Wild type (AS499) and *smc6-9* (CCG1761); (b) Wild type (BY4741) and *smc6-1* (YTR608); and (c) Wild type (BY4741) and *nse2ΔC* (YMB539) mutant cells were treated as previously described. Samples were taken every 20 minutes for FACS and PFGE analysis. FACS analysis (left panel) and PFGE (middle panel) show that all strains start replication on time but the mutants fail to resolve sister chromosomes after S phase. Note that chromosomes fail to enter into the PFG after S phase and stay in the well even at late time points in *smc5/6* mutants. Arrows point to the chromosome used for quantification (right panel). Data from three independent experiments were used for quantification. Note that all *smc5/6* mutants tested show the same behaviour.

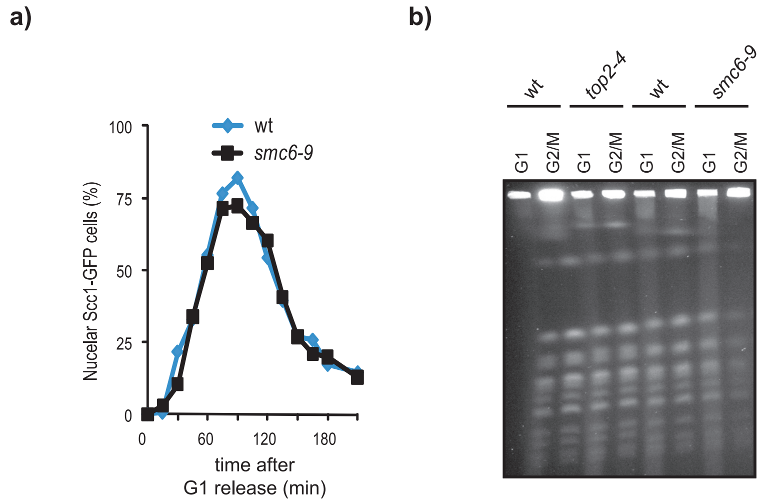

Figure 24. ***smc5/6*** **mutants accumulate protein/topological-independent linkages after an MMS pulse**

> a) *smc6-9* mutant cells do not show cohesin removal defects after an MMS pulse. Wild-type (YTR1154) and *smc6-9* (YTR1156) mutant cells expressing a GFP-tagged version of Scc1 were treated as previously described. Samples were taken after G1 release and microscopically examined for nuclear Scc1-GFP signal. Note the parallel appearance and disappearance of nuclear Scc1-GFP signal in both strains. b) Contrary to *smc6-9* cells, chromosomes in *top2-4* mutant cells can be resolved in a PFG. Wild-type (AS499), *top2-4* (YTR1268) and *smc6-9* (CCG1761) mutant cells were arrested in G1 with alpha factor. Once arrested, they were treated with 0.01% MMS (wild type and *smc6-9* cells) and shifted to 37ºC for 30 minutes. Then, cells were released into a nocodazole block (G2/M). Samples from G1 and G2/M arrests were processed for PFGE. Note that chromosomes from wild type and *top2-4* cells enter the gel in G2/M, while those from *smc6-9* cells are defective.

Next, we studied the nature of the DNA-mediated linkages that prevent chromosome segregation in *smc6* mutants. The segregation defects shown in *smc5/6* mutant cells indicate that these structures should still be present at anaphase onset. In nocodazole-arrested cells, the levels of replication and recombination intermediates are almost undetectable in wild type cells in a two-dimensional gel electrophoresis. In contrast, *smc6-9* mutant cells display low but readily detectable levels of SCJs and ongoing replication forks in the *ARS305* on chromosome III (see Figure 25). This result indicates that *smc6-9* mutant cells accumulate SCJs and replication intermediates throughout the genome when exposed to alkylating DNA damage.

The presence of ongoing replication forks was confirmed by DNA combing analysis. Wild type and *smc6-9* mutant cells were treated with an MMS pulse. Then, cells were released into S phase in the presence of bromodeoxyuridine (BrdU) and nocodazole to label replicated DNA and arrest cells in metaphase, respectively. The number of unreplicated gaps (BrdU-negative) was scored as well as the overall percentage of DNA replication. It should be noted that the MMS pulse does not affect the gap frequency in wild type cells; besides, unchallenged *smc6-9* cells display the same frequency of replication gaps as wild type cells. In contrast, *smc6-9* mutant cells display a ~2.5 times increase in the number of unreplicated gaps relative to wild type cells after an MMS pulse. The estimated failure in DNA replication completion increases from 6.5% in wild type cells to 16.3% in *smc6-9* mutant cells. Additionally, the average length of chromosome fibres is significantly shorter in *smc6-9* cells, suggesting that *smc6-9* fibres are more fragile. This could be due to the presence of sister chromatid linkages, which could also minimize the calculated amount of unreplicated chromosomal DNA. It is worth noting that, although the percentages of unreplicated gaps are relatively high in both strains, most of the chromosomes have been replicated in metaphase-arrested cells. According to the obtained data by 2D gels and DNA combing analysis, we concluded that the Smc5/6 complex is required for completion of genome replication in response to MMS-induced DNA damage. Therefore, persistent chromosomal linkages in *smc5/6* mutant cells arise from at least, two different different types of structures, incomplete replication and sister chromatid junctions.

a)

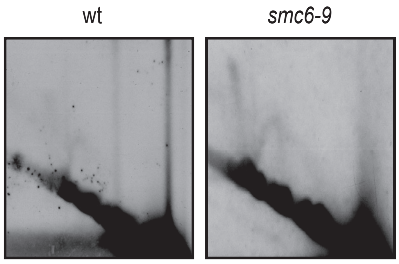

b)

	wt	*smc6-9*
Number of fibers	166	242
Total DNA (Mb)	47	57
Fiber length (Kb)	282	236
Gap length (Kb)	59	57
BrdU track length (Kb)	215	145
Gaps/Mb	1,1	2,7
% unreplicated	6,5	16,3

c)

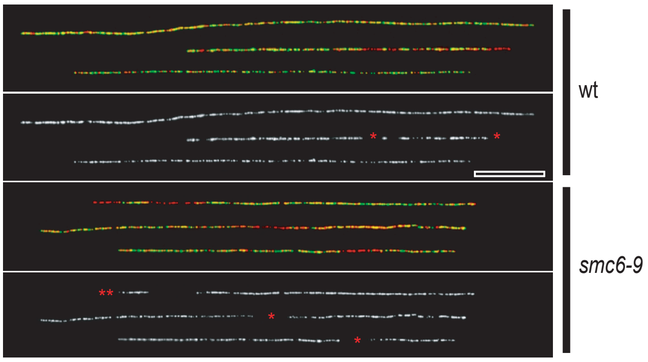

Figure 25. ***smc6*** **mutant cells accumulate SCJs and unfinished replication intermediates after an MMS pulse**

a) *Smc6-9* mutant cells show SCJs and ongoing replication forks after an MMS pulse. Wild type (CCG3227) and *smc6-9* (CCG3229) mutant cells were treated as previously described. Cells were subsequently blocked in metaphase with nocodazole. Samples were taken for 2D gel analysis and probed for the *ARS305*. Note the presence of replication intermediates and SCJs in *smc6-9* cells. b) *Smc6-9* mutant cells show a higher percentage of unreplicated DNA after an MMS pulse. Wild type (CCG3227) and *smc6-9* (CCG3229) mutant cells were treated as in (a) except that they were released from the G1 block in the presence of bromodeoxyuridine (BrdU) to label newly replicated DNA. Once arrested in G2/M, samples were taken for DNA combing. Absolute values for number of examined fibres, total DNA, mean values for length of fibres, gap length, BrdU track length and gaps per megabase were measured. Experiment carried out by Dr. Audrey Ceschia in Dr. Pasero´s lab. c) Representative fibres from (b). Red corresponds to DNA; green, BrdU; white, BrdU channel alone. Asterisks mark unreplicated gaps. Bar, 50 kb.

4.1.6. Suppression of SCJ formation has a beneficial effect on *smc5/6* mutants

The thermosensitivity of *smc6-9* mutant cells is partially suppressed by deletion of *RAD52*, a key component of the homologous recombination pathway (Torres-Rosell et al., 2005), probably because SCJ formation is deleterious when the function of the Smc5/6 complex is compromised.

Formation of SCJs depends on a functional HR pathway and the template switch branch of the postreplicational repair (Branzei et al., 2008). In accordance with this, the MMS sensitivity of *smc6-9* mutant cells is significantly suppressed by deletion of *RAD52* (see Figure 26). Analysis using PFGE revealed that *rad52⊿* mutant cells display chromosome resolution defects after an MMS pulse. These failures might be due to incomplete chromosome replication, since the HR pathway is required for replication fork progression in MMS (Vazquez et al., 2008). Even though deletion of *RAD52* alone prevents completion of chromosome replication, its deletion in *smc6-9* cells is able to improve resolution of chromosomes, an effect that is more evident for large chromosomes (see Figure 26).

In order to ensure that we had captured metaphase conditions, cells were synchronized in G1, and subjected to a 0.01% MMS pulse before release into a nocodazole block. As shown in Figure 26, the *smc6-9* mutant defects still show partial rescue by deletion of *RAD52*. This result is supported by the fact that *mms21-11 rad51⊿* (Branzei et al., 2006) and *smc6-9 rad51⊿* (Sollier et al., 2009) mutants do not accumulate significant SCJs when replicating in the presence of MMS compared to single *smc5/6* mutants. Therefore, *smc5/6* mutants accumulate SCJs at damaged forks in a recombination-dependent manner.

To determine whether the template switch branch of the postreplicational repair pathway has a detrimental effect when Smc5/6 function is compromised, we used *mms2* null cells, which channel repair of MMS-induced DNA lesions into the error-prone branch of the PRR pathway. As seen in Figure 27, the phenotype of *smc6-9* mutant cells can be partially rescued by deletion of *MMS2* on MMS plates, suggesting that promotion of TLS polymerases to the detriment of the template switch branch is beneficial in *smc6* mutants. Similar to deletion of *RAD52*, *MMS2* deletion increases chromosome entering in a PFG. This result is supported by the fact that *smc6-P4 mms2⊿* mutant cells show a reduced level of SCJs compared to *smc6-P4* single mutant cells in 2D gels, which correlates with a better growth on MMS plates (Choi et al., 2010). Therefore, preventing SCJ formation via template switching is beneficial when the function of the Smc5/6 complex is compromised.

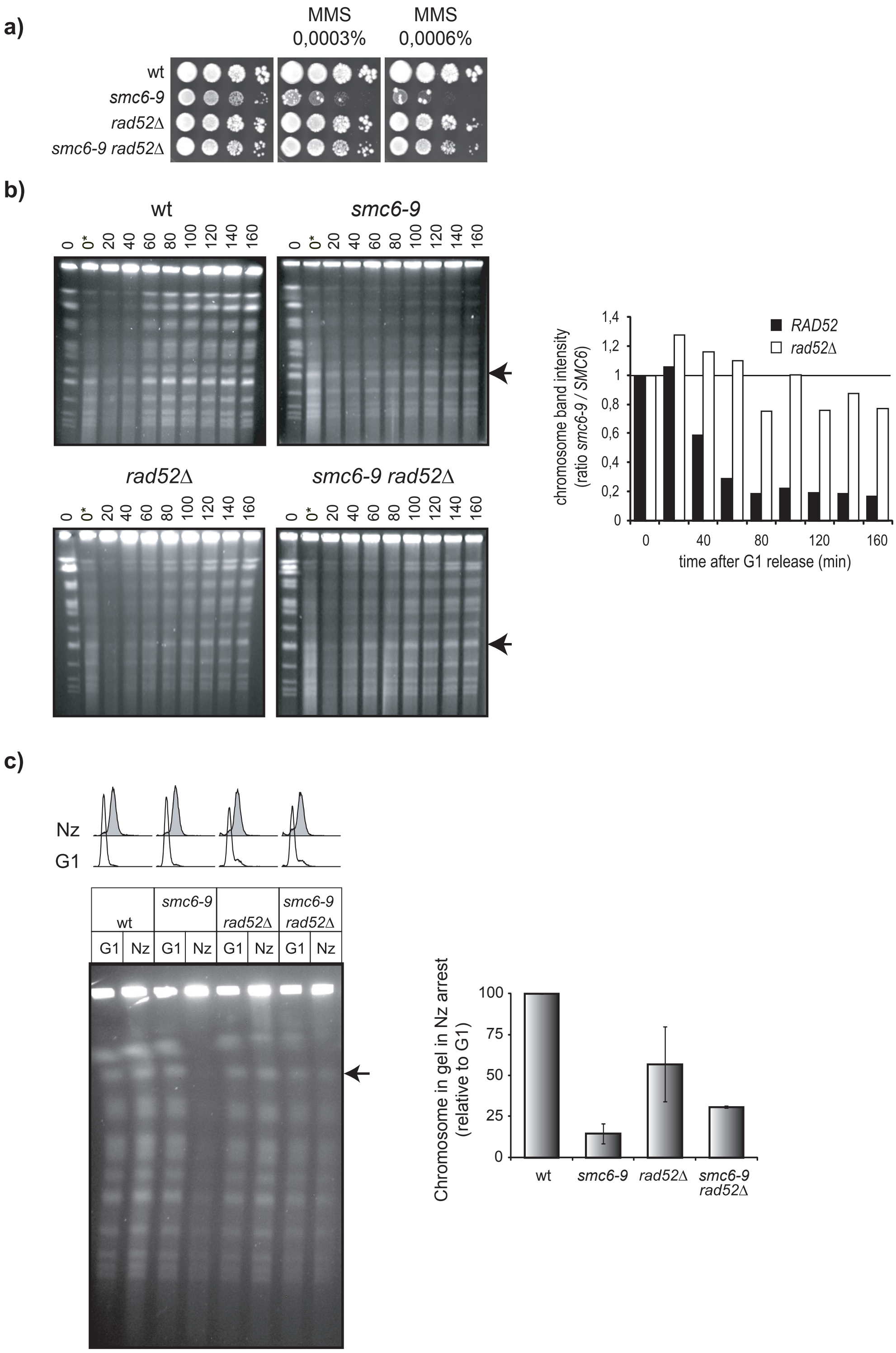

Figure 26. Homologous recombination has a negative effect in *smc5/6* mutant cells

a) Deletion of *RAD52* partially suppresses the MMS sensitivity in *smc6-9* mutant cells. Serial dilutions of wild type (AS499), *smc6-9* (CCG1761), *rad52⊿* (CCG1800) and *smc6-9 rad52⊿* (CCG1804) cells. They were spotted on YPD plates or YPD plates containing the indicated amount of MMS. Note that deletion of *RAD52* significantly suppresses MMS sensitivity in *smc6-9* mutant cells. b) Deletion of *RAD52* improves chromosome resolution in *smc6-9* mutant cells.

Wild type (AS499), *smc6-9* (CCG1761), *rad52⊿* (CCG1800) and *smc6-9 rad52⊿* (CCG1804) cells were arrested in G1 with alpha factor at 25ºC. Then, they were shifted to 37ºC (time 0) and simultaneously treated with 0.01% MMS for 30 minutes (time 0*). Then, cells were washed twice with pre-warmed medium to release them from the G1 block and remove MMS. Samples were taken every 20 minutes after G1 release. Wild type cells show entry of chromosomes into the gel after S phase (60 minutes onwards). Note that, relative to wild type cells, both *rad52⊿* and *smc6-9* strains display chromosome resolution defects after S phase. However, *smc6-9* failures can be partially suppressed by deletion of *RAD52* (compare right top and bottom gels). Arrow points to the chromosome used for quantification. Note that the *smc6-9* allele has little effect on chromosome resolution on a *rad52⊿* background. Experiment performed in Luis Aragon´s lab c) Deletion of *RAD52* improves chromosome resolution in *smc6-9* mutant cells. Wild type (AS499), *smc6-9* (CCG1761), *rad52⊿* (CCG1800) and *smc6-9 rad52⊿* (CCG1804) cells were treated as previously described. After G1 release, cells were blocked in G2/M with nocodazole (Nz). Note that the chromosome resolution defects seen in *smc6-9* mutant cells can be partially suppressed by deletion of *RAD52*. Arrow points to the chromosome used for quantification. Data from two independent experiments were used for quantification.

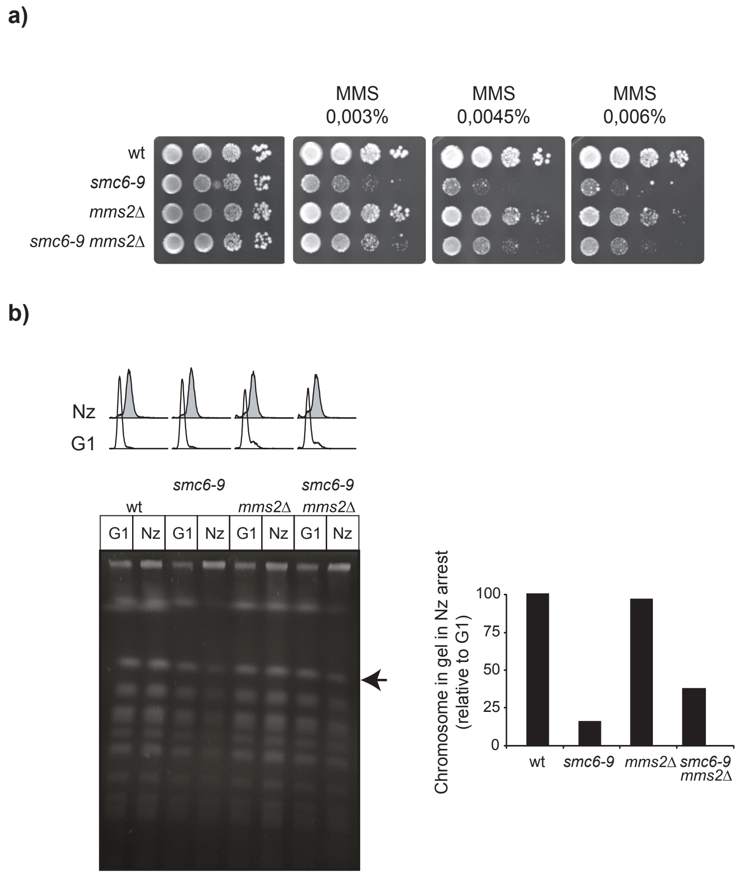

Figure 27. Blocking the template switch pathway is beneficial in *smc6-9* mutant cells

a) Deletion of *MMS2* partially suppresses the MMS sensitivity in *smc6-9* mutant cells. Serial dilutions of wild type (AS499), *smc6-9* (CCG1761), *mms2⊿* (YTR454) and s*mc6-9 mms2⊿* (YTR456) cells. They were spotted on YPD plates containing different MMS concentrations and incubated for 3 days at 25ºC. Note that deletion of MMS2 partially suppresses the MMS sensitivity in s*mc6-9* mutant cells. b) Deletion of *MMS2* improves chromosome resolution in *smc6-9* mutant cells. Wild type (AS499), *smc6-9* (CCG1761), *mms2⊿* (YTR454) and *smc6-9 mms2⊿* (YTR456). Cells were treated as in fig. 26c. Note that the chromosome resolution defects seen in *smc6-9* mutant cells can be partially suppressed by deletion of *MMS2*.

4.1.7. Smc6 promotes resolution of SCJs

In order to test whether the Smc5/6 complex has a role in the removal of sister chromatid junctions (SCJs), we designed an experiment to re-activate the Smc5/6 complex after their generation. Smc5/6 re-activation would help to eliminate DNA-mediated linkages only if the complex were required for their dissolution. *smc6-1 GALp-SMC6* cells were arrested in G1 and released into S phase in the presence of 0.033% MMS. After 3 hours, a sample was taken as a control for SCJ accumulation. The culture was then split into two, and galactose was added to one half to induce expression of wild type *SMC6*. Samples were taken 2 and 3 hours after galactose addition and processed for two-dimensional gel electrophoresis analysis. As shown in Figure 28, reactivation of wild type *SMC6* allows removal of SCJs. In contrast, SCJs remain in cells that do not express wild type *SMC6* (glucose conditions). Signal quantification showed that SCJs are 2.5 times lower in the induced culture (galactose), compared to the non-induced culture (glucose), at the two time points tested. These results indicate that, similarly to Sgs1 and Top3 (Liberi et al., 2005), Smc6 is involved in removal of DNA-mediated linkages.

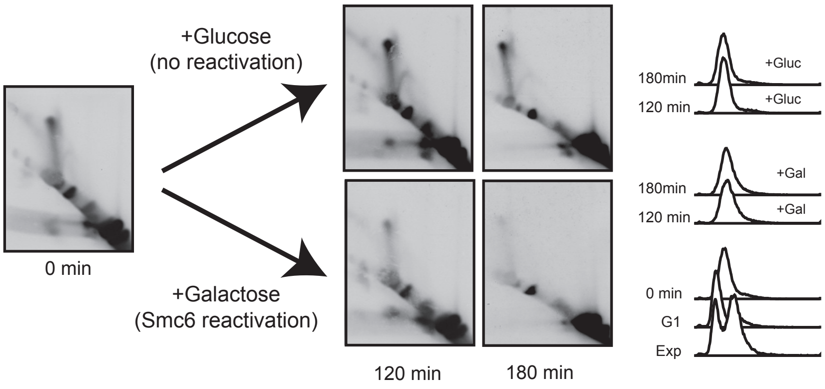

Figure 28. Smc6 promotes SCJs resolution ***in vivo***

smc6-1 GALp-SMC6 (YTR633) cells were grown in YP raffinose and arrested in G1. Then, cells were released into 0.033% MMS for 3 hours. Afterwards, the culture was split into two and galactose was added to one half to induce expression of wild type *SMC6* and glucose to the other half as a control for no expression. Samples were taken at the indicated times and processed for 2D gel analysis. Note that *SMC6* reactivation allows removal of SCJs.

The reduction of SCJs should correlate with an increase in chromosome resolution in a PFG. To test this idea, *smc6-1 GALp-SMC6* cells were arrested in G1 and treated with a 30 minutes pulse of 0.01% MMS before releasing them into a metaphase block. Once arrested in G2/M, the culture was split in two. The *GAL* promoter was induced in one half by addition of galactose, and repressed in the other by glucose. Both cultures were kept arrested in nocodazole for the rest of the experiment. Western blot analysis indicates that Smc6 protein is detected 20 minutes after induction of the *GAL* promoter, and accumulates above wild type levels after 40 minutes of expression (see Figure 29). As expected, *SMC6* reactivation increases chromosome entry into the PFG 20 minutes after induction, indicating resolution of DNA-mediated linkages. The entry is most obvious for the two most retarded chromosomes in the gel, probably chromosomes XII and IV, which can barely be detected and quantified in the non-reactivated culture conditions (glucose). Quantification of the bands in the PFG shows active linkage resolution for all medium-sized chromosomes (~3 times more present after 30 minutes than in the nocodazole arrest) (see Figure 29).

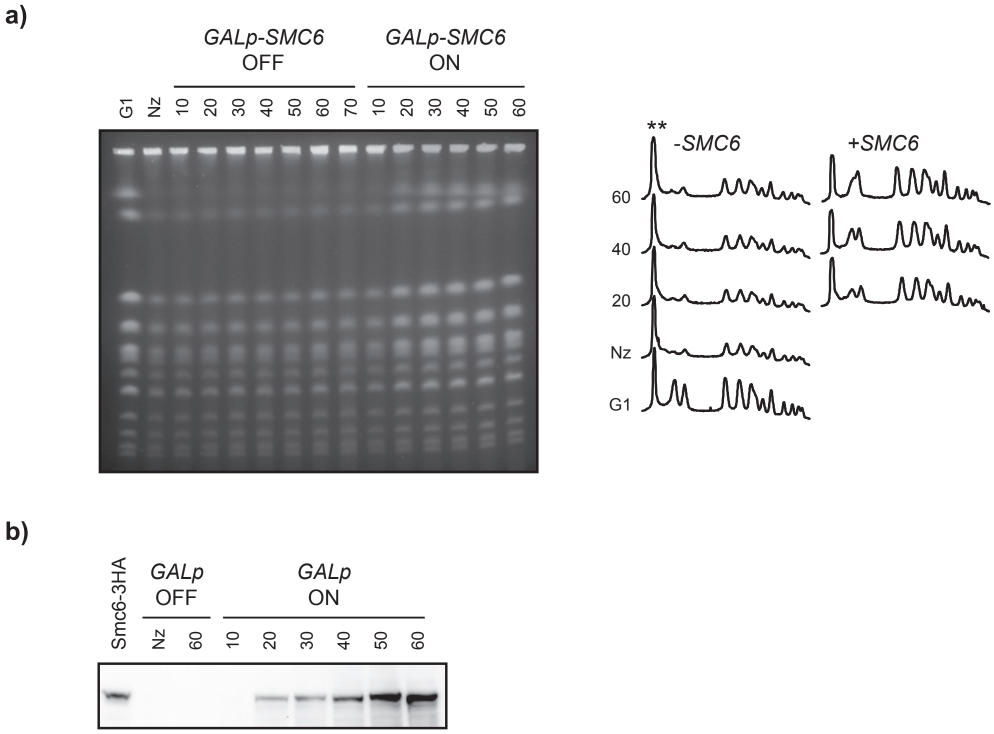

Figure 29. ***SMC6*** **reactivation increases chromosome resolution in a PFGE**

a) Smc6 reactivation increases chromosome resolution in a PFGE. *smc6-1 GALp-SMC6* (YTR633) cells growing in YPraf were arrested and treated with an MMS pulse as previously described. Then, cells were released in the absence of MMS and arrested in G2/M with nocodazole. Once blocked in G2/M, the culture was split into two and galactose or glucose was added to a final concentration of 2%. Samples were taken for PFGE analysis at the indicated times after induction of the *GAL* promoter. Lane profile quantification (right panel) shows that only *SMC6* re-activation allows entry of chromosomes into the gel. Asterisks denote signal from well.
b) Smc6 expression after *SMC6* reactivation. Smc6 can be detected after 20 minutes of *GAL* promoter induction.

Finally, SCJ reduction, which improves chromosome resolution after *SMC6* reactivation, should ameliorate the segregation problems detected in *smc5/6* mutants after an MMS pulse. To test this idea, we repeated the same previous procedure, except that both cultures were released from the nocodazole block into anaphase. Microscopic analysis indicates that both cultures complete mitosis and enter a new cell cycle with similar kinetics (see Figure 30). As expected from the previous results, *smc6-1 GALp-SMC6* cells that progress into anaphase in raffinose media display nuclear segregation defects, since most of the cells that re-bud display unequal separation of nuclei. These failures are paralleled by the appearance of cells with less than 1N (<1N) DNA content by FACS (see Figure 30). In contrast, *smc6-1* cells that progress into anaphase after expression of wild type *SMC6* display virtually no defects in nuclear segregation.

The reversibility of the chromosome segregation failures confirms that, rather than a function in preventing the appearance of sister chromatid junctions, Smc5/6 has a role in their resolution. Smc5/6 probably triggers a fast reaction, since chromosome resolution is a relatively quick event after SMC6 re-activation (20 minutes onwards). It is worth noting that although such a reaction might be carried out in S phase during a normal cell cycle, Smc5/6 can perform its function even in metaphase-arrested cells.

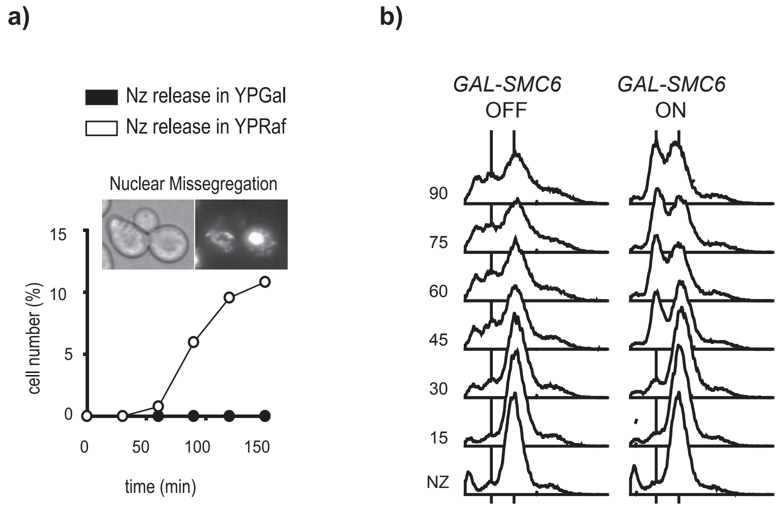

Figure 30. ***SMC6* reactivation prevents nuclear missegregation after an MMS pulse**

smc6-1 GALp-SMC6 (YTR633) cells were treated as previously described, except that cells were released from the metaphase block and allowed to enter anaphase. 20 minutes before the nocodazole release, galactose was added to one half of the culture to induce expression of wild type *SMC6* from the *GAL* promoter, while the other half was kept in raffinose. Note that *SMC6* reactivation prevents nuclear missegregation (left panel) and the appearance of cells with <1 DNA content (right panel).

4.2. Characterization of the Nse2 SUMO ligase activity regulation

Although multiple experiments in yeast and human cells have demonstrated that Nse2 is indeed an E3 SUMO ligase that is required for efficient DNA repair (Andrews et al., 2005; Potts and Yu, 2005; Stephan et al., 2011a; Zhao and Blobel, 2005) little is known about how the activity of this enzyme is regulated and which factors control its ability to transfer SUMO.

4.2.1. Detection of SUMOylated proteins *in vivo*

In order to determine whether a candidate protein is SUMOylated, Smt3, the *S. cerevisiae* SUMO protein, was tagged at its N-terminus with a 6HisFLAG tag and the protein of interest was tagged at its C-terminus with either HA or myc epitope tags. Cells were grown to mid-log phase and total cell protein was extracted under denaturing conditions in 8 M urea to block the activity of SUMO peptidases. After protein extraction, all SUMOylated proteins were purified using nickel-conjugated agarose (Ni-NTA) beads. Subsequent Western blot analysis with an antibody against either the myc or HA epitope revealed the SUMOylated forms of the protein of interest (see Figure 31 and materials and methods for more details).

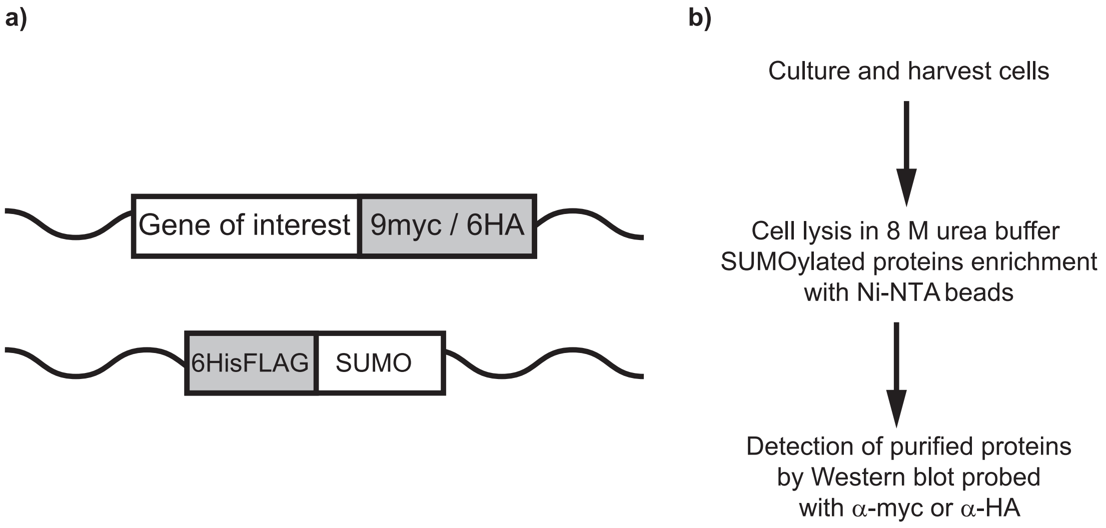
a)
Gene of interest
9myc / 6HA
6HisFLAG
SUMO
b)
Culture and harvest cells
Cell lysis in 8 M urea buffer
SUMOylated proteins enrichment
with Ni-NTA beads
Detection of purified proteins
by Western blot probed
with α-myc or α-HA

Figure 31. Strategy for purification of SUMO-conjugated proteins

a) Representation of the constructs used to study the SUMOylation of candidate proteins. The 6HisFLAG epitope tag was inserted at the N-terminus of Smt3 and either myc or 6HA epitope tag was inserted at the C-terminus of the target protein. b) Diagram showing the strategy used for SUMO-conjugate detection. Cells were grown in liquid media until mid-log phase. Then, cells were harvested and lysed under denaturing conditions. After protein extraction, the SUMOylated proteins were purified using Ni-NTA beads. Finally, after protein elution, the SUMOylated target proteins were detected by Western blot using an antibody against the myc or HA epitope tag.

The size of the candidate protein in the protein extract lane (PE) reflects the unmodified protein, whereas any slower migrating higher weight bands in the pull-down lane (PD) of the 6HisFLAG-tagged samples reflect the SUMO-conjugated forms of the candidate protein. Although the number and the abundance of the SUMOylated forms differ between proteins, the amount of the SUMO-modified protein relative to the unmodified form is always very low in the PE lane. Frequently, multiple bands can be detected in the PD. They correspond to different SUMOylated forms of the protein, such as single modifications on several sites, chains of SUMO at a single site, or a combination of both (Windecker and Ulrich, 2008). Moreover, it must be considered that a combination of SUMO with other modifications such as ubiquitilation, acetylation or phosphorylation is also possible.

4.2.2. Several subunits of the Smc5/6 complex are SUMOylated in an Nse2-dependent manner

Since the initial description of Nse2 as a SUMO ligase, several subunits of the Smc5/6 complex have been shown to be SUMOylated in different organisms: Smc5 and Nse2 in budding yeast (Zhao and Blobel, 2005); Nse2, Nse3, Nse4 and Smc6 in fission yeast (Andrews et al., 2005; Pebernard et al., 2008b); Nse2 and Smc6 in humans (Potts and Yu, 2005).

First we tested the SUMOylation of all subunits in the Smc5/6 complex. As seen in Figure 32, Smc5, Smc6, Nse2, Nse3 and Nse4 are all SUMOylated, as evidenced by the slower migrating forms detected in the SUMO pull-downs (PD). In contrast, Nse1, Nse5 and Nse6 are either not SUMO targets, or are modified at levels that are not detectable in our pull-down analysis.

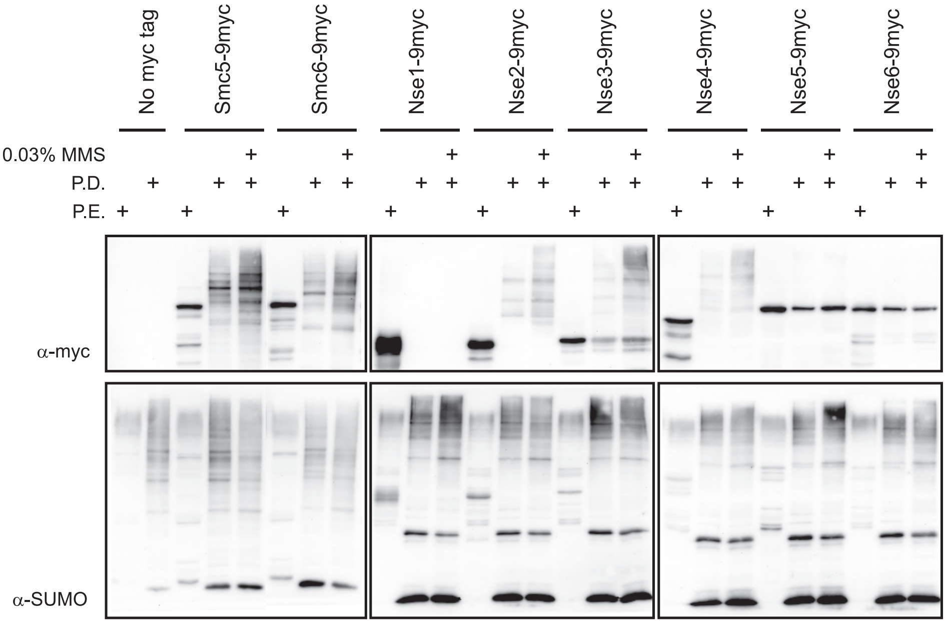

Figure 32. Several subunits of the Smc5/6 complex are SUMOylated and the SUMOylation increases in response to MMS

6HisFLAG-SUMO was pulled down under denaturing conditions in exponentially growing cells expressing the indicated 9myc versions of the Smc5/6 complex subunits at the endogenous locus (Smc5-9myc (YMB794), Smc6-9myc (YTR844), Nse1-9myc (YTR846), Nse2-9myc (YTR852), Nse3-9myc (YTR854), Nse4-9myc (YTR856), Nse5-9myc (YTR850), Nse6-9myc (YTR848)). Cells were treated with 0.03% MMS for 2 hours where indicated. Note the appearance of slower mobility forms in the pull-down (PD), indicative of modification by SUMO, and the increase in the SUMOylation levels upon MMS treatment. Abbreviations: MMS, methyl methanesulfonate; PD, pull-down; PE, Protein Extract.

Interestingly, an increase in the SUMOylation levels of the Smc5/6 complex subunits is detected when cells are treated with MMS. This suggests further activation of the SUMO ligase in response to DNA damage.

To determine the E3 SUMO ligase responsible for the SUMOylation of the Smc5/6 complex, the genes encoding the mitotic SUMO E3 ligases *SIZ1* and *SIZ2* were deleted, either alone or in combination. In order to inactivate the SUMO ligase activity of Nse2, the C-terminal part was deleted, generating the *nse2ΔC* mutant that lacks the Siz/PIAS (SP)-RING domain. As seen in Figure 33, the SUMOylation of Smc5 is not affected in siz1, *siz2* or *siz1-2* null cells. However, the SUMOylated forms of Smc5 are greatly reduced in the *nse2ΔC* mutant, indicating that its SUMOylation is highly dependent on Nse2, but not on Siz1 or Siz2. Interestingly, in the *siz2Δ* and *siz1-2Δ* mutant backgrounds, an increased Smc5 SUMOylation is detected. This may be due to a higher activity of Nse2 in these cells. A similar effect has been reported for other Nse2-dependent substrates in *siz1-2* null cells (Albuquerque et al., 2013). As with Smc5, the SUMOylation of Smc6 and the kleisin subunit, Nse4, of the Smc5/6 complex are highly Nse2-dependent (see Figure 33).

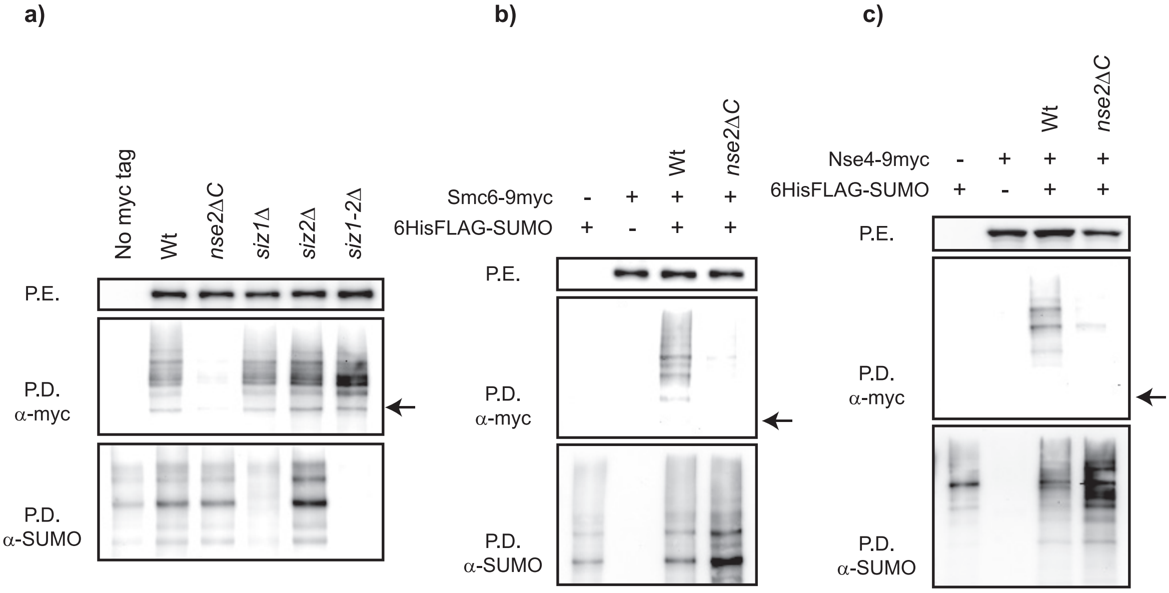

Figure 33. The SUMOylation of Smc5, Smc6 and Nse4 are Nse2-dependent

a) Smc5 SUMOylation is Nse2-dependent. Cells expressing 6HisFLAG-SUMO and Smc5-9myc in a wild type (YTR794), *nse2ΔC* (YTR793), *siz1Δ* (YTR811), *siz2Δ* (YTR813), or *siz1-2Δ* (YTR823) background were used. An untagged strain (YTR557) was used as a control for the anti-myc antibody. They were processed as previously described. Note that the SUMOylation of Smc5 depends on the SUMO ligase activity of Nse2. Note also that most SUMOylation in the cell is Siz1/2-dependent, while in the *nse2ΔC* background the levels of some SUMO conjugates are increased. Arrow points to unmodified Smc5. b) Smc6 SUMOylation is Nse2-dependent. Cells expressing 6HisFLAG-SUMO and Smc6-9myc in a wild type (YTR844) and *nse2ΔC* (YMB1773) background were used. As controls, untagged strains (YTR557 (no 9myc tag) and YTR28 (no 6HisFLAG-SUMO tag)) are also shown. They were processed as previously described. Note that the SUMOylation of Smc6 depends on the SUMO ligase activity of Nse2. Arrow points to unmodified Smc6. c) Nse4 SUMOylation is Nse2-dependent. Cells expressing 6HisFLAG-SUMO and Nse4-9myc in a wild type (YTR856) and *nse2ΔC* (YMB1110) background were used. As controls, untagged strains (YTR557 (no 9myc tag) and YTR83 (no 6HisFLAG tag)) are also shown. They were processed as previously described. Note that the SUMOylation of Nse4 depends on the SUMO ligase activity of Nse2. Arrow points to unmodified Nse4. Abbreviations: PD, pull-down; PE, protein extract.

The anti-SUMO blot of the PD revealed that deletion of *SIZ1* and *SIZ2* genes largely abolishes SUMOylation in *S. cerevisiae* (Johnson and Gupta, 2001). However, the levels of some SUMO conjugates are increased in the *nse2ΔC* background. This effect might be a response to endogenous DNA damage present in this mutant. This idea is supported by the fact that *mms21Δsl* and *mms21-11* mutants, which are SUMO ligase-defective cells, show slow growth, similar to *nse2ΔC* cells, spontaneous activation of the DNA damage checkpoint and an enhanced frequency of chromosome breakage (Rai et al., 2011).

In order to circumvent this problem, we decided to test the effect of a controlled inactivation of Nse2. For this purpose, the auxin-induced degron (AID) system was used. The AID system allows rapid and reversible degradation of target proteins in response to auxin (indole-3-acetic acid; IAA). This strategy allows the generation of efficient conditional mutants of essential genes in yeast, as well as cell lines (Nishimura et al., 2009). Since all members of the Smc5/6 complex are required for viability in *S. cerevisiae*, the lethality of the *nse2-aid* mutant in the presence of 1 mM indole-3-acetic acid (IAA) indicates that the specific degradation of Nse2 is strong enough to compromise the viability of the cell (see Figure 34). Then, we decided to analyse the impact of the specific degradation of Nse2 in the SUMOylation of Smc5 and Smc6. As seen in Figure 34, the addition of IAA to a final concentration of 1 mM for 2 hours causes a significant impairment in Smc5 and Smc6 SUMOylation without affecting the global SUMOylation pattern.

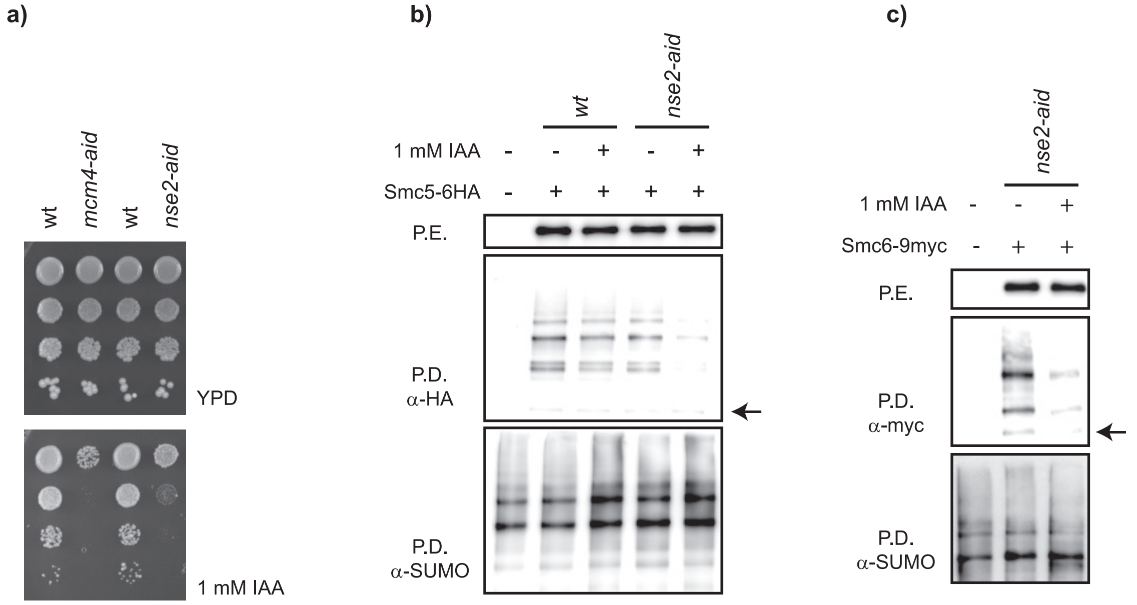

Figure 34. Nse2 degradation decreases the SUMOylation levels of the Smc5/6 complex

a) *nse2-aid* mutant cells are sensitive to indole-3-acetic acid (IAA). Serial dilutions of wild type (YTR1355), *mcm4-aid* (YTR1356), wild type (YTR1435) and *nse2-aid* (YTR1557) cells. They were spotted on YPD plates or YPD plates containing 1 mM IAA at 25ºC for 3 days and then photographed. Note that both mutants are sensitive to IAA indicating that the specific degradation of Nse2 and Mcm4 are strong enough to compromise the viability of the cell. b) Smc5 SUMOylation is impaired in *nse2-aid* cells when treated with IAA. Cells expressing Smc5-6HA in a wild type (YTR1435) and *nse2-aid* (YTR1557) background were used. As a control, an untagged strain (YTR557) is also shown. Where indicated, IAA was added to a final concentration of 1 mM and incubated for 2 hours. Samples were taken and processed as previously described. Note that Smc5 SUMOylation decreases in *nse2-aid* mutant cells when treated with IAA. Arrow points to unmodified Smc5. c) Smc6 SUMOylation is impaired in *nse2-aid* cells when treated with IAA. Cells expressing Smc6-9myc in an *nse2-aid* background (YTR1899) were used. Where indicated, IAA was added to a final concentration of 1 mM and incubated for 2 hours. Samples were taken and processed as previously described. Note that Smc6 SUMOylation decreases in the *nse2-aid* mutant when treated with IAA. Arrow points to unmodified Smc6. Abbreviations: PD, pull-down; PE, protein extract; IAA, indole-3-acetic acid.

4.2.3. Nse2 binding to Smc5 is essential for viability and required for the Smc5/6 complex SUMOylation

The crystal structure of Nse2 bound to the coiled coils of Smc5 shows that Nse2 forms a bipartite structure. The N-terminal domain (NTD) contributes to Smc5 binding, and the C-terminal domain (CTD) contains a variant Siz/PIAS (SP)-RING structure that has no contact with Smc5. Four segments in the NTD of Nse2 make the largest contributions to Smc5 binding. These include: the T1 region, which is the most N-terminal region of Nse2 wrapped around Smc5; the α2 and α3 helices, which contact with Smc5 in a parallel fashion; and the T2 region, which is composed of six residues located between the α1 and the α2 (Duan et al., 2009a).

To reduce the interaction between Nse2 and Smc5, we mutated 4 amino acids in the T1 region (Pro9, Val12, Leu14 and His15) and 2 amino acids in the T2 region (Leu25 and Leu30) to alanine generating an Smc5-binding-deficient Nse2 (*nse2-5BD*) mutant. These mutations have been previously reported to disrupt the interaction between Nse2 and Smc5 to different degrees (Duan et al., 2009a). This new allele was expressed from a *pRS315* vector under the *GAL* promoter. Then, the interaction between 3HA-tagged Nse2 and 9myc-tagged Smc5 was tested *in vivo*. Cells were grown in SC raffinose media overnight. When cells reached mid-log phase, galactose was added to a final concentration of 2% to activate the expression of either the wild type *NSE2* or *nse2-5BD* for two hours. Then, samples were taken, Nse2-3HA was immunoprecipitated (see materials and methods for more details) and the Nse2 binding to Smc5 was analysed by Western blot. As seen in Figure 35, the interaction between *nse2-5BD* and Smc5 is drastically reduced.

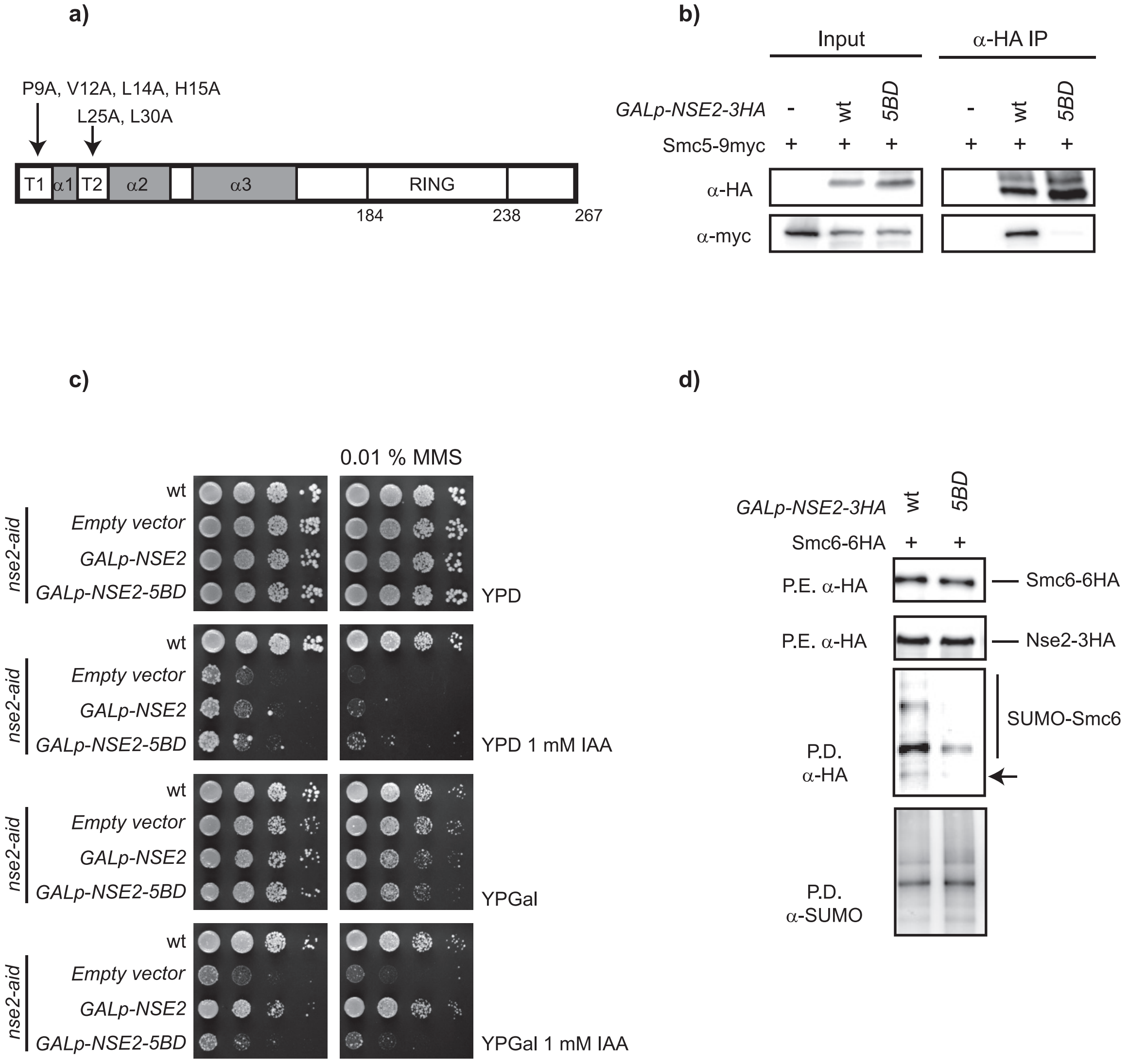
a)
P9A, V12A, L14A, H15A
L25A, L30A
T1
α1
T2
α2
α3
RING
184
238
267
b)
Input
α-HA IP
GALp-NSE2-3HA
-
wt
5BD
-
wt
5BD
Smc5-9myc
+
+
+
+
+
+
α-HA
α-myc
c)
0.01 % MMS
wt
nse2-aid
Empty vector
GALp-NSE2
GALp-NSE2-5BD
YPD
YPD 1 mM IAA
YPGal
YPGal 1 mM IAA
d)
GALp-NSE2-3HA
wt
5BD
Smc6-6HA
+
+
P.E. α-HA
Smc6-6HA
P.E. α-HA
Nse2-3HA
SUMO-Smc6
P.D.
α-HA
P.D.
α-SUMO

Figure 35. The Nse2 docking to Smc5 is essential for viability and required for Smc6 SUMOylation

a) Schematic map of Nse2 representing the different Smc5 interacting segments. Four amino acids in the T1 region (Pro9, Val12, Leu14 and His15) and 2 amino acids in the T2 region (Leu25 and Leu30) were mutated to alanine generating a Smc5 binding-deficient *nse2* (*nse2-5BD*) mutant. b) The *nse2-5BD* mutant protein is not able to interact with Smc5. Cells expressing Smc5-9myc (YTR912) were grown in SC raff media overnight. When cells reached mid-log phase, galactose was added to a final concentration of 2% to activate the expression of either wild type *NSE2* (YMB2141) or *nse2-5BD* (YMB2142) for two hours. Then, samples were taken and Nse2-3HA was immunoprecipitated. Finally, the Nse2 binding to Smc5 was analysed by Western blot. Note that the *nse2-5BD* mutant protein is not able to interact with Smc5. c) The Nse2-Smc5 interaction is essential for viability. Serial dilutions of wild type (YMB1852), *nse2-aid* (YMB1899), and *nse2-aid* with either wild type *GALp-NSE2* (YMB2137) or *GALp-nse2-5BD* (YMB2138) cells. They were spotted on YPD and YPgal plates. Where indicated, IAA was added to a final concentration of 1 mM and MMS to a final concentration of 0.01%. Note that *nse2-5BD* is not able to complement a lack of endogenous Nse2. d) The Nse2-Smc5 interaction is required for Smc6 SUMOylation. Cells expressing 6HisFLAG-SUMO and Smc6-6HA in the *nse2-aid* background either with *GALp-NSE2* or *GALp-nse2-5BD* (YMB2137 and YMB 2138, respectively) were grown in SC raffinose media overnight. When cells reached mid-log phase, galactose was added to a final concentration of 2% and IAA was added to a final concentration of 1 mM and incubated for 2 hours. Then, cells were harvested and lysed under denaturing conditions. After protein extraction, the SUMOylated proteins were purified using Ni-NTA beads. Finally, after protein elution, the SUMOylated proteins were detected by Western blot using an antibody against the HA epitope tag. Note that the *nse2-5BD* allele cannot maintain the SUMOylation of Smc6 when the endogenous Nse2 is degraded. Arrow points to unmodified Smc6. Abbreviations: A, alanine; H, histidine; L, leucine; P, proline; V, valine; PD, pull-down; PE, protein extract; IAA, indole-3-acetic acid.

Afterwards, we determined whether the *nse2-5BD* mutant was able to complement a lack of the endogenous Nse2. To test this, the mutant allele was inserted in the *nse2-aid* background. As seen in Figure 35, only wild type Nse2 is able to suppress the growth defects and MMS sensitivity of *nse2-aid* mutant cells in the presence of IAA. This result indicates that mutations in Nse2 that affect the interaction with Smc5 are lethal. This result is consistent with the notion that the interaction between Nse2 and Smc5 is necessary for the essential function(s) of the Smc5/6 complex (Duan et al., 2009a).

Finally, we decided to test whether the interaction between Nse2 and Smc5 was required for the SUMOylation of the Smc5/6 complex. To test this, the SUMOylation of Smc6 was analysed in the *nse2-aid* background in which the *nse2-5BD* allele had been previously inserted. Cells were grown in SC raffinose media overnight. When cells reached mid-log phase, IAA and galactose were added to promote the degradation of the endogenous Nse2 and activate the expression of either the wild type *NSE2* or the *nse2-5BD,* respectively. After two hours, samples were taken and the SUMOylation levels of Smc6 were analysed. As seen in Figure 35, the *nse2-5BD* mutant is not able to maintain the SUMOylation levels of Smc6 when the endogenous Nse2 is depleted. This suggests that the SUMOylation of the Smc5/6 complex reports the SUMO ligase activity of Nse2 associated with the complex. This result is in accordance with the hypothesis that Nse2 docks to Smc5 to reach its chromatin-associated substrates (Ulrich, 2014).

4.2.4. The Ubc9 fusion-directed SUMOylation suppresses the phenotype of *nse2ΔC* mutant cells

In comparison to the large population of E2 and E3s in the ubiquitin system, the small number of SUMO ligases opens the question of how SUMOylation is regulated. SUMOylation is essential for DNA damage repair, and mutations in E1, E2 or SUMO all lead to a higher DNA damage sensitivity (Bergink and Jentsch, 2009).

NSE2 was originally called *MMS21*, from a screen in *S. cerevisiae* for mutants sensitive to MMS (Prakash and Prakash, 1977a). Later, it was described as a member of a large complex involved in DNA repair (Zhao and Blobel, 2005). Despite the requirement of the Nse2 protein for cell viability in yeast, its SUMO ligase activity is not essential (Andrews et al., 2005; McDonald et al., 2003; Zhao and Blobel, 2005). Inactivating mutations in the Siz/PIAS (SP)-RING domain of Nse2 in budding and fission yeast (*nse2-SA*, *mms21-11, mms21-CH*, *mms21Δsl, mms21-H202A*, or *mms21-C221A*) that disrupt the SUMO ligase domain, result in hypersensitivity towards different types of DNA damage, including hydroxyurea, ionizing radiation, methyl methanesulfonate and ultraviolet light (Andrews et al., 2005; McDonald et al., 2003; Pebernard et al., 2004; Potts and Yu, 2005; Rai et al., 2011; Zhao and Blobel, 2005).

In the previous section, we demonstrated that *nse2ΔC* mutant cells behave like other *smc5/6* mutants; accumulating recombination intermediates, which lead to chromosome missegregation after an MMS pulse (see Figure 23). Contrary to other SUMO ligase mutants (*siz1*Δ, *siz2Δ*, and double *siz1-2Δ*), the *nse2ΔC* mutant shows a slow growth phenotype, is thermosensitive and hypersensitive to MMS (see Figure 36).

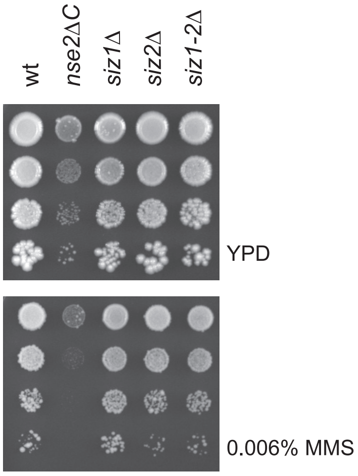

Figure 36. ***nse2ΔC*** **mutant cells are sensitive to MMS**

Serial dilutions of wild type (YTR557), *nse2ΔC* (YTR570), *siz1Δ* (YTR569), s*iz2Δ* (YTR571) and *siz1-2Δ* (YTR572) cells. They were spotted on YPD plates. Where indicated, MMS was added to a final concentration of 0.006%. Cells were grown at 25°C for 3 days and then photographed. Note that only the *nse2ΔC* mutant is sensitive to MMS.

As seen in Figure 35, SUMOylation of Smc5/6 subunits also requires binding of the E3 to its substrate, which indicates that Nse2 most likely promotes SUMOylation by recruiting Ubc9 through its Siz/PIAS (SP)-RING domain and by promoting the formation of an E2-SUMO-E3-target complex. If the phenotype of the *nse2⊿C* mutant were due to its inability to specifically SUMOylate its substrates, the recovery of the SUMOylation levels would alleviate its phenotype. It is accepted that E3 SUMO ligases can facilitate SUMOylation by bringing Ubc9 and its substrates into close proximity. To explore this possibility, we integrated a second copy of *UBC9* fused to the 3´-end of the endogenous *NSE2* gene and to the *nse2⊿C* mutant allele to force recruitment of the E2 in the vicinity of the E3. Ubc9 fusion-directed SUMOylation (UFDS), in which Ubc9 (SUMO E2) is fused to the C-terminus of a target protein, is a technique developed in mammalian cells to increase the amount of specific SUMOylation targets (Jakobs et al., 2007). Our group has used this technique previously to characterize the importance of the SUMOylation of the cohesin complex in *S. cerevisiae* (Almedawar et al., 2012).

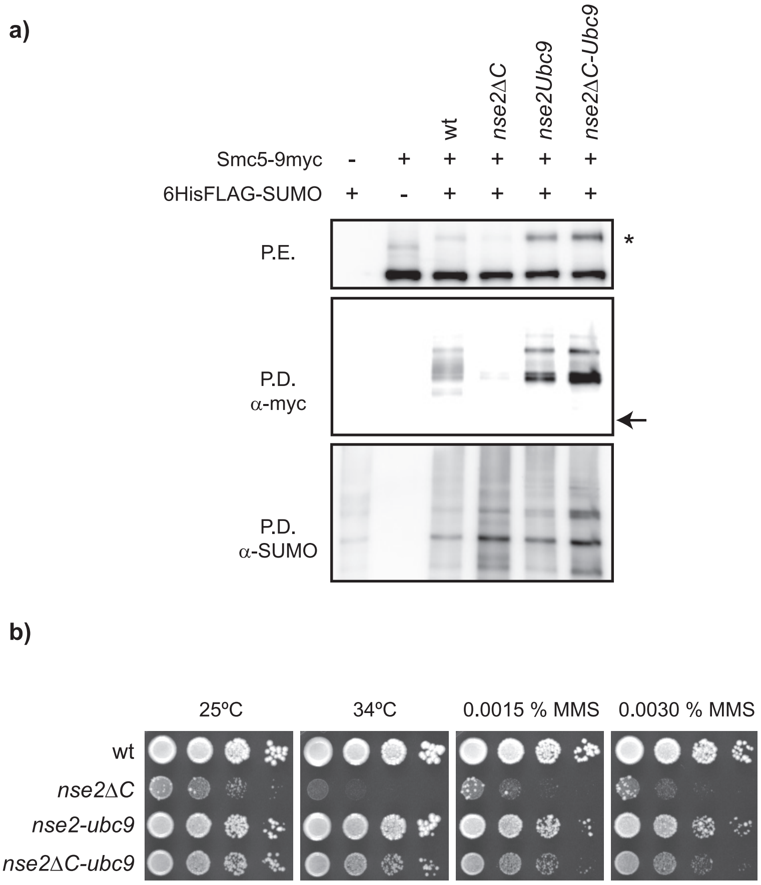

Figure 37. The Ubc9 fusion-directed SUMOylation suppresses the phenotype of the *nse2⊿C* mutant

a) Ubc9 fusion to Nse2 increases Smc5 SUMOylation. Cells expressing Smc5-9myc in a wild-type (YTR794), *nse2⊿C* (YTR793), *nse2-ubc9* (YTR1766), and *nse2⊿C-ubc9* (YTR1768) background were used. As controls, untagged strains (no 6HisFLAG tag (YTR27) and no 9myc tag (YTR557)) are also shown. Note that the SUMOylation of Smc5 increases in the E2-E3 fusions. Arrow points to unmodified Smc5 and stars indicate the SUMOylated form of Smc5 seen in the protein extract. Abbreviations: PD, pull-down; PE, protein extract.

b) The phenotype of the nse2ΔC mutant is partially suppressed by the E2-E3 fusion. Serial dilutions of wild type (YTR557), *nse2ΔC* (YTR570), *nse2-ubc9* (YTR1766) and *nse2ΔC-ubc9* (YTR1768) cells. They were spotted on YPD plates with the indicated amount of MMS. Cells were grown at 25ºC or 34ºC for 3 days and then photographed. Note that the phenotype of the *nse2ΔC* is partially suppressed by the *nse2ΔC-Ubc9* fusion.

In order to determine whether the constitutive recruitment of Ubc9 to the complex was able to increase the SUMOylation levels of Smc5, exponentially growing cells expressing Smc5-9myc and 6HisFLAG-Smt3 in a wild type, *nse2ΔC*, *nse2-ubc9* and *nse2ΔC-ubc9* background were used. As seen in Figure 37, the Nse2-Ubc9 and *nse2ΔC*-Ubc9 fusions increase the SUMOylation levels of Smc5. This indicates that this fusion is functional and displays higher levels of Smc5 SUMOylation, as expected from constitutive recruitment of both the E2 and E3 enzymes. In accordance, we observed that the Ubc9 fusion-directed SUMOylation partially suppresses most of the *nse2ΔC* mutant sensitivities towards temperature and MMS-induced DNA damage (see Figure 37). These experiments allowed us to conclude that the artificial recruitment of Ubc9 increases the SUMOylation levels of the complex and alleviates the DNA damage sensitivity of the *nse2ΔC* mutant, which indicates that the main function of the Siz/PIAS (SP)-RING domain of Nse2 is the recruitment of Ubc9 (E2).

4.2.5. Nse2-mediated SUMOylation requires an active and intact Smc5/6 complex

The previous observations suggest that Nse2 binds to the Smc5/6 complex to reach its substrates and promote DNA repair. Therefore, we decided to test the influence of the different components of the Smc5/6 complex on the E3 SUMO ligase activity of Nse2. Since Smc5 is a target of Nse2 (Zhao and Blobel, 2005), the binding site for Nse2 in the complex (Duan et al., 2009a), and shows a strong SUMOylation (see Figure 32), we used its SUMOylation levels as an *in vivo* reporter for the activity of the Smc5/6-associated SUMO ligase.

The Smc5/6 complex has been dissected into apparently different sub-entities: the Smc5-Smc6, the Nse1-Nse3 and the Nse5-Nse6 heterodimers, plus the Nse2 SUMO ligase and the Nse4 kleisin subunit (Duan et al., 2009b; Hudson et al., 2011; Pebernard et al., 2006; Sergeant et al., 2005). In order to analyze the contribution of each sub-complex to the SUMO ligase activity of Nse2, we used various approaches to individually down-regulate the different subunits.

In order to determine the contribution of the Nse1-Nse3 heterodimer, the *nse3-2* hypomorphic allele was used. *nse3-2* thermosensitive cells are sensitive to MMS to a similar extent as other *smc5/6* mutants (see Figure 38), indicating that the activity of the Smc5/6 complex is impaired in this mutant. We started by testing whether the interaction between Nse3 and Smc5 was affected in the *nse3-2* background. To do this, cells expressing Smc5-6FLAG and either wild type Nse3-9myc or *nse3-2-9myc* were used. When cells reached mid-log phase, the culture was split into two, and one half was shifted to 37ºC for 2 hours to inactivate *nse3*. Then, cells were harvested, Smc5-6FLAG was immunoprecipitated, and the Nse3 binding to Smc5 was analyzed by Western blot. As seen in Figure 38, the Smc5-Nse3 interaction is weaker in *nse3-2* mutant cells than in wild type cells at the permissive temperature, and this interaction is drastically reduced upon shift to the restrictive temperature.

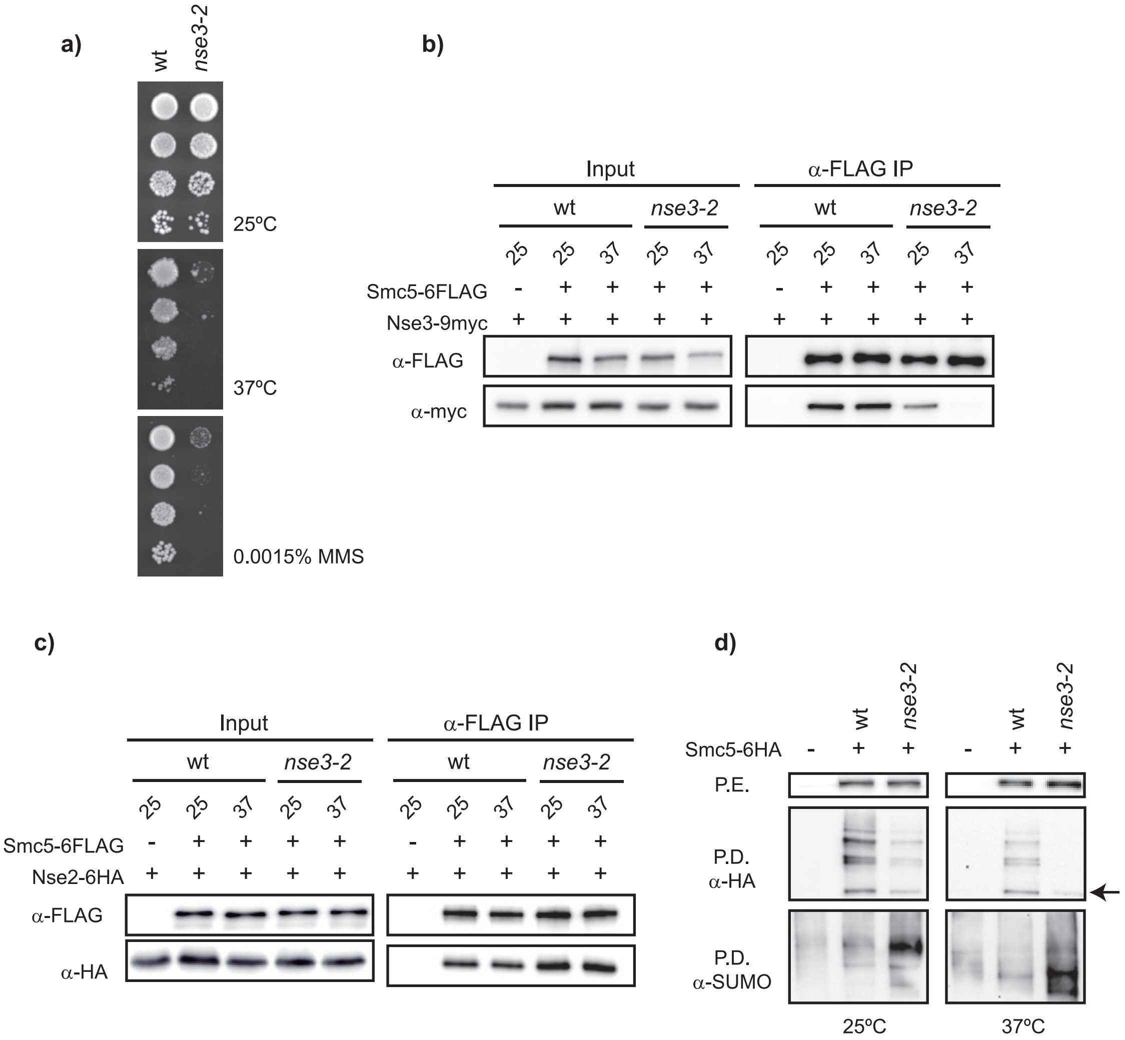
a)
wt
nse3-2
25ºC
37ºC
0.0015% MMS
b)
Input
α-FLAG IP
wt
nse3-2
wt
nse3-2
25 25 37 25 37
25 25 37 25 37
Smc5-6FLAG - + + + + - + + + +
Nse3-9myc + + + + + + + + + +
α-FLAG
α-myc
c)
Input
α-FLAG IP
wt
nse3-2
wt
nse3-2
25 25 37 25 37
25 25 37 25 37
Smc5-6FLAG - + + + + - + + + +
Nse2-6HA + + + + + + + + + +
α-FLAG
α-HA
d)
wt
nse3-2
wt
nse3-2
Smc5-6HA - + + - + +
P.E.
P.D.
α-HA
P.D.
α-SUMO
25ºC
37ºC

Figure 38. The SUMO ligase activity of Nse2 is reduced when the Nse3 docking to Smc5 is impaired

a) *nse3-2* mutant cells are sensitive to MMS. Serial dilutions of wild type (YTR337) and *nse3-2* (YTR788) cells. They were spotted on YPD plates and grown at 25ºC or 37ºC for 3 days and then photographed. Where indicated, MMS was added to a final concentration of 0.0015%. Note that *nse3-2* mutant cells are thermosensitive and sensitive to MMS. b) The Nse3-Smc5 interaction is impaired in *nse3-2* mutant cells. Cells expressing Smc5-6FLAG and either wild type Nse3-9myc (YMB1424) or *nse3-2-9myc* (YMB1330) were used. As a control for unspecific binding of Nse3 to the beads, an Nse3-9myc (YTR82) strain was used. When cells reached mid-log phase, the culture was split into two and one half was shifted to 37ºC for 2 hours to inactivate *nse3*. Then, cells were harvested; Smc5-6FLAG was immunoprecipitated and the Nse3 binding to Smc5 was analyzed by Western blot. Note that the interaction between Nse3 and Smc5 is weaker in *nse3-2* than in wild type cells and is further reduced at the restrictive temperature.

c)The interaction between Nse2 and Smc5 is not affected in *nse3-2* cells. Cells expressing Smc5-6FLAG and Nse2-6HA in a wild type (YMB1448) and *nse3-2* background (YMB1430) were used. As a control for unspecific binding of Nse2 to the beads, an Nse2-6HA (YMB2210) strain was used. When cells reached mid-log phase, the culture was split into two and one half was shifted to 37ºC for 2 hours to inactivate *nse3*. Then, cells were harvested; Smc5-6FLAG was immunoprecipitated and the Nse2 binding to Smc5 was analysed by Western blot. Note that the interaction between Nse2 and Smc5 is not affected in *nse3-2* cells
d) Smc5 SUMOylation is impaired in an *nse3-2* background. Cells expressing Smc5-6HA and 6HisFLAG-SUMO in a wild type (YMB1117) and *nse3-2* background (YMB1345) were used. When cells reached mid-log phase, the culture was split into two and one half was shifted to 37ºC for 2 hours to inactivate *nse3-2*. Cells were harvested and the SUMOylation levels of Smc5 were analyzed as previously described. Note that the *nse3-2* mutant shows reduced levels of Smc5 SUMOylation at both the permissive and the restrictive temperatures. Arrow points to unmodified Smc5. Abbreviations: MMS, methyl methanesulfonate; PD, pull-down; PE, protein extract.

Since the *nse3-2* allele affects the integrity of the Smc5/6 complex, it was important to know whether the Nse2-Smc5 interaction was also affected. To answer this question the interaction between Nse2 and Smc5 was determined in the *nse3-2* background. Cells expressing Smc5-6FLAG and Nse2-6HA were used. When cells reached mid-log phase the culture was split into two and one half was shifted to 37ºC for 2 hours to inactivate *nse3*. Then, cells were harvested, Smc5-6FLAG was immunoprecipitated, and the Nse2 binding to Smc5 was analysed by Western blot. As seen in Figure 38, the interaction between the SUMO ligase Nse2 and Smc5 is not affected in *nse3-2* mutant cells.

Finally we analysed the SUMOylation levels of Smc5 in the *nse3-2* background. To do this, when cells reached mid-log phase, the culture was split into two and one half was shifted to 37ºC for 2 hours to inactivate *nse3*. Then, cells were harvested and the SUMOylation levels of Smc5 were analyzed. As seen in Figure 38, despite wild type levels of Nse2 recruitment to Smc5, and a global up-regulation of protein SUMOylation (similar to *nse2ΔC*), *nse3-2* mutant cells show reduced levels of Smc5 SUMOylation at both the permissive and the restrictive temperatures. These results indicate that the SUMO ligase activity of Nse2 is impaired when the interaction between Nse3 and the rest of the Smc5/6 complex is compromised.

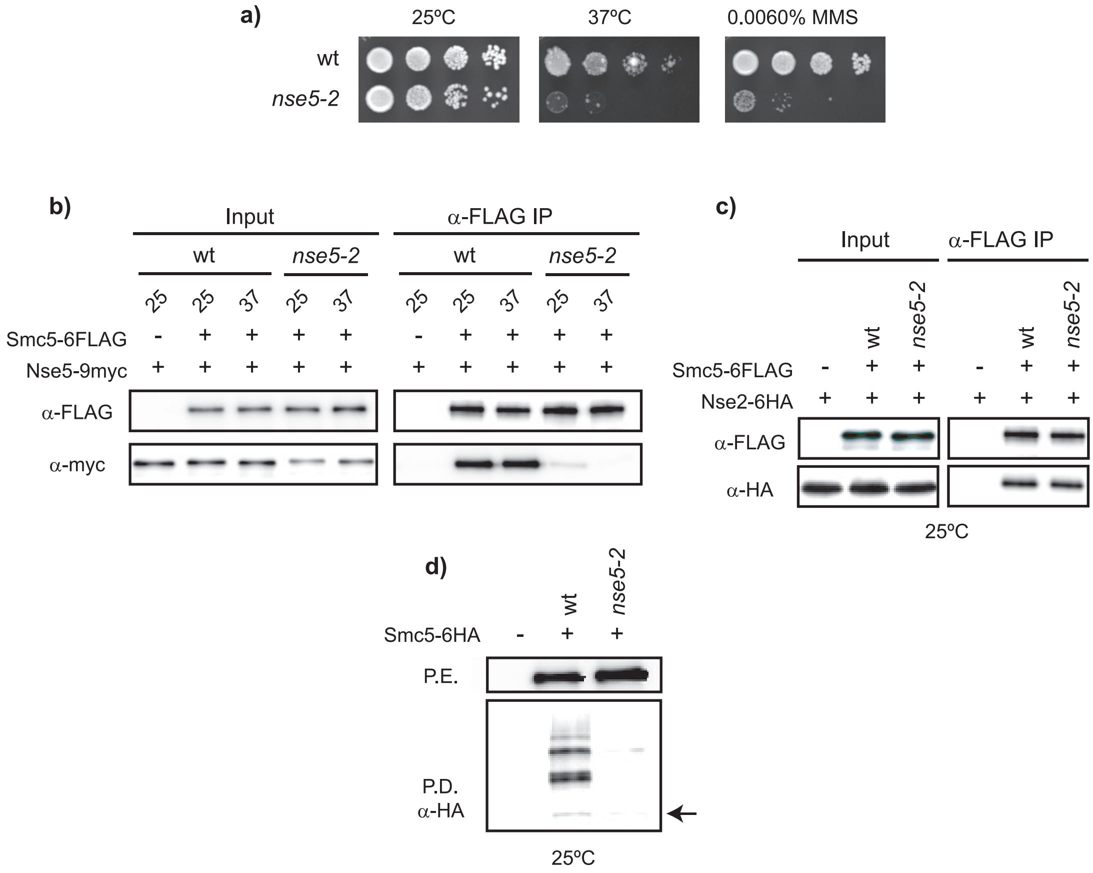

Figure 39. The SUMO ligase activity of Nse2 is impaired when the Nse5 docking to Smc5 is impaired

a) nse5-2 mutant cells are sensitive to MMS. Serial dilutions of wild type (YTR337) and *nse5-2* (YTR786) cells. They were spotted on YPD plates, grown at 25ºC or 37ºC for 3 days and then photographed. Where indicated, MMS was added to a final concentration of 0.006%. Note that *nse5-2* mutant cells are thermosensitive and sensitive to MMS. b) The Nse5-Smc5 interaction is impaired in *nse5-2* mutant cells. Cells expressing Smc5-6FLAG and either wild type Nse5-9myc (YMB1410) or *nse5-2-9myc* (YMB1432) were used. When cells reached mid-log phase, the culture was split into two and one half was shifted to 37ºC for 2 hours to inactivate *nse5*. Then, cells were harvested; Smc5-6FLAG was immunoprecipitated and the Nse5 binding to Smc5 was analysed by Western blot. Note that the interaction between Nse5 and Smc5 is weaker in *nse5-2* mutant cells than in wild type cells at the permissive temperature and it is drastically reduced at the restrictive temperature. c) The interaction between Nse2 and Smc5 is not affected in *nse5-2* mutant cells. Cells expressing Smc5-6FLAG and Nse2-6HA in a wild type (YMB1446) or *nse5-2* background (YMB1432) were used. As a control for unspecific binding of Nse2 to the beads, an Nse2-6HA (YMB2210) strain was used. When cells reached mid-log phase, the culture was split into two and one half was shifted to 37ºC for 2 hours to inactivate *nse5*. Then, cells were harvested, Smc5-6FLAG was immunoprecipitated and the Nse2 binding to Smc5 was analysed by Western blot. Note that the interaction between Nse2 and Smc5 is not affected in the *nse5-2* background. d) Smc5 SUMOylation is affected in an *nse5-2* background. Cells expressing Smc5-6HA and 6HisFLAG-SUMO in a wild type (YMB1117) or *nse5-2* background (YMB1120) were used. When cells reached mid-log phase, cells were harvested and the SUMOylation levels of Smc5 were analyzed as previously described. Note that the *nse5-2* mutant shows reduced levels of Smc5 SUMOylation even at the permissive temperature. Arrow points to unmodified Smc5. Abbreviations: MMS, methyl methanesulfonate; PD, pull-down; PE, protein extract.

Nse5 is another subunit of the Smc5/6 complex, which heterodimerizes with Nse6. It has been described that Nse5 interacts with Ubc9 (SUMO E2 conjugating enzyme), Siz2 (SUMO E3 ligase), and Smt3 (SUMO) by two-hybrid analysis (Hazbun et al., 2003). *nse5* hypomorphic alleles show reduced levels of Smc5 SUMOylation (Bustard et al., 2012). Since this effect was not clearly understood, we decided to characterize the *nse5-2* mutant to explain this phenomenon. *nse5-2* mutant cells behave like other *smc5/6* mutants: it is thermosensitive and sensitive to the DNA damaging agent MMS (see Figure 39). Moreover, the *nse5-2* mutant protein interacts weakly with Smc5, suggesting that the integrity of the complex might become compromised, even at the permissive temperature (see Figure 39). However, the Smc5-Nse2 interaction is not affected, not even after the shift to the restrictive temperature. Like in the *nse3-2* background, in spite of a stable Nse2-Smc5 interaction, the levels of Smc5 SUMO-conjugates are almost undetectable in *nse5-2* cells even at the permissive temperature (see Figure 39). These observations indicate that the SUMO ligase activity of Nse2 is affected when the interaction between Nse5 and the rest of the Smc5/6 complex is compromised.

Previously, we determined the requirements of the Nse1-Nse3 and the Nse5-Nse6 subcomplexes for the SUMO ligase activity of Nse2. In order to test whether a functional Smc6 protein was also required for the activation of Nse2, we analysed the SUMOylation levels of Smc5 in cells that express the *SMC6* gene from a regulatable *GAL* promoter. *GALp-SMC6* cells expressing Smc5-9myc were grown in YP galactose until mid-log phase. Then, the culture was split into two. One half was maintained in galactose and the other half was shifted to YPD to repress the expression of *SMC6* for 12 hours. Afterwards, cells were harvested and the SUMOylation levels of Smc5 were determined as previously described. We observed that shutting off the promoter leads to a drastic reduction in Smc5 SUMOylation (see Figure 40).

Then, we determined whether the repression of *SMC6* was affecting the Nse2-Smc5 interaction. To test this, the interaction between Nse2 and Smc5 was determined in a *GALp-SMC6* background in the absence of Smc6 (glucose). *GALp-SMC6* cells expressing Smc5-9myc and Nse2-6HA were grown in YP galactose until mid-log phase. Then, the culture was shifted to YPD to repress the expression of *SMC6* for 12 hours. Afterwards, cells were harvested, Nse2-6HA was immunoprecipitated and the Nse2 binding to Smc5 was analysed by Western blot. As seen in Figure 40, under these conditions, Nse2 still binds to Smc5. However, we noticed that down-regulation of *SMC6* leads to a reduction of the protein levels of Nse2 (see Figure 40). In order to circumvent this problem, we also tested Smc5 SUMOylation when the thermosensitive *smc6-1* allele was expressed under its own promoter from an ectopic location in a *GALp-SMC6* strain. Wild type, *GALp-SMC6* and *smc6-1 GALp-SMC6* cells expressing Smc5-9myc were grown in SC galactose until mid-log phase. Then, the culture was split into two. One half was maintained in galactose and the other half was shifted to SC glucose to repress the expression of SMC6 for 12 hours. Then, cells were harvested and the SUMOylation levels of Smc5 were determined. As shown in Figure 40, the SUMO ligase activity of Nse2 could not be restored by the expression of the *smc6-1* mutant allele.

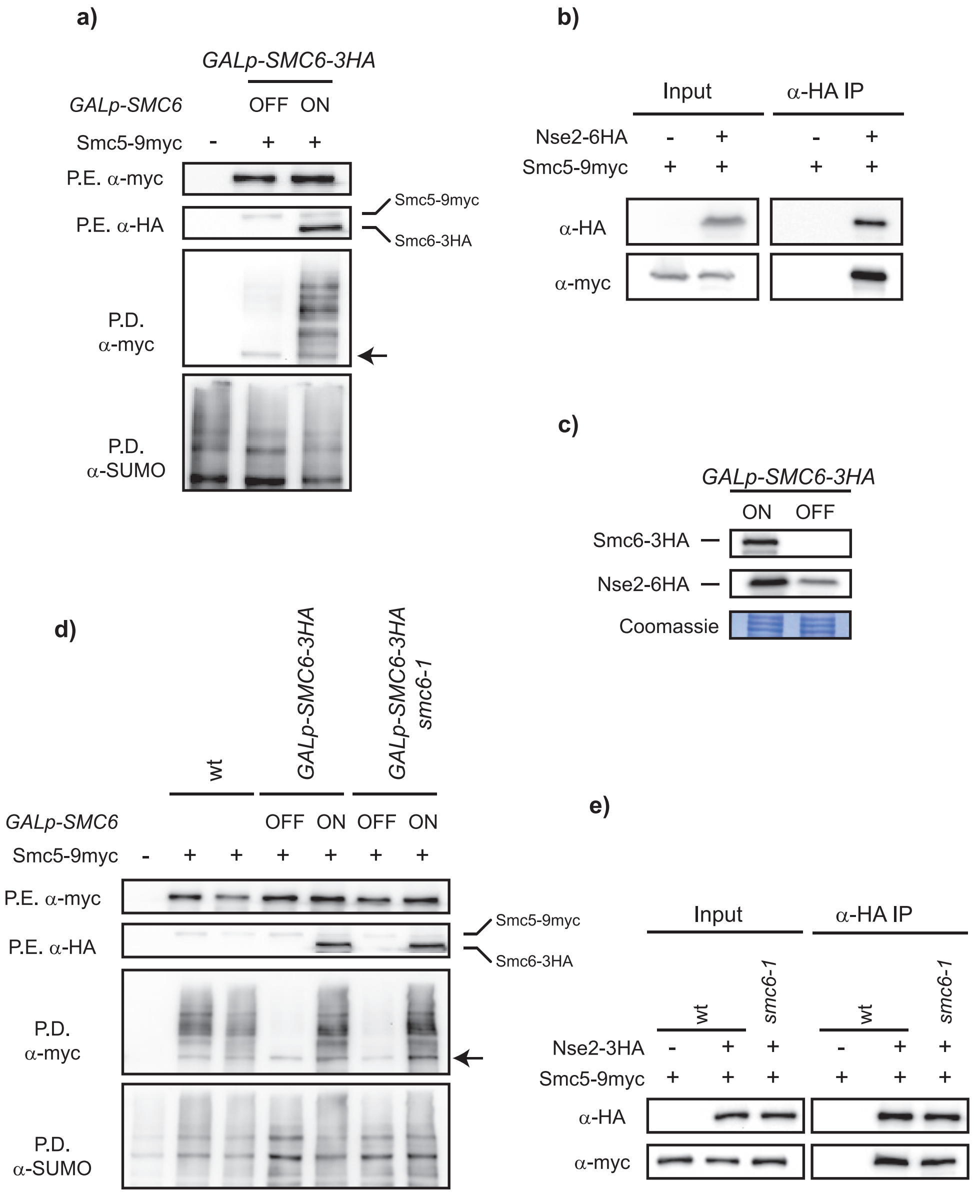
a)
GALp-SMC6-3HA
GALp-SMC6
OFF ON
Smc5-9myc - + +
P.E. α-myc
P.E. α-HA
Smc5-9myc
Smc6-3HA
P.D. α-myc
P.D. α-SUMO
b)
Input
α-HA IP
Nse2-6HA - + - +
Smc5-9myc + + + +
α-HA
α-myc
c)
GALp-SMC6-3HA
ON OFF
Smc6-3HA
Nse2-6HA
Coomassie
d)
wt
GALp-SMC6-3HA
GALp-SMC6-3HA smc6-1
GALp-SMC6
OFF ON OFF ON
Smc5-9myc - + + + + + +
P.E. α-myc
P.E. α-HA
Smc5-9myc
Smc6-3HA
P.D. α-myc
P.D. α-SUMO
e)
Input
α-HA IP
wt
smc6-1
wt
smc6-1
Nse2-3HA - + + - + +
Smc5-9myc + + + + + +
α-HA
α-myc

Figure 40. A functional *SMC6* is required for the activation of the Nse2 SUMO ligase

a) *SMC6* down-regulation has a negative effect on Smc5 SUMOylation. *GALp-SMC6* cells expressing Smc5-9myc and 6HisFLAG-SUMO (YMB1444) were grown in YP galactose until mid-log phase. Then, the culture was split into two. One half was maintained in galactose and the other half was shifted to YPD to repress the expression of *SMC6* for 12 hours. After this, cells were harvested and the SUMOylation levels of Smc5 were determined as previously described. Note that shutting the promoter off leads to a drastic reduction in Smc5 SUMOylation. Arrow points to unmodified Smc5. b) Nse2 is able to interact with Smc5 in the absence of Smc6. *GALp-SMC6* cells expressing Smc5-9myc and Nse2-6HA (YMB2045) were used. As a control for Smc5 unspecific binding, cells expressing Smc5-9myc (YTR794) used. They were grown in YP galactose until mid-log phase. Then, the culture was shifted to YPD to repress the expression of *SMC6* for 12 hours. After this, cells were harvested, Nse2-6HA was immunoprecipitated and the Nse2 binding to Smc5 was analysed by Western blot. Note that under these conditions, Nse2 still binds to Smc5. c) *SMC6* down-regulation leads to a reduction of the Nse2 protein levels. *GALp-SMC6* cells expressing Nse2-6HA (YMB2045) cells were grown in YP galactose until mid-log phase. Then, the culture was split into two. One half was maintained in galactose and the other half was shifted to YPD to repress the expression of SMC6 for 12 hours. After this, cells were harvested and the protein levels of Nse2 and Smc6 were determined by Western blot. Note that the down-regulation of *SMC6* leads to a reduction in the protein levels of Nse2. d) Smc5 SUMOylation is impaired when *SMC6* is compromised. Wild type (YTR794), *GALp-SMC6* (YMB1444), and *smc6-1 GALp-SMC6* (YMB1556) cells expressing Smc5-9myc and 6HisFLAG-SUMO were grown in SC galactose until mid-log phase. Then, the culture was split into two. One half was maintained in galactose and the other half was shifted to SC glucose to repress the expression of SMC6 for 12 hours. After this, cells were harvested and the SUMOylation levels of Smc5 were determined as previously described. Note that Smc5 is not SUMOylated when *SMC6* is compromised. Arrow points to unmodified Smc5. e) The Nse2-Smc5 interaction is not affected in the *smc6-1* background. Wild type (YMB2315) and *smc6-1 GALp-SMC6* (YMB2309) cells expressing Smc5-9myc and Nse2-6HA were grown in SC galactose until mid-log phase. Then, the culture was shifted to SC glucose to repress the expression of *SMC6* for 12 hours. After this, cells were harvested, Nse2-6HA was immunoprecipitated and the Nse2 binding to Smc5 was analyzed by Western blot. Note that in the *smc6-1* background, Nse2 interacts with Smc5 with the same efficiency as in wild type cells. Abbreviations: PD, pull-down; PE, protein extract.

Finally, we decided to determine whether the *smc6-1* allele was affecting the Nse2-Smc5 interaction. To test this, wild type and *smc6-1 GALp-SMC6* cells expressing Smc5-9myc and Nse2-6HA were grown in SC galactose until mid-log phase. Then, the culture was shifted to SC glucose to repress the expression of *SMC6* for 12 hours. After this, cells were harvested, Nse2-6HA was immunoprecipitated and the Nse2 binding to Smc5 was analysed by Western blot. As seen in Figure 40, in the *smc6-1* background, Nse2 interacts with Smc5 with the same efficiency as in wild type cells. Since the Nse2-Smc5 interaction is not affected in *smc6-1* cells, these results indicate that the SUMO ligase activity of Nse2 is impaired when Smc6 is not fully functional.

Given that these results indicate that the integrity of the Smc5/6 complex affects the SUMO ligase activity of Nse2, we decided to test the effect of controlled inactivation of specific subunits, including the Nse4 kleisin, using the auxin-induced degron (AID) system. Since all members of the Smc5/6 complex are required for viability in *S. cerevisiae*, the lethality of the *nse4-aid*, *nse5-aid* and *nse6-aid* mutants in the presence of 1 mM of IAA indicates that the specific degradation of these subunits is strong enough to compromise the viability of the cell (see Figure 41). Then, we analysed the impact of the specific degradation of these subunits in the SUMOylation of Smc5. As seen in Figure 41, the addition of IAA to a final concentration of 1 mM for 2 hours causes a significant reduction in the SUMOylation levels of Smc5.

In summary, our observations indicate that inactivation of the Nse1-Nse3 heterodimer, the Nse5-Nse6 heterodimer, the Nse4 kleisin subunit or Smc6 all lead to reduced levels of the Nse2-dependent SUMOylation of Smc5. Therefore, an active and intact Smc5/6 complex is required for the activity of its associated SUMO ligase.

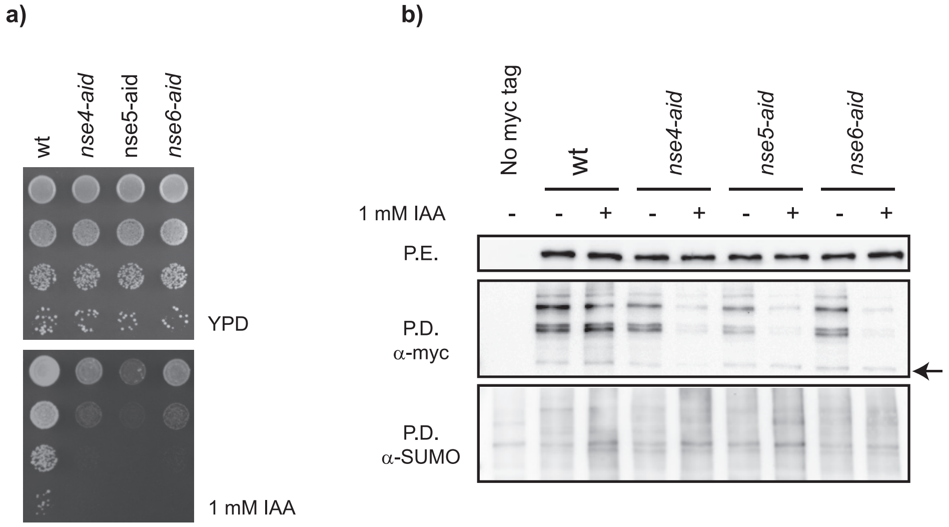

Figure 41. The auxin-induced degradation of Nse4, Nse5 and Nse6 decreases the SUMOylation levels of Smc5

a) Fusion of Nse4, Nse5 or Nse6 to the AID moiety renders cells sensitive to IAA. Serial dilutions of wild type (YTR1435), *nse4-aid* (YTR1452), *nse5-aid* (YTR1454) and *nse6-aid* (YTR1456) cells. They were spotted on YPD plates or YPD plates containing 1 mM of IAA. Note that all mutants are sensitive to IAA indicating that the specific degradation of these subunits is strong enough to compromise the viability of the cell. b) Smc5 SUMOylation is impaired in the *nse4-aid*, *nse5-aid* and *nse6-aid* backgrounds when treated with IAA. Cells expressing Smc5-6HA and 6HisFLAG-SUMO in wild type (YTR1435), *nse4-aid* (YTR1452), *nse5-aid* (YTR1454) and *nse6-aid* (YTR1456) backgrounds were used. Where indicated, IAA was added to a final concentration of 1 mM and incubated for 2 hours. Samples were taken and processed as previously described. Note that the SUMOylation of Smc5 decreases in all mutants when treated with IAA. Arrow points to unmodified Smc5. Abbreviations: IAA, indole-3-acetic acid; PD, pull-down; PE, protein extract.

Finally, we wanted to determine whether the integrity of the Smc5/6 complex was also affecting the ability of Nse2 to transfer SUMO to other targets outside the Smc5/6 complex. Several cohesin subunits are modified by SUMO in budding yeast: Smc1, Smc3, Scc1, Scc3 and Pds5 (Almedawar et al., 2012; Denison et al., 2005; Stead et al., 2003; Takahashi et al., 2008). To determine whether the SUMOylation of the cohesin complex was Nse2-dependent, the SUMOylation levels of Smc1 and Smc3 were determined in the *nse2ΔC* mutant background. Similar to what has been described (Takahashi et al., 2008), the abundance of SUMO conjugates is greatly reduced in the *nse2ΔC* mutant (see Figure 42). This experiment allowed us to conclude that the SUMOylation of Smc1 and Smc3 are highly dependent on the SUMO ligase domain of Nse2.

Then, we wanted to know whether the integrity of the Smc5/6 complex was affecting the ability of Nse2 to SUMOylate the cohesin complex. To test this, the SUMOylation levels of Smc3 were determined in cells that express the *SMC6* gene from a regulatable

GAL promoter. *GALp-SMC6* cells expressing Smc3-9myc were grown in YP galactose until mid-log phase. Then, the culture was split into two. One half was maintained in galactose, and the other half was shifted to YPD to repress the expression of *SMC6* for 12 hours. After this, cells were harvested and the SUMOylation levels of Smc3 were determined as previously described. We observed that shutting the promoter off leads to a drastic reduction of Smc3 SUMOylation (see Figure 42). However, since we noticed that down-regulation of *SMC6* leads to a reduction of the protein levels of Nse2 (see Figure 40); we decided to test whether the SUMOylation levels of Smc3 were affected in an *nse5-2* background. As previously seen for Smc5, Smc3 SUMOylation levels are almost undetectable in *nse5-2* cells at the permissive temperature (see Figure 42). These observations indicate that the ability of Nse2 to transfer SUMO to substrates outside, as well as inside, the Smc5/6 complex is impaired when the integrity or the functionality of the Smc5/6 complex is compromised.

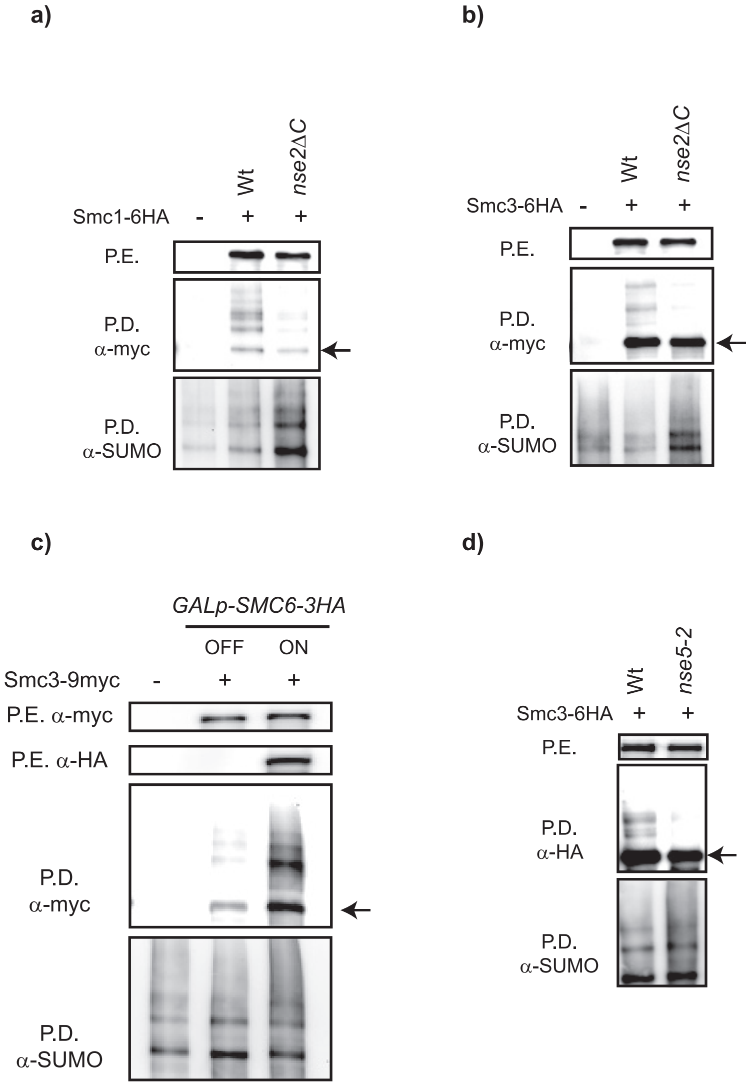
a)
b)
Wt
nse2ΔC
Smc1-6HA - + +
P.E.
P.D.
α-myc
P.D.
α-SUMO
Wt
nse2ΔC
Smc3-6HA - + +
P.E.
P.D.
α-myc
P.D.
α-SUMO
c)
d)
GALp-SMC6-3HA
OFF ON
Smc3-9myc - + +
P.E. α-myc
P.E. α-HA
P.D.
α-myc
P.D.
α-SUMO
Wt
nse5-2
Smc3-6HA + +
P.E.
P.D.
α-HA
P.D.
α-SUMO

Figure 42. The SUMOylation of the cohesin complex is impaired when the integrity of the Smc5/6 complex is compromised

a) Smc1 SUMOylation is Nse2-dependent. Cells expressing Smc1-6HA and 6HisFLAG-SUMO in a wild type (YMB2214) and *nse2ΔC* (YMB2162) background were processed as previously described. Note that the SUMOylation of Smc1 depends on the SUMO ligase activity of Nse2. b) Smc3 SUMOylation is Nse2-dependent. Cells expressing Smc3-6HA and 6HisFLAG-SUMO in a wild type (YMB2164) and *nse2ΔC* (YMB2166) background were processed as previously described. Note that the SUMOylation of Smc3 depends on the SUMO ligase activity of Nse2. c) *SMC6* down-regulation impairs Smc3 SUMOylation. *GALp-SMC6* cells expressing 6HisFLAG-SUMO and Smc3-9myc (YMB1830) were grown in YP galactose until mid-log phase. Then, the culture was split into two. One half was maintained in galactose and the other half was shifted to YPD to repress the expression of *SMC6* for 12 hours. After this, cells were harvested and the SUMOylation levels of Smc3 were determined as previously described. Note that shutting the promoter off leads to a drastic reduction in Smc3 SUMOylation. d) Smc3 SUMOylation is impaired in *nse5-2* cells. Cells expressing Smc3-6HA and 6HisFLAG-SUMO in a wild type (YMB2164) and *nse5-2* background (YMB2266) were used. When cells reached mid-log phase, they were harvested and the SUMOylation levels of Smc3 were analysed as previously described. Note that *nse5-2* mutant cells show reduced levels of Smc3 SUMOylation even at the permissive temperature. Abbreviations: PD, pull-down; PE, protein extract.

4.2.6. Esc2 promotes the SUMO ligase activity of Nse2

Genetic analysis suggest that Esc2 may function with Nse2. Both *NSE2* and *ESC2* suppress duplication-mediated gross chromosomal rearrangements (GCRs) and are epistatic with each other (Albuquerque et al., 2013). Moreover, they both prevent the formation of X-shaped DNA replication intermediates at damaged forks (Choi et al., 2010; Mankouri et al., 2009; Sollier et al., 2009). Esc2 contains SUMO-like domains and no known enzymatic activity (Ohya et al., 2008), but physically interacts with components of the SUMO pathway, including Ubc9 and Smt3 (SUMO) itself (Sollier et al., 2009). In *S. pombe*, crystallographic analysis shows that the SUMO E2 Ubc9 forms a non-covalent complex with Esc2 that acts in the Nse2 SUMO E3 ligase-dependent pathway for DNA repair (Prudden et al., 2011).

According to the previous data, we decided to test whether the interaction between Esc2 and the Smc5/6 complex was conserved in *S. cerevisiae*. As seen in Figure 43, Esc2 interacts with Smc5 *in vivo*. Similar results were obtained in a preliminary study in *S. pombe* (Boddy et al., 2003). Then, we decided to check whether the SUMO ligase activity of Nse2 was affected in *esc2* null cells. To verify this, exponentially growing cells expressing Smc5-9myc and 6HisFLAG-Smt3 in a wild type and *esc2Δ* background were grown until they reached mid-log phase. Then, the culture was split into two, and one half was treated with MMS to a final concentration of 0.033%. After two hours, cells were harvested and the Smc5 SUMOylation levels were determined. As seen in Figure 43, the Smc5 SUMOylation levels are reduced in *esc2* null cells. This indicates that Esc2 positively regulates Nse2 activity *in vivo*. Recently, it has been described that some Nse2-dependent SUMO targets show reduced SUMOylation levels in the *esc2Δ* background (Albuquerque et al., 2013). These data are consistent with a role for Esc2 in promoting the formation of an active complex between Ubc9 and the Smc5/6 complex.

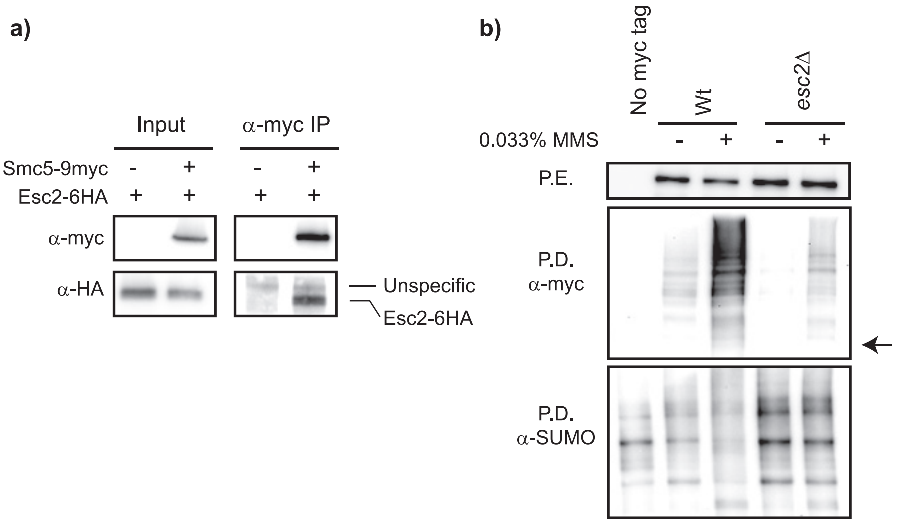

Figure 43. The Smc5 SUMOylation is impaired in *esc2⊿* null cells

a) Esc2 interacts with Smc5 *in vivo*. Cells expressing Smc5-9myc and Esc2-6HA (YMB1815) were used. As a control for unspecific Esc2 binding to the beads, cells expressing Esc2-6HA (YMB1817) are also shown. Cells were harvested, Smc5-9myc was immunoprecipitated and the Esc2 binding to Smc5 was analysed by Western blot. Note that Esc2 binds to Smc5. b) Esc2 promotes Smc5 SUMOylation. Cells expressing Smc5-9myc and 6HisFLAG-SUMO in a wild type (YMB1458) and *esc2⊿* (YMB1839) background were used. When they reached mid-log phase, the culture was split into two and one half was treated with MMS to a final concentration of 0.033%. After two hours, cells were harvested and the SUMOylation levels were determined. Note that Smc5 SUMOylation levels are reduced in *esc2* null cells. Arrow points to unmodified Smc5. Abbreviations: PD, pull-down; PE, protein extract.

4.2.7. The ATPase function of Smc5 is required for the Nse2-dependent SUMOylation

The results presented so far predict that the activity of Smc5 will also be crucial for the activation of its associated SUMO ligase. For this purpose, we introduced mutations in the nucleotide binding domains of Smc5 to weaken its interaction with ATP and block its ATPase activity (K75I and D1014A) (Roy et al., 2011). The ATPase-mutant allele was expressed in cells that drive the expression of their endogenous wild type *SMC5* gene from a regulatable *GAL* promoter. As previously described, the ATPase-defective *smc5* allele is lethal (Roy et al., 2011) (See Figure 44). The next question was to know whether the lethality seen in this mutant stemmed from defects in recruitment to chromatin. To test this, the recruitment to chromatin was determined by a protein chromatin-binding assay (Liang and Stillman, 1997). Cells expressing an ectopic copy of wild type Smc5-9myc or *smc5-K75I-9myc* were used. As seen in Figure 44, we did not observe major alterations in chromatin binding for the ATPase-defective *smc5* mutant protein compared to wild type Smc5. These results are supported by *in vitro* experiments, which showed that Smc5 binds efficiently to DNA in the absence of ATP (Roy et al., 2011).

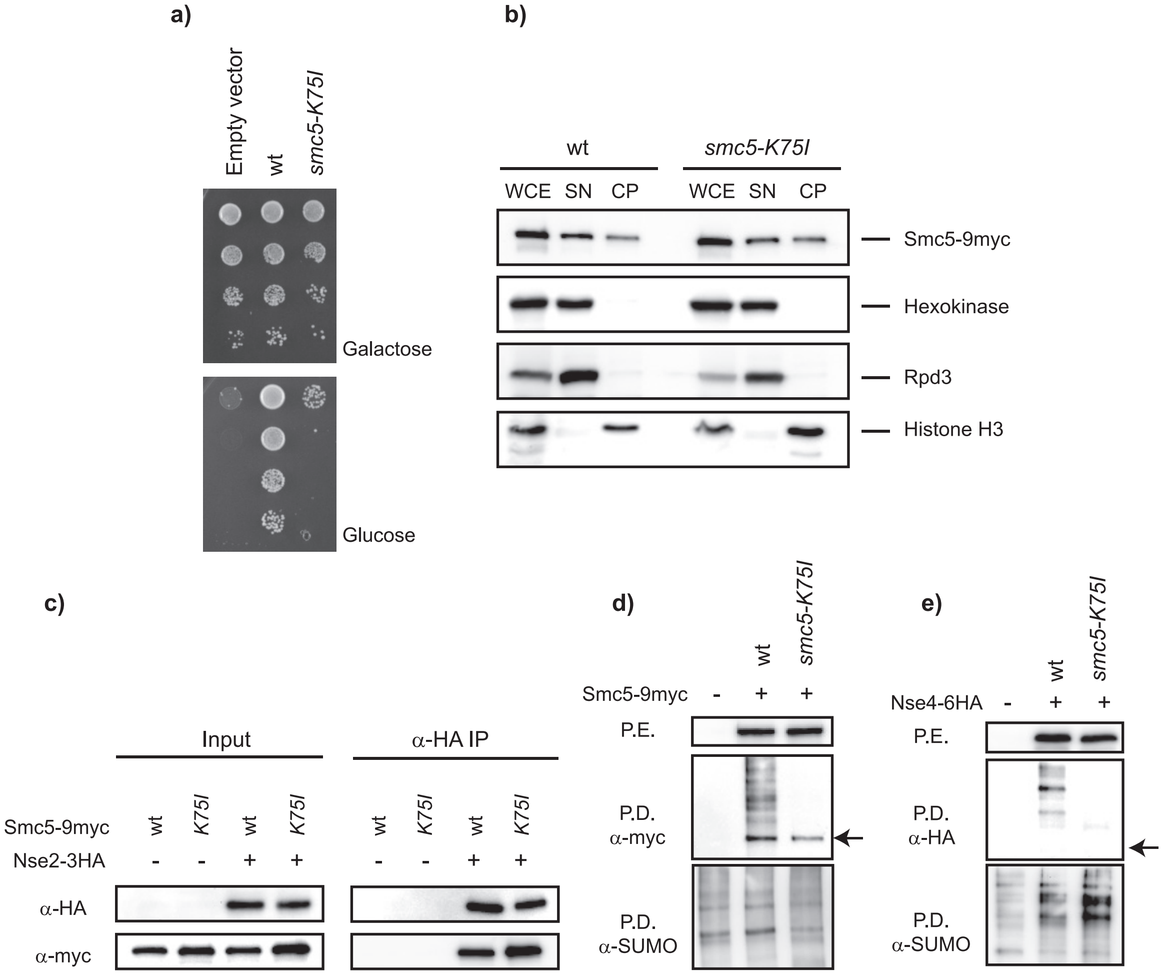
a)
Empty vector
wt
smc5-K75I
Galactose
Glucose
b)
wt
smc5-K75I
WCE SN CP
WCE SN CP
Smc5-9myc
Hexokinase
Rpd3
Histone H3
c)
Input
α-HA IP
Smc5-9myc
Nse2-3HA
wt K75I wt K75I
- - + +
α-HA
α-myc
d)
wt
smc5-K75I
Smc5-9myc - + +
P.E.
P.D. α-myc
P.D. α-SUMO
e)
wt
smc5-K75I
Nse4-6HA - + +
P.E.
P.D. α-HA
P.D. α-SUMO

Figure 44. The ATPase function of the Smc5/6 complex is required for activation of the Nse2 SUMO ligase

a) The ATPase-deficient *smc5* allele is lethal. Serial dilutions of *GALp-SMC5* cells containing either an empty vector (YMB1081), wild type *SMC5* (YMB1916) or *smc5-K75I* (YMB2145). They were spotted on SC galactose or SC glucose at 25ºC for 3 days and then photographed. Note that the *smc5-K75I* mutant is not able to complement the lack of the endogenous Smc5. b) The ATPase-deficient *smc5* shows no major alterations in chromatin binding. Cells expressing an ectopic copy of wild type Smc5-9myc (YMB1925) or *smc5-K75I-9myc* (YMB1949) were used. Controls for a chromatin bound protein (histone H3), nuclear (Rpd3) and cytoplasmic soluble (Hexokinase) proteins are also shown. Note that no major alterations in chromatin binding for ATPase-defective *smc5* mutant protein compared to wild type Smc5 were detected. c) The ATPase activity of Smc5 is not required for the Nse2-Smc5 interaction. Cells expressing Nse2-3HA with either wild type Smc5-9myc (YMB1950) or *smc5-K75I-9my*c (YMB1951) were used. As a control for unspecific Smc5 binding to the beads, cells expressing Smc5-9myc (YMB1925) or *smc5-K75I-9myc* (YMB1949) are also shown. Cells were harvested, Nse2-3HA was immunoprecipitated and the Nse2 binding to Smc5 was analysed by Western blot. Note that Nse2 binds with similar efficiency to either wild type or ATPase-defective smc5 mutant proteins. d) The ATPase-deficient Smc5 is not SUMOylated. Cells expressing 6HisFLAG-Smt3 and an ectopic copy of wild type Smc5-9myc (YMB1925) or *smc5-K75I-9myc* (YMB1949) were used. Note that the *smc5-K75I* mutant is not SUMOylated. Arrow points to unmodified Smc5.

e) Nse4 is not SUMOylated in *smc5-K75I* mutant cells. *GALp-SMC5* cells expressing Nse4-6HA and 6HisFLAG-SUMO with either wild type Smc5 (YMB1937) or *smc5-K75I* (YMB1938) were grown in SC galactose until mid-log phase. Then, the culture was shifted into SC glucose to down-regulate the expression of the endogenous *SMC5* for 12 hours. After this, cells were harvested and the SUMOylation levels of Nse4 were determined as previously described. Note that Nse4 is not SUMOylated when Smc5 cannot bind ATP. Arrow points to unmodified Nse4. Abbreviations: K, lysine; I, isoleusine; PD, pull-down; PE, protein extract.

To investigate whether the ATP binding was required for the recruitment of the SUMO ligase, cells expressing Nse2-3HA and an ectopic copy of wild type Smc5-9myc or *smc5-K75I-9myc* were used. As seen in Figure 44, Nse2 binds with similar efficiency to either wild type or ATPase-defective *smc5* mutant proteins, indicating that the ATPase activity of Smc5 is not required for the Nse2-Smc5 interaction. However, we were unable to detect SUMOylation of the ATPase-defective *smc5* protein, which indicates that the *smc5-K75I* mutant is not SUMOylated by its accompanying SUMO ligase.

Finally, we wanted to know whether the ATPase-defective mutant was able to affect the SUMOylation of other subunits in the Smc5/6 complex. To test this, *GALp-SMC5* cells expressing Nse4-6HA and either wild type Smc5 or *smc5-K75I* were grown in SC galactose until mid-log phase. Then, the culture was shifted into SC glucose to down-regulate the expression of the endogenous *SMC5* for 12 hours. After this, cells were harvested and the SUMOylation levels of Nse4 were determined. As seen in Figure 44, the SUMOylation deficiency is not only restricted to Smc5, and the Nse4 kleisin subunit in the complex is also not SUMOylated when Smc5 cannot bind ATP. Altogether, these experiments demonstrate that the Smc5/6 complex operates as a giant E3 SUMO ligase, which is sensitive to the ATPase activity of the Smc5/6 complex.

We speculated that the ATPase-inactive *smc5* mutant protein may fail to recruit Ubc9, thereby precluding SUMOylation. If this hypothesis were correct, artificial recruitment of Ubc9 to Smc5/6 would eliminate the SUMOylation differences between wild type and ATPase mutant Smc5 proteins. To explore this possibility, we integrated a second copy of *UBC9* fused to the 3´-end of the endogenous *NSE2* gene to force recruitment of the E2 in the vicinity of the E3. As previously shown in Figure 37, this fusion is functional and is able to increase the SUMOylation levels of Smc5. The E3-E2 fusion interacts with the same efficiency with both the ATPase active and inactive *smc5* proteins (see Figure 45). This confirms that the Smc5-Nse2 interaction is not affected in the ATPase mutant. Strikingly, in spite of this constitutive recruitment of Ubc9 to the Smc5/6 complex, Smc5 SUMOylation is still lower than wild type and so SUMOylation must require an ATP-dependent step, indicating that the ATPase mutant complex is held in an inactive state for SUMOylation (see Figure 45). Moreover, these results demonstrate that the ATPase function of Smc5 is part of the ligase mechanism that assists Ubc9 function. Therefore, the Smc5/6 complex operates as a giant E3 SUMO ligase, which is sensitive to the integrity, the functionality and the ATPase activity of Smc5.

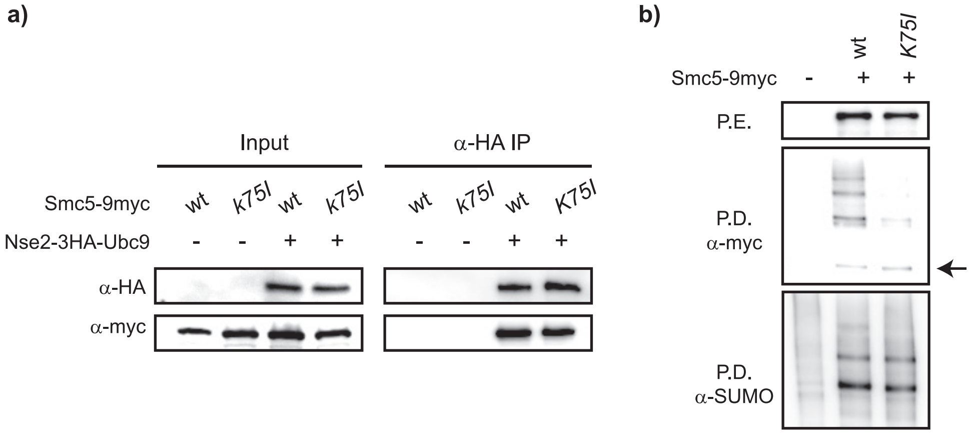

Figure 45. ***smc5-K75I*** **is not SUMOylated in Nse2-Ubc9 cells**

a) The E3-E2 (Nse2-Ubc9) fusion interacts with the same efficiency with both the ATPase active and inactive smc5 proteins. Cells expressing Nse2-3HA-Ubc9 with either wild type Smc5-9myc (YMB2230) or *smc5-K75I-9myc* (YMB2231) were used. As controls for Smc5 unspecific binding to the beads, cells expressing Smc5-9myc (YMB1925) and *smc5-K75I-9myc* (YMB1949) are also shown. Cells were harvested, Nse2-3HA-Ubc9 was immunoprecipitated and the Nse2-3HA-Ubc9 binding to Smc5 was analyzed by Western blot. Note that Nse2-Ubc9 binds with similar efficiency to either wild type Smc5 or ATPase-defective *smc5* mutant proteins. b) The ATPase-deficient *smc5* is not SUMOylated in the presence of the Nse2-Ubc9 fusion. Nse2-3HA-Ubc9 cells expressing 6HisFLAG-SUMO and an ectopic copy of wild type Smc5-9myc (YMB2230) or *smc5-K75I-9myc* (YMB2231) were used. When cells reached mid-log phase, they were harvested and the SUMOylation levels of Smc5 were analyzed. Note that the *smc5-K75I* mutant is not SUMOylated. Arrow points to unmodified Smc5. Abbreviations: PD, pull-down; PE, protein extract.

4.3. Characterization of the Smc5/6 complex SUMOylation in response to DNA damage

The SUMOylation levels of all the SUMOylated Smc5/6 subunits increase in response to MMS-induced DNA damage (Figure 32), which indicates a further activation of the SUMO ligase activity of Nse2. Since little is known about this, we decided to investigate which factors control this phenomenon.

4.3.1. The DNA damage checkpoint in not required for the MMS-induced SUMOylation of Smc5

First, we decided to determine whether the MMS-induced SUMOylation was controlled by the DNA damage checkpoint. To test this, exponentially growing cells expressing Smc5-9myc and 6HisFLAG-Smt3 in a wild type, *mre11Δ*, *mec1Δ* or *rad53Δ* background were grown until they reached mid-log phase. Then, the culture was split into two and one half was treated with MMS to a final concentration of 0.033%. After two hours, cells were harvested and SUMOylation levels were determined. As seen in Figure 46, the MMS-induced SUMOylation of Smc5 is not affected either in the *mre11Δ*, *mec1Δ* or *rad53Δ* mutant background, indicating that, at least, these elements are not required for this response.

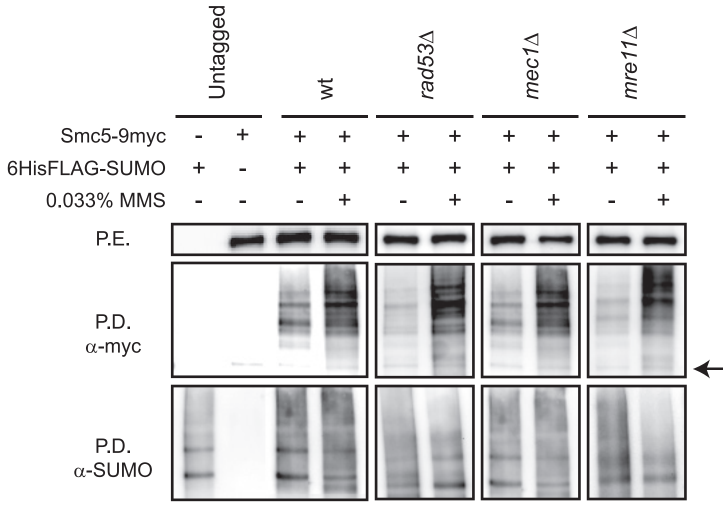
Untagged
wt
rad53Δ
mec1Δ
mre11Δ
Smc5-9myc - + + + + + + + + +
6HisFLAG-SUMO + - + + + + + + + +
0.033% MMS - - - + - + - + - +
P.E.
P.D.
α-myc
P.D.
α-SUMO

Figure 46. The MMS-induced SUMOylation of Smc5 is not controlled by Mre11, Mec1 or Rad53

Cells expressing 6HisFLAG-SUMO and Smc5-9myc in a wild type (YMB1738), *rad53Δ* (YMB1606), *mec1Δ* (YMB1608), *mre11Δ* (YMB1530) background and untagged strains (no 9myc tag (YTR557) and no 6HisFLAG-Smt3 (YTR912)) were grown until they reached mid-log phase. Then, the cultures were split into two and one half of each was treated with MMS to a final concentration of 0.033%. After two hours, cells were harvested and SUMOylation levels were determined. Note that the MMS-induced SUMOylation is not affected in these mutant backgrounds. Arrow points to unmodified Smc5. Abbreviations: PD, pull-down; PE, protein extract.

4.3.2. SCJ formation activates the Nse2-dependent SUMOylation

Since the Smc5/6 complex is closely involved in the resolution of sister chromatid junctions (SCJs) that are formed at damaged replication forks, one possibility is that the activity of the SUMO ligase Nse2 might be enhanced by the formation of these DNA structures that appear as a consequence of the replication fork restart and the DNA damage by-pass mechanisms. In MMS, formation of SCJs depends on a functional homologous recombination pathway and the template switch branch of the postreplicational repair (Branzei et al., 2008). If this hypothesis were correct, impeding the formation of these structures would prevent the MMS-induced SUMOylation of Smc5.

To verify this, exponentially growing cells expressing Smc5-9myc in a wild type and *rad52Δ* background were grown until they reached mid-log phase. Then, the culture was split into two and one half was treated with MMS to a final concentration of 0.033%. After two hours, cells were harvested and the Smc5 SUMOylation levels were determined. As seen in Figure 47, *RAD52* deletion prevents the MMS-induced SUMOylation of Smc5. These results indicate that the activity of the Smc5/6 complex is enhanced in response to MMS, leading to a further activation of the SUMO ligase activity of Nse2, presumably due to formation of recombination-dependent pathological structures at damaged forks.

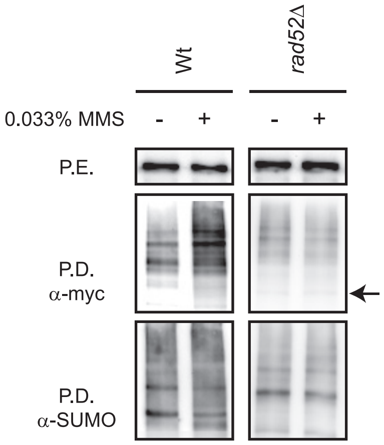

Figure 47. Homologous recombination is required for the MMS-induced SUMOylation of Smc5

Cells expressing Smc5-9myc and 6HisFLAG-SUMO in a wild type (YMB1458) and *rad52Δ* (YMB1536) background were grown until they reached mid-log phase. Then, the culture was split into two and one half was treated with MMS to a final concentration of 0.033%. After two hours, cells were harvested and the SUMOylation levels were determined. Note that there is no MMS-induced SUMOylation of Smc5 in the *rad52Δ* background. Arrow points to unmodified Smc5. Abbreviations: PD, pull-down; PE, protein extract.

Since MMS induces SCJ formation, which enhances the activity of Nse2, similar results should be observed in hydroxyurea-stalled replication forks in checkpoint-deficient (*rad53Δ*) cells, where stalling leads to fork collapse. When DNA replication forks in wild-type cells stall because of deoxynucleoside triphosphate (dNTP) depletion with hydroxyurea (HU), they remain competent to resume replication after removal of HU; however, this is not the case in *rad53Δ* cells, which have widespread replication fork collapse after HU removal (Desany et al., 1998; Lopes et al., 2001; Tercero et al., 2003). *smc5* mutants show marked sensitivity to HU and the budding yeast Smc5/6 complex is found at collapsed replication forks (Lindroos et al., 2006). To verify this hypothesis, exponentially growing cells expressing Smc5-9myc and 6HisFLAG-Smt3 in a wild type and *rad53Δ* backgrounds were grown until they reached mid-log phase. Then, the culture was split into two and one half was treated with HU to a final concentration of 0.2 M. After two hours, cells were harvested and the Smc5 SUMOylation levels were determined. As seen in Figure 48, Smc5 SUMOylation increases in response to HU in *rad53* null cells. This result is in accordance with previous work in *S. pombe*, where it was described that Nse4 SUMOylation increases in response to HU in a *rad53Δ* background (Pebernard et al., 2008b).

Altogether, these results indicate that the SUMO ligase activity of Nse2 is enhanced in response to SCJ formation, presumably at damaged forks.

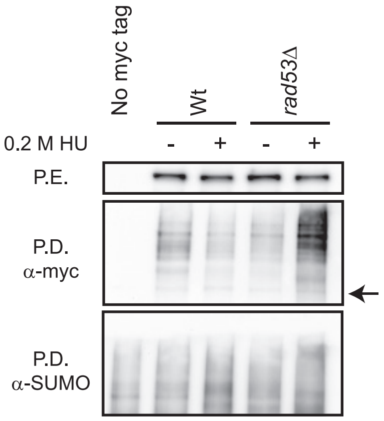

Figure 48. Replication fork collapse in HU activates the SUMO ligase activity of Nse2

Cells expressing Smc5-9myc and 6HisFLAG-SUMO in a wild type (YMB1738) and *rad53Δ* (YMB1606) background were grown until they reached mid-log phase. Then, the culture was split into two and one half was treated with HU to a final concentration of 0.2 M. After two hours, cells were harvested and the SUMOylation levels were determined. Note that there is an HU-induced SUMOylation of Smc5 in *rad53* null cells. Arrow points to unmodified Smc5. Abbreviations: PD, pull-down; PE, protein extract.

4.4. Identification of the SUMOylation sites of Smc5

Since Smc5 is a target of Nse2 (Zhao and Blobel, 2005) and interacts directly with Nse2 (Duan et al., 2009a), we decided to identify the SUMOylation sites of Smc5. The aim was to generate a *smc5-SUMO-deficient* mutant (*smc5-SD*) to study the function of Smc5 SUMOylation.

4.4.1. Smc5 is not SUMOylated at the Ubc9 consensus sites

A consensus sequence for SUMOylation has been identified based on its interaction with Ubc9, ΨKXE/D, where Ψ represents a bulky aliphatic residue, usually isoleucine, leucine or valine and X represents any amino acid (Bernier-Villamor et al., 2002; Johnson and Blobel, 1999). However, a number of proteins not subject to SUMOylation contain this motif, and other physiological targets of SUMOylation are not SUMOylated at this consensus motif (Wilkinson and Henley, 2010).

In order to predict the SUMOylation sites of Smc5, the sequence was analysed with SUMOsp 2.0, which is a SUMOylation site prediction program based on the Ubc9 consensus motif and previously identified SUMOylation sites (Ren et al., 2009). The analysis revealed 17 putative lysines (K) in Smc5, one located in the ATPase domain of Smc5 (K31) and 16 distributed throughout the rest of the protein (see Figure 49 for more details). All putative lysines but K31 were mutated to arginine (R) to try to block Smc5 SUMOylation.

The *smc5(K-16-R)* mutant allele was synthesized by GenScript (Piscataway, USA) and cloned into an *YCpLac22* vector under its own promoter. To test the phenotype of this allele, it was expressed in cells that drive the expression of their endogenous wild type *SMC5* gene from a regulatable *GAL* promoter. As seen in Figure 49, *smc5(K-16-R)* is able to complement the lack of expression of the endogenous wild type *SMC5* (+ glucose), indicating that this mutant is viable but shows a mild growth defect in MMS. Furthermore, when the SUMOylation pattern of Smc5 was analysed, no difference between wild type Smc5 and *smc5(K-16-R)* was detected, which allowed us to conclude that Smc5 is not SUMOylated at its canonical Ubc9 consensus sites.

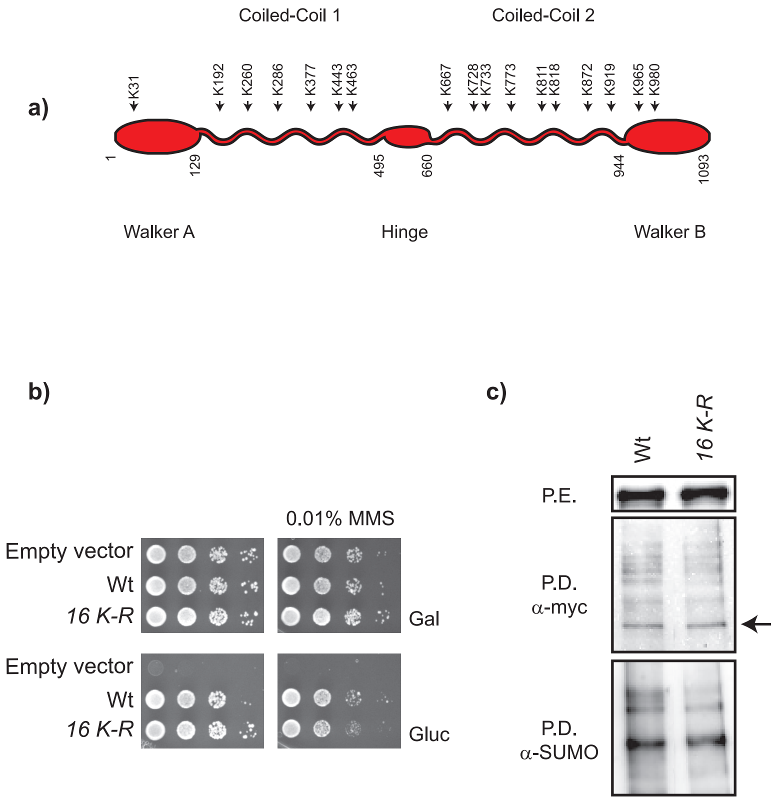
a)
Coiled-Coil 1
Coiled-Coil 2
K31
K192
K260
K286
K377
K443
K463
K667
K728
K733
K773
K811
K818
K872
K919
K965
K980
1
129
495
660
944
1093
Walker A
Hinge
Walker B
b)
0.01% MMS
Empty vector
Wt
16 K-R
Gal
Empty vector
Wt
16 K-R
Gluc
c)
Wt
16 K-R
P.E.
P.D.
α-myc
P.D.
α-SUMO

Figure 49. Smc5 is not SUMOylated at the Ubc9 consensus sites

a) Putative SUMOylation sites of Smc5. Potential Ubc9 SUMOylation sites were identified with the SUMOsp 2.0 software. Note that K31 is located in the ATPase domain of Smc5. b) The *smc5(K-16-R)* mutant is viable. Serial dilutions of *GALp-SMC5* cells containing either an empty vector (YMB1081), wild type *SMC5* (YMB1074) or *smc5-16-K-R* (YMB1920) were spotted on SC galactose or SC glucose at 25ºC for 3 days and then photographed. Where indicated, MMS was added to a final concentration of 0.01%. Note that the *smc5(K-16-R)* mutant is viable and shows a mild growth defect in MMS. c) *smc5(K-16-R)* mutant protein is SUMOylated as wild type Smc5. Cells expressing 6HisFLAG-SUMO and an ectopic copy of wild type Smc5-9myc (YTR953) or *smc5(K-16-R)-9myc* (YTR954) were used. When cells reached mid-log phase, they were harvested and the SUMOylation levels of Smc5 were analyzed. Note that there is no difference between wild type Smc5 and *smc5-16-K-R* mutant proteins. Arrow points to unmodified Smc5.

4.4.2. Smc5 is SUMOylated in both coiled-coils

Since mutating the consensus Ubc9 SUMOylation sites to arginine failed, we decided to mutate all lysines in Smc5 to arginine but K75, which is necessary for ATPase function, generating the *smc5(K-all-R)* mutant. To do this, this mutant allele was synthesized by GenScript (Piscataway, USA). As seen in Figure 50, the *smc5(K-all-R)* mutant is not able to complement the lack of expression of the endogenous wild type *SMC5* (+ glucose), indicating that this mutant is not viable, and is not SUMOylated.

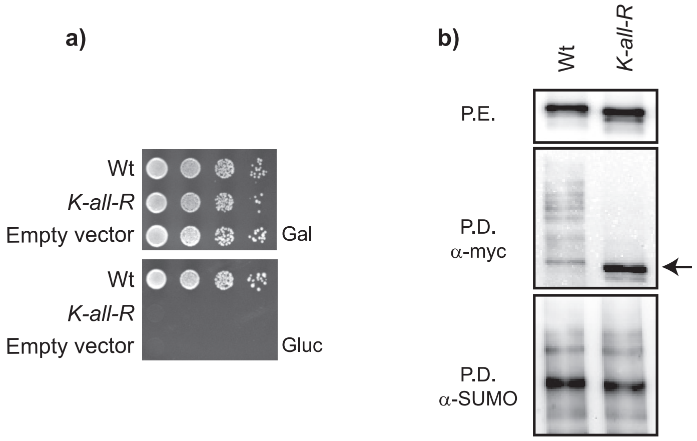

Figure 50. The *smc5-K-all-*R **mutant is lethal**

a) The *smc5(K-all-R)* mutant is not viable. Serial dilutions of *GALp-SMC5* cells containing either an empty vector (YMB1081), wild type *SMC5* (YMB1074) or s*mc5(K-all-R)* (YMB1080) were spotted on SC galactose or SC glucose at 25ºC for 3 days and then photographed. Note that the *smc5(K-all-R)* mutant is not viable. b) The *smc5(K-all-R)* mutant is not SUMOylated. Cells expressing 6HisFLAG-SUMO and an ectopic copy of wild type Smc5-9myc (YTR953) or *smc5-K-all-*R*-9myc* (YMB1072) were used. When cells reached mid-log phase, they were harvested and the SUMOylation levels of Smc5 were analyzed. Note that there is no SUMOylation in the *smc5-K-all-*R mutant protein. Arrows points to unmodified Smc5.

Then, we decided to mutate all the lysines present in each domain. Smc5 has 116 lysines: 11 in the walker A (WA), 47 in the coiled-coil 1 (CC1), 15 in the hinge (H), 33 in the coiled-coil 2 (CC2) and 10 in the walker B (WB). First, we amplified by PCR the plasmid containing the wild type *SMC5* using a pair of primers that amplify the whole plasmid except the domain to be mutated. Second, we amplified by PCR the plasmid containing the *smc5-K-all-*R mutant allele with a pair of primers that only amplifies the region that we want to mutate. Afterwards, the products were treated with *DpnI* to degrade the template plasmid and they were co-transformed into *E.coli MC1061* (*recA*+). The PCR fragments should recombine inside *E. coli* generating a new plasmid with the mutated insert (see Figure 51). This strategy allowed us to mutate all lysines in the walker A, except K75, *smc5(wa K-*R*)*; in the hinge, *smc5(h K-*R*)*; in the walker B, s*mc5(wb K-*R*)*; in the coiled coil 1, *smc5(cc1 K-*R*)*; in the coiled coil 2, *smc5(cc2 K-*R*)*; and, in the coiled coil 1 and 2, simultaneously, s*mc5(cc1,2 K-*R*)*.

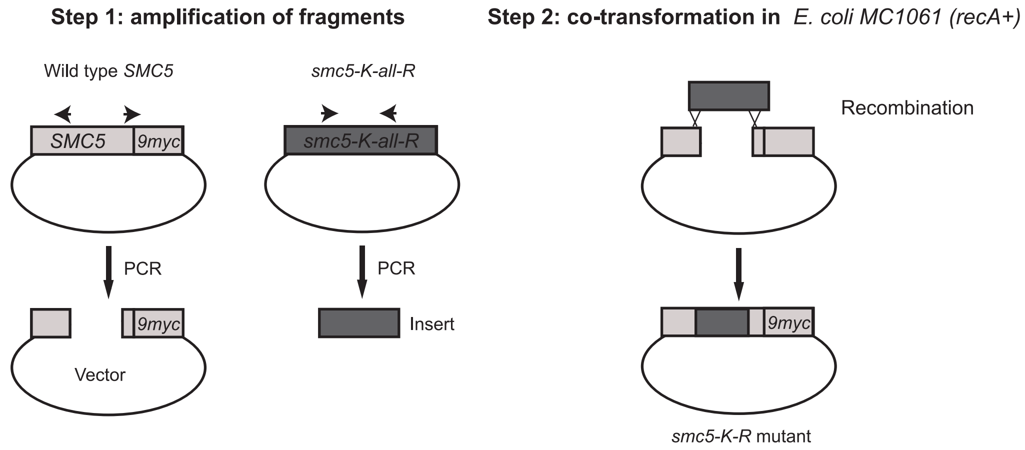

Figure 51. Strategy used to generate *smc5-single-domain-K-R* mutants

The wild type *SMC5* plasmid was amplified by PCR using a pair of primers that were able to amplify the whole plasmid except the wanted domain. Then, the *smc5-K-all-R* mutant plasmid was amplified with a pair of primers that only amplified the region that we wanted to mutate. Then, the PCR products were treated with *DpnI* and were co-transformed into *E.coli MC1061* (*recA+*). PCR fragments will recombine inside *E. coli* generating a new plasmid with the mutated insert.

Then, we tested whether these mutants were sensitive to MMS. They were expressed in cells that drive the expression of their endogenous wild type *SMC5* gene from a regulatable *GAL* promoter. As seen in Figure 52, *smc5(wa K-R)*, *smc5(h K-R)* and *smc5(wb K-R)* are able to complement the lack of expression of the endogenous *SMC5*. Although, *smc5(wa K-R)* and *smc5(wb K-R)* show a discrete slow growth phenotype in the presence the of MMS, when the SUMOylation pattern was analysed, no difference was observed in the *smc5(h K-R)* and a slight global reduction was observed in the *smc5(wa K-R)* and *smc5(wb K-R)* mutant without any difference in the band distribution compared to wild type Smc5, which may correspond to a global down-regulation of Smc5 SUMOylation. This experiment allowed us to conclude that Smc5 is not SUMOylated in the walker A, hinge or walker B.

Since Nse2 binds to the coiled-coils of Smc5, it is more likely that the lysines of this region could accept SUMO. However, as seen in Figure 52, the single *smc5(cc1 K-R)* and *smc5(cc2 K-R)* mutants are able to complement the lack of expression of the endogenous *SMC5* and show no growth defects in the presence of MMS. However, interestingly the *smc5(cc1,2 K-R)* double mutant is hypersensitive to MMS. The combination of the *smc5(cc1 K-R)* and *smc5(cc2 K-R)* mutants showed that there are some lysines able to accept SUMO in both coiled-coils domains of Smc5, therefore, Smc5 SUMOylation is significantly impaired in the *smc5(cc1,2 K-R)*. These experiments allowed us to conclude that a lack of SUMOylation in the coiled-coils of Smc5 confers sensitivity to the alkylating agent MMS, which indicates that the SUMOylation of the complex is important for the DNA damage response.

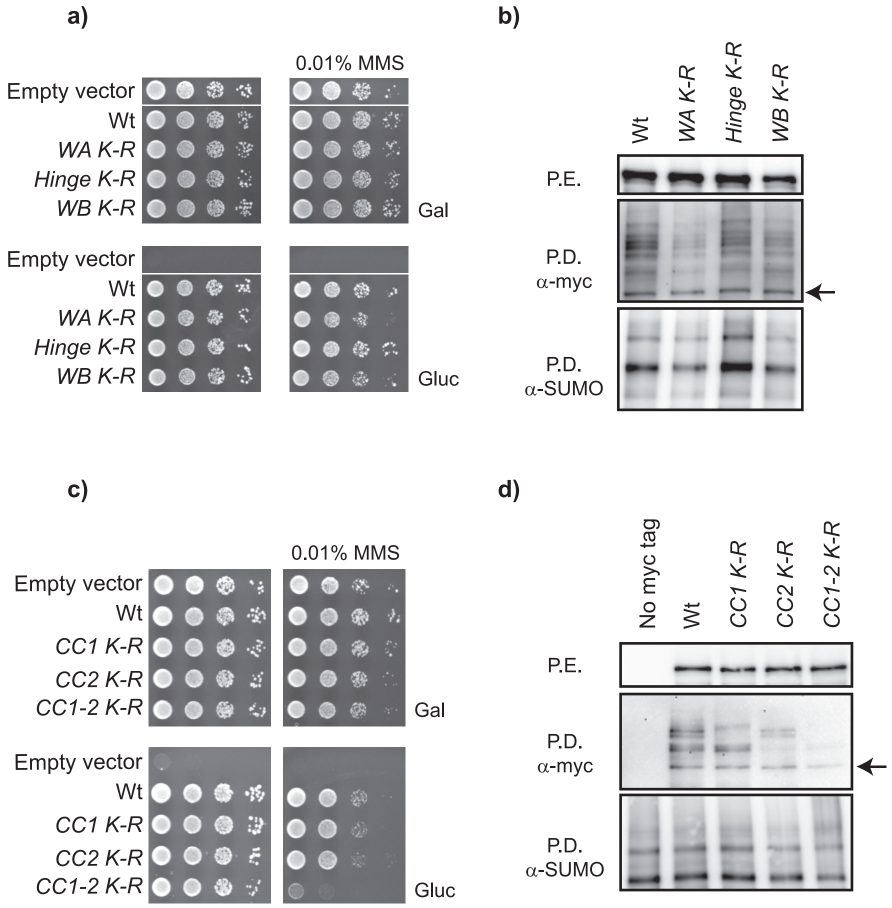
a)
0.01% MMS
Empty vector
Wt
WA K-R
Hinge K-R
WB K-R
Gal
Empty vector
Wt
WA K-R
Hinge K-R
WB K-R
Gluc
b)
Wt
WA K-R
Hinge K-R
WB K-R
P.E.
P.D.
α-myc
P.D.
α-SUMO
c)
0.01% MMS
Empty vector
Wt
CC1 K-R
CC2 K-R
CC1-2 K-R
Gal
Empty vector
Wt
CC1 K-R
CC2 K-R
CC1-2 K-R
Gluc
d)
No myc tag
Wt
CC1 K-R
CC2 K-R
CC1-2 K-R
P.E.
P.D.
α-myc
P.D.
α-SUMO

Figure 52 Smc5 is SUMOylated in both coiled-coils

a) *smc5(wa K-R)*, *smc5(h K-R),* and *smc5(wb K-R)* mutants are viable. Serial dilutions of *GALp-SMC5* cells containing either an empty vector (YMB1081), wild type *SMC5* (YMB1074), *smc5(wa K-R)* (YMB1075), *smc5(h K-R)* (YMB1076) or *smc5(wb K-R)* (YMB1077). They were spotted on SC galactose or SC glucose at 25ºC for 3 days and then photographed. Where indicated, MMS was added to a final concentration of 0.01%. Note that these mutants are able to complement the lack of expression of the endogenous *SMC5*. b) Smc5 is not SUMOylated in the walker A, hinge or walker B. Cells expressing 6HisFLAG-SUMO and an ectopic copy of wild type *SMC5* (YTR1921), *smc5(wa K-R)* (YMB1922), *smc5(h K-R)* (YMB1923) or *smc5(wb K-R)* (YMB1924) were used. When cells reached mid-log phase, they were harvested and the SUMOylation levels of Smc5 were analyzed. Note that the SUMOylation pattern is not affected in these mutants. Arrow points to unmodified Smc5. c) *smc5(cc1,2 K-R)* mutant is hypersensitive to MMS. Serial dilutions of *GALp-SMC5* cells containing either an empty vector (YMB1081), wild type *SMC5* (YMB1916), s*mc5(cc1 K-R)* (YMB1918), *smc5(cc2 K-R)* (YMB1919) or *smc5(cc1,2 K-R)* (YMB1917) were spotted on SC galactose or SC glucose at 25ºC for 3 days and then photographed. Where indicated, MMS was added to a final concentration of 0.01%. Note that the double *smc5(cc1,2 K-R)* mutant is hypersensitive to MMS. d) Both coiled-coils of Smc5 accept SUMO. Cells expressing 6HisFLAG-SUMO and an ectopic copy of wild type Smc5-9myc (YTR1925), *smc5(cc1 K-R)-9myc* (YMB1926), *smc5(cc2 K-R)-9myc* (YMB1927) or *smc5(cc1,2 K-R)-9myc* (YMB1928) were used. When cells reached mid-log phase, they were harvested and the SUMOylation levels of Smc5 were analysed. Note that there are lysines SUMOylated in both coiled-coils.

It has been described that the Smc5/6 complex is recruited to either side of a DSB in budding yeast (de et al., 2006; Lindroos et al., 2006). Based on this, we decided to test whether the recruitment of the Smc5/6 complex to an HO endonuclease-mediated DSB was affected in the *smc5(cc1,2 K-R)* mutant. Either wild type SMC5-9myc or *smc5(cc1,2 K-R)-9myc* mutant allele was integrated into the endogenous locus of *SMC5* in a strain that contains the HO endonuclease, which cuts at the *MAT* locus on chromosome III, under the inducible *GAL* promoter. This strain has the *HMR* and *HML* loci deleted, and therefore repair cannot occur. Thus, in galactose a single unrepairable break is formed. Cells were grown in YP raffinose until they reached mid-log phase. Then, a sample was taken as time 0, before DSB induction, and galactose was added to a final concentration of 2% to induce the HO cut to create a single DSB per cell. After two hours, cells were harvested and processed for ChIP analysis (see materials and methods for more details). Real-time PCR analysis of the ChIP was performed to quantify Smc5 recruitment to the DSB as described in (Shroff et al., 2004). As seen in Figure 53, the recruitment of the *smc5(cc1,2 K-R)* mutant protein to the DSBs is impaired, which indicates that Smc5 SUMOylation could be necessary for the recruitment onto DNA. Although these results are in accordance with the fact that *nse5-1* mutant cells, that display a strong impairment in Smc5 SUMOylation, also show a reduced recruitment of Smc5/6 to stalled forks in HU (Bustard et al., 2012), we must be very critical of this result because the *smc5(cc1,2 K-R)* has many lysines replaced with arginine, which could be provoking a significant structural change that might affect its DNA binding. Further studies will be required to identify the specific lysines required for Smc5 SUMOylation and analyse the phenotype of a less severe mutant.

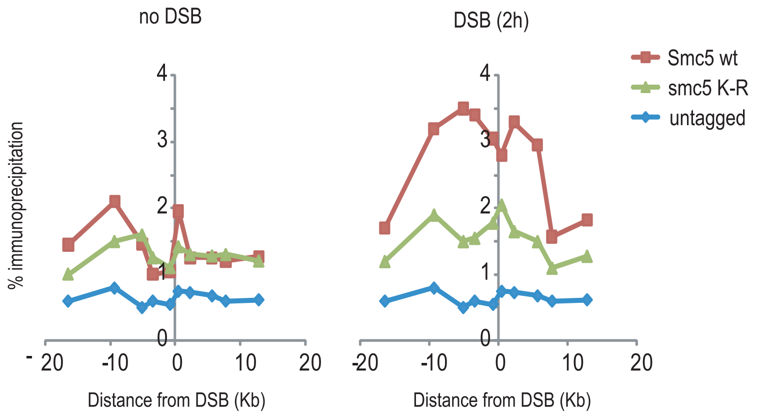

Figure 53. Recruitment of *smc5(cc1,2 K-R)* to DSBs is impaired

Cells expressing either wild type Smc5-9myc (YTR1178), *smc5(cc1,2 K-R)9-myc* (YTR1172) or untagged Smc5 (YTR1162) in a *GAL HO hmlΔ hmrΔ* background were grown in YP raffinose until they reached mid-log phase. Then, a sample was taken as time 0, before DSB induction, and galactose was added to a final concentration of 2% to induce a DSB. After two hours, cells were harvested and processed for ChIP analysis. Real-time PCR analysis of the ChIP was performed to quantify Smc5 recruitment. Note that the recruitment of the *smc5-(cc1,2 KR)* mutant protein to the DSB is impaired.

4.5. The role of the Smc5/6 complex in replisome swivelling

It has been proposed that the Smc5/6 complex reduces the accumulation of positive supercoiling ahead of the replication machinery through assisting fork rotation (Kegel et al., 2011).

Briefly, during DNA replication the parental DNA molecule becomes overwound, or positively supercoiled, in the region ahead of the advancing replication fork (Alexandrov et al., 1999; Peter et al., 1998). To allow fork progression, this superhelical tension must be removed by topoisomerases, which catalyse transient breaks in the DNA (Wang, 2002). Relaxation of superhelical tension becomes problematic as the length of the unreplicated DNA becomes shorter because there is less room to contain the positive supercoils resulting from fork movement, and less room for topoisomerases to act in order to remove them. This is especially important during replication termination when two replisomes converge (Sundin and Varshavsky, 1981). Champoux and Been in 1980 proposed a model in which if the replication fork were free to rotate along the axis of the DNA helix, the positive superhelical stress in front of the fork would diffuse through the replication fork and redistribute both ahead and behind the fork, resulting in sister chromatid intertwinings in its wake (Postow et al., 2001; Wang, 2002). These intertwinings of the daughter duplexes are defined as precatenanes (Peter et al., 1998), because they will catenate sister chromatids if they are not removed by topoisomerases before the completion of replication (Lucas et al., 2001; Zechiedrich et al., 1997).

4.5.1. *top2-td* mutant cells accumulate catenated plasmids

Top2 is the only type II topoisomerase that can resolve catenated double-stranded DNA is budding yeast (Wang, 2002). Extensive studies have shown that reduction of Top2 function inhibits decatenation of plasmid molecules during S phase, which prevents normal chromosome segregation causing chromosome breakage and cell death (Baxter and Diffley, 2008; DiNardo et al., 1984; Hirano et al., 1986; Holm et al., 1985).

In order to deplete Top2 specifically *in vivo*, we used a strain in which the endogenous *TOP2* gene was replaced with a heat-inducible degron allele (*top2-td*) expressed under a doxycycline-repressible promoter. This mutant is unable to grow under restrictive conditions in which the promoter is repressed (+doxycycline); the degron–specific E3 ubiquitin ligase, Ubr1, is induced (+Galactose); and the culture is shifted to the restrictive temperature (37ºC) (Baxter and Diffley, 2008). Wild type and *top2-td* mutant cells were arrested in G1 with alpha factor. Once arrested, cultures were shifted to the restrictive conditions for one hour to deplete Top2. Then, cells were released from the G1 arrest into fresh media containing galactose, doxycycline and nocodazole at 37ºC to arrest them in metaphase. To examine the presence of catenated dimers after Top2 depletion, we followed the fate of the centromeric plasmid *pRS316*. As previously published (Baxter and Diffley, 2008), the supercoiled monomeric plasmid is converted during S phase into a form that migrates considerably more slowly in *top2-td* mutant cells but not in wild type cells, consistent with it being a catenated dimer (see Figure 54).

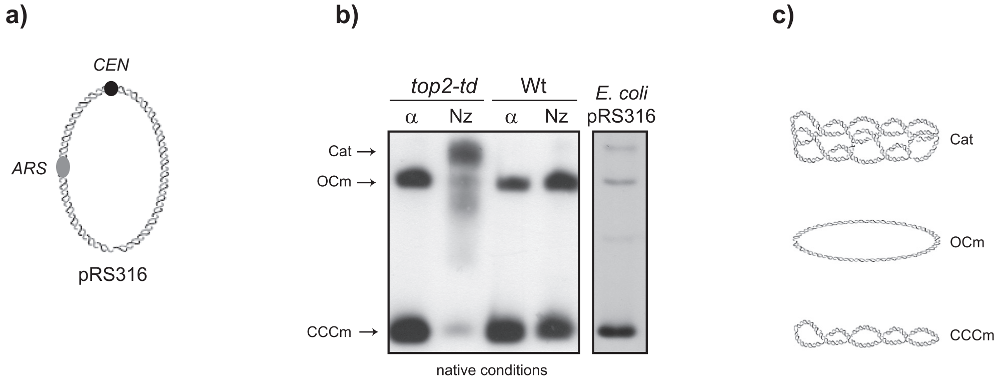

Figure 54. Top2 depletion provokes accumulation of catenated dimers

a) Diagram of the centromeric *pRS316* plasmid used in these experiments. Note that this plasmid contains an origin of replication and a centromere. b) Top2-depleted cells show an accumulation of catenated dimers. Wild type cells (CCG9119) and *top2-td* mutant cells (CCG9120) were grown in synthetic complete media without uracil + 2% raffinose to mid-log phase at 25ºC and transferred into YP + 2% raffinose for 1 hour before being arrested in G1 with alpha factor. Once arrested, 2% galactose (to activate Ubr1 expression) and 25 ng/ml doxycycline (to repress *TOP2* transcription) were added for 45 minutes. Then, cultures were shifted to 37ºC for 1 hour to deplete Top2. Cells were released from the G1 arrest into YPgal fresh media containing 25 ng/ml doxycycline at 37ºC and arrested in metaphase with nocodazole. Samples were taken and genomic DNA was prepared according to standard methods before one-dimensional gel electrophoresis using native conditions. Note that the supercoiled monomeric plasmids present before S phase are converted into catenated dimers in the top2-td mutant. c) Different topological forms of the *pRS316*. Catenated dimers, as well as relaxed and supercoiled monomers are depicted. Abbreviations: CCCm (covalently closed circular monomer), OCm (open circular monomer), and Cat (catenated dimers).

It is well established that there are three different forms of catenanes: those formed by two nicked plasmids (CatAs), those formed by one nicked plasmid and the other covalently closed (CatBs) and those formed by two covalently closed plasmids (CatCs)(Sundin and Varshavsky, 1981). In addition, the plasmids can be catenated just once (Ca=1) or multiple times (Ca ≥2) (Bates and Maxwell, 1997) (see Figure 55). In order to identify the different types of catenated plasmid present in *S. cerevisiae*, Top2 was depleted as previously described and DNA was purified and analyzed by 2D gel electrophoresis (Martin-Parras et al., 1998). This approach allowed us to confirm that all three catenated forms of the *pRS316* are present in budding yeast. As previously described in *E. coli* cells (Martinez-Robles et al., 2009) and in budding yeast (Baxter and Diffley, 2008), the most abundant form corresponds to CatCs followed by CatBs; whereas CatAs are barely visible, indicating that CatBs and CatAs result from nicking during DNA preparation. (see Figure 55).

In order to resolve the different catenanes according to their catenation number, DNA samples were treated with the nicking endonuclease *Nb-BsmI* that provokes single-stranded breaks (Xu et al., 2007) converting all forms of catenanes into CatAs. As clearly shown in Figure 55, 2D gels revealed that after *Nb-BsmI* nicking, those signals that were identified as CatBs and CatCs disappeared while the intensity and complexity of the signal corresponding to CatAs was notably enhanced.

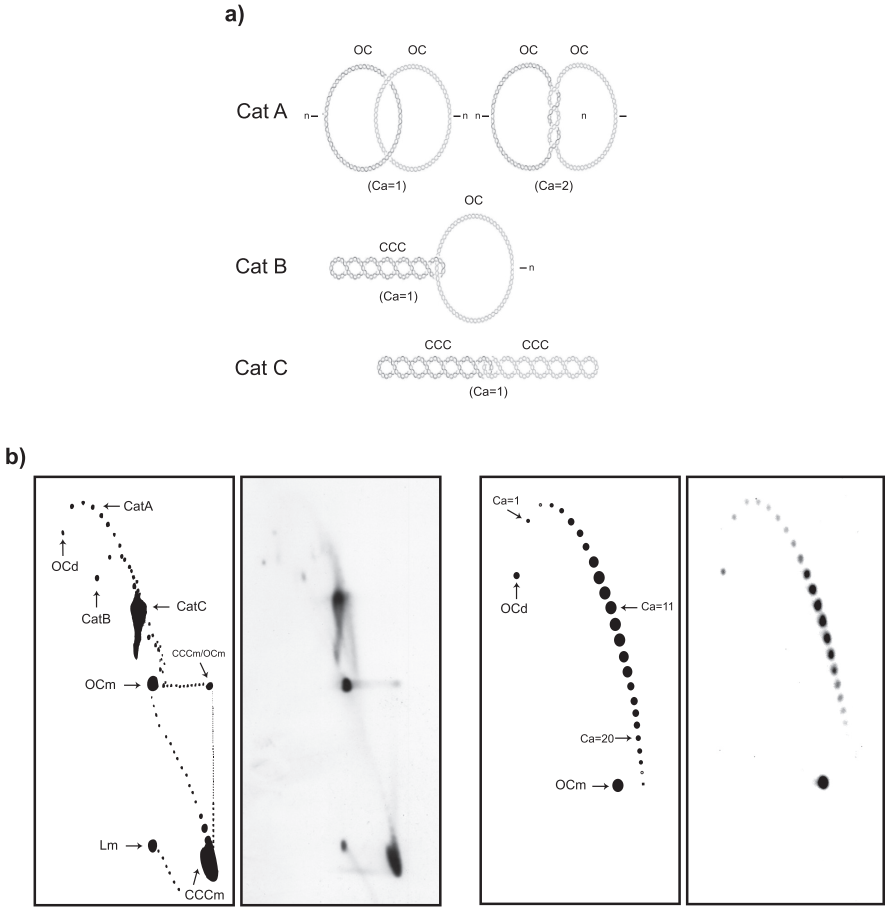

Figure 55. Visualization of catenated dimers by 2D gel electrophoresis

a) Diagram representing different forms of catenanated plasmids as projected in a plane. Two pairs of nicked catenated rings (CatAs) are represented. The one on the left is catenated once (Ca=1) whereas the one on the right is catenated twice (Ca=2). CatBs are formed by one nicked plasmid and the other covalently closed. Finally, CatCs are formed by two covalently closed plasmids (CatCs). b) Visualization of catenated plasmids by 2D gel electrophoresis. Plasmid DNA from Top2-depleted cells arrested in metaphase was purified using native conditions and analyzed by 2D gel electrophoresis. Note that the most abundant form corresponds to CatCs followed by CatBs and CatAs. c) Resolution of catenated dimers according to their catenation number (Ca). DNA samples from (b) were treated with the nicking endonuclease *Nb-BsmI* and analyzed by 2D gel electrophoresis. Note that the signal corresponding to CatBs and CatCs disappeared while the one corresponding to the CatAs was significantly enhanced. Arrows point to dimers catenated once (Ca=1), dimers catenated eleven times (Ca=11) and dimers catenated twenty times (Ca=20). Abbreviations: CCCm (covalently closed circular monomer), OCm (open circular monomer), Lm (linear monomer), OCd (open circular dimer), and Cats (catenated dimers).

4.5.2. Catenane distribution is not altered in *smc6-9* mutant cells

If, as previously proposed (Kegel et al., 2011), Smc5/6 had a role in assisting replisome swivelling, a non-functional *smc5/6* complex would reduce the ability of the replication fork to rotate along the axis of the DNA helix. This would lead to an accumulation of positive supercoiling ahead of the replication machinery and a decrease in the formation of precatenanes behind the replication fork.

To test this, the topological status of the *pRS316* plasmid after one round of replication in the absence of Top2 and Smc5/6 function was investigated. Wild type, *smc6-9*, *top2-td* and *top2-td smc6-9* cells were arrested in G1 with alpha factor. Once arrested, cultures were shifted to the restrictive conditions for one hour to deplete Top2 and inactivate the *smc5/6* complex. Then, cells were released from the G1 arrest into fresh media at 37ºC under restrictive conditions and arrested in metaphase. As seen in Figure 56, only *top2-td* and *top2-td smc6-9* mutant cells show an accumulation of catenated dimers. Interestingly the global amount of supercoiled catenanes detected is slightly decreased in *top2-td smc6-9* mutant cells. The global amount of supercoiled catenanes could be affected either by DNA replication problems or by nicking of the sample during the DNA extraction. In order to circumvent this problem, we decided to resolve the catenanes according to their catenation number (Ca). To do this, DNA samples were treated with the nicking endonuclease *Nb-BsmI* that introduces single-stranded breaks into both intertwined plasmids converting all catenanes into CatAs. Surprisingly, when the catenane abundance was determined, there was no difference in the catenane distribution, which indicates that replication fork swivelling is not impaired in smc6-9 mutant cells (see Figure 56).

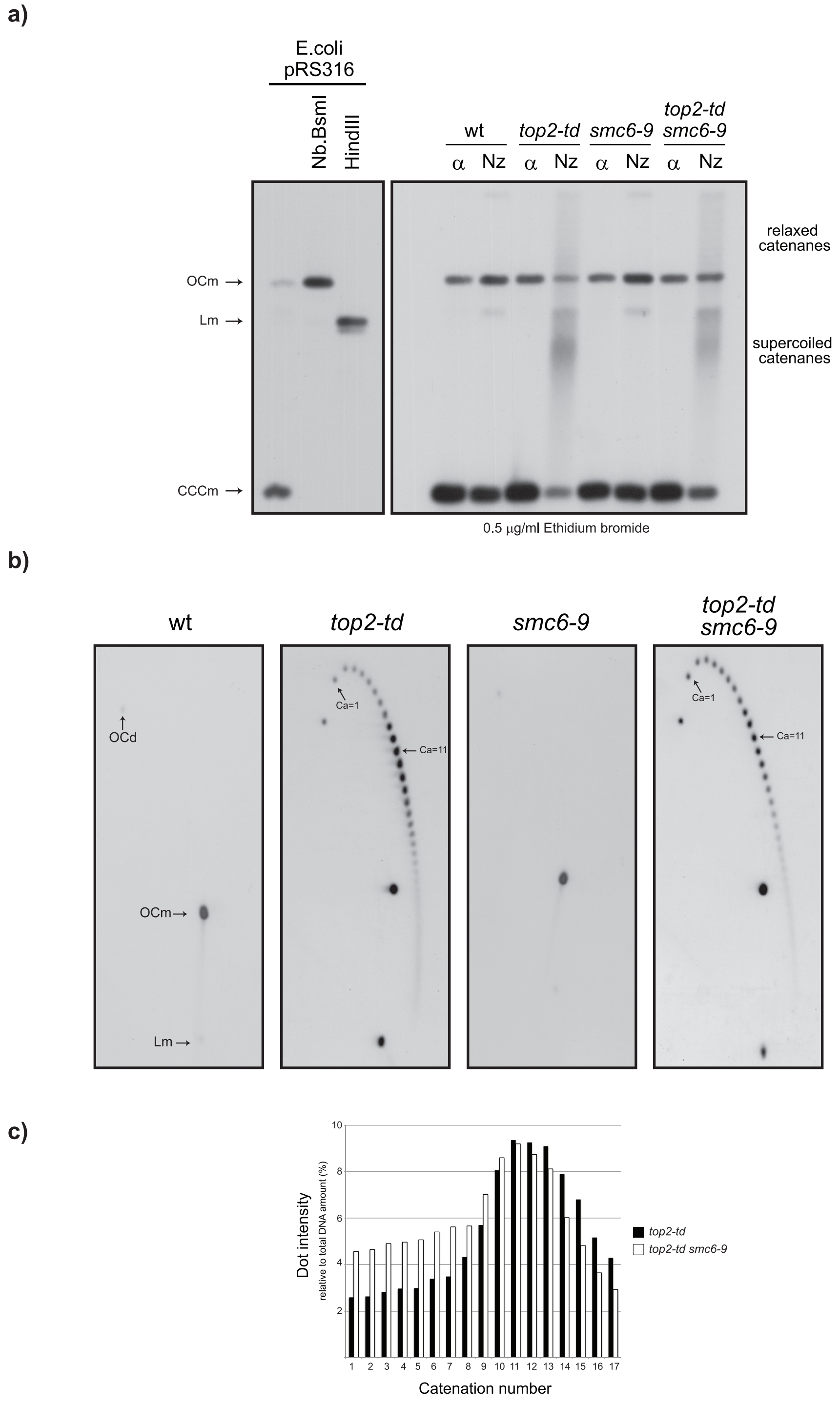

Figure 56. Catenane distribution is not affected in *smc6-9* mutant cells in a *top2-td* background

a) *top2-td* and *top2-td smc6-9* cells accumulate catenated plasmids. Wild type (CCG9119), *top2-td* (CCG9120), *smc6-9* (CCG10435), *smc6-9 top2-td* (CCG10542) cells were grown in synthetic complete media without uracil + 2% raffinose to mid-log phase at 25ºC and transferred into YP + 2% raffinose for 1 hour before being arrested in G1 with alpha factor. Once arrested, 2% galactose (to activate Ubr1 expression) and 25 ng/ml doxycycline (to repress *TOP2* transcription) were added for 45 minutes. Then, cultures were shifted to 37ºC for 1 hour to deplete Top2 and inactivate *smc6*. Cells were released from the G1 arrest into YPgal fresh media containing 25 ng/ml doxycycline at 37ºC and arrested in metaphase with nocodazole. Samples were taken and genomic DNA was prepared according to standard methods. DNA electrophoresis was performed in the presence of 0.5 µg/ml ethidium bromide. Note that only *top2-td* and *top2-td smc6-9* mutant cells show an accumulation of catenated plasmids. The presence of ethidium bromide in the gel allows differentiation between the supercoiled catenanes, which run faster than the relaxed monomer; and the relaxed catenanes, which show a slower mobility under these conditions. Purified, linearized and relaxed *pRS316* plasmids are also shown. b) *top2-td* and *top2-td smc6-9* cells show the same catenane distribution. DNA samples from the previous experiment were treated with the nicking endonuclease *Nb-BsmI* and analyzed by 2D gel electrophoresis. Arrows point to dimers catenated once (Ca=1) and dimers catenated eleven times (Ca=11). c) Quantification of catenane distribution in *top2-td* and *top2-td smc6-9* cells. Using non-saturated film exposures, the relative intensity of each spot was assessed with Image J software and the results are depicted in the histogram. Note that there is no significant difference in the catenane distribution in presence or absence of a functional *SMC6*. Abbreviations: CatAs (catenanes A), OCm (open circular monomer), OCd (open circular dimer), and Lm (linear monomer).

In order to confirm these results, we decided to repeat these experiments in a *top2-4* termosensitive background. In this case, *top2-4* and *top2-4 smc6-9* cells were arrested in G1 with alpha factor. Once arrested, cultures were shifted to 37ºC to inactivate *top2* and *smc6* for one hour. Then, cells were allowed to enter S phase at the restrictive temperature and arrested in metaphase with nocodazole. As previously shown in the *top2-td* background, the double *top2-4 smc6-9* mutant shows the same catenane distribution as the single *top2-4* mutant (see Figure 57). This data indicates that, since the catenane distribution is not affected in *smc6-9* mutant cells, the swivelling of the replisome is not affected, at least, with this allele.

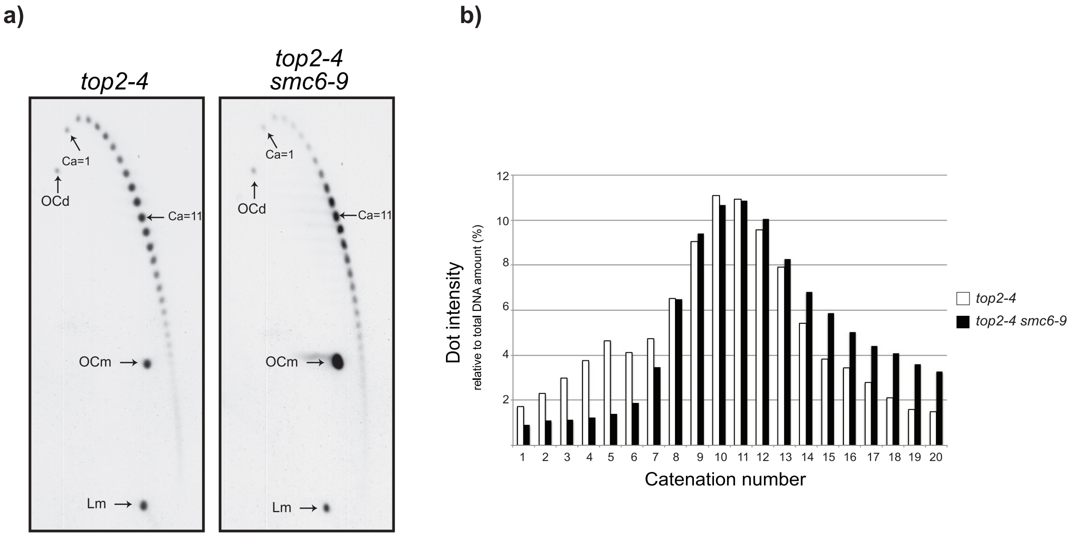

Figure 57. Catenane distribution is not impaired in *smc6-9* mutant cells in a *top2-4* background

a) *top2-4* and *top2-4 smc6-9* cells show the same catenane distribution. *top2-4* (CCG8603), *top2-4 smc6-9* (CCG10649) cells were grown in synthetic complete media without uracil + 2% glucose to midlog phase at 25ºC and transferred into YPD for 1 hour before being arrested in G1 with alpha factor. Once arrested, cultures were shifted to 37ºC for 1 hour to inactivate *top2* and *smc5/6*. Then, cells were released from the G1 arrest into YPD fresh media at 37ºC and arrested in metaphase with nocodazole. Samples were taken and genomic DNA was prepared according to standard methods. DNA samples were treated with the nicking endonuclease *Nb-BsmI* and analyzed by 2D gel electrophoresis. Arrows point to dimers catenated once (Ca=1) and dimers catenated eleven times (Ca=11). b) Quantification of catenane distribution in *top2-4* and *top2-4 smc6-9* cells. Using non-saturated film exposures, the relative intensity of each spot was assessed with Image J software and the results are depicted in the histogram. Note that there is no significant difference in the catenane distribution. Abbreviations: CatAs (catenanes A), OCm (open circular monomer), OCd (open circular dimer), and Lm (linear monomer).

4.5.3. Catenane distribution is not impaired in *smc6-56* mutant cells

Since the previous findings do not corroborate what has been previously published, we decided to repeat these experiments using the same *smc6* mutant that the authors used, the *smc6-56* hypomorphic allele. *top2-4* and t*op2-4 smc6-56* cells were arrested in G1 with alpha factor. Once arrested, cultures were shifted to 37ºC to inactivate *top2* and *smc6* for one hour. Then, cells were allowed to enter S phase at the restrictive temperature and arrested in metaphase with nocodazole. As previously shown in the *smc6-9* mutant, the double *top2-4 smc6-56* mutant shows the same catenane distribution as the single *top2-4* mutant (see Figure 58). Therefore, since the catenane distribution is not affected in *smc6-56* mutant cells, the swivelling of the replisome is also not affected in this allele. This data is contrary to what has been published by Kegel and colleagues (Kegel et al., 2011). One possible explanation is that they based their conclusion on the global amount of catenanes seen in mono-dimensional gel electrophoresis. As previously stated, the global amount of catenanes can be affected by DNA replication, which will reduce the global abundance. In order to circumvent this issue, DNA samples must be nicked, which allows the quantification of catenane distribution.

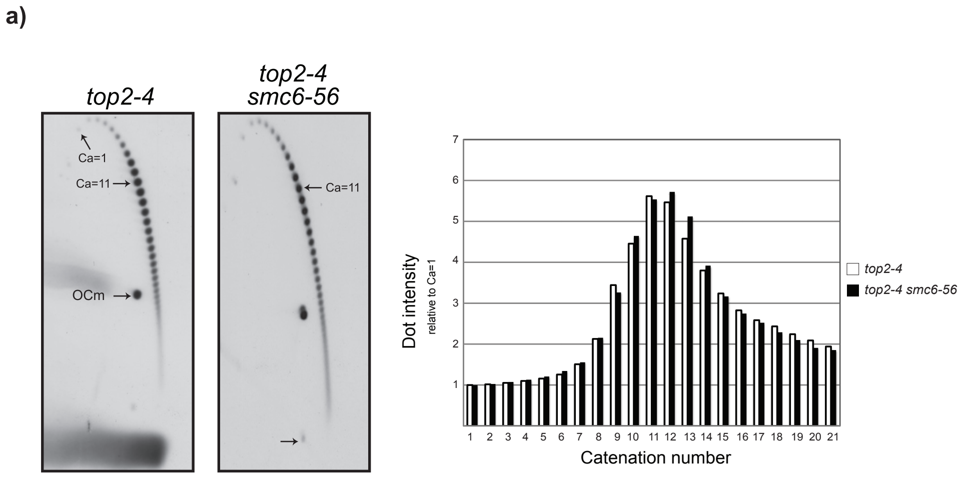

Figure 58. Catenane distribution is not impaired in *smc6-56* mutant cells

a) *top2-4* and *top2-4 smc6-56* cells show the same catenane distribution. *top2-4* (CCG8603), *top2-4 smc6-56* (CCG9295) cells were grown in synthetic complete media without uracil + 2% glucose to midlog phase at 25ºC and transferred into YPD for 1 hour before being arrested in G1 with alpha factor. Once arrested, cultures were shifted to 37ºC for 1 hour to inactivate *top2* and *smc6*. Then, cells were released from the G1 arrest into YPD fresh media at 37ºC and arrested in metaphase with nocodazole. Samples were taken and genomic DNA was prepared according to standard methods. DNA samples were treated with the nicking endonuclease *Nb-BsmI* and analysed by 2D gel electrophoresis. Arrows point to dimers catenated once (Ca=1) and dimers catenated eleven times (Ca=11). b) Quantification of catenane distribution in *top2-4* and t*op2-4 smc6-56* cells. Using non-saturated film exposures, the relative intensity of each spot was assessed with Image J software and the results are depicted in the histogram. Note that there is no significant difference in the catenane distribution. Abbreviations: CatAs (catenanes A), OCm (open circular monomer), OCd (open circular dimer), and Lm (linear monomer).

4.5.4. *smc5-4* mutant cells accumulate more catenanes

Finally, we decided to test another *smc5/6* mutant, whose function is highly compromised. For this purpose, we used the *smc5-4* hypomorphic allele. This mutant shows slow growth at permissive temperature, which indicates that the essential function of the Smc5/6 complex must be highly impaired. *top2-td* and *top2-td smc5-4* cells were arrested in G1 with alpha factor. Once arrested, cultures were shifted to the restrictive conditions for one hour to deplete Top2 and inactivate s*mc5* . Then, cells were released from the G1 arrest into fresh media at 37ºC under restrictive conditions and arrested in metaphase. As seen in Figure 59, *top2-td smc5-4* mutant cells show a significant increase in accumulation of catenanes compared to *top2-td*, which indicates that the replication fork swivels more in the *smc5-4* mutant background.

Since different *smc5/6* mutants show different replisome swivelling behaviour, depending on the allele, further work is required to determine the role of the Smc5/6 complex in fork swivelling.

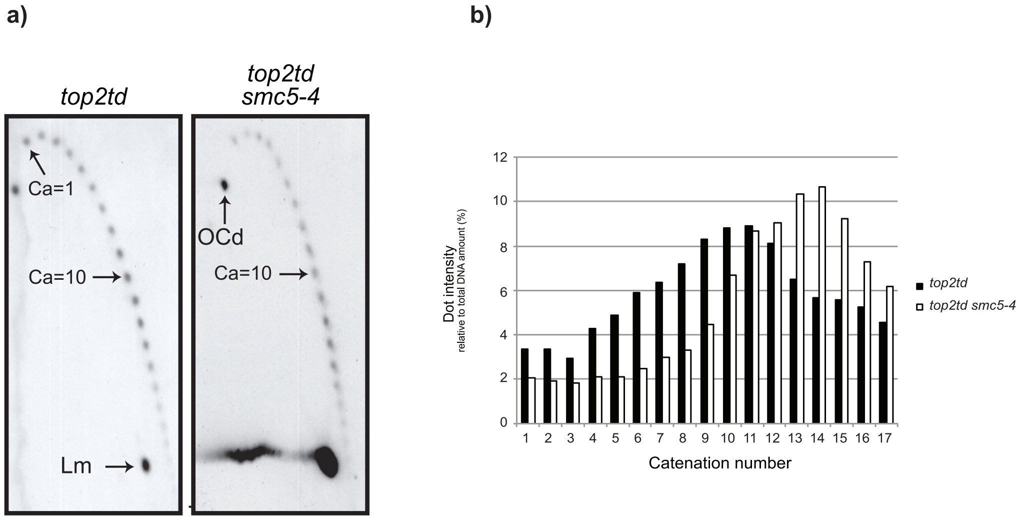

Figure 59. ***smc5-4* mutant cells show a higher accumulation of catenanes**

a) *top2-td smc5-4* cells show more catenations. *top2-td* (CCG9120), *top2-td smc5-4* (CCG8604) cells were grown in synthetic complete media without uracil + 2% raffinose to mid-log phase at 25ºC and transferred into YP + 2% raffinose for 1 hour before being arrested in G1 with alpha factor. Once arrested, 2% galactose (to activate Ubr1 expression) and 25 ng/ml doxycycline (to repress *TOP2* transcription) were added for 45 minutes. Then, cultures were shifted to 37ºC for 1 hour to deplete Top2 and inactivate smc5/6. Cells were released from the G1 arrest into YPgal fresh media containing 25 ng/ml doxycycline at 37ºC and arrested in metaphase with nocodazole. Samples were taken and genomic DNA was prepared according to standard methods. DNA samples were treated with the nicking endonuclease *Nb-BsmI* and analysed by 2D gel electrophoresis. Arrows point to dimers catenated once (Ca=1) and dimers catenated eleven times (Ca=11). b) Quantification of catenane distribution in *top2-td* and t*op2-td smc5-4* cells. Note that *top2-td smc5-4* mutant cells show a higher accumulation of catenanes.

DISCUSSION

5.1. The role of the Smc5/6 complex in sister chromatid disjunction

Since the initial identification of *SMC6* and *NSE2* (Nasim and Smith, 1975; Prakash and Prakash, 1977a), the Smc5/6 complex has been linked to DNA damage repair. Subsequent studies have uncovered mutations in every subunit of the Smc5/6 complex that render cells sensitive to DNA damaging agents, such as UV, ionizing radiation (IR), methyl methanesulfonate (MMS), Mitomycin C, and hydroxyurea (HU) in yeast, *Arabidopsis*, chicken, *Drosophila*, mouse, *Xenopus*, and humans; reviewed in (Wu and Yu, 2012).

The *smc6-9* mutant allele was first described as a mutant that fails to segregate the distal part of chromosome XII at the restrictive temperature due to the presence of sister chromatid junctions (SCJs) and replication intermediates in the rDNA at anaphase onset (Torres-Rosell et al., 2005; Torres-Rosell et al., 2007a). However, the fact that the entire deletion of the rDNA array does not suppress the thermosensitivity of *smc6-9* mutant cells, indicates that the Smc5/6 complex has additional essential non-nucleolar functions (Torres-Rosell et al., 2005). Based on this, we decided to determine whether the Smc5/6 complex has a genome-wide function in chromosome segregation.

5.1.1. *smc5/6* mutants are able to complete bulk DNA replication when replicating in the presence of MMS

Alkylating damage by MMS is normally used as a method to induce blocks in replication fork progression as it disturbs DNA replication in a dose-dependent manner (Groth et al., 2010). Briefly, if the MMS-induced DNA damage is not repaired, mainly by BER (Boiteux and Jinks-Robertson, 2013) before the cells enter S phase, the alkylated bases will either force the replisome to replicate through the damaged site or to activate some bypass mechanism, such as template switching or homologous recombination (Jackson and Durocher, 2013).

In order to determine whether *smc5/6* mutants have replication problems in the presence of MMS, wild type, *smc6-9* and *nse2ΔC* mutant cells were arrested in G1 with alpha factor at the permissive temperature. After G1 arrest, cells were shifted to 37ºC for 30 minutes to inactivate the *smc5/6* complex and then released into fresh media containing 0.02% MMS at 37ºC. As previously described (Tercero and Diffley, 2001), wild type cells go through a very long and slow S phase when replicating in the presence of MMS. As shown in Figure 17, *smc6-9* and *nse2ΔC* mutant cells enter S phase and complete bulk DNA replication with wild type kinetics, indicating that fork progression is not further compromised in these mutants. Under these conditions, the DNA damage checkpoint becomes activated, which arrests cells in G2/M.

Two-dimensional gel electrophoresis indicates that *smc6* mutants accumulate sister chromatid junctions (SCJs) when replicating in the presence of MMS in the *ARS305* (see Figure 18) in a way that wild type cells do not. Apart from our study (Bermudez-Lopez et al., 2010), a parallel work using the *smc6-9* allele also showed the same behaviour (Sollier et al., 2009). Furthermore, similar results have been obtained using different *smc5/6* mutants: *mms21-CH* (Branzei et al., 2006), *mms21-11* and *smc6-P4* (Chen et al., 2009; Chen et al., 2013; Choi et al., 2010), *smc6-56* (Yong-Gonzales et al., 2012), and *mms21-SP* (Chavez et al., 2011). Together, the aforementioned data provide compelling support for the idea that *smc5/6* mutants accumulate SCJs when replicating in the presence of MMS.

5.1.2. An MMS pulse allowed characterization of the genome-wide segregation problems in *smc5/6* mutant cells

Although MMS-induced DNA damage has been extensively used, its effects on chromosome segregation had not been previously assessed because activation of the DNA damage checkpoint precludes anaphase entry (Tercero and Diffley, 2001).

In order to circumvent this problem, we set up a more physiological approach based on a pulse of 0.01% MMS for 30 minutes while cells are arrested in G1. Then, cells are washed thoroughly and allowed to enter into S phase in the absence of the DNA alkylating agent. As seen in Figure 19, wild type cells do not experience a significant delay in cell cycle entry or progression through S phase, and start chromosome segregation with similar kinetics to unchallenged cells. Therefore, this condition does not activate the DNA damage checkpoint in wild type cells. However, when the DNA damage bypass mechanisms are blocked, either inactivating homologous recombination (*rad52* null cells) or the error-free branch of the postreplicational repair (*rad5* null cells), cells show an activation of Rad53 and arrest in G2/M (see Figure 19). This indicates that the experimental conditions used are acute enough to require HR and template switch to overcome the MMS-induced DNA damage.

These experimental conditions allowed us to study the requirements for chromosome segregation after low-dose DNA damage. BER (*mag1Δ, apn1Δ, apn2Δ*), NER (*rad1Δ, rad10Δ, rad2Δ*), the DNA damage and S phase checkpoints (*ddc1Δ, rad9Δ, rad24Δ, mrc1*Δ), DNA helicases (*mph1Δ, sgs1Δ, srs2Δ, rrm3Δ*), DNA topoisomerases (*top1Δ, top2Δ*), and other DNA nucleases (*exo1Δ, slx1Δ, slx4Δ, mms4Δ, mus81Δ, rad27Δ, mre11Δ, sae2Δ, dna2-1, yen1Δ*) are not individually required for bulk chromosome segregation after a G1 MMS pulse. These results indicate that although these genes have a role in coping with higher MMS concentrations (Hickson and Mankouri, 2011; Schwartz and Heyer, 2011), they are either not essential or collectively cooperate in the removal of the few SCJs formed in response to a low dose of DNA damage. For example, there is evidence that Mms4/Mus81 might be a back-up mechanism employed by cells to remove the mitotic SCJs not dissolved by Sgs1/Top3 during S phase, and Yen1 can be used as a second back-up mechanism in anaphase to eliminate those escaping from Sgs1/Top3 and Mms4/Mus81 (Matos and West, 2014). One should take into account that our experimental procedures were not sensitive enough to detect small contributions to dissolution of chromosome linkages, since only the bulk of DNA masses were analysed by microscopy. A more detailed analysis of individual loci resolution will be required to conclusively ascertain their requirement in segregation of damaged chromosomes.

In striking contrast to the battery of deleted genes described above, *smc5/6* mutants display an abnormally high proportion of nuclear segregation defects following an MMS pulse, as revealed by FACS and microscopy. A more detailed analysis using chromosomal tags revealed that *smc6-9* mutant cells fail to segregate centromeric regions (chromosome III and XII) and the rDNA centromeric flank (see Figure 21). These segregation problems indicate that the SCJ removal defects in *smc6-9* mutant cells are scattered throughout the genome. Therefore, the role of the Smc5/6 complex in chromosome segregation is not restricted to the rDNA array, the major binding site identified for the Smc5/6 complex in budding yeast (Lindroos et al., 2006; Torres-Rosell et al., 2005), and even centromeric regions can experience resolution defects during anaphase after MMS-induced DNA damage. The nuclear segregation failures in *smc5/6* mutants are observed in response to MMS treatment, and not in unchallenged conditions, presumably because MMS increases the frequency of replication fork stalling and SCJ formation.

5.1.3. *smc5/6* mutants accumulate replication and recombination intermediates after an MMS pulse

Cells have to maintain sister chromatids together during S phase. This is essential for chromosome biorientation and segregation. However, when cells enter anaphase, all linkages between sister chromatids must be resolved in order to allow chromosome segregation. Therefore, failures to remove these connections can threaten genome integrity. The segregation problems detected in *smc5/6* mutants must be due to persistent sister chromatid linkages present at the anaphase onset. These linkages can be generated by: (i) proteins, such as those provided by cohesin, and resolved by separase at the metaphase to anaphase transition; (ii) catenations, generated by transcription and replication, and resolved by Top2 and condensin in G2/M; and (iii) DNA-mediated linkages, which arise during DNA replication and repair.

It is accepted that PFGE prevents chromosomes containing replication forks or branched recombination intermediates from entering the gel (Azvolinsky et al., 2006). Once S phase is completed, and these structures disappear, chromosomes enter into the gel (80 minutes onwards). Pulsed field gel electrophoresis (PFGE) experiments revealed that chromosomes do not enter the gel, but remain in the well while cells are in S phase (40 to 80 minutes). Contrary to wild type cells, *smc6-9*, *smc6-1* and *nse2ΔC* mutant chromosomes fail to enter the gel even at later time points suggesting that DNA linkages persist. This is more obvious for larger chromosomes, which suggest that they are more likely to carry DNA linkages, as expected for random DNA damage (see Figure 23).

It has been proposed that the Smc5/6 complex has a role in cohesin removal in *S. pombe* (Outwin et al., 2009). However, Scc1-GFP signal appears during S phase and disappears when cells enter into anaphase with the same kinetics in wild type and *smc6-9* mutant cells (see Figure 24). This result, together with the PFGE analysis, which only scores protein-independent linkages, demonstrates that the chromosome resolution defects observed in *smc5/6* mutant cells are cohesin-independent. In accordance, nocodazole-arrested *smc6-9* mutant cells display low but readily detectable levels of SCJs and ongoing replication forks (see Figure 25) and a 2.5 times increase in the number of unreplicated gaps relative to wild type cells after a pulse of MMS. Therefore, two types of structures might prevent chromosome segregation in *smc5/6* mutants: first, SCJs arising during DNA replication; and second, the presence of ongoing replication forks at the onset of anaphase.

5.1.4. The Smc5/6 complex has a role in resolution of SCJs

The fact that different *smc5/6* mutants accumulate SCJs when replicating in the presence of MMS (Bermudez-Lopez et al., 2010; Branzei et al., 2006; Chavez et al., 2011; Chen et al., 2009; Chen et al., 2013; Choi et al., 2010; Sollier et al., 2009; Yong-Gonzales et al., 2012), indicates that Smc5/6 is not required for the generation of these structures.

Several lines of evidence indicate that SCJ formation has a deleterious effect when the function of the Smc5/6 complex is compromised: first, the thermosensitivity of *smc6-9* mutant cells is partially suppressed by deletion of *RAD52*, a key component of the homologous recombination pathway (Torres-Rosell et al., 2005). In accordance with this, the MMS sensitivity of *smc6-9* mutant cells is also significantly suppressed in *rad52* null cells (see Figure 26). A more detailed analysis revealed that *RAD52* deletion is able to improve chromosome resolution by PFGE in *smc6-9* mutant cells, an effect that is more evident for large chromosomes (see Figure 26). This result is supported by the fact that *mms21-11 rad51Δ* (Branzei et al., 2006) and *smc6-9 rad51Δ* (Sollier et al., 2009) mutants do not accumulate SCJs when replicating in the presence of MMS. Therefore, *smc5/6* mutants accumulate SCJs at damaged forks in a recombination-dependent manner. Second, *SHU* complex deletion reduces the accumulation of SCJs, which improves the tolerance of *smc6* mutants towards replication stress (Branzei et al., 2006; Choi et al., 2010; Sollier et al., 2009). Third, *MPH1* deletion strongly reduces the accumulation of SCJs in *smc5/6* mutants, which correlates with a notably higher resistance to MMS (Chavez et al., 2011; Chen et al., 2009; Chen et al., 2013; Choi et al., 2010). Finally, blocking the error-free branch of the postreplicational repair (*mms2* null cells) partially rescues the MMS sensitivity of smc6-9 mutant cells and improves chromosome resolution by PFGE (see Figure 27). This result is supported by the fact that *smc6-P4 mms2Δ* mutant cells show a reduced level of SCJs compared to *smc6-P4* single mutant, which correlates with a better growth on MMS plates (Choi et al., 2010). Therefore, preventing SCJ formation is beneficial when the function of the Smc5/6 complex is compromised.

The accumulation of SCJs in *smc5/6* mutants might be due to the inability to prevent their appearance (anti-recombinogenic) or to resolve them. It has been proposed that Smc5/6 modulates Mph1 to prevent recombination at blocked forks and/or that the complex helps to resolve recombination structures formed by Mph1. Interestingly, *MPH1* deletion suppresses the lethality of *smc6* and *nse2* null cells, allowing slow growth of the double mutants (Chen et al., 2009). This indicates that a failure to prevent and/or resolve recombination structures at naturally occurring fork blocks could be one part of the essential role of the Smc5/6 complex.

In order to determine whether the Smc5/6 complex has a role in resolving SCJs, we designed an experiment to re-activate the Smc5/6 complex after generation of SCJs. Smc5/6 reactivation would affect SCJ levels only if the complex were required for their dissolution. As seen in Figure 28, two-dimensional gel electrophoresis showed that reactivation of *SMC6* allows the removal of SCJs accumulated in *smc6-1* mutant cells, which correlates with an increase in chromosome resolution in a PFGE (see Figure 29), and suppression of the nuclear missegregation phenotype in *smc6-1* mutant cells after an MMS pulse in G1 (see Figure 30). These results show that the physical linkages between sister chromatids can be dissolved upon reactivation of *SMC6*, indicating that the complex must have an active role in their removal. However, recent data indicate that the Smc5/6 complex also prevents and eliminates inappropriate recombination intermediates in meiosis: Smc5/6-Nse2 antagonises rogue joint molecules via two mechanisms: destabilising early intermediates and resolving DNA joint molecules through coordination of DNA helicases and resolvases at D-loops and HJs, respectively (Xaver et al., 2013).

5.1.5. How does the Smc5/6 complex resolve SCJs?

Smc5/6 probably triggers a fast reaction, since chromosome resolution is also a relatively quick event after *SMC6* reactivation (20 minutes onwards, see Figure 29). It is worth noting that although such a reaction is most likely carried out in S phase during a normal cell cycle, Smc5/6 can perform its function even in metaphase-arrested cells.

Sequence prediction and homology searches indicate that there is no subunit in the Smc5/6 complex with helicase or DNA cleavage activity. This suggests that Smc5/6 most probably detects and signals for the removal of DNA linkages but does not catalyse the resolution reaction itself. The presence of some subunits of the Smc5/6 complex with regulatory activity, such as Nse2 (SUMO ligase) and Nse1 (ubiquitin ligase), support this idea (Doyle et al., 2010; Zhao and Blobel, 2005). Interestingly, *nse2ΔC* mutant cells display similar defects to *smc6* mutant cells, which indicates that SUMOylation is also important for removing SCJs. Thus, unlike cohesin and condensin, and in addition to its structural role on DNA, we propose that the Smc5/6 complex assists dissolution of DNA linkages through SUMOylation of other proteins. This hypothesis is supported by the fact that *MMS21* reactivation resolves SCJs accumulated in *mms21-sp* cells, a SUMO ligase-defective mutant, exposed to MMS (Chavez et al., 2010). The most obvious Smc5/6 targets for the removal of DNA linkages are enzymes with DNA cleavage activity or helicase-topoisomerase pairs. On the other hand, if the linkages are due to unfinished replication structures, these might require either reactivation of stalled replisomes or help unzipping the unreplicated dsDNA. The latter could be achieved through uncoupling of the replicative helicase and the DNA synthesis machinery. Non-replicative DNA helicases could also have a role in resolution of unreplicated regions. Supporting this idea, it has been proposed that FANC and BLM could mediate resolution of unfinished intermediates during anaphase by unzipping the unreplicated dsDNA in mammalian cells (Naim and Rosselli, 2009). However, it should be noted that the yeast homologue of BLM (Sgs1) appears not to be defective in gross nuclear separation (under our experimental approach), suggesting that it is unlikely to be regulated by Smc5/6, at least in budding yeast. Besides, Sgs1 is not SUMOylated by Nse2 in yeast (Branzei et al., 2006). Given the plethora of telomere proteins SUMOylated by Nse2 in humans (Potts and Yu, 2007), it is highly probable that the Smc5/6 complex will regulate more than one target for the removal of chromosome linkages. Based on this, further work will be required to identify the relevant targets of the Smc5/6 complex in chromosome resolution.

5.2. Characterization of the Nse2 SUMO ligase activity regulation

Although multiple experiments have demonstrated that Nse2 is an E3 SUMO ligase essential for the maintenance of genome stability, and most of its substrates, including the Smc5/6 and cohesin complexes, play important roles in chromosome segregation and repair (Stephan et al., 2011b), little is known about how the activity of this enzyme is regulated and which factors control its ability to transfer SUMO.

5.2.1. Nse2 docking to Smc5 is required for the Smc5/6 complex SUMOylation and DNA damage repair

Since the initial description of Nse2 as a SUMO ligase, several subunits of the Smc5/6 complex have been shown to be SUMOylated in different organisms: Smc5 and Nse2 in budding yeast (Zhao and Blobel, 2005); Nse2, Nse3, Nse4 and Smc6 in fission yeast (Andrews et al., 2005; Pebernard et al., 2008b); Nse2 and Smc6 in humans (Potts and Yu, 2005).

As seen in Figure 32, Smc5, Smc6, Nse2, Nse3 and Nse4 are all SUMOylated. In contrast, Nse1, Nse5 and Nse6 are either not SUMO targets, or are modified at levels that are not detectable in our pull-down analysis. As previously described, Smc5 and Nse4 are SUMOylated in an Nse2-dependent manner (see Figure 33). Interestingly, although Smc6 had been proposed not to be a target of Nse2 (Takahashi et al., 2008), in our hands, the SUMOylation of Smc6 is highly Nse2-dependent (see Figure 33). It is worth noting that, in response to MMS-induced DNA damage, an increase of the SUMOylation levels is detected, which suggests a further activation of the SUMO ligase activity in response to DNA damage (see below for more details).

nse2ΔC mutant cells show increased levels of some SUMO conjugates. This effect might be a response to endogenous DNA damage present in this background. This idea is supported by the fact that *mms21Δsl* and *mms21-11* cells, which are SUMO ligase-defective mutants, show slow growth, similar to *nse2ΔC* cells, spontaneous activation of the DNA damage checkpoint and an enhanced frequency of chromosome breakage (Rai et al., 2011). In order to circumvent this problem, we used the auxin-induced degradation of Nse2, which allows rapid and reversible degradation of target proteins in response to auxin (indole-3-acetic; IAA) (Nishimura et al., 2009). *nse2-AID* mutant cells are sensitive to auxin, which indicates that the degradation is strong enough to compromise the viability of the cell (see Figure 34); and show reduced levels of Smc5 and Smc6 SUMOylation in the presence of auxin, without displaying the up-regulation of SUMO conjugates seen in the *nse2ΔC* mutant.

To test the relationship between the docking state of Nse2 to the Smc5/6 complex and its DNA repair function, we constructed the *nse2-5BD* mutant allele (P9A, V12A, L14A, H15A, L25A, L30A), which has been previously shown to disturb the interaction with Smc5 (Duan et al., 2009a). Combining the *nse2-AID* allele with the ectopic expression of the *nse2-5BD* mutant protein, allowed us to conclude that Nse2 cannot promote Smc6 SUMOylation and DNA damage repair when it is not bound to Smc5 (see Figure 35). Although this result is in accordance with the hypothesis that Nse2 docks to Smc5 to reach its chromatin-associated substrates (Ulrich, 2014), one possible caveat to the approach used above is that the same mutations that prevent Nse2 docking to Smc5 might hinder its direct interaction with other targets. To address this issue, my laboratory colleagues replaced specific residues within the coiled coil domain of the Smc5 protein to disrupt its binding to the SUMO ligase without affecting the *NSE2* gene. Using this approach we could confirm that the function of Nse2 in DNA repair and chromosome segregation requires its binding to the Smc5/6 complex.

5.2.2. The phenotype of *nse2ΔC* mutant cells is suppressed by its fusion to Ubc9

Ubc9, an SUMO E2 conjugating enzyme, can directly transfer SUMO to its targets. This occurs by direct interaction between Ubc9 and its substrates, most typically through recognition of a SUMOylation consensus motif (ΨKXE, where Ψ represents a hydrophobic amino acid and X any amino acid). However, SUMOylation of most proteins in budding yeast requires the presence of a SUMO E3 ligase. This is manifested by the observation that a double deletion of the E3 ligases *SIZ1* and *SIZ2* leads to extremely low levels of SUMO conjugates (see Figure 33). In the case of substrates that directly interact with Ubc9, the presence of an E3 SUMO ligase might promote the correct orientation of the Ubc9-SUMO thioester for catalysis, as is the case for RanBP2 (Reverter and Lima, 2005). In other cases, such as the Siz/PIAS-dependent SUMOylation of PCNA, the E3 establishes additional contacts with the substrate (Yunus and Lima, 2009), a situation that might be especially relevant for SUMOylation of lysines that are not part of a consensus motif. As seen in Figure 35, SUMOylation of Smc5/6 subunits requires binding of the Nse2 to its substrate, what indicates that Nse2 most probably promotes SUMOylation by recruiting Ubc9 through its Siz/PIAS (SP)-RING domain and by promoting the formation of an E2-SUMO-E3-target complex. Supporting this idea, we have observed that the DNA repair deficiency and low Smc5 SUMOylation levels in *nse2ΔC* mutant cells can be suppressed by its fusion to Ubc9 (see Figure 37), indicating that the main function of the Siz/PIAS (SP)-RING domain is the recruitment of the E2 enzyme.

5.2.3. Nse2-mediated SUMOylation requires an active and intact Smc5/6 complex

The previous observations suggest that Nse2 binds to the Smc5/6 complex to reach its substrates and promote DNA repair. Yet, and more appealingly, the structural and the SUMO-mediated signaling functions present in Smc5/6 might be coordinated to enhance DNA repair. Therefore, we decided to test the influence of different Smc5/6 subcomplexes on the E3 SUMO ligase activity. Since Smc5 is a target of Nse2 (Zhao and Blobel, 2005), the binding site for Nse2 in the complex (Duan et al., 2009a), and shows a strong SUMOylation (see Figure 32), we used its SUMOylation levels as an *in vivo* reporter for the activity of the Smc5/6-associated SUMO ligase. The Smc5/6 complex can be dissected into different sub-complexes (Duan et al., 2009b), including the Smc5-Smc6, Nse1-Nse3 and Nse5-Nse6 heterodimers, plus the Nse2 SUMO ligase and the Nse4 kleisin subunit. We used various approaches to analyze the contribution of each of them.

First, we studied the contribution of the Nse1-Nse3 heterodimer using the thermosensitive and MMS-sensitive *nse3-2* mutant allele. Co-immunoprecipitation analysis showed that the Smc5-Nse3 interaction is weaker in *nse3-2* cells, and becomes severely impaired upon shift to the restrictive temperature (see Figure 38). Interestingly, *nse3-2* mutant cells show reduced levels of Smc5 SUMOylation, even at the permissive temperature. However, the Smc5-Nse2 protein interaction is not affected in *nse3-2* cells (see Figure 38), indicating that binding of a functional Nse3 to Smc5 is required for the SUMO ligase activation *in vivo.*

Second, we tested the contribution of Nse5. It has been described that Nse5 interacts with Ubc9 (SUMO E2), Siz2 (SUMO E3), and Smt3 (SUMO) by two hybrid studies (Hazbun et al., 2003). Like *nse3-2*, the *nse5-2* allele is also impaired in most Smc5/6 functions, including MMS repair, rDNA segregation and nucleolar exclusion of recombination factors (Torres-Rosell et al., 2007a). *nse5-2* mutant protein interacts weakly with Smc5, even at the permissive temperature, while the Smc5-Nse2 interaction is not affected in *nse5-2* cells (see Figure 39). In spite of normal binding of Nse2 to Smc5, a severe impairment in Smc5 SUMOylation is observed in *nse5-2* mutant cells. These observations indicate that proper recruitment of Nse5 to Smc5/6 is required for the SUMO ligase activity of Nse2. These results are supported by the fact that, *nse5-1* mutant cells also show reduced levels of Smc5 SUMOylation (Bustard et al., 2012).

Third, we tested the contribution of Smc6. Repression of *SMC6* expression leads to a drastic reduction in Smc5 SUMOylation (see Figure 40). Co-immunoprecipitation analysis showed the Nse2 still binds to Smc5 under these conditions, although there is a substantial reduction in total Nse2 protein levels. Similar behaviour has been reported in DT40 cells, where down-regulation of *SMC5* leads to a reduction of Smc6 and Nse2, which suggests that the intracellular abundance of different Smc5/6 subunits might be co-regulated. Interestingly though, the SUMO ligase activity of Nse2 could not be restored to wild type levels by the expression of the hypomorphic *smc6-1* allele (see Figure 40). Therefore, since neither the Nse2 protein levels nor its interaction with Smc5 are affected in *smc6-1* mutant cells, these results indicate that the Nse2 SUMO ligase is not active when *SMC6* function is impaired.

Fourth, we found that the auxin-induced destruction of specific Smc5/6 subunits, such as Nse4, Nse5, and Nse6, leads to a rapid loss of Smc5 SUMOylation (see Figure 41), which reinforces the idea that the integrity of the Smc5/6 complex is required for Nse2 activation.

Finally, we checked the contribution of different Smc5/6 subunits to the SUMOylation of cohesin. As seen in Figure 42, Smc1 and Smc3 SUMOylation levels are lower in *nse2ΔC* mutant cells than in wild type cells; Smc3 SUMOylation is lower when the expression of *SMC6* is compromised; and Smc3 SUMOylation levels also decrease in *nse5-2* mutant cells. Therefore, hypomorphic alleles of the Smc5/6 complex, which lower the E3 activity of Nse2 towards Smc5, also prevent Nse2-dependent modification of cohesin subunits, which indicates that these requirements can be extended to other targets outside the Smc5/6 complex.

In summary, our observations indicate that inactivation of the Nse1-Nse3, the Nse5-Nse6 heterodimer, the Nse4 kleisin subunit or Smc6 all lead to reduced levels of Nse2-dependent SUMOylation. Therefore, an active and intact Smc5/6 complex is required for the activity of its associated SUMO ligase. Our results suggest that the Smc5/6 complex functions as a giant SUMO E3 enzyme, and the different sub-entities present in the Smc5/6 complex are required for SUMOylation of Nse2 targets. We hypothesise that the non-SMC elements, as well as Smc6, could directly participate in Nse2 activation as we have shown here for Smc5. A second possibility is that the *nse* mutants analysed might diminish the ATPase activity of the complex. For example, the kleisin subunit in the cohesin complex is known to regulate the ATPase activity of the SMC heads (Arumugam et al., 2006), and loss of Nse4 could block Smc5/6 in an analogous manner. A third option is that *nse* malfunction might indirectly diminish the ATPase activity by precluding Smc5/6 recruitment to damaged DNA (Bustard et al., 2012). It has been proposed that the Nse5-Nse6 sub-complex might regulate chromatin association of Smc5/6 through opening of the Smc5-Smc6 hinge interface (Duan et al., 2009b), analogously to what occurs during chromatin loading of cohesin (Gruber et al., 2006). Interestingly, Nse5 is known to directly interact with proteins of the SUMO pathway, including Ubc9 and SUMO (Bustard et al., 2012; Hazbun et al., 2003); therefore, it is tempting to speculate that this sub-complex might play specific roles in SUMO conjugation through recruitment of Ubc9. Still, it is worth noting that Nse2 remains bound to Smc5 (despite down-regulation of Smc5 SUMOylation) in all the thermosensitive *smc5/6* mutants tested; indicating that further steps are required of activation of Nse2.

5.2.4. Esc2 promotes the SUMO ligase activity of Nse2

It is widely accepted that Esc2 may function within the Nse2-dependent SUMOylation pathway. Both *NSE2* and *ESC2* suppress duplication-mediated gross chromosomal rearrangements (GCRs), are epistatic with each other (Albuquerque et al., 2013), and prevent the accumulation of SCJs at damaged forks (Choi et al., 2010; Mankouri et al., 2009; Sollier et al., 2009).

As seen in Figure 43, Esc2 interacts with the Smc5/6 complex *in vivo* and promotes the SUMO ligase activity of Nse2. This result is corroborated by a preliminary study conducted in *S. pombe* (Boddy et al., 2003) where they described the interaction between Esc2 and the Smc5/6 complex. Similar to the impairment in Smc5 SUMOylation shown in this study, it has been described that Esc2 is required for efficient SUMOylation of Nse2-targets outside the Smc5/6 complex, such as Rpa135, Smc1, Smc3, Smc2 and Smc4 (RNA pol I, cohesin and condensin, respectively), which reinforces the idea that Esc2 positively regulates Nse2 activity *in vivo* (Albuquerque et al., 2013). In *S. pombe*, it has been proposed that Esc2 could bring Ubc9-SUMO thioester species into proximity with the Nse2 SUMO E3 ligase to facilitate target SUMOylation through transient interaction with the Smc5/6 complex (Prudden et al., 2011).

The transient interaction between Esc2 and the Smc5/6 complex might regulate the ability of Nse2 to transfer SUMO to its substrates, thereby preventing Nse2-dependent hyperSUMOylation due to the constitutive recruitment of the E3 SUMO ligase to the Smc5/6 complex.

5.2.5. The ATPase function of Smc5 is required for Nse2-dependent SUMOylation

Since the essential function of SMC complexes in chromosome maintenance requires the ATPase activity of its SMC subunits, we decided to introduce specific mutations in the walker A and walker B nucleotide binding domains of Smc5 (K75I or D1014A, respectively) to weaken its interaction with ATP and block its ATPase activity (Arumugam et al., 2003; Hirano et al., 2001). As previously described, we observed that the ATPase mutations in *SMC5* are lethal (Roy et al., 2011), underlining the essential function of the ATPase in chromosome maintenance. Nse2 binds with similar efficiency to *smc5(K75I)* or *smc5(D1014A)* mutant proteins compared to wild type Smc5, which indicates that there is no ATP-dependent modulation of the Smc5-Nse2 interaction. However, SUMOylation of the ATPase-defective *smc5* proteins was almost undetectable (see Figure 44), showing that they are not modified by their accompanying E3. The SUMOylation deficiency observed in cells expressing *smc5(K75I)* mutant protein also affects other subunits in the complex, such as the kleisin subunit, as well as the cohesin complex (data not shown). Therefore, the ATPase activity of Smc5 is required for the SUMO ligase activity of Nse2. This effect does not seem to stem from diminished recruitment to chromatin, since *in vitro* experiments showed that Smc5 binds efficiently to DNA in the absence of ATP (Roy et al., 2011), and we did not observe alterations in the *in vivo* chromatin binding of *smc5* ATPase mutant proteins using a chromatin fractionation assay (see Figure 44).

Importantly, the fact that the constitutive recruitment of Ubc9 to Nse2 is not able to SUMOylate the *smc5(K75I)* mutant protein indicates that the ATPase activity of Smc5 is required for activation of the Nse2-dependent branch of the SUMO pathway, after E2 recruitment (see Figure 45). Although the Siz/PIAS (SP)-RING domain of Nse2 may fail to interact with the E2 when Smc5 is not bound to ATP, we think that this possibility is unlikely, because an E3-E2 fusion, also still requires the ATPase function for SUMOylation. Therefore, Nse2 must be held in an inactive state. This could encompass various situations, ranging from the incapacity to properly orient the Ubc9-SUMO thioester species, the trapping of the molecule in a transition state for SUMOylation, or the direct inhibition of Ubc9 activity. A more detailed understanding of the Nse2-Ubc9-SUMO interaction structure, as well as the participation of Smc5/6 structural elements will be required to understand this issue. In conclusion, we propose that the Smc5/6 complex functions as a giant SUMO E3 enzyme that requires: (i) Esc2, (ii) a functional and intact complex, and (iii) the ATPase activity of Smc5.

5.2.6. How could Nse2 sense ATP binding by Smc5?

The SUMO ligase binds in the middle of the coiled coil domain of Smc5. Based on the structure of the Nse2-Smc5 interaction (Duan et al., 2009a), and the length of the coiled coil, Nse2 most likely docks at a distance of 16-24 nm from the ATPase heads. It is possible that the communication between the ATPase heads and the SUMO ligase is propagated through conformational changes in the Smc5-Nse2 molecule. In collaboration with Dr. Claire Wyman (Rotterdam, Netherlands) we performed atomic force microscopy experiments, which revealed that ATP binding provokes a conformational change leading to more compacted SMC molecules characterized by increased height. These ATP-dependent conformational changes may well involve the coiled coil domain, including the SUMO ligase bound to it.

The coiled coil domains in SMC proteins display a wide variety of conformations, most probably due to the presence of kinks at specific disruptions in these domains (Yoshimura et al., 2002). The coiled coil flexibility in SMC proteins might be important to accommodate chromatin fibres inside the ring structure, and it might also help to bring different domains of the molecule into closer contact (Mc et al., 2007). ATPases are known to couple ATP binding and hydrolysis to mechanical work, and coiled coil domains can transmit this information to other regions of the molecule (Carter et al., 2008; Kinoshita et al., 2009). In the case of dynein, the communication is enabled by a change in the registry of the two short alpha-helical chains in the coiled coils (Carter et al., 2008). Other possibilities include the rotation of the ATPase heads along the coiled coil axis, as is the case for Rad50 (Hopfner et al., 2000), or folding of the molecule at specific articulated disruptions, as has been hypothesized for the cohesin complex (Gruber et al., 2006). It is therefore likely that the communication between the ATPase heads and the SUMO ligase is propagated through conformational changes in the Smc5/6-Nse2 molecule involving the coiled coil domains. In relation to the latter, we have observed that the conserved proline residues in the coiled coil disruptions of Smc5 are required for full activation of Nse2. Mutations of these residues to glutamic acid prevent the activation of the SUMO ligase and proper repair of MMS-induced damage. Overall, these observations strongly support the idea that ATP hydrolysis provokes a conformational change that is propagated along the coiled coils, and this allows activation of its accompanying SUMO ligase.

5.3. Characterization of the Smc5/6 complex SUMOylation in response to DNA damage

Previous sections emphasize the importance of the intimate relationship between the Nse2 SUMO ligase and its binding site, the Smc5/6 complex. The Nse2 branch of the SUMO pathway and the Smc5/6 complex are both required to prevent the accumulation and promote the removal of pathological replication-dependent recombinogenic structures at damaged forks (Bermudez-Lopez et al., 2010; Branzei et al., 2006; Chen et al., 2009; Chen et al., 2013; Sollier et al., 2009; Yong-Gonzales et al., 2012). Similarly, in meiosis the Smc5/6 complex is also required to properly control the production and removal of recombination intermediates (Copsey et al., 2013; Wehrkamp-Richter et al., 2012; Xaver et al., 2013).

MMS-induced DNA damage provokes an increase in the SUMOylation levels of all the SUMOylated subunits in the Smc5/6 complex (Figure 32), which reflects a further activation of Nse2. This is in accordance with the fact that the Nse2-dependent SUMOylation is required to promote resolution of SCJs that appear during perturbed DNA replication (Bermudez-Lopez et al., 2010; Chavez et al., 2010). Interestingly, *RAD52* deletion, which reduces the accumulation of SCJs (Branzei et al., 2006), prevents the MMS-induced SUMOylation of Smc5 (Figure 47). This indicates that the SUMO ligase activity of Nse2 is enhanced by the presence of SCJs generated during the DNA damage bypass and replication fork recovery process. Based on this, deleting *SHU*, *MMS2* and *MPH1* (factors that promote SCJ formation in the presence of MMS-induced DNA damage) might have the same effect.

In *S. pombe*, the Smc5/6 complex is recruited to stalled replication forks and is proposed to play a role during HU-induced replication fork stalling by maintaining fork conformation, allowing the loading of homologous recombination factors, such as Rad52 and replication factor A (Ampatzidou et al., 2006; Irmisch et al., 2009). In budding yeast, recruitment of the Smc5/6 complex has been detected only at HU-stalled replication forks in checkpoint-deficient (*rad53* mull) cells, where stalling leads to fork collapse (Bustard et al., 2012; Lindroos et al., 2006). As seen in Figure 48, Smc5 SUMOylation increases in response to HU in *rad53* null cells (Figure 48), which indicates that the SUMO ligase activity of Nse2 increases most likely in response to SCJ formation due to replication fork collapse. This result is supported by the fact that Nse4 SUMOylation increases also in response to HU in *rad53* null cells in *S. pombe* (Pebernard et al., 2008b). Altogether, these results indicate that the SUMO ligase activity of Nse2 is enhanced in response to SCJs produced at damaged replication forks.

5.4. Identification of the Smc5 SUMOylation sites

Since Smc5 is a target of Nse2 (Zhao and Blobel, 2005), the binding site for Nse2 in the complex (Duan et al., 2009a), and shows a strong SUMOylation (see Figure 32), we decided to determine its SUMOylation sites.

In order to predict the SUMOylation sites of Smc5, the sequence was first analyzed with SUMOsp 2.0, which is a SUMOylation site prediction program based on Ubc9 consensus motifs and previously identified SUMOylation sites (Ren et al., 2009). As seen in Figure 49, the program identified 17 putative lysines in Smc5, one located in the ATPase domain of Smc5 (K31) and 16 distributed throughout the rest of the protein. In order to prevent the SUMOylation, all putative lysines (K), but K31, were mutated to arginine (R). As seen in Figure 49, *smc5(K-16-R)* shows the same SUMOylation pattern as wild type Smc5, which indicates that Smc5 is not SUMOylated at Ubc9 consensus sites. This result is in accordance with the fact that a number of proteins not subject to SUMOylation contain this motif, and other physiological targets of SUMOylation are not SUMOylated on this consensus motif (Wilkinson and Henley, 2010), which limits the accuracy of SUMOylation site prediction programs.

Next, we decided to mutate all lysines present in Smc5, but K75 which is necessary for ATPase function, generating the *smc5(K-all-R)*. As expected, this mutant allele is not SUMOylated and it is not able to complement the lack of expression of the endogenous wild type *SMC5*, which indicates that this mutant is not viable. Afterwards, we decided to mutate the lysines present in each domain separetely. As seen in Figure 52, mutating the lysines in the nucleotide binding domains, walker A (*smc5(wa K-R)*) or walker B (*smc5(wb K-R)*), showed a discrete but reproducible slow growth in MMS and a slight global reduction in the SUMOylation levels with the same band pattern. This suggests that the mutations inserted in the nucleotide binding domains of Smc5 might have a minor deleterious effect on the ATPase activity of Smc5, which could compromise the Nse2 SUMO ligase activity, provoking a global down-regulation of Smc5 SUMOylation. However, this effect must be very small because these mutants are viable and the ATPase activity of Smc5 is essential for the viability of the cell (Roy et al., 2011). Finally, the combination of *smc5(cc1 K-R)*, *smc5(cc2 K-R)* and *smc5(cc1,2 K-R)* allowed us to demonstrate that Smc5 is SUMOylated in both coiled coils, and the lack of SUMOylation in both domains renders cells sensitive to MMS.

Since Smc5/6 is recruited to DSBs to promote sister chromatid recombination in budding yeast (de et al., 2006) , we decided to test whether the recruitment of the *smc5(cc1,2 K-R)* to an HO endonuclease-mediated DSB was affected. As seen in Figure 53, the recruitment of the *smc5(cc1,2 K-R)* is impaired, which indicates that Smc5 SUMOylation could be necessary for the recruitment onto DNA upon damage. Although these results are in accordance with the fact that *nse5-1* mutant cells, which display a strong impairment of Smc5 SUMOylation, show a reduced recruitment of Smc5/6 to stalled forks by HU (Bustard et al., 2012), we must be very critical with this result because the *smc5(cc1,2 K-R)* has many lysines mutated to arginine, which could be provoking a significant structural change able to affect its DNA binding independently of SUMOylation. Further studies will be required to identify the specific lysines required for Smc5 SUMOylation and analyse its phenotype.

5.5. The role of the Smc5/6 complex in chromosome topology

The Smc5/6 complex has been strongly associated with DNA repair. However, several lines of evidence indicate that it could also influence chromosome topology. First, ChIP-on-chip analysis shows that the Smc5/6 complex associates with all chromosomes during DNA replication, and the frequency of Smc5/6 chromosome arm-binding sites increases with chromosome length (Lindroos et al., 2006). Second, *smc5/6* hypomorphic alleles show a late replication delay that specifically affects longer chromosomes (Kegel et al., 2011), a phenotype that is also detected in cells lacking functional Top1 (Wang, 2002). Third, the amount of chromosomal-associated Smc5/6 increases in *top2-4* mutants (Kegel et al., 2011). Fourth, the fission yeast *smc6-74* mutant is synthetically lethal with temperature sensitive *top2-191* at semipermissive temperatures (Verkade et al., 1999). Finally, the Smc5/6 complex is required for on-time progression of DNA replication and subsequent binding of Topo IIα onto replicated chromatids in mammalian cells (Gallego-Paez et al., 2014; Gomez et al., 2013).

Linked to this, it has been proposed that the Smc5/6 complex assists replication fork rotation, preventing the accumulation of positive supercoils ahead of the replication machinery (Kegel et al., 2011). If this is true, a non-functional *smc5/6* complex would reduce the ability of the replication fork to rotate along the axis of the DNA, leading to an accumulation of positive supercoiling ahead of the replication machinery and a decrease in the formation of precatenanes behind the replication fork.

To test this, we analysed the topological status of the *pRS316* plasmid after one round of replication in the absence of Top2 and Smc5/6 function. As seen in Figure 56, one-dimensional gel electrophoresis shows that *top2-td* and *top2-td smc6-9* mutant cells both accumulate catenated dimers. Interestingly, the amount of supercoiled catenated dimers is slightly decreased in *top2-td smc6-9* mutant cells compared to *top2-td* cells. The amount of supercoiled catenated dimers could be affected either by DNA replication problems or by nicking of the sample during DNA extraction. Therefore, one-dimensional gel electrophoresis analysis is not reliable. In order to circumvent this problem, we decided to resolve the catenanes according to their catenation number regarding any contribution of supercoiling state or accidental nicking. To do this, DNA samples were treated with a nicking endonuclease enzyme to relax all catenated dimers and samples were then subjected to two-dimensional gel electrophoresis analysis. Surprisingly, when the catenane distribution was determined, there was no difference using two different approaches to inactivate Top2 function (*top2-td and top2-4*) (see Figure 56 and Figure 57). This data indicates that swivelling of the replisome is not affected, at least in *smc6-9* mutant cells.

Since the previous findings do not support what has been previously published (Kegel et al., 2011), we decided to characterize the same *smc5/6* mutant that the authors used, the *smc6-56* hypomorphic allele. As seen in Figure 58, *top2-4 smc6-56* mutant cells also show the same catenane distribution as *top2-4* cells. These data are directly contradictory to what was proposed by Kegel and colleagues. One possible explanation is that they based their conclusion on the global amount of supercoiled catenanes seen in a one-dimensional gel electrophoresis. The one-dimensional gel in our hands replicates what was published; unfortunately the additional analysis possible only through the two-dimensional gel electrophoresis brings to the opposite conclusion -that catenane distribution is not affected by *smc6-9* or *smc6-56* mutants. Surprisingly, the highly compromised *smc5-4* hypomorphic allele in fact shows a higher accumulation of catenanes in the same system, which indicates that Smc5/6 might have the opposite role, preventing unscheduled replication fork swivelling. Given the discrepancy between our results and the published data, further work will be required to fully understand the contribution of the Smc5/6 complex to chromosome topology.

CONCLUSIONS

Conclusions

1) *smc5/6* mutants accumulate sister chromatid junctions (SCJs) during replication in the presence of methyl methanesulfonate (MMS).

2) A 30 minute pulse of 0.01% MMS in G1 does not affect cell cycle progression in wild type cells.

3) *smc5/6* mutants display genome segregation defects after an MMS pulse.

4) *smc5/6* mutants accumulate SCJs and unfinished replication intermediates after an MMS pulse.

5) Suppression of SCJ formation is beneficial when Smc5/6 function is compromised.

6) The Smc5/6 complex promotes resolution of sister chromatid junctions.

7) The Nse2-Smc5 interaction is required for SUMOylation of Nse2 targets.

8) The main function of the Siz/PIAS (SP)-RING domain of Nse2 is to recruit Ubc9.

9) Nse2-mediated SUMOylation requires an active and intact Smc5/6 complex.

10) Esc2 promotes Nse2-dependent SUMOylation.

11) The ATPase function of Smc5 is part of the ligase mechanism that triggers SUMOylation via Nse2.

12) Up-regulation of Smc5 SUMOylation upon DNA damage depends on an active homologous recombination pathway.

13) Smc5 SUMOylation in both coiled coils is important for its recruitment to DSBs.

14) Two-dimensional gel electrophoresis revealed that *smc6* mutants cells do not alter catenane formation.

15) *smc5-4 top2* mutant cells accumulate more catenanes compared to single *top2* mutant cells.

REFERENCE LIST

Reference list

1. Albuquerque, C.P., Wang, G., Lee, N.S., Kolodner, R.D., Putnam, C.D., and Zhou, H. (2013). Distinct SUMO ligases cooperate with Esc2 and Slx5 to suppress duplication-mediated genome rearrangements. PLoS. Genet. 9, e1003670.
2. Alcasabas, A.A., Osborn, A.J., Bachant, J., Hu, F., Werler, P.J., Bousset, K., Furuya, K., Diffley, J.F., Carr, A.M., and Elledge, S.J. (2001). Mrc1 transduces signals of DNA replication stress to activate Rad53. Nat. Cell Biol. 3, 958-965.
3. Alexandrov, A.I., Cozzarelli, N.R., Holmes, V.F., Khodursky, A.B., Peter, B.J., Postow, L., Rybenkov, V., and Vologodskii, A.V. (1999). Mechanisms of separation of the complementary strands of DNA during replication. Genetica 106, 131-140.
4. Allers, T., and Lichten, M. (2000). A method for preparing genomic DNA that restrains branch migration of Holliday junctions. Nucleic Acids Res. 28, e6.
5. Almedawar, S., Colomina, N., Bermudez-Lopez, M., Pocino-Merino, I., and Torres-Rosell, J. (2012). A SUMO-dependent step during establishment of sister chromatid cohesion. Curr. Biol. 22, 1576-1581.
6. Ampatzidou, E., Irmisch, A., O'Connell, M.J., and Murray, J.M. (2006). Smc5/6 is required for repair at collapsed replication forks. Mol. Cell Biol. 26, 9387-9401.
7. Anderson, D.E., Losada, A., Erickson, H.P., and Hirano, T. (2002). Condensin and cohesin display different arm conformations with characteristic hinge angles. J. Cell Biol. 156, 419-424.
8. Andrews, E.A., Palecek, J., Sergeant, J., Taylor, E., Lehmann, A.R., and Watts, F.Z. (2005). Nse2, a component of the Smc5-6 complex, is a SUMO ligase required for the response to DNA damage. Mol. Cell Biol. 25, 185-196.
9. Arends, M.J. (2013). Pathways of colorectal carcinogenesis. Appl. Immunohistochem. Mol. Morphol. 21, 97-102.
10. Arnaudeau, C., Lundin, C., and Helleday, T. (2001). DNA double-strand breaks associated with replication forks are predominantly repaired by homologous recombination involving an exchange mechanism in mammalian cells. J. Mol. Biol. 307, 1235-1245.
11. Arumugam, P., Gruber, S., Tanaka, K., Haering, C.H., Mechtler, K., and Nasmyth, K. (2003). ATP hydrolysis is required for cohesin's association with chromosomes. Curr. Biol. 13, 1941-1953.
12. Arumugam, P., Nishino, T., Haering, C.H., Gruber, S., and Nasmyth, K. (2006). Cohesin's ATPase activity is stimulated by the C-terminal Winged-Helix domain of its kleisin subunit. Curr. Biol. 16, 1998-2008.
13. Azvolinsky, A., Dunaway, S., Torres, J.Z., Bessler, J.B., and Zakian, V.A. (2006). The S. cerevisiae Rrm3p DNA helicase moves with the replication fork and affects replication of all yeast chromosomes. Genes Dev. 20, 3104-3116.
14. Azzam, R., Chen, S.L., Shou, W., Mah, A.S., Alexandru, G., Nasmyth, K., Annan, R.S., Carr, S.A., and Deshaies, R.J. (2004). Phosphorylation by cyclin B-Cdk underlies release of mitotic exit activator Cdc14 from the nucleolus.

Science 305, 516-519.

15. Bartkova, J., Horejsi, Z., Koed, K., Kramer, A., Tort, F., Zieger, K., Guldberg, P., Sehested, M., Nesland, J.M., Lukas, C., Orntoft, T., Lukas, J., and artek, J. (2005). DNA damage response as a candidate anti-cancer barrier in early human tumorigenesis. Nature 434, 864-870.
16. Bates, A.D., and Maxwell, A. (1989). DNA gyrase can supercoil DNA circles as small as 174 base pairs. EMBO J. 8, 1861-1866.
17. Bates, A.D., and Maxwell, A. (1997). DNA topology: topoisomerases keep it simple. Curr. Biol. 7, R778-R781.
18. Baxter, J., and Diffley, J.F. (2008). Topoisomerase II inactivation prevents the completion of DNA replication in budding yeast. Mol. Cell 30, 790-802.
19. Baxter, J., Sen, N., Martinez, V.L., De Carandini, M.E., Schvartzman, J.B., Diffley, J.F., and Aragon, L. (2011). Positive supercoiling of mitotic DNA drives decatenation by topoisomerase II in eukaryotes. Science 331, 1328-1332.
20. Behlke-Steinert, S., Touat-Todeschini, L., Skoufias, D.A., and Margolis, R.L. (2009). SMC5 and MMS21 are required for chromosome cohesion and mitotic progression. Cell Cycle 8, 2211-2218.
21. Bell, S.P., and Stillman, B. (1992). ATP-dependent recognition of eukaryotic origins of DNA replication by a multiprotein complex. Nature 357, 128-134.
22. Bergink, S., and Jentsch, S. (2009). Principles of ubiquitin and SUMO modifications in DNA repair. Nature 458, 461-467.
23. Bermudez-Lopez, M., Ceschia, A., de, P.G., Colomina, N., Pasero, P., Aragon, L., and Torres-Rosell, J. (2010). The Smc5/6 complex is required for dissolution of DNA-mediated sister chromatid linkages. Nucleic Acids Res. 38, 6502-6512.
24. Bernier-Villamor, V., Sampson, D.A., Matunis, M.J., and Lima, C.D. (2002). Structural basis for E2-mediated SUMO conjugation revealed by a complex between ubiquitin-conjugating enzyme Ubc9 and RanGAP1. Cell 108, 345-356.
25. Bhat, M.A., Philp, A.V., Glover, D.M., and Bellen, H.J. (1996). Chromatid segregation at anaphase requires the barren product, a novel chromosome-associated protein that interacts with Topoisomerase II. Cell 87, 1103-1114.
26. Blackburn, E.H. (2001). Switching and signaling at the telomere. Cell 106, 661- 673.
27. Blanco, M.G., Matos, J., and West, S.C. (2014). Dual control of Yen1 nuclease activity and cellular localization by Cdk and Cdc14 prevents genome instability. Mol. Cell 54, 94-106.
28. Bloom, J., and Cross, F.R. (2007). Multiple levels of cyclin specificity in cell-cycle control. Nat. Rev. Mol. Cell Biol. 8, 149-160.
29. Boddy, M.N., Shanahan, P., McDonald, W.H., Lopez-Girona, A., Noguchi, E., Yates III, J.R., and Russell, P. (2003). Replication checkpoint kinase Cds1 regulates recombi national repair protein Rad60. Mol. Cell Biol. 23, 5939-5946.
30. Bodnar, A.G., Ouellette, M., Frolkis, M., Holt, S.E., Chiu, C.P., Morin, G.B., Harley, C.B., Shay, J.W., Lichtsteiner, S., and Wright, W.E. (1998). Extension of life-span by introduction of telomerase into normal human cells. Science 79, 349-352.
31. Boiteux, S., and Guillet, M. (2004). Abasic sites in DNA: repair and biological consequences in Saccharomyces cerevisiae. DNA Repair (Amst) 3, 1-12.

32. Boiteux, S., and Jinks-Robertson, S. (2013). DNA repair mechanisms and the bypass of DNA damage in Saccharomyces cerevisiae. Genetics 193, 1025-1064.
33. Bouck, D.C., Joglekar, A.P., and Bloom, K.S. (2008). Design features of a mitotic spindle: balancing tension and compression at a single microtubule kinetochore interface in budding yeast. Annu. Rev. Genet. 42, 335-359.
34. Branzei, D., and Foiani, M. (2005). The DNA damage response during DNA replica tion. Curr. Opin. Cell Biol. 17, 568-575.
35. Branzei, D., and Foiani, M. (2009). The checkpoint response to replication stress. DNA Repair (Amst) 8, 1038-1046.
36. Branzei, D., Sollier, J., Liberi, G., Zhao, X., Maeda, D., Seki, M., Enomoto, T., Ohta,K., and Foiani, M. (2006). Ubc9- and mms21-mediated sumoylation countacts recombinogenic events at damaged replication forks. Cell 127, 509-522.
37. Branzei, D., Vanoli, F., and Foiani, M. (2008). SUMOylation regulates Rad18-mediated template switch. Nature 456, 915-920.
38. Braschi, E., Zunino, R., and McBride, H.M. (2009). MAPL is a new mitochonrial SUMO E3 ligase that regulates mitochondrial fission. EMBO Rep. 10, 748-754.
39. Brewer, B.J., and Fangman, W.L. (1987). The localization of replication origins on ARS plasmids in S. cerevisiae. Cell 51, 463-471.
40. Brouwer, A.K., Schimmel, J., Wiegant, J.C., Vertegaal, A.C., Tanke, H.J., and Dirks, R.W. (2009). Telomeric DNA mediates de novo PML body formation. Mol. Biol. Cell 20, 4804-4815.
41. Bustard, D.E., Menolfi, D., Jeppsson, K., Ball, L.G., Dewey, S.C., Shirahige, K., Sjogren, C., Branzei, D., and Cobb, J.A. (2012). During replication stress, non-SMC element5 (NSE5) is required for Smc5/6 protein complex functionality at stalled forks. J. Biol. Chem. 287, 11374-11383.
42. Bylebyl, G.R., Belichenko, I., and Johnson, E.S. (2003). The SUMO isopeptidase Ulp2 prevents accumulation of SUMO chains in yeast. J. Biol. Chem. 278, 44113-44120.
43. Byun, T.S., Pacek, M., Yee, M.C., Walter, J.C., and Cimprich, K.A. (2005). Funcional uncoupling of MCM helicase and DNA polymerase activities activates the ATR-dependent checkpoint. Genes Dev. 19, 1040-1052.
44. Cadet, J., Sage, E., and Douki, T. (2005). Ultraviolet radiation-mediated damage to cel lular DNA. Mutat. Res. 571, 3-17.
45. Caldecott, K.W. (2008). Single-strand break repair and genetic disease. Nat. Rev. Genet. 9, 619-631.
46. Calzada, A., Hodgson, B., Kanemaki, M., Bueno, A., and Labib, K. (2005). Molecular anatomy and regulation of a stable replisome at a paused eukaryotic DNA replication fork. Genes Dev. 19, 1905-1919.
47. Carter, A.P., Garbarino, J.E., Wilson-Kubalek, E.M., Shipley, W.E., Cho, C., Milligan, R.A., Vale, R.D., and Gibbons, I.R. (2008). Structure and functional role of dynein's microtubule-binding domain. Science 322, 1691-1695.
48. Cerritelli, S.M., and Crouch, R.J. (2009). Ribonuclease H: the enzymes in eukaryotes. FEBS J. 276, 1494-1505.
49. Chang, D.J., and Cimprich, K.A. (2009). DNA damage tolerance: when it's OK to make mistakes. Nat. Chem. Biol. 5, 82-90.
50. Chang, D.J., Lupardus, P.J., and Cimprich, K.A. (2006). Monoubiquitination of prolif erating cell nuclear antigen induced by stalled replication requires

uncoupling of DNA polymerase and mini-chromosome mainteance helicase activities. J. Biol. Chem. 281, 32081-32088.

51. Chavez, A., Agrawal, V., and Johnson, F.B. (2011). Homologous recombination-dependent rescue of deficiency in the structural maintenance of chromo somes (Smc) 5/6 complex. J. Biol. Chem. 286, 5119-5125.
52. Chavez, A., George, V., Agrawal, V., and Johnson, F.B. (2010). Sumoylation and the structural maintenance of chromosomes (Smc) 5/6 complex slow senes cence through recombination intermediate resolution. J. Biol. Chem. 285, 11922-11930.
53. Chen, Y.H., Choi, K., Szakal, B., Arenz, J., Duan, X., Ye, H., Branzei, D., and Zhao, X. (2009). Interplay between the Smc5/6 complex and the Mph1 helicase in recombinational repair. Proc. Natl. Acad. Sci. U. S. A 106, 21252-21257.
54. Chen, Y.H., Szakal, B., Castellucci, F., Branzei, D., and Zhao, X. (2013). DNA damage checkpoint and recombinational repair differentially affect the replication stress tolerance of Smc6 mutants. Mol. Biol. Cell 24, 2431-2441.
55. Cheng, C.H., Lo, Y.H., Liang, S.S., Ti, S.C., Lin, F.M., Yeh, C.H., Huang, H.Y., and Wang, T.F. (2006). SUMO modifications control assembly of synaptonemal complex and polycomplex in meiosis of Saccharomyces cerevisiae. Genes Dev. 20, 2067-2081.
6. Chiolo, I., Minoda, A., Colmenares, S.U., Polyzos, A., Costes, S.V., and Karpen, G.H. (2011). Double-strand breaks in heterochromatin move outside of a dynamic HP1a domain to complete recombinational repair. Cell 144, 732-744.
57. Choi, K., Szakal, B., Chen, Y.H., Branzei, D., and Zhao, X. (2010). The Smc5/6 complex and Esc2 influence multiple replication-associated recombination processes in Saccharomyces cerevisiae. Mol. Biol. Cell 21, 2306-2314.
58. Chu, W.K., and Hickson, I.D. (2009). RecQ helicases: multifunctional genome caretak ers. Nat. Rev. Cancer 9, 644-654.
59. Chung, I., Leonhardt, H., and Rippe, K. (2011). De novo assembly of a PML nuclea subcompartment occurs through multiple pathways and induces telomere elongation. J. Cell Sci. 124, 3603-3618.
60. Ciosk, R., Shirayama, M., Shevchenko, A., Tanaka, T., Toth, A., Shevchenko, A., and Nasmyth, K. (2000). Cohesin's binding to chromosomes depends on a separate complex consisting of Scc2 and Scc4 proteins. Mol. Cell 5, 243-254.
61. Conradt, B., Shaw, J., Vida, T., Emr, S., and Wickner, W. (1992). In vitro reactions of vacuole inheritance in Saccharomyces cerevisiae. J. Cell Biol. 119, 1469-1479.
62. Cooper, S. (2006). Checkpoints and restriction points in bacteria and eukaryotic cells. Bioessays 28, 1035-1039.
63. Copsey, A., Tang, S., Jordan, P.W., Blitzblau, H.G., Newcombe, S., Chan, A.C., Newn ham, L., Li, Z., Gray, S., Herbert, A.D., Arumugam, P., Hochwagen, A., Hunter, N., andHoffmann, E. (2013). Smc5/6 coordinates formation and resolution of joint molecules with chromosome morphology to ensure meiotic divisions. PLoS. Genet. 9, e1004071.
64. Cost, G.J., and Cozzarelli, N.R. (2006). Smc5p promotes faithful chromosome trans mission and DNA repair in Saccharomyces cerevisiae. Genetics 172, 2185-2200.
65. Cotta-Ramusino, C., Fachinetti, D., Lucca, C., Doksani, Y., Lopes, M., Sogo, J.,

and Foiani, M. (2005). Exo1 processes stalled replication forks and counter acts fork reversal in checkpoint-defective cells. Mol. Cell 17, 153-159.

66. Cremona, C.A., Sarangi, P., and Zhao, X. (2012). Sumoylation and the DNA damage response. Biomolecules. 2, 376-388.
67. Crow, Y.J., Leitch, A., Hayward, B.E., Garner, A., Parmar, R., Griffith, E., Ali, M., Sem ple, C., Aicardi, J., Babul-Hirji, R., Baumann, C., Baxter, P., Bertini, E., Chandler, K.E., Chitayat, D., Cau, D., Dery, C., Fazzi, E., Goizet, C., King, M.D. Klepper, J., Lambe, D., Lanzi, G., Lyall, H., Martinez-Frias, M.L., Mathieu, M., McKeown, C., Monier, A., Oade, Y., Quarrell, O.W., Rittey, C.D., Rogers, R.C., Sanchis, A., Stephenson, J.B., acke, U., Till, M., Tolmie, J.L., Tomlin, P., Voit, T., Weschke, B., Woods, C.G., Lebon, P., Bonthron, D.T., Ponting, C.P., and Jackson, A.P. (2006). Mutations in genes encoding ribonuclease H2 subunits cause Aicardi-Goutieres yndrome and mimic congenital viral brain infection. Nat. Genet. 38, 910-916.
68. D'Ambrosio, C., Schmidt, C.K., Katou, Y., Kelly, G., Itoh, T., Shirahige, K., and Uhl mann, F. (2008). Identification of cis-acting sites for condensin loading onto bud ding yeast chromosomes. Genes Dev. 22, 2215-2227.
69. D'Ambrosio, L.M., and Lavoie, B.D. (2014). Pds5 Prevents the PolySUMO-Dependent Separation of Sister Chromatids. Curr. Biol. 24, 361-371.
70. Da Silva-Ferrada, E., Lopitz-Otsoa, F., Lang, V., Rodriguez, M.S., and Matthiesen, R. (2012). Strategies to Identify Recognition Signals and Targets of SUMOylation. Biochem. Res. Int. 2012, 875148.
71. Das-Bradoo, S., Nguyen, H.D., Wood, J.L., Ricke, R.M., Haworth, J.C., and Bielinsky, A.K. (2010). Defects in DNA ligase I trigger PCNA ubiquitylation at Lys 107. Nat. Cell Biol. 12, 74-79.
72. Davies, A.A., Huttner, D., Daigaku, Y., Chen, S., and Ulrich, H.D. (2008). Activation of ubiquitin-dependent DNA damage bypass is mediated by replication protein a. Mol. Cell 29, 625-636.
73. de, P.G., Cortes-Ledesma, F., Ira, G., Torres-Rosell, J., Uhle, S., Farmer, S., wang, J.Y., Machin, F., Ceschia, A., McAleenan, A., Cordon-Preciado, V., Clemente-Blanco, A., Vilella-Mitjana, F., Ullal, P., Jarmuz, A., Leitao, B., Bressan, D., Dotwala, F., Papusha, A., Zhao, X., Myung, K., Haber, J.E., Aguilera, A., and ragon, L. (2006). Smc5-Smc6 mediate DNA double-strand-break repair by promoting sister-chromatid recombination. Nat. Cell Biol. 8, 1032-1034.

74. de, P.G., Torres-Rosell, J., and Aragon, L. (2009). The unnamed complex: what do we know about Smc5-Smc6? Chromosome. Res. 17, 251-263.
75. Delacote, F., and Lopez, B.S. (2008). Importance of the cell cycle phase for the choice of the appropriate DSB repair pathway, for genome stability maintenance: the trans-S double-strand break repair model. Cell Cycle 7, 33-38.
76. Denison, C., Rudner, A.D., Gerber, S.A., Bakalarski, C.E., Moazed, D., and Gygi, S.P. (2005). A proteomic strategy for gaining insights into protein sumoylation in yeast. MolCell Proteomics. 4, 246-254.
77. Desany, B.A., Alcasabas, A.A., Bachant, J.B., and Elledge, S.J. (1998). Recovery from DNA replicational stress is the essential function of the S-phase checkpoint pathway. Genes Dev. 12, 2956-2970.
78. Deshpande, A.M., and Newlon, C.S. (1996). DNA replication fork pause sites

dependent on transcription. Science 272, 1030-1033.
79. Desterro, J.M., Thomson, J., and Hay, R.T. (1997). Ubch9 conjugates SUMO but not ubiquitin. FEBS Lett. 417, 297-300.
80. Dianov, G.L., and Hubscher, U. (2013). Mammalian base excision repair: the forgotten archangel. Nucleic Acids Res. 41, 3483-3490.
81. DiNardo, S., Voelkel, K., and Sternglanz, R. (1984). DNA topoisomerase II mutant of Saccharomyces cerevisiae: topoisomerase II is required for segregation of daughter molecules at the termination of DNA replication. Proc. Natl. Acad. Sci. U. S. A 81, 2616-2620.
82. Dirick, L., Bohm, T., and Nasmyth, K. (1995). Roles and regulation of Cln-Cdc28 ki nases at the start of the cell cycle of Saccharomyces cerevisiae. EMBO J. 14, 4803-4813.
83. Doyle, J.M., Gao, J., Wang, J., Yang, M., and Potts, P.R. (2010). MAGE-RING protein complexes comprise a family of E3 ubiquitin ligases. Mol. Cell 39, 963-974.
84. Dreier, M.R., Bekier, M.E., and Taylor, W.R. (2011). Regulation of sororin by Cdk1-mediated phosphorylation. J. Cell Sci. 124, 2976-2987.
85. Duan, X., Sarangi, P., Liu, X., Rangi, G.K., Zhao, X., and Ye, H. (2009a). Structural and functional insights into the roles of the Mms21 subunit of the Smc5/6 complex. Mol. Cell 35, 657-668.
86. Duan, X., Yang, Y., Chen, Y.H., Arenz, J., Rangi, G.K., Zhao, X., and Ye, H. (2009b). Architecture of the Smc5/6 Complex of Saccharomyces cerevisiae Reveals a Unique Interaction between the Nse5-6 Subcomplex and the Hinge Regions of Smc5 and Smc6. J. Biol. Chem. 284, 8507-8515.
87. Earnshaw, W.C., Halligan, B., Cooke, C.A., Heck, M.M., and Liu, L.F. (1985). Topoi somerase II is a structural component of mitotic chromosome scaffolds. J. Cell Biol. 100, 1706-1715.
88. Earnshaw, W.C., and Laemmli, U.K. (1983). Architecture of metaphase chromosomes and chromosome scaffolds. J. Cell Biol. 96, 84-93.
89. Elsasser, S., Gali, R.R., Schwickart, M., Larsen, C.N., Leggett, D.S., Muller, B., Feng, M.T., Tubing, F., Dittmar, G.A., and Finley, D. (2002). Proteasome subunit Rpn1 binds ubiquitin-like protein domains. Nat. Cell Biol. 4, 725-730.
90. Enoch, T., and Nurse, P. (1990). Mutation of fission yeast cell cycle control genes abol ishes dependence of mitosis on DNA replication. Cell 60, 665-673.
91. Enserink, J.M., and Kolodner, R.D. (2010). An overview of Cdk1-controlled targets and processes. Cell Div. 5, 11.
92. Fagarasanu, A., Mast, F.D., Knoblach, B., and Rachubinski, R.A. (2010). Molecular mechanisms of organelle inheritance: lessons from peroxisomes in yeast. Nat. Rev. Mol.Cell Biol. 11, 644-654.
93. Farmer, S., San-Segundo, P.A., and Aragon, L. (2011). The Smc5-Smc6 complex is re quired to remove chromosome junctions in meiosis. PLoS. One. 6,e20948.
94. Fay, A., Misulovin, Z., Li, J., Schaaf, C.A., Gause, M., Gilmour, D.S., and Dorsett, D. (2011). Cohesin selectively binds and regulates genes with paused RNA polymer ase. Curr. Biol. 21, 1624-1634.
95. Feng, W., Di Rienzi, S.C., Raghuraman, M.K., and Brewer, B.J. (2011a). Replication stress-induced chromosome breakage is correlated with replication

fork progression and is preceded by single-stranded DNA formation. G3. (Bethesda.) 1, 327-335.

96. Feng, Y., Gao, J., and Yang, M. (2011b). When MAGE meets RING: insights into biological functions of MAGE proteins. Protein Cell 2, 7-12.
97. Finn, K., Lowndes, N.F., and Grenon, M. (2012). Eukaryotic DNA damage checkpoint activation in response to double-strand breaks. Cell Mol. Life Sci. 69, 1447-1473.
98. Foley, E.A., and Kapoor, T.M. (2013). Microtubule attachment and spindle assembly checkpoint signalling at the kinetochore. Nat. Rev. Mol. Cell Biol. 14, 25-37.
99. Forsburg, S.L., and Nurse, P. (1991). Cell cycle regulation in the yeasts Saccharomyces cerevisiae and Schizosaccharomyces pombe. Annu. Rev. Cell Biol. 7, 227-256.
100. Fousteri, M.I., and Lehmann, A.R. (2000). A novel SMC protein complex in Schizosaccharomyces pombe contains the Rad18 DNA repair protein. EMBO J. 19, 1691-1702.
101. Freeman, L., Aragon-Alcaide, L., and Strunnikov, A. (2000). The condensin complex governs chromosome condensation and mitotic transmission of rDNA. J. Cell Biol. 149, 811-824.
102. Fujioka, Y., Kimata, Y., Nomaguchi, K., Watanabe, K., and Kohno, K. (2002). Identification of a novel non-structural maintenance of chromosomes (SMC) component of the SMC5-SMC6 complex involved in DNA repair. J. Biol. Chem. 277, 21585-21591.
103. Fussner, E., Ching, R.W., and Bazett-Jones, D.P. (2011). Living without 30nm chromatin fibers. Trends Biochem. Sci. 36, 1-6.
104. Fussner, E., Strauss, M., Djuric, U., Li, R., Ahmed, K., Hart, M., Ellis, J., and Bazett-Jones, D.P. (2012). Open and closed domains in the mouse genome are configured as 10-nm chromatin fibres. EMBO Rep. 13, 992-996.
105. Gallego, C., Gari, E., Colomina, N., Herrero, E., and Aldea, M. (1997). The Cln3 cyclin is down-regulated by translational repression and degradation during the G1 arrest caused by nitrogen deprivation in budding yeast. EMBO J. 16, 7196-7206.
106. Gallego-Paez, L.M., Tanaka, H., Bando, M., Takahashi, M., Nozaki, N., Nakato, R., Shirahige, K., and Hirota, T. (2014). Smc5/6-mediated regulation of replication progression contributes to chromosome assembly during mitosiin human cells. Mol. Biol. Cell 25, 302-317.
107. Gambus, A., Jones, R.C., Sanchez-Diaz, A., Kanemaki, M., van, D.F., Edmondson, R.D., and Labib, K. (2006). GINS maintains association of Cdc45 with MCM in replisome progression complexes at eukaryotic DNA replication forks. Nat. Cell Biol. 8, 358-366.
108. Gandhi, R., Gillespie, P.J., and Hirano, T. (2006). Human Wapl is a cohesin-binding protein that promotes sister-chromatid resolution in mitotic prophase. Curr. Biol. 16, 2406-2417.
109. Gao, C., Ho, C.C., Reineke, E., Lam, M., Cheng, X., Stanya, K.J., Liu, Y., Chakraborty, S., Shih, H.M., and Kao, H.Y. (2008). Histone deacetylase 7 promotes PML sumoylation and is essential for PML nuclear body formation. Mol. Cell Biol. 28, 5658-5667.
110. Gavin, K.A., Hidaka, M., and Stillman, B. (1995). Conserved initiator proteins in eukaryotes. Science 270, 1667-1671.

111. Geiss-Friedlander, R., and Melchior, F. (2007). Concepts in sumoylation: a decade on. Nat. Rev. Mol. Cell Biol. 8, 947-956.

112. Genois, M.M., Paquet, E.R., Laffitte, M.C., Maity, R., Rodrigue, A., Ouellette, M., and Masson, J.Y. (2014). DNA repair pathways in trypanosomaids: from DNA repair to drug resistance. Microbiol. Mol. Biol. Rev. 78, 40-73.

113. Gerlich, D., Koch, B., Dupeux, F., Peters, J.M., and Ellenberg, J. (2006). Live-cell imaging reveals a stable cohesin-chromatin interaction after but not before DNA replication Curr. Biol. 16, 1571-1578.

114. Gietz, R.D., and Sugino, A. (1988). New yeast-Escherichia coli shuttle vectors constructed with in vitro mutagenized yeast genes lacking six-base pair restriction sites. Gene 74, 527-534.

115. Gilbert, D.M. (2007). Replication origin plasticity, Taylor-made: inhibition vs recruitment of origins under conditions of replication stress. Chromosoma 116, 341-347.

116. Goffeau, A., Barrell, B.G., Bussey, H., Davis, R.W., Dujon, B., Feldmann, H., Galibert, F., Hoheisel, J.D., Jacq, C., Johnston, M., Louis, E.J., Mewes, H.W., Murakami, Y., Philippsen, P., Tettelin, H., and Oliver, S.G. (1996). Life with 6000 genes. Science 274, 546, 563-546, 567.

117. Gomez, R., Jordan, P.W., Viera, A., Alsheimer, M., Fukuda, T., Jessberger, R., Llano, E., Pendas, A.M., Handel, M.A., and Suja, J.A. (2013). Dynamic localization of SMC5/6 complex proteins during mammalian meiosis and mitosis suggests functions in distinct chromosome processes. J. Cell Sci. 126, 4239-4252.

118. Gong, L., Kamitani, T., Fujise, K., Caskey, L.S., and Yeh, E.T. (1997). Preferential interaction of sentrin with a ubiquitin-conjugating enzyme, Ubc9. J. Biol. Chem. 272, 28198-28201.

119. Gong, L., Li, B., Millas, S., and Yeh, E.T. (1999). Molecular cloning and characterization of human AOS1 and UBA2, components of the sentrin.activating enzyme complex. FEBS Lett. 448, 185-189.

120. Gordon, D.J., Resio, B., and Pellman, D. (2012). Causes and consequences of aneuploidy in cancer. Nat. Rev. Genet. 13, 189-203.

121. Goshima, G., and Yanagida, M. (2000). Establishing biorientation occurs with precocious separation of the sister kinetochores, but not the arms, in the early spindle of budding yeast. Cell 100, 619-633.

122. Grawunder, U., Wilm, M., Wu, X., Kulesza, P., Wilson, T.E., Mann, M., and Lieber, M.R. (1997). Activity of DNA ligase IV stimulated by complex formation with XRCC4 protein in mammalian cells. Nature 388, 492-495.

123. Gregoire, S., and Yang, X.J. (2005). Association with class IIa histone deacetylases upregulates the sumoylation of MEF2 transcription factors. Mol. Cell Biol. 25, 2273-2287.

124. Groth, A., Rocha, W., Verreault, A., and Almouzni, G. (2007). Chromatin challenges during DNA replication and repair. Cell 128, 721-733.

125. Groth, P., Auslander, S., Majumder, M.M., Schultz, N., Johansson, F., Petermann, E., and Helleday, T. (2010). Methylated DNA causes a physical block to replication forks independently of damage signalling, O(6)-methylguanine or DNA single-strand breaks and results in DNA damage. J. Mol. Biol. 402, 70-82.

126. Gruber, S., Arumugam, P., Katou, Y., Kuglitsch, D., Helmhart, W., Shirahige, K., and Nasmyth, K. (2006). Evidence that loading of cohesin onto

chromosomes involves opening of its SMC hinge. Cell 127, 523-537.

127. Guacci, V., Koshland, D., and Strunnikov, A. (1997). A direct link between sister chromatid cohesion and chromosome condensation revealed through the analysis of MCD1 in S. cerevisiae. Cell 91, 47-57.

128. Guerineau, M., Kriz, Z., Kozakova, L., Bednarova, K., Janos, P., and Palecek, J. (2012). Analysis of the Nse3/MAGE-binding domain of the Nse4/EID family proteins. PLoS. One. 7, e35813.

129. Guillou, E., Ibarra, A., Coulon, V., Casado-Vela, J., Rico, D., Casal, I., Schwob, E., Losada, A., and Mendez, J. (2010). Cohesin organizes chromatin loops at DNA replication factories. Genes Dev. 24, 2812-2822.

130. Guo, D., Li, M., Zhang, Y., Yang, P., Eckenrode, S., Hopkins, D., Zheng, W., Purohit, S., Podolsky, R.H., Muir, A., Wang, J., Dong, Z., Brusko, T., Atkinon, M., Pozzilli, P., Zeidler, A., Raffel, L.J., Jacob, C.O., Park, Y., Serrano-Rios, M., Larrad, M.T., Zhang, Z., Garchon, H.J., Bach, J.F., Rotter, J.I., She, .X., and Wang, C.Y. (2004). A functional variant of SUMO4, a new I kappa B alpha modifier, is associated with type 1 diabetes. Nat. Genet. 36, 837-841.

131. Haering, C.H., Lowe, J., Hochwagen, A., and Nasmyth, K. (2002). Molecular architecture of SMC proteins and the yeast cohesin complex. Mol. Cell 9, 773-788.

132. Hang, L.E., Liu, X., Cheung, I., Yang, Y., and Zhao, X. (2011). SUMOylation regulates telomere length homeostasis by targeting Cdc13. Nat. Struct. Mol. Biol. 18, 920-926.

133. Harley, C.B., Futcher, A.B., and Greider, C.W. (1990). Telomeres shorten during ageing of human fibroblasts. Nature 345, 458-460.

134. Hartlerode, A.J., and Scully, R. (2009). Mechanisms of double-strand break repair in somatic mammalian cells. Biochem. J. 423, 157-168.

135. Hartwell, L.H., Culotti, J., Pringle, J.R., and Reid, B.J. (1974). Genetic control of the cell division cycle in yeast. Science 183, 46-51.

136. Hartwell, L.H., and Weinert, T.A. (1989). Checkpoints: controls that ensure the order of cell cycle events. Science 246, 629-634.

137. Hazbun, T.R., Malmstrom, L., Anderson, S., Graczyk, B.J., Fox, B., Riffle, M., Sundin, B.A., Aranda, J.D., McDonald, W.H., Chiu, C.H., Snydsman, B.E., Bradley, P., Muller, E.G., Fields, S., Baker, D., Yates, J.R., III, and Davis, T.N. (2003). Assigning function to yeast proteins by integration of technologies. Mol. Cell 12, 1353-1365.

138. Heermann, D.W. (2012). Mitotic chromosome structure. Exp. Cell Res. 318, 1381-1385.

139. Hennessy, K.M., Lee, A., Chen, E., and Botstein, D. (1991). A group of interacting yeast DNA replication genes. Genes Dev. 5, 958-969.

140. Henson, J.D., Neumann, A.A., Yeager, T.R., and Reddel, R.R. (2002). Alternative lengthening of telomeres in mammalian cells. Oncogene 21, 598-610.

141. Hickey, C.M., Wilson, N.R., and Hochstrasser, M. (2012). Function and reguation of SUMO proteases. Nat. Rev. Mol. Cell Biol. 13, 755-766.

142. Hickson, I.D., and Mankouri, H.W. (2011). Processing of homologous recombination repair intermediates by the Sgs1-Top3-Rmi1 and Mus81-Mms4 complexes. Cell Cycle 10, 3078-3085.

143. Hirano, M., Anderson, D.E., Erickson, H.P., and Hirano, T. (2001). Bimodal

activation of SMC ATPase by intra- and inter-molecular interactions. EMBO J. 20, 3238-3250.

144. Hirano, M., and Hirano, T. (2002). Hinge-mediated dimerization of SMC protein is essential for its dynamic interaction with DNA. EMBO J. 21, 5733-5744.
145. Hirano, M., and Hirano, T. (2004). Positive and negative regulation of SMC-DNA interactions by ATP and accessory proteins. EMBO J. 23, 2664-2673.
146. Hirano, T. (2000). Chromosome cohesion, condensation, and separation. Annu. Rev. Biochem. 69, 115-144.
147. Hirano, T. (2005). Condensins: organizing and segregating the genome. Curr. Biol. 15, R265-R275.
148. Hirano, T. (2012). Condensins: universal organizers of chromosomes with diverse functions. Genes Dev. 26, 1659-1678.
149. Hirano, T., Funahashi, S., Uemura, T., and Yanagida, M. (1986). Isolation and characterization of Schizosaccharomyces pombe cutmutants that block nuclear division but not cytokinesis. EMBO J. 5, 2973-2979.
150. Hirano, T., Kobayashi, R., and Hirano, M. (1997). Condensins, chromosome condensation protein complexes containing XCAP-C, XCAP-E and a Xenopus homolog of the Drosophila Barren protein. Cell 89, 511-521.
151. Hirano, T., and Mitchison, T.J. (1994). A heterodimeric coiled-coil protein required for mitotic chromosome condensation in vitro. Cell 79, 449-458.
152. Hochstrasser, M. (2001). SP-RING for SUMO: new functions bloom for a ubiquitin-like protein. Cell 107, 5-8.
153. Hoege, C., Pfander, B., Moldovan, G.L., Pyrowolakis, G., and Jentsch, S. (2002). RAD6-dependent DNA repair is linked to modification of PCNA by ubiquitin and SUMO. Nature 419, 135-141.
154. Hoeijmakers, J.H. (2001). Genome maintenance mechanisms for preventing cancer. Nature 411, 366-374.
155. Hoffman, C.S. (2001). Preparation of yeast DNA. Curr. Protoc. Mol. Biol. Chapter 13, Unit13.
156. Holm, C., Goto, T., Wang, J.C., and Botstein, D. (1985). DNA topoisomerase II is required at the time of mitosis in yeast. Cell 41, 553-563.
157. Holm, C., Stearns, T., and Botstein, D. (1989). DNA topoisomerase II must act at mitosis to prevent nondisjunction and chromosome breakage. Mol. Cell Biol. 9, 159-168.
158. Hopfner, K.P., Karcher, A., Shin, D.S., Craig, L., Arthur, L.M., Carney, J.P., andTainer, J.A. (2000). Structural biology of Rad50 ATPase: ATP-driven conformational control in DNA double-strand break repair and the ABC-ATPase superfamily. Cell 101, 789-800.
159. Horsfield, J.A., Anagnostou, S.H., Hu, J.K., Cho, K.H., Geisler, R., Lieschke, G., Crosier, K.E., and Crosier, P.S. (2007). Cohesin-dependent regulation of Runx genes. Development 134, 2639-2649.
160. Hsieh, P., and Yamane, K. (2008). DNA mismatch repair: molecular mechanism, cancer, and ageing. Mech. Ageing Dev. 129, 391-407.
161. Hu, B., Itoh, T., Mishra, A., Katoh, Y., Chan, K.L., Upcher, W., Godlee, C., Roig, M.B., Shirahige, K., and Nasmyth, K. (2011). ATP hydrolysis is required for relocating cohesin from sites occupied by its Scc2/4 loading complex. Curr. Biol. 21, 12-24.

162. Hu, B., Liao, C., Millson, S.H., Mollapour, M., Prodromou, C., Pearl, L.H., Piper, P.W., and Panaretou, B. (2005). Qri2/Nse4, a component of the essential Smc5/6 DNA repair complex. Mol. Microbiol. 55, 1735-1750.
163. Huang, L., Yang, S., Zhang, S., Liu, M., Lai, J., Qi, Y., Shi, S., Wang, J., Wang, Y., Xie, Q., and Yang, C. (2009). The Arabidopsis SUMO E3 ligase AtMMS21, a homologue of NSE2/MMS21, regulates cell proliferation in the root. Plant J. 60, 666-678.
164. Hudson, J.J., Bednarova, K., Kozakova, L., Liao, C., Guerineau, M., Colnaghi, R., Vidot, S., Marek, J., Bathula, S.R., Lehmann, A.R., and Palecek, J. (2011). Interactions between the Nse3 and Nse4 components of the SMC5-6 complex identify evolutionarily conserved interactions between MAGE and EID Families. PLoS. One. 6, e17270.
165. Ilves, I., Petojevic, T., Pesavento, J.J., and Botchan, M.R. (2010). Activation of the MCM2-7 helicase by association with Cdc45 and GINS proteins. Mol. Cell 37, 247-258.
166. Irmisch, A., Ampatzidou, E., Mizuno, K., O'Connell, M.J., and Murray, J.M. (2009). Smc5/6 maintains stalled replication forks in a recombination-competent conformation. EMBO J. 28, 144-155.
167. Jackson, D.A., and Pombo, A. (1998). Replicon clusters are stable units of chromosome structure: evidence that nuclear organization contributes to the eficient activation and propagation of S phase in human cells. J. Cell Biol. 140, 1285-1295.
168. Jackson, S.P., and Durocher, D. (2013). Regulation of DNA damage responses by ubiquitin and SUMO. Mol. Cell 49, 795-807.
169. Jakobs, A., Koehnke, J., Himstedt, F., Funk, M., Korn, B., Gaestel, M., and Niedenthal, R. (2007). Ubc9 fusion-directed SUMOylation (UFDS): a method to analyze function of protein SUMOylation. Nat. Methods 4, 245-250.
170. Janke, C., Magiera, M.M., Rathfelder, N., Taxis, C., Reber, S., Maekawa, H., Moreno-Borchart, A., Doenges, G., Schwob, E., Schiebel, E., and Knop, M. (2004). A versatile toolbox for PCR-based tagging of yeast genes: new fluorescent proteins, more markers and promoter substitution cassettes. Yeast 21, 947-962.
171. Janssen, A., van der Burg, M., Szuhai, K., Kops, G.J., and Medema, R.H. (2011). Chromosome segregation errors as a cause of DNA damage and structural chromosome aberrations. Science 333, 1895-1898.
172. Jaspersen, S.L., and Winey, M. (2004). The budding yeast spindle pole body: structure, duplication, and function. Annu. Rev. Cell Dev. Biol. 20, 1-28.
173. Johnson, E.S., and Blobel, G. (1997). Ubc9p is the conjugating enzyme for the ubiquitin-like protein Smt3p. J. Biol. Chem. 272, 26799-26802.
174. Johnson, E.S., and Blobel, G. (1999). Cell cycle-regulated attachment of the ubiquitin-related protein SUMO to the yeast septins. J. Cell Biol. 147, 981-994.
175. Johnson, E.S., and Gupta, A.A. (2001). An E3-like factor that promotes SUMO conjugation to the yeast septins. Cell 106, 735-744.
176. Jossen, R., and Bermejo, R. (2013). The DNA damage checkpoint response to replication stress: A Game of Forks. Front Genet. 4, 26.
177. Kagey, M.H., Melhuish, T.A., and Wotton, D. (2003). The polycomb protein Pc2 is a SUMO E3. Cell 113, 127-137.
178. Kahyo, T., Nishida, T., and Yasuda, H. (2001). Involvement of PIAS1 in the sumoylation of tumor suppressor p53. Mol. Cell 8, 713-718.

179. Kearsey, S.E., and Cotterill, S. (2003). Enigmatic variations: divergent modes of regulating eukaryotic DNA replication. Mol. Cell 12, 1067-1075.
180. Kegel, A., Betts-Lindroos, H., Kanno, T., Jeppsson, K., Strom, L., Katou, Y., Itoh, T., Shirahige, K., and Sjogren, C. (2011). Chromosome length influences replication-induced topological stress. Nature 471, 392-396.
181. Kegel, A., and Sjogren, C. (2010). The Smc5/6 complex: more than repair? Cold Spring Harb. Symp. Quant. Biol. 75, 179-187.
182. Kerscher, O. (2007). SUMO junction-what's your function? New insights through SUMO-interacting motifs. EMBO Rep. 8, 550-555.
183. Kerscher, O., Felberbaum, R., and Hochstrasser, M. (2006). Modification of proteins by ubiquitin and ubiquitin-like proteins. Annu. Rev. Cell Dev. Biol. 22, 159-180.
184. Kim, K.P., Weiner, B.M., Zhang, L., Jordan, A., Dekker, J., and Kleckner, N. (2010). Sister cohesion and structural axis components mediate homolog bias of meiotic recombination. Cell 143, 924-937.
185. Kimura, K., Hirano, M., Kobayashi, R., and Hirano, T. (1998). Phosphorylation and activation of 13S condensin by Cdc2 in vitro. Science 282, 487-490.
186. Kinoshita, E., van der Linden, E., Sanchez, H., and Wyman, C. (2009). RAD50, an SMC family member with multiple roles in DNA break repair: how does ATP affect function? Chromosome. Res. 17, 277-288.
187. Kitagawa, R., Bakkenist, C.J., McKinnon, P.J., and Kastan, M.B. (2004). Phosphorylation of SMC1 is a critical downstream event in the ATM-NBS1-BRCA1 pathway. Genes Dev. 18, 1423-1438.
188. Kitajima, T.S., Sakuno, T., Ishiguro, K., Iemura, S., Natsume, T., Kawashima, S.A., and Watanabe, Y. (2006). Shugoshin collaborates with protein phosphatase 2A to protect cohesin. Nature 441, 46-52.
189. Knop, M., Siegers, K., Pereira, G., Zachariae, W., Winsor, B., Nasmyth, K., and Schiebel, E. (1999). Epitope tagging of yeast genes using a PCR-based strategy: more tags and improved practical routines. Yeast 15, 963-972.
190. Kobayashi, T., Heck, D.J., Nomura, M., and Horiuchi, T. (1998). Expansion and contraction of ribosomal DNA repeats in Saccharomyces cerevisiae: requirement replication fork blocking (Fob1) protein and the role of RNA polymerase I. Genes Dev. 12, 3821-3830.
191. Kolodner, R.D., Putnam, C.D., and Myung, K. (2002). Maintenance of genome stability in Saccharomyces cerevisiae. Science 297, 552-557.
192. Kotaja, N., Karvonen, U., Janne, O.A., and Palvimo, J.J. (2002). PIAS proteins modulate transcription factors by functioning as SUMO-1 ligases. Mol. Cell Biol. 22, 5222-5234.
193. Krejci, L., Van, K.S., Li, Y., Villemain, J., Reddy, M.S., Klein, H., Ellenberger, T., and Sung, P. (2003). DNA helicase Srs2 disrupts the Rad51 presynaptic filament. Nature 423, 305-309.
194. Krude, T., Jackman, M., Pines, J., and Laskey, R.A. (1997). Cyclin/Cdk-dependent initiation of DNA replication in a human cell-free system. Cell 88, 109-119.
195. Kushnirov, V.V. (2000). Rapid and reliable protein extraction from yeast. Yeast 16, 857-860.
196. Labib, K., and de, P.G. (2011). Surviving chromosome replication: the many roles of the S-phase checkpoint pathway. Philos. Trans. R. Soc. Lond B Biol. Sci. 366, 3554-

3561.

197. Labib, K., Tercero, J.A., and Diffley, J.F. (2000). Uninterrupted MCM2-7 function required for DNA replication fork progression. Science 288, 1643-1647.

198. Lander, E.S., Linton, L.M., Birren, B., Nusbaum, C., Zody, M.C., Baldwin, J., Devon, K., Dewar, K., Doyle, M., FitzHugh, W., Funke, R., Gage, D., Harris, K., Heaford, A., Howland, J., Kann, L., Lehoczky, J., LeVine, R., McEwan, P., McKernan, K., Meldrim, J., Mesirov, J.P., Miranda, C., Morris, W., Naylor, J., Raymond, C., Rosetti, M., Santos, R., Sheridan, A., Sougnez, C., Stange-Thomann, N., Stojanovic, N., Subramanian, A., Wyman, D., Rogers, J., Sulston, J., Ainscough, R., Beck, S., Bentley, D., Burton, J., Clee, C., Carter, N., Coulson, A., Deadman, R., Deloukas, P., Dunham, A., Dunham, I., Durbin, R., French, L., Grafham, D., Gregory, S., Hubbard, T., Humphray, S., Hunt, A., Jones, M., Lloyd, C., McMurray, A., Matthews, L., Mercer, S., Milne, S., Mullikin, J.C., Mungall, A., Plumb, R., Ross, M., Shownkeen, R., Sims, S., Waterston, R.H., Wilson, R.K., Hillier, L.W., McPherson, J.D., Marra, M.A., Mardis, E.R., Fulton, L.A., Chinwalla, A.T., Pepin, K.H., Gish, W.R., Chissoe, S.L., Wendl, M.C., Delehaunty, K.D., Miner, T.L., Delehaunty, A., Kramer, J.B., Cook, L.L., Fulton, R.S., Johnson, D.L., Minx, P.J., Clifton, S.W., Hawkins, T., Branscomb, E., Predki, P., Richardson, P., Wenning, S., Slezak, T., Doggett, N., Cheng, J.F., Olsen, A., Lucas, S., Elkin, C., Uberbacher, E., Frazier, M., Gibbs, R.A., Muzny, D.M., Scherer, S.E., Bouck, J.B., Sodergren, E.J., Worley, K.C., Rives, C.M., Gorrell, J.H., Metzker, M.L., Naylor, S.L., Kucherlapati, R.S., Nelson, D.L., Weinstock, G.M., Sakaki, Y., Fujiyama, A., Hattori, M., Yada, T., Toyoda, A., Itoh, T., Kawagoe, C., Watanabe, H., Totoki, Y., Taylor, T., Weissenbach, J., Heilig, R., Saurin, W., Artiguenave, F., Brottier, P., Bruls, T., Pelletier, E., Robert, C., Wincker, P., Smith, D.R., Doucette-Stamm, L., Rubenfield, M., Weinstock, K., Lee, H.M., Dubois, J., Rosenthal, A., Platzer, M., Nyakatura, G., Taudien, S., Rump, A., Yang, H., Yu, J., Wang, J., Huang, G., Gu, J., Hood, L., Rowen, L., Madan, A., Qin, S., Davis, R.W., Federspiel, N.A., Abola, A.P., Proctor, M.J., Myers, R.M., Schmutz, J., Dickson, M., Grimwood, J., Cox, D.R., Olson, M.V., Kaul, R., Raymond, C., Shimizu, N., Kawasaki, K., Minoshima, S., Evans, G.A., Athanasiou, M., Schultz, R., Roe, B.A., Chen, F., Pan, H., Ramser, J., Lehrach, H., Reinhardt, R., McCombie, W.R., de la Bastide, M., Dedhia, N., Blocker, H., Hornischer, K., Nordsiek, G., Agarwala, R., Aravind, L., Bailey, J.A., Bateman, A., Batzoglou, S., Birney, E., Bork, P., Brown, D.G., Burge, C.B., Cerutti, L., Chen, H.C., Church, D., Clamp, M., Copley, R.R., Doerks, T., Eddy, S.R., Eichler, E.E., Furey, T.S., Galagan, J., Gilbert, J.G., Harmon, C., Hayashizaki, Y., Haussler, D., Hermjakob, H., Hokamp, K., Jang, W., Johnson, L.S., Jones, T.A., Kasif, S., Kaspryzk, A., Kennedy, S., Kent, W.J., Kitts, P., Koonin, E.V., Korf, I., Kulp, D., Lancet, D., Lowe, T.M., McLysaght, A., Mikkelsen, T., Moran, J.V., Mulder, N., Pollara, V.J., Ponting, C.P., Schuler, G., Schultz, J., Slater, G., Smit, A.F., Stupka, E., Szustakowski, J., Thierry-Mieg, D., Thierry-Mieg, J., Wagner, L., Wallis, J., Wheeler, R., Williams, A., Wolf, Y.I., Wolfe, K.H., Yang, S.P., Yeh, R.F., Collins, F., Guyer, M.S., Peterson, J., Felsenfeld, A., Wetterstrand, K.A., Patrinos, A., Morgan, M.J., de, J.P., Catanese, J.J., Osoegawa, K., Shizuya, H., Choi, S., and Chen, Y.J. (2001). Initial sequencing and analysis of the human genome. Nature 409, 860-921.

199. Lavoie, B.D., Hogan, E., and Koshland, D. (2002). In vivo dissection of the chro mosome condensation machinery: reversibility of condensation distinguishes con tributions of condensin and cohesin. J. Cell Biol. 156, 805-815.

200. Lee, G.W., Melchior, F., Matunis, M.J., Mahajan, R., Tian, Q., and Anderson, P. (1998). Modification of Ran GTPase-activating protein by the small ubiquitin-related

modifier SUMO-1 requires Ubc9, an E2-type ubiquitin-conjugating enzyme homologue. J. Biol. Chem. 273, 6503-6507.

201. Lehmann, A.R. (2005). The role of SMC proteins in the responses to DNA damage. DNA Repair (Amst) 4, 309-314.

202. Lehmann, A.R., Walicka, M., Griffiths, D.J., Murray, J.M., Watts, F.Z., McCready, S., and Carr, A.M. (1995). The rad18 gene of Schizosaccharomyces pombe defines a new subgroup of the SMC superfamily involved in DNA repair. Mol. Cell Biol. 15, 7067-7080.

203. Lei, M., Kawasaki, Y., Young, M.R., Kihara, M., Sugino, A., and Tye, B.K. (1997). Mcm2 is a target of regulation by Cdc7-Dbf4 during the initiation of DNA synthesis. Genes Dev. 11, 3365-3374.

204. Lengronne, A., Katou, Y., Mori, S., Yokobayashi, S., Kelly, G.P., Itoh, T., Watanabe, Y., Shirahige, K., and Uhlmann, F. (2004). Cohesin relocation from sites of chromosomal loading to places of convergent transcription. Nature 430, 573-578.

205. Lengronne, A., Pasero, P., Bensimon, A., and Schwob, E. (2001). Monitoring S phase progression globally and locally using BrdU incorporation in TK(+) yeast strains. Nucleic Acids Res. 29, 1433-1442.

206. Leung, G.P., Lee, L., Schmidt, T.I., Shirahige, K., and Kobor, M.S. (2011). Rtt107 is required for recruitment of the SMC5/6 complex to DNA double strand breaks. J. Biol. Chem. 286, 26250-26257.

207. Lewis, C.D., and Laemmli, U.K. (1982). Higher order metaphase chromosome structure: evidence for metalloprotein interactions. Cell 29, 171-181.

208. Li, S.J., and Hochstrasser, M. (1999). A new protease required for cell-cycle progression in yeast. Nature 398, 246-251.

209. Li, S.J., and Hochstrasser, M. (2000). The yeast ULP2 (SMT4) gene encodes a novel protease specific for the ubiquitin-like Smt3 protein. Mol. Cell Biol. 20, 2367-2377.

210. Li, X., and Heyer, W.D. (2008). Homologous recombination in DNA repair and DNA damage tolerance. Cell Res. 18, 99-113.

211. Liang, C., and Stillman, B. (1997). Persistent initiation of DNA replication and chromatin-bound MCM proteins during the cell cycle in cdc6 mutants. Genes Dev. 11, 3375-3386.

212. Liberi, G., Maffioletti, G., Lucca, C., Chiolo, I., Baryshnikova, A., Cotta-Ramusino, C., Lopes, M., Pellicioli, A., Haber, J.E., and Foiani, M. (2005). Rad51-dependent DNA structures accumulate at damaged replication forks in sgs1 mutants defective in the yeast ortholog of BLM RecQ helicase. Genes Dev. 19, 339-350.

213. Lilienthal, I., Kanno, T., and Sjogren, C. (2013). Inhibition of the Smc5/6 complex during meiosis perturbs joint molecule formation and resolution without significantly changing crossover or non-crossover levels. PLoS. Genet. 9, e1003898.

214. Lin, D., Tatham, M.H., Yu, B., Kim, S., Hay, R.T., and Chen, Y. (2002). Identification of a substrate recognition site on Ubc9. J. Biol. Chem. 277, 21740-21748.

215. Lin, W., Jin, H., Liu, X., Hampton, K., and Yu, H.G. (2011). Scc2 regulates gene expression by recruiting cohesin to the chromosome as a transcriptional activator during yeast meiosis. Mol. Biol. Cell 22, 1985-1996.

216. Lindahl, T. (1993). Instability and decay of the primary structure of DNA. Nature 362, 709-715.

217. Lindroos, H.B., Strom, L., Itoh, T., Katou, Y., Shirahige, K., and Sjogren, C. (2006).

Chromosomal association of the Smc5/6 complex reveals that it functions in differently regulated pathways. Mol. Cell 22, 755-767.

218. Lombard, D.B., Chua, K.F., Mostoslavsky, R., Franco, S., Gostissa, M., and Alt, F.W. (2005). DNA repair, genome stability, and aging. Cell 120, 497-512.

219. Longhese, M.P., Clerici, M., and Lucchini, G. (2003). The S-phase checkpoint and its regulation in Saccharomyces cerevisiae. Mutat. Res. 532, 41-58.

220. Lopes, M., Cotta-Ramusino, C., Pellicioli, A., Liberi, G., Plevani, P., Muzi-Falconi, M., Newlon, C.S., and Foiani, M. (2001). The DNA replication checkpoint response stabilizes stalled replication forks. Nature 412, 557-561.

221. Losada, A., and Hirano, T. (2005). Dynamic molecular linkers of the genome: the first decade of SMC proteins. Genes Dev. 19, 1269-1287.

222. Lucas, I., Germe, T., Chevrier-Miller, M., and Hyrien, O. (2001). Topoisomerase II can unlink replicating DNA by precatenane removal. EMBO J. 20, 6509-6519.

223. Luger, K., Mader, A.W., Richmond, R.K., Sargent, D.F., and Richmond, T.J. (1997). Crystal structure of the nucleosome core particle at 2.8 A resolution. Nature 389, 251-260.

224. Luo, H., Li, Y., Mu, J.J., Zhang, J., Tonaka, T., Hamamori, Y., Jung, S.Y., Wang, Y., and Qin, J. (2008). Regulation of intra-S phase checkpoint by ionizing radiation (IR)-dependent and IR-independent phosphorylation of SMC3. J. Biol. Chem. 283, 19176-19183.

225. Malkova, A., Ivanov, E.L., and Haber, J.E. (1996). Double-strand break repair in the absence of RAD51 in yeast: a possible role for break-induced DNA replication. Proc. Natl. Acad. Sci. U. S. A 93, 7131-7136.

226. Mallory, J.C., and Petes, T.D. (2000). Protein kinase activity of Tel1p and Mec1p, two Saccharomyces cerevisiae proteins related to the human ATM protein kinase. Proc. Natl. Acad. Sci. U. S. A 97, 13749-13754.

227. Mankouri, H.W., and Hickson, I.D. (2007). The RecQ helicase-topoisomerase III-Rmi1 complex: a DNA structure-specific 'dissolvasome'? Trends Biochem. Sci. 32, 538-546.

228. Mankouri, H.W., Ngo, H.P., and Hickson, I.D. (2009). Esc2 and Sgs1 act in function ally distinct branches of the homologous recombination repair pathway in Saccha romyces cerevisiae. Mol. Biol. Cell 20, 1683-1694.

229. Martin-Parras, L., Lucas, I., Martinez-Robles, M.L., Hernandez, P., Krimer, D.B., Hy rien, O., and Schvartzman, J.B. (1998). Topological complexity of different popu lations of pBR322 as visualized by two-dimensional agarose gel electrophoresis. Nucleic Acids Res. 26, 3424-3432.

230. Martinez-Robles, M.L., Witz, G., Hernandez, P., Schvartzman, J.B., Stasiak, A., and Krimer, D.B. (2009). Interplay of DNA supercoiling and catenation during the segregation of sister duplexes. Nucleic Acids Res. 37, 5126-5137.

231. Matic, I., Schimmel, J., Hendriks, I.A., van Santen, M.A., van de Rijke, F., van, D.H., Gnad, F., Mann, M., and Vertegaal, A.C. (2010). Site-specific identification of SUMO-2 targets in cells reveals an inverted SUMOylation motif and a hydropho bic cluster SUMOylation motif. Mol. Cell 39, 641-652.

232. Matic, I., van, H.M., Schimmel, J., Macek, B., Ogg, S.C., Tatham, M.H., Hay, R.T., La mond, A.I., Mann, M., and Vertegaal, A.C. (2008). In vivo identification of human small ubiquitin-like modifier polymerization sites by high accuracy

mass spectrometry and an in vitro to in vivo strategy. Mol. Cell Proteomics. 7, 132-144.

233. Matos, J., Blanco, M.G., and West, S.C. (2013). Cell-cycle kinases coordinate the reso lution of recombination intermediates with chromosome segregation. Cell Rep. 4, 76-86.

234. Matos, J., and West, S.C. (2014). Holliday junction resolution: regulation in space and time. DNA Repair (Amst) 19, 176-181.

235. Mazon, G., Mimitou, E.P., and Symington, L.S. (2010). SnapShot: Homologous re combination in DNA double-strand break repair. Cell 142, 646, 646.

236. Mc, I.J., Muller, E.G., Weitzer, S., Snydsman, B.E., Davis, T.N., and Uhlmann, F. (2007). In vivo analysis of cohesin architecture using FRET in the budding yeast Saccharomyces cerevisiae. EMBO J. 26, 3783-3793.

237. McAleenan, A., Cordon-Preciado, V., Clemente-Blanco, A., Liu, I.C., Sen, N., Leonard, J., Jarmuz, A., and Aragon, L. (2012). SUMOylation of the alpha-kleisin subunit of cohesin is required for DNA damage-induced cohesion. Curr. Biol. 22, 1564-1575.

238. McClendon, A.K., Rodriguez, A.C., and Osheroff, N. (2005). Human topoisomerase Ialpha rapidly relaxes positively supercoiled DNA: implications for enzyme action ahead of replication forks. J. Biol. Chem. 280, 39337-39345.

239. McDonald, W.H., Pavlova, Y., Yates, J.R., III, and Boddy, M.N. (2003). Novel essential DNA repair proteins Nse1 and Nse2 are subunits of the fission yeast Smc5-Smc6 complex. J. Biol. Chem. 278, 45460-45467.

240. McDowell, G.S., Kucerova, R., and Philpott, A. (2010). Non-canonical ubiquitylation of the proneural protein Ngn2 occurs in both Xenopus embryos and mammalian cells. Biochem. Biophys. Res. Commun. 400, 655-660.

241. Melby, T.E., Ciampaglio, C.N., Briscoe, G., and Erickson, H.P. (1998). The symmetri cal structure of structural maintenance of chromosomes (SMC) and MukB proteins: long, antiparallel coiled coils, folded at a flexible hinge. J. Cell Biol. 142, 1595-1604.

242. Melchior, F. (2000). SUMO--nonclassical ubiquitin. Annu. Rev. Cell Dev. Biol. 16, 5 91-626.

243. Mendez, J., and Stillman, B. (2003). Perpetuating the double helix: molecular ma chines at eukaryotic DNA replication origins. Bioessays 25, 1158-1167.

244. Michaelis, C., Ciosk, R., and Nasmyth, K. (1997). Cohesins: chromosomal proteins that prevent premature separation of sister chromatids. Cell 91, 35-45.

245. Mimitou, E.P., and Symington, L.S. (2008). Sae2, Exo1 and Sgs1 collaborate in DNA double-strand break processing. Nature 455, 770-774.

246. Mimura, S., and Takisawa, H. (1998). Xenopus Cdc45-dependent loading of DNA polymerase alpha onto chromatin under the control of S-phase Cdk. EMBO J. 17, 5699-5707.

247. Miyabe, I., Morishita, T., Hishida, T., Yonei, S., and Shinagawa, H. (2006). Rhp51-dependent recombination intermediates that do not generate checkpoint signal are accumulated in Schizosaccharomyces pombe rad60 and smc5/6 mutants after release from replication arrest. Mol. Cell Biol. 26, 343-353.

248. Miyazaki, T., Tsai, H.F., and Bennett, J.E. (2006). Kre29p is a novel nuclear protein i nvolved in DNA repair and mitotic fidelity in Candida glabrata. Curr. Genet. 50,

11-22.

249. Mohideen, F., Capili, A.D., Bilimoria, P.M., Yamada, T., Bonni, A., and Lima, C.D. (2009). A molecular basis for phosphorylation-dependent SUMO conjugation by the E2 UBC9. Nat. Struct. Mol. Biol. 16, 945-952.

250. Mol, C.D., Parikh, S.S., Putnam, C.D., Lo, T.P., and Tainer, J.A. (1999). DNA repair mechanisms for the recognition and removal of damaged DNA bases. Annu. Rev. Biophys. Biomol. Struct. 28, 101-128.

251. Monnat, R.J., Jr. (2010). Human RECQ helicases: roles in DNA metabolism, mutagenesis and cancer biology. Semin. Cancer Biol. 20, 329-339.

252. Morgan, D.O. (1999). Regulation of the APC and the exit from mitosis. Nat. Cell Biol. 1, E47-E53.

253. Morikawa, H., Morishita, T., Kawane, S., Iwasaki, H., Carr, A.M., and Shinagawa, H. (2004). Rad62 protein functionally and physically associates with the smc5/smc6 protein complex and is required for chromosome integrity and recombination repair in fission yeast. Mol. Cell Biol. 24, 9401-9413.

254. Morin, I., Ngo, H.P., Greenall, A., Zubko, M.K., Morrice, N., and Lydall, D. (2008). Checkpoint-dependent phosphorylation of Exo1 modulates the DNA damage response. EMBO J. 27, 2400-2410.

255. Morita, Y., Kanei-Ishii, C., Nomura, T., and Ishii, S. (2005). TRAF7 sequesters c-Myb to the cytoplasm by stimulating its sumoylation. Mol. Biol. Cell 16, 5433-5444.

256. Mukhopadhyay, D., and Dasso, M. (2007). Modification in reverse: the SUMO proteases. Trends Biochem. Sci. 32, 286-295.

257. Mullen, J.R., and Brill, S.J. (2008). Activation of the Slx5-Slx8 ubiquitin ligase by poly-small ubiquitin-like modifier conjugates. J. Biol. Chem. 283, 19912-19921.

258. Naim, V., and Rosselli, F. (2009). The FANC pathway and BLM collaborate during mitosis to prevent micro-nucleation and chromosome abnormalities. Nat. Cell Biol. 11, 761-768.

259. Nasim, A., and Smith, B.P. (1975). Genetic control of radiation sensitivity in Schizosaccharomyces pombe. Genetics 79, 573-582.

260. Nasmyth, K., and Haering, C.H. (2005). The structure and function of SMC and kleisin complexes. Annu. Rev. Biochem. 74, 595-648.

261. Nedelcheva-Veleva, M.N., Krastev, D.B., and Stoynov, S.S. (2006). Coordination of DNA synthesis and replicative unwinding by the S-phase checkpoint pathways. Nucleic Acids Res. 34, 4138-4146.

262. Nelson, J.D., Denisenko, O., and Bomsztyk, K. (2006). Protocol for the fast chromatin immunoprecipitation (ChIP) method. Nat. Protoc. 1, 179-185.

263. Nick McElhinny, S.A., Kumar, D., Clark, A.B., Watt, D.L., Watts, B.E., Lundstrom, E.B., Johansson, E., Chabes, A., and Kunkel, T.A. (2010). Genome instability due to ribonucleotide incorporation into DNA. Nat. Chem. Biol. 6, 774-781.

264. Nishida, T., and Yasuda, H. (2002). PIAS1 and PIASxalpha function as SUMO-E3 ligases toward androgen receptor and repress androgen receptor-dependent transcription. J. Biol. Chem. 277, 41311-41317.

265. Nishimura, K., Fukagawa, T., Takisawa, H., Kakimoto, T., and Kanemaki, M. (2009). An auxin-based degron system for the rapid depletion of proteins in nonplant cells. Nat. Methods 6, 917-922.

266. Nishiyama, T., Ladurner, R., Schmitz, J., Kreidl, E., Schleiffer, A., Bhaskara, V., Bando,

M., Shirahige, K., Hyman, A.A., Mechtler, K., and Peters, J.M. (2010). Sororin mediates sister chromatid cohesion by antagonizing Wapl. Cell 143, 737-749.

267. Noel, J.F., and Wellinger, R.J. (2011). Abrupt telomere losses and reduced end-resection can explain accelerated senescence of Smc5/6 mutants lacking telomerase. DNA Repair (Amst) 10, 271-282.
268. O'Neill, B.M., Szyjka, S.J., Lis, E.T., Bailey, A.O., Yates, J.R., III, Aparicio, O.M., and Romesberg, F.E. (2007). Pph3-Psy2 is a phosphatase complex required for Rad53 dephosphorylation and replication fork restart during recovery from DNA damage. Proc. Natl. Acad. Sci. U. S. A 104, 9290-9295.
269. Ohya, T., Arai, H., Kubota, Y., Shinagawa, H., and Hishida, T. (2008). A SUMO-like domain protein, Esc2, is required for genome integrity and sister chromatid cohesion in Saccharomyces cerevisiae. Genetics 180, 41-50.
270. Ono, T., Fang, Y., Spector, D.L., and Hirano, T. (2004). Spatial and temporal regulation of Condensins I and II in mitotic chromosome assembly in human cells. Mol. Biol. Cell 15, 3296-3308.
271. Ono, T., Losada, A., Hirano, M., Myers, M.P., Neuwald, A.F., and Hirano, T. (2003). Differential contributions of condensin I and condensin II to mitotic chromosome architecture in vertebrate cells. Cell 115, 109-121.
272. Onoda, F., Takeda, M., Seki, M., Maeda, D., Tajima, J., Ui, A., Yagi, H., and Enomoto, T. (2004). SMC6 is required for MMS-induced interchromosomal and sister chromatid recombinations in Saccharomyces cerevisiae. DNA Repair (Amst) 3, 429-439.
273. Osborn, A.J., Elledge, S.J., and Zou, L. (2002). Checking on the fork: the DNA-replication stress-response pathway. Trends Cell Biol. 12, 509-516.
274. Outwin, E.A., Irmisch, A., Murray, J.M., and O'Connell, M.J. (2009). Smc5-Smc6-dependent removal of cohesin from mitotic chromosomes. Mol. Cell Biol. 29, 4363-4375.
275. Owerbach, D., McKay, E.M., Yeh, E.T., Gabbay, K.H., and Bohren, K.M. (2005). A proline-90 residue unique to SUMO-4 prevents maturation and sumoylation. Biochem. Biophys. Res. Commun. 337, 517-520.
276. Pacek, M., and Walter, J.C. (2004). A requirement for MCM7 and Cdc45 in chromosome unwinding during eukaryotic DNA replication. EMBO J. 23, 3667-3676.
277. Painter, R.B. (1977). Inhibition of initiation of HeLa cell replicons by methyl methanesulfonate. Mutat. Res. 42, 299-303.
278. Palecek, J., Vidot, S., Feng, M., Doherty, A.J., and Lehmann, A.R. (2006). The Smc5-Smc6 DNA repair complex. bridging of the Smc5-Smc6 heads by the KLEISIN, Nse4, and non-Kleisin subunits. J. Biol. Chem. 281, 36952-36959.
279. Papouli, E., Chen, S., Davies, A.A., Huttner, D., Krejci, L., Sung, P., and Ulrich, H.D. (2005). Crosstalk between SUMO and ubiquitin on PCNA is mediated by recruitment of the helicase Srs2p. Mol. Cell 19, 123-133.
280. Paques, F., and Haber, J.E. (1999). Multiple pathways of recombination induced by double-strand breaks in Saccharomyces cerevisiae. Microbiol. Mol. Biol. Rev. 63, 349-404.
281. Parker, J.L., Bucceri, A., Davies, A.A., Heidrich, K., Windecker, H., and Ulrich, H.D. (2008). SUMO modification of PCNA is controlled by DNA. EMBO J. 27, 2422-2431.

282. Pauli, A., Althoff, F., Oliveira, R.A., Heidmann, S., Schuldiner, O., Lehner, C.F., Dick son, B.J., and Nasmyth, K. (2008). Cell-type-specific TEV protease cleavage reveals cohesin functions in Drosophila neurons. Dev. Cell 14, 239-251.
283. Pebernard, S., McDonald, W.H., Pavlova, Y., Yates, J.R., III, and Boddy, M.N. (2004). Nse1, Nse2, and a novel subunit of the Smc5-Smc6 complex, Nse3, play a crucial role in meiosis. Mol. Biol. Cell 15, 4866-4876.
284. Pebernard, S., Perry, J.J., Tainer, J.A., and Boddy, M.N. (2008a). Nse1 RING-like domain supports functions of the Smc5-Smc6 holocomplex in genome stability. Mol. Biol. Cell 19, 4099-4109.
285. Pebernard, S., Schaffer, L., Campbell, D., Head, S.R., and Boddy, M.N. (2008b). Lo calization of Smc5/6 to centromeres and telomeres requires heterochromatin and SUMO, respectively. EMBO J. 27, 3011-3023.
286. Pebernard, S., Wohlschlegel, J., McDonald, W.H., Yates, J.R., III, and Boddy, M.N. (2006). The Nse5-Nse6 dimer mediates DNA repair roles of the Smc5-Smc6 complex. Mol. Cell Biol. 26, 1617-1630.
287. Perry, J.J., Tainer, J.A., and Boddy, M.N. (2008). A SIM-ultaneous role for SUMO and ubiquitin. Trends Biochem. Sci. 33, 201-208.
288. Peter, B.J., Ullsperger, C., Hiasa, H., Marians, K.J., and Cozzarelli, N.R. (1998). The structure of supercoiled intermediates in DNA replication. Cell 94, 819-827.
289. Petes, T.D. (1979). Yeast ribosomal DNA genes are located on chromosome XII. Proc. Natl. Acad. Sci. U. S. A 76, 410-414.
290. Pfander, B., Moldovan, G.L., Sacher, M., Hoege, C., and Jentsch, S. (2005). SUMO-modified PCNA recruits Srs2 to prevent recombination during S phase. Nature 436, 428-433.
291. Pichler, A., Gast, A., Seeler, J.S., Dejean, A., and Melchior, F. (2002). The nucleoporin RanBP2 has SUMO1 E3 ligase activity. Cell 108, 109-120.
292. Pichler, A., Knipscheer, P., Oberhofer, E., van Dijk, W.J., Korner, R., Olsen, J.V., Jentsch, S., Melchior, F., and Sixma, T.K. (2005). SUMO modification of the ubiquitin-conjugating enzyme E2-25K. Nat. Struct. Mol. Biol. 12, 264-269.
293. Postow, L., Crisona, N.J., Peter, B.J., Hardy, C.D., and Cozzarelli, N.R. (2001). Topological challenges to DNA replication: conformations at the fork. Proc. Natl. Acad. Sci. U. S. A 98, 8219-8226.
294. Potts, P.R. (2009). The Yin and Yang of the MMS21-SMC5/6 SUMO ligase complex in homologous recombination. DNA Repair (Amst) 8, 499-506.
295. Potts, P.R., Porteus, M.H., and Yu, H. (2006). Human SMC5/6 complex promotes sister chromatid homologous recombination by recruiting the SMC1/3 cohesin complex to double-strand breaks. EMBO J. 25, 3377-3388.
296. Potts, P.R., and Yu, H. (2005). Human MMS21/NSE2 is a SUMO ligase required for DNA repair. Mol. Cell Biol. 25, 7021-7032.
297. Potts, P.R., and Yu, H. (2007). The SMC5/6 complex maintains telomere length in ALT cancer cells through SUMOylation of telomere-binding proteins. Nat. Struct. Mol. Biol. 14, 581-590.
298. Prakash, L., and Prakash, S. (1977a). Isolation and characterization of MMS-sensitive mutants of Saccharomyces cerevisiae. Genetics 86, 33-55.
299. Prakash, S., and Prakash, L. (1977b). Increased spontaneous mitotic segregation in MMS-sensitive mutants of Saccharomyces cerevisiae. Genetics 87, 229-236.

300. Prakash, S., and Prakash, L. (2000). Nucleotide excision repair in yeast. Mutat. Res. 451, 13-24.
301. Prudden, J., Perry, J.J., Nie, M., Vashisht, A.A., Arvai, A.S., Hitomi, C., Guenther, G., Wohlschlegel, J.A., Tainer, J.A., and Boddy, M.N. (2011). DNA repair and global sumoylation are regulated by distinct Ubc9 noncovalent complexes. Mol. Cell Biol. 31, 2299-2310.
302. Pruyne, D., and Bretscher, A. (2000). Polarization of cell growth in yeast. J. Cell Sci. 113 (Pt 4), 571-585.
303. Pruyne, D., Legesse-Miller, A., Gao, L., Dong, Y., and Bretscher, A. (2004). Mechanisms of polarized growth and organelle segregation in yeast. Annu. Rev. Cell Dev. Biol. 20, 559-591.
304. Rai, R., Varma, S.P., Shinde, N., Ghosh, S., Kumaran, S.P., Skariah, G., and Laloraya, S. (2011). Small ubiquitin-related modifier ligase activity of Mms21 is required for maintenance of chromosome integrity during the unperturbed mitotic cell division cycle in Saccharomyces cerevisiae. J. Biol. Chem. 286, 14516-14530.
305. Remeseiro, S., and Losada, A. (2013). Cohesin, a chromatin engagement ring. Curr. Opin. Cell Biol. 25, 63-71.
306. Ren, J., Gao, X., Jin, C., Zhu, M., Wang, X., Shaw, A., Wen, L., Yao, X., and Xue, Y. (2009). Systematic study of protein sumoylation: Development of a site-specific predictor of SUMOsp 2.0. Proteomics. 9, 3409-3412.
307. Resnick, M.A. (1976). The repair of double-strand breaks in DNA; a model involving recombination. J. Theor. Biol. 59, 97-106.
308. Reverter, D., and Lima, C.D. (2005). Insights into E3 ligase activity revealed by a SUMO-RanGAP1-Ubc9-Nup358 complex. Nature 435, 687-692.
309. Ricke, R.M., van Ree, J.H., and van Deursen, J.M. (2008). Whole chromosome istability and cancer: a complex relationship. Trends Genet. 24, 457-466.
310. Roberts, J.J., Pascoe, J.M., Plant, J.E., Sturrock, J.E., and Crathorn, A.R. (1971). Quantitative aspects of the repair of alkylated DNA in cultured mammalian cells. I. The effect on HeLa and Chinese hamster cell survival of alkylation of cellular macromolecules. Chem. Biol. Interact. 3, 29-47.
311. Rodriguez, M.S., Dargemont, C., and Hay, R.T. (2001). SUMO-1 conjugation in vivo requires both a consensus modification motif and nuclear targeting. J. Biol. Chem. 276, 12654-12659.
312. Rosas-Acosta, G., Russell, W.K., Deyrieux, A., Russell, D.H., and Wilson, V.G. (2005). A universal strategy for proteomic studies of SUMO and other ubiquitin-like modifiers. Mol. Cell Proteomics. 4, 56-72.
313. Roy, M.A., Siddiqui, N., and D'Amours, D. (2011). Dynamic and selective DNA-binding activity of Smc5, a core component of the Smc5-Smc6 complex. Cell Cycle 10, 690-700.
314. Sacher, M., Pfander, B., and Jentsch, S. (2005). Identification of SUMO-protein conjugates. Methods Enzymol. 399, 392-404.
315. Saitoh, H., and Hinchey, J. (2000). Functional heterogeneity of small ubiquitin-related protein modifiers SUMO-1 versus SUMO-2/3. J. Biol. Chem. 275, 6252-6258.
316. Sakuno, T., Tada, K., and Watanabe, Y. (2009). Kinetochore geometry defined by cohesion within the centromere. Nature 458, 852-858.
317. Sale, J.E., Lehmann, A.R., and Woodgate, R. (2012). Y-family DNA polymerases and

their role in tolerance of cellular DNA damage. Nat. Rev. Mol. Cell Biol. 13, 141-152.

318. Sampson, D.A., Wang, M., and Matunis, M.J. (2001). The small ubiquitin-like modifier-1 (SUMO-1) consensus sequence mediates Ubc9 binding and is essential for SUMO-1 modification. J. Biol. Chem. 276, 21664-21669.
319. Sancar, A. (2008). Structure and function of photolyase and in vivo enzymology: 50th anniversary. J. Biol. Chem. 283, 32153-32157.
320. Sanchez, Y., Desany, B.A., Jones, W.J., Liu, Q., Wang, B., and Elledge, S.J. (1996). Regulation of RAD53 by the ATM-like kinases MEC1 and TEL1 in yeast cell cycle checkpoint pathways. Science 271, 357-360.
321. Sanchez-Diaz, A., Marchesi, V., Murray, S., Jones, R., Pereira, G., Edmondson, R., Allen, T., and Labib, K. (2008). Inn1 couples contraction of the actomyosin ring to membrane ingression during cytokinesis in budding yeast. Nat. Cell Biol. 10, 395-406.
322. Sassanfar, M., and Samson, L. (1990). Identification and preliminary characterization of an O6-methylguanine DNA repair methyltransferase in the yeast Saccharomyces cerevisiae. J. Biol. Chem. 265, 20-25.
323. Schleiffer, A., Kaitna, S., Maurer-Stroh, S., Glotzer, M., Nasmyth, K., and Eisenhaber, F. (2003). Kleisins: a superfamily of bacterial and eukaryotic SMC protein partners. Mol. Cell 11, 571-575.
324. Schmidt, D., and Muller, S. (2002). Members of the PIAS family act as SUMO ligases for c-Jun and p53 and repress p53 activity. Proc. Natl. Acad. Sci. U. S. A 99, 2872-2877.
325. Schmidt, D., Schwalie, P.C., Ross-Innes, C.S., Hurtado, A., Brown, G.D., Carroll, J.S., Flicek, P., and Odom, D.T. (2010). A CTCF-independent role for cohesin in tissue-specific transcription. Genome Res. 20, 578-588.
326. Schulz, S., Chachami, G., Kozaczkiewicz, L., Winter, U., Stankovic-Valentin, N., Haas, P., Hofmann, K., Urlaub, H., Ovaa, H., Wittbrodt, J., Meulmeester, E., and Melchior, F. (2012). Ubiquitin-specific protease-like 1 (USPL1) is a SUMO isopeptidase with essential, non-catalytic functions. EMBO Rep. 13, 930-938.
327. Schwartz, E.K., and Heyer, W.D. (2011). Processing of joint molecule intermediates by structure-selective endonucleases during homologous recombination in eukaryotes. Chromosoma 120, 109-127.
328. Schwarz, S.E., Matuschewski, K., Liakopoulos, D., Scheffner, M., and Jentsch, S. (1998). The ubiquitin-like proteins SMT3 and SUMO-1 are conjugated by the UBC9 E2 enzyme. Proc. Natl. Acad. Sci. U. S. A 95, 560-564.
329. Segurado, M., and Diffley, J.F. (2008). Separate roles for the DNA damage checkpoint protein kinases in stabilizing DNA replication forks. Genes Dev. 22, 1816-1827.
330. Segurado, M., and Tercero, J.A. (2009). The S-phase checkpoint: targeting the replication fork. Biol. Cell 101, 617-627.
331. Seitan, V.C., Hao, B., Tachibana-Konwalski, K., Lavagnolli, T., Mira-Bontenbal, H., Brown, K.E., Teng, G., Carroll, T., Terry, A., Horan, K., Marks, H., Adams, D.J., Schatz, D.G., Aragon, L., Fisher, A.G., Krangel, M.S., Nasmyth, K., and Merkenschlager, M. (2011). A role for cohesin in T-cell receptor rearrangement and thymocyte differentiation. Nature 476, 467-471.
332. Sergeant, J., Taylor, E., Palecek, J., Fousteri, M., Andrews, E.A., Sweeney, S., Shina

gawa, H., Watts, F.Z., and Lehmann, A.R. (2005). Composition and architecture of the Schizosaccharomyces pombe Rad18 (Smc5-6) complex. Mol. Cell Biol. 25, 172-184.

333. Sheedy, D.M., Dimitrova, D., Rankin, J.K., Bass, K.L., Lee, K.M., Tapia-Alveal, C., Harvey, S.H., Murray, J.M., and O'Connell, M.J. (2005). Brc1-mediated DNA repair and damage tolerance. Genetics 171, 457-468.

334. Sheltzer, J.M., Blank, H.M., Pfau, S.J., Tange, Y., George, B.M., Humpton, T.J., Brito, I.L., Hiraoka, Y., Niwa, O., and Amon, A. (2011). Aneuploidy drives genomic insta bility in yeast. Science 333, 1026-1030.

335. Shin, E.J., Shin, H.M., Nam, E., Kim, W.S., Kim, J.H., Oh, B.H., and Yun, Y. (2012). DeSUMOylating isopeptidase: a second class of SUMO protease. EMBO Rep. 13, 339-346.

336. Shintomi, K., and Hirano, T. (2009). Releasing cohesin from chromosome arms in early mitosis: opposing actions of Wapl-Pds5 and Sgo1. Genes Dev. 23, 2224-2236.

337. Shirayama, M., Toth, A., Galova, M., and Nasmyth, K. (1999). APC(Cdc20) promotes exit from mitosis by destroying the anaphase inhibitor Pds1 and cyclin Clb5. Na ture 402, 203-207.

338. Shroff, R., Arbel-Eden, A., Pilch, D., Ira, G., Bonner, W.M., Petrini, J.H., Haber, J.E., and Lichten, M. (2004). Distribution and dynamics of chromatin modifica tion induced by a defined DNA double-strand break. Curr. Biol. 14, 1703-1711.

339. Simpson-Lavy, K.J., and Johnston, M. (2013). SUMOylation regulates the SNF1 pro tein kinase. Proc. Natl. Acad. Sci. U. S. A 110, 17432-17437.

340. Sjogren, C., and Nasmyth, K. (2001). Sister chromatid cohesion is required for pos treplicative double-strand break repair in Saccharomyces cerevisiae. Curr. Biol. 11, 991-995.

341. Smogorzewska, A., and de, L.T. (2004). Regulation of telomerase by telomeric pro teins. Annu. Rev. Biochem. 73, 177-208.

342. Sollier, J., Driscoll, R., Castellucci, F., Foiani, M., Jackson, S.P., and Branzei, D. (2009). The Saccharomyces cerevisiae Esc2 and Smc5-6 proteins promote sister chromatid junction-mediated intra-S repair. Mol. Biol. Cell 20, 1671-1682.

343. Song, J., Zhang, Z., Hu, W., and Chen, Y. (2005). Small ubiquitin-like modifier (SUMO) recognition of a SUMO binding motif: a reversal of the bound orienta tion. J. Biol. Chem. 280, 40122-40129.

344. Sonoda, E., Matsusaka, T., Morrison, C., Vagnarelli, P., Hoshi, O., Ushiki, T., Nojima, K., Fukagawa, T., Waizenegger, I.C., Peters, J.M., Earnshaw, W.C., and Takeda, S. (2001). Scc1/Rad21/Mcd1 is required for sister chromatid cohesion and kinetochore function in vertebrate cells. Dev. Cell 1, 759-770.

345. Soulas-Sprauel, P., Rivera-Munoz, P., Malivert, L., Le, G.G., Abramowski, V., Revy, P., and de Villartay, J.P. (2007). V(D)J and immunoglobulin class switch recombina tions: a paradigm to study the regulation of DNA end-joining. Oncogene 26, 7780-7791.

346. St-Pierre, J., Douziech, M., Bazile, F., Pascariu, M., Bonneil, E., Sauve, V., Ratsima, H., and D'Amours, D. (2009). Polo kinase regulates mitotic chromosome conden sation by hyperactivation of condensin DNA supercoiling activity. Mol. Cell 34, 416-426.

347. Stead, K., Aguilar, C., Hartman, T., Drexel, M., Meluh, P., and Guacci, V. (2003).

Pds5p regulates the maintenance of sister chromatid cohesion and is sumoylated to promote the dissolution of cohesion. J. Cell Biol. 163, 729-741.
348. Stegmeier, F., and Amon, A. (2004). Closing mitosis: the functions of the Cdc14 phosphatase and its regulation. Annu. Rev. Genet. 38, 203-232.
349. Stelter, P., and Ulrich, H.D. (2003). Control of spontaneous and damage-induced mutagenesis by SUMO and ubiquitin conjugation. Nature 425, 188-191.
350. Stephan, A.K., Kliszczak, M., Dodson, H., Cooley, C., and Morrison, C.G. (2011a). Roles of vertebrate Smc5 in sister chromatid cohesion and homologous recombinational repair. Mol. Cell Biol. 31, 1369-1381.
351. Stephan, A.K., Kliszczak, M., and Morrison, C.G. (2011b). The Nse2/Mms21 SUMO ligase of the Smc5/6 complex in the maintenance of genome stability. FEBS Lett. 585, 2907-2913.
352. Strukov, Y.G., and Belmont, A.S. (2009). Mitotic chromosome structure: reproducibility of folding and symmetry between sister chromatids. Biophys. J. 96, 1617-1628.
353. Stukenberg, P.T., Studwell-Vaughan, P.S., and O'Donnell, M. (1991). Mechanism of the sliding beta-clamp of DNA polymerase III holoenzyme. J. Biol. Chem. 266, 11328-11334.
354. Stukenberg, P.T., Turner, J., and O'Donnell, M. (1994). An explanation for lagging strand replication: polymerase hopping among DNA sliding clamps. Cell 78, 877-887.
355. Subramaniam, S., Sixt, K.M., Barrow, R., and Snyder, S.H. (2009). Rhes, a striatal specific protein, mediates mutant-huntingtin cytotoxicity. Science 324, 1327-1330.
356. Sundin, O., and Varshavsky, A. (1981). Arrest of segregation leads to accumulation of highly intertwined catenated dimers: dissection of the final stages of SV40 DNA replication. Cell 25, 659-669.
357. Svendsen, J.M., and Harper, J.W. (2010). GEN1/Yen1 and the SLX4 complex: Solutions to the problem of Holliday junction resolution. Genes Dev. 24, 521-536.
358. Symington, L.S., and Gautier, J. (2011). Double-strand break end resection and repair pathway choice. Annu. Rev. Genet. 45, 247-271.
359. Takahashi, Y., Dulev, S., Liu, X., Hiller, N.J., Zhao, X., and Strunnikov, A. (2008). Cooperation of sumoylated chromosomal proteins in rDNA maintenance. PLoS. Genet. 4, e1000215.
360. Takata, M., Sasaki, M.S., Sonoda, E., Morrison, C., Hashimoto, M., Utsumi, H., Yamaguchi-Iwai, Y., Shinohara, A., and Takeda, S. (1998). Homologous recombination and non-homologous end-joining pathways of DNA double-strand break repair have overlapping roles in the maintenance of chromosomal integrity in vertebrate cells. EMBO J. 17, 5497-5508.
361. Takayama, Y., Kamimura, Y., Okawa, M., Muramatsu, S., Sugino, A., and Araki, H. (2003). GINS, a novel multiprotein complex required for chromosomal DNA replication in budding yeast. Genes Dev. 17, 1153-1165.
362. Tanaka, K., and Russell, P. (2001). Mrc1 channels the DNA replication arrest signal to checkpoint kinase Cds1. Nat. Cell Biol. 3, 966-972.
363. Tanaka, T.U., Stark, M.J., and Tanaka, K. (2005). Kinetochore capture and bi-orientation on the mitotic spindle. Nat. Rev. Mol. Cell Biol. 6, 929-942.
364. Taylor, E.M., Copsey, A.C., Hudson, J.J., Vidot, S., and Lehmann, A.R. (2008). Idetification of the proteins, including MAGEG1, that make up the human SMC5-6

protein complex. Mol. Cell Biol. 28, 1197-1206.

365. Taylor, E.M., Moghraby, J.S., Lees, J.H., Smit, B., Moens, P.B., and Lehmann, A.R. (2001). Characterization of a novel human SMC heterodimer homologous to the Schizosaccharomyces pombe Rad18/Spr18 complex. Mol. Biol. Cell 12, 1583-1594.
366. Tercero, J.A., and Diffley, J.F. (2001). Regulation of DNA replication fork progression through damaged DNA by the Mec1/Rad53 checkpoint. Nature 412, 553-557.
367. Tercero, J.A., Longhese, M.P., and Diffley, J.F. (2003). A central role for DNA replica tion forks in checkpoint activation and response. Mol. Cell 11, 1323-1336.
368. Terret, M.E., Sherwood, R., Rahman, S., Qin, J., and Jallepalli, P.V. (2009). Cohesin acetylation speeds the replication fork. Nature 462, 231-234.
369. Thadani, R., Uhlmann, F., and Heeger, S. (2012). Condensin, chromatin crossbarring and chromosome condensation. Curr. Biol. 22, R1012-R1021.
370. Thomas, S.E., Soltani-Bejnood, M., Roth, P., Dorn, R., Logsdon, J.M., Jr., and McKee, B.D. (2005). Identification of two proteins required for conjunction and regular segregation of achiasmate homologs in Drosophila male meiosis. Cell 123, 555-568.
371. Torres-Rosell, J., de, P.G., Cordon-Preciado, V., Farmer, S., Jarmuz, A., Machin, F., Pasero, P., Lisby, M., Haber, J.E., and Aragon, L. (2007a). Anaphase onset before complete DNA replication with intact checkpoint responses. Science 315, 1411-1415.
372. Torres-Rosell, J., Machin, F., Farmer, S., Jarmuz, A., Eydmann, T., Dalgaard, J.Z., and Aragon, L. (2005). SMC5 and SMC6 genes are required for the segregation of repetitive chromosome regions. Nat. Cell Biol. 7, 412-419.
373. Torres-Rosell, J., Sunjevaric, I., de, P.G., Sacher, M., Eckert-Boulet, N., Reid, R., Jentsch, S., Rothstein, R., Aragon, L., and Lisby, M. (2007b). The Smc5-Smc6 com plex and SUMO modification of Rad52 regulates recombinational repair at the ribosomal gene locus. Nat. Cell Biol. 9, 923-931.
374. Tourriere, H., Versini, G., Cordon-Preciado, V., Alabert, C., and Pasero, P. (2005). Mrc1 and Tof1 promote replication fork progression and recovery independently of Rad53. Mol. Cell 19, 699-706.
375. Tsang, C.K., Li, H., and Zheng, X.S. (2007a). Nutrient starvation promotes condensin loading to maintain rDNA stability. EMBO J. 26, 448-458.
376. Tsang, C.K., Wei, Y., and Zheng, X.F. (2007b). Compacting DNA during the inter phase: condensin maintains rDNA integrity. Cell Cycle 6, 2213-2218.
377. Tsuyama, T., Inou, K., Seki, M., Seki, T., Kumata, Y., Kobayashi, T., Kimura, K., Hanaoka, F., Enomoto, T., and Tada, S. (2006). Chromatin loading of Smc5/6 is duced by DNA replication but not by DNA double-strand breaks. Biochem. Biophys. Res. Commun. 351, 935-939.
378. Uhlmann, F., Lottspeich, F., and Nasmyth, K. (1999). Sister-chromatid separation at anaphase onset is promoted by cleavage of the cohesin subunit Scc1. Nature 400, 37-42.
379. Ui, A., Seki, M., Ogiwara, H., Onodera, R., Fukushige, S., Onoda, F., and Enomoto, T. (2005). The ability of Sgs1 to interact with DNA topoisomerase III is essential for damage-induced recombination. DNA Repair (Amst) 4, 191-201.
380. Ullal, P., Vilella-Mitjana, F., Jarmuz, A., and Aragon, L. (2011). Rtt107 phosphoryla tion promotes localisation to DNA double-stranded breaks (DSBs) and recombina

tional repair between sister chromatids. PLoS. One. 6, e20152.

381. Ulrich, H.D. (2014). Two-way communications between ubiquitin-like modifiers and DNA. Nat. Struct. Mol. Biol. 21, 317-324.

382. Ulrich, H.D., and Walden, H. (2010). Ubiquitin signalling in DNA replication and repair. Nat. Rev. Mol. Cell Biol. 11, 479-489.

383. van der Veen, A.G., and Ploegh, H.L. (2012). Ubiquitin-like proteins. Annu. Rev. Biochem. 81, 323-357.

384. Vazquez, M.V., Rojas, V., and Tercero, J.A. (2008). Multiple pathways cooperate to facilitate DNA replication fork progression through alkylated DNA. DNA Repair (Amst) 7, 1693-1704.

385. Venter, J.C., Adams, M.D., Myers, E.W., Li, P.W., Mural, R.J., Sutton, G.G., Smith, H.O., Yandell, M., Evans, C.A., Holt, R.A., Gocayne, J.D., Amanatides, P., Ballew, R.M., Huson, D.H., Wortman, J.R., Zhang, Q., Kodira, C.D., Zheng, X.H., Chen, L., Skupski, M., Subramanian, G., Thomas, P.D., Zhang, J., Gabor Miklos, G.L., Nelson, C., Broder, S., Clark, A.G., Nadeau, J., McKusick, V.A., Zinder, N., Levine, A.J., Roberts, R.J., Simon, M., Slayman, C., Hunkapiller, M., Bolanos, R., Delcher, A., Dew, I., Fasulo, D., Flanigan, M., Florea, L., Halpern, A., Hannenhalli, S., Kravitz, S., Levy, S., Mobarry, C., Reinert, K., Remington, K., Abu-Threideh, J., Beasley, E., Biddick, K., Bonazzi, V., Brandon, R., Cargill, M., Chandramouliswaran, I., Charlab, R., Chaturvedi, K., Deng, Z., Di, F., V, Dunn, P., Eilbeck, K., Evangelista, C., Gabrielian, A.E., Gan, W., Ge, W., Gong, F., Gu, Z., Guan, P., Heiman, T.J., Higgins, M.E., Ji, R.R., Ke, Z., Ketchum, K.A., Lai, Z., Lei, Y., Li, Z., Li, J., Liang, Y., Lin, X., Lu, F., Merkulov, G.V., Milshina, N., Moore, H.M., Naik, A.K., Narayan, V.A., Neelam, B., Nusskern, D., Rusch, D.B., Salzberg, S., Shao, W., Shue, B., Sun, J., Wang, Z., Wang, A., Wang, X., Wang, J., Wei, M., Wides, R., Xiao, C., Yan, C., Yao, A., Ye, J., Zhan, M., Zhang, W., Zhang, H., Zhao, Q., Zheng, L., Zhong, F., Zhong, W., Zhu, S., Zhao, S., Gilbert, D., Baumhueter, S., Spier, G., Carter, C., Cravchik, A., Woodage, T., Ali, F., An, H., Awe, A., Baldwin, D., Baden, H., Barnstead, M., Barrow, I., Beeson, K., Busam, D., Carver, A., Center, A., Cheng, M.L., Curry, L., Danaher, S., Davenport, L., Desilets, R., Dietz, S., Dodson, K., Doup, L., Ferriera, S., Garg, N., Gluecksmann, A., Hart, B., Haynes, J., Haynes, C., Heiner, C., Hladun, S., Hostin, D., Houck, J., Howland, T., Ibegwam, C., Johnson, J., Kalush, F., Kline, L., Koduru, S., Love, A., Mann, F., May, D., McCawley, S., McIntosh, T., McMullen, I., Moy, M., Moy, L., Murphy, B., Nelson, K., Pfannkoch, C., Pratts, E., Puri, V., Qureshi, H., Reardon, M., Rodriguez, R., Rogers, Y.H., Romblad, D., Ruhfel, B., Scott, R., Sitter, C., Smallwood, M., Stewart, E., Strong, R., Suh, E., Thomas, R., Tint, N.N., Tse, S., Vech, C., Wang, G., Wetter, J., Williams, S., Williams, M., Windsor, S., Winn-Deen, E., Wolfe, K., Zaveri, J., Zaveri, K., Abril, J.F., Guigo, R., Campbell, M.J., Sjolander, K.V., Karlak, B., Kejariwal, A., Mi, H., Lazareva, B., Hatton, T., Narechania, A., Diemer, K., Muruganujan, A., Guo, N., Sato, S., Bafna, V., Istrail, S., Lippert, R., Schwartz, R., Walenz, B., Yooseph, S., Allen, D., Basu, A., Baxendale, J., Blick, L., Caminha, M., Carnes-Stine, J., Caulk, P., Chiang, Y.H., Coyne, M., Dahlke, C., Mays, A., Dombroski, M., Donnelly, M., Ely, D., Esparham, S., Fosler, C., Gire, H., Glanowski, S., Glasser, K., Glodek, A., Gorokhov, M., Graham, K., Gropman, B., Harris, M., Heil, J., Henderson, S., Hoover, J., Jennings, D., Jordan, C., Jordan, J., Kasha, J., Kagan, L., Kraft, C., Levitsky, A., Lewis, M., Liu, X., Lopez, J., Ma, D., Majoros, W., McDaniel, J., Murphy, S., Newman, M., Nguyen, T., Nguyen, N., and Nodell, M. (2001). The sequence of the human genome. Science 291, 1304-1351.

386. Verkade, H.M., Bugg, S.J., Lindsay, H.D., Carr, A.M., and O'Connell, M.J. (1999).

Rad18 is required for DNA repair and checkpoint responses in fission yeast. Mol. Biol. Cell 10, 2905-2918.

387. Vertegaal, A.C., Andersen, J.S., Ogg, S.C., Hay, R.T., Mann, M., and Lamond, A.I. (2006). Distinct and overlapping sets of SUMO-1 and SUMO-2 target proteins revealed by quantitative proteomics. Mol. Cell Proteomics. 5, 2298-2310.
388. Verver, D.E., van Pelt, A.M., Repping, S., and Hamer, G. (2013). Role for rodent Smc6 in pericentromeric heterochromatin domains during spermatogonial differentiation and meiosis. Cell Death. Dis. 4, e749.
389. Wahl, M.C., and Sundaralingam, M. (2000). B-form to A-form conversion by a 3'-terminal ribose: crystal structure of the chimera d(CCACTAGTG)r(G). Nucleic Acids Res. 28, 4356-4363.
390. Walker, J.R., Corpina, R.A., and Goldberg, J. (2001). Structure of the Ku heterodimer bound to DNA and its implications for double-strand break repair. Nature 412, 607-614.
391. Wan, Y., Zuo, X., Zhuo, Y., Zhu, M., Danziger, S.A., and Zhou, Z. (2013). The functional role of SUMO E3 ligase Mms21p in the maintenance of subtelomeric silencing in budding yeast. Biochem. Biophys. Res. Commun. 438, 746-752.
392. Wang, J.C. (2002). Cellular roles of DNA topoisomerases: a molecular perspective. Nat. Rev. Mol. Cell Biol. 3, 430-440.
393. Wang, L.H., Schwarzbraun, T., Speicher, M.R., and Nigg, E.A. (2008). Persistence of DNA threads in human anaphase cells suggests late completion of sister chromatid decatenation. Chromosoma 117, 123-135.
394. Warner, J.R. (1999). The economics of ribosome biosynthesis in yeast. Trends Biochem. Sci. 24, 437-440.
395. Wasch, R., and Cross, F.R. (2002). APC-dependent proteolysis of the mitotic cyclin Clb2 is essential for mitotic exit. Nature 418, 556-562.
396. Watanabe, K., Pacher, M., Dukowic, S., Schubert, V., Puchta, H., and Schubert, I. (2009). The STRUCTURAL MAINTENANCE OF CHROMOSOMES 5/6 complex promotes sister chromatid alignment and homologous recombination after DNA damage in Arabidopsis thaliana. Plant Cell 21, 2688-2699.
397. Watson, J.D., and Crick, F.H. (1953). Molecular structure of nucleic acids; a structure for deoxyribose nucleic acid. Nature 171, 737-738.
398. Watt, D.L., Johansson, E., Burgers, P.M., and Kunkel, T.A. (2011). Replication of ribonucleotide-containing DNA templates by yeast replicative polymerases. DNA Repair (Amst) 10, 897-902.
399. Weger, S., Hammer, E., and Heilbronn, R. (2005). Topors acts as a SUMO-1 E3 ligas for p53 in vitro and in vivo. FEBS Lett. 579, 5007-5012.
400. Wehrkamp-Richter, S., Hyppa, R.W., Prudden, J., Smith, G.R., and Boddy, M.N. (2012). Meiotic DNA joint molecule resolution depends on Nse5-Nse6 of the Smc5-Smc6 holocomplex. Nucleic Acids Res. 40, 9633-9646.
401. Wendt, K.S., Yoshida, K., Itoh, T., Bando, M., Koch, B., Schirghuber, E., Tsutsumi, S., Nagae, G., Ishihara, K., Mishiro, T., Yahata, K., Imamoto, F., Aburatani, H., Nakao, M., Imamoto, N., Maeshima, K., Shirahige, K., and Peters, J.M. (2008). Cohesin mediates transcriptional insulation by CCCTC-binding factor. Nature 451, 796-801.
402. Westhorpe, F.G., and Straight, A.F. (2013). Functions of the centromere and kine

tochore in chromosome segregation. Curr. Opin. Cell Biol. 25, 334-340.

403. Wilkinson, K.A., and Henley, J.M. (2010). Mechanisms, regulation and consequences of protein SUMOylation. Biochem. J. 428, 133-145.
404. Windecker, H., and Ulrich, H.D. (2008). Architecture and assembly of poly-SUMO chains on PCNA in Saccharomyces cerevisiae. J. Mol. Biol. 376, 221-231.
405. Wu, L., and Hickson, I.D. (2003). The Bloom's syndrome helicase suppresses crossing over during homologous recombination. Nature 426, 870-874.
406. Wu, N., Kong, X., Ji, Z., Zeng, W., Potts, P.R., Yokomori, K., and Yu, H. (2012). Scc1 sumoylation by Mms21 promotes sister chromatid recombination through counteracting Wapl. Genes Dev. 26, 1473-1485.
407. Wu, N., and Yu, H. (2012). The Smc complexes in DNA damage response. Cell Biosci. 2, 5.
408. Wyatt, M.D., and Pittman, D.L. (2006). Methylating agents and DNA repair responses: Methylated bases and sources of strand breaks. Chem. Res. Toxicol. 19, 1580-1594.
409. Xaver, M., Huang, L., Chen, D., and Klein, F. (2013). Smc5/6-mms21 prevents and eliminates inappropriate recombination intermediates in meiosis. PLoS. Genet. 9, e1004067.
410. Xu, D., Bai, J., Duan, Q., Costa, M., and Dai, W. (2009). Covalent modifications of histones during mitosis and meiosis. Cell Cycle 8, 3688-3694.
411. Xu, P., Yuan, D., Liu, M., Li, C., Liu, Y., Zhang, S., Yao, N., and Yang, C. (2013). AtMMS21, an SMC5/6 complex subunit, is involved in stem cell niche maintenance and DNA damage responses in Arabidopsis roots. Plant Physiol 161, 1755-1768.
412. Xu, S.Y., Zhu, Z., Zhang, P., Chan, S.H., Samuelson, J.C., Xiao, J., Ingalls, D., and Wilson, G.G. (2007). Discovery of natural nicking endonucleases Nb.BsrDI and Nb.BtsI and engineering of top-strand nicking variants from BsrDI and BtsI. Nucleic Acids Res. 35, 4608-4618.
413. Yang, J., Bachrati, C.Z., Ou, J., Hickson, I.D., and Brown, G.W. (2010). Human topoisomerase IIIalpha is a single-stranded DNA decatenase that is stimulated by BLM and RMI1. J. Biol. Chem. 285, 21426-21436.
414. Yang, S.H., Galanis, A., Witty, J., and Sharrocks, A.D. (2006). An extended consensus motif enhances the specificity of substrate modification by SUMO. EMBO J. 25, 5083-5093.
415. Yang, X.J., and Gregoire, S. (2006). A recurrent phospho-sumoyl switch in transcriptional repression and beyond. Mol. Cell 23, 779-786.
416. Yao, N.Y., and O'Donnell, M. (2010). SnapShot: The replisome. Cell 141, 1088, 1088.
417. Yazdi, P.T., Wang, Y., Zhao, S., Patel, N., Lee, E.Y., and Qin, J. (2002). SMC1 is a downstream effector in the ATM/NBS1 branch of the human S-phase checkpoint. Genes Dev. 16, 571-582.
418. Yeager, T.R., Neumann, A.A., Englezou, A., Huschtscha, L.I., Noble, J.R., and Reddel, R.R. (1999). Telomerase-negative immortalized human cells contain a novel type of promyelocytic leukemia (PML) body. Cancer Res. 59, 4175-4179.
419. Yi, C., and He, C. (2013). DNA repair by reversal of DNA damage. Cold Spring Harb. Perspect. Biol. 5, a012575.
420. Yong-Gonzales, V., Hang, L.E., Castellucci, F., Branzei, D., and Zhao, X. (2012). The Smc5-Smc6 complex regulates recombination at centromeric regions and affects

kinetochore protein sumoylation during normal growth. PLoS. One. 7, e51540.

421. Yoshimura, S.H., Hizume, K., Murakami, A., Sutani, T., Takeyasu, K., and Yanagida, M. (2002). Condensin architecture and interaction with DNA: regulatory non-SMC subunits bind to the head of SMC heterodimer. Curr. Biol. 12, 508-513.
422. Young, P., Deveraux, Q., Beal, R.E., Pickart, C.M., and Rechsteiner, M. (1998). Characterization of two polyubiquitin binding sites in the 26 S protease subunit 5a. J. Biol. Chem. 273, 5461-5467.
423. Yunus, A.A., and Lima, C.D. (2009). Structure of the Siz/PIAS SUMO E3 ligase Siz1 and determinants required for SUMO modification of PCNA. Mol. Cell 35, 669-682.
424. Zechiedrich, E.L., Khodursky, A.B., and Cozzarelli, N.R. (1997). Topoisomerase IV, not gyrase, decatenates products of site-specific recombination in Escherichia coli. Genes Dev. 11, 2580-2592.
425. Zegerman, P., and Diffley, J.F. (2009). DNA replication as a target of the DNA damage checkpoint. DNA Repair (Amst) 8, 1077-1088.
426. Zhang, J., Shi, X., Li, Y., Kim, B.J., Jia, J., Huang, Z., Yang, T., Fu, X., Jung, S.Y., Wang, Y., Zhang, P., Kim, S.T., Pan, X., and Qin, J. (2008). Acetylation of Smc3 by Eco1 is required for S phase sister chromatid cohesion in both human and yeast. Mol. Cell 31, 143-151.
427. Zhang, S., Qi, Y., Liu, M., and Yang, C. (2013). SUMO E3 ligase AtMMS21 regulates drought tolerance in Arabidopsis thaliana(F). J. Integr. Plant Biol. 55, 83-95.
428. Zhao, X., and Blobel, G. (2005). A SUMO ligase is part of a nuclear multiprotein complex that affects DNA repair and chromosomal organization. Proc. Natl. Acad. Sci. U. S. A 102, 4777-4782.
429. Zou, L., and Elledge, S.J. (2003). Sensing DNA damage through ATRIP recognition of RPA-ssDNA complexes. Science 300, 1542-1548.